Integrated Modelling of Moisture Release, Transport and Buffering in Housing

Anastasios Markopoulos B.Eng., M.Sc.

A thesis submitted for the
Degree of Doctor of Philosophy

Energy Systems Research Unit,
Department of Mechanical and Aerospace Engineering, University of Strathclyde, Glasgow, UK

December 2014

Signed:

Date:

Contents

Abstract

A significant proportion of damage in buildings is moisture related, contributing to the reduction of building energy and thermal efficiency. The presence of surface mould growth, indicating high indoor relative humidity and surface condensation effects, is also recognised to impact on the integrity of building materials and occupants' health.

The work in this thesis is focused on the advancement of moisture modelling within whole building hygrothermal simulation, given the increasing use of simulation tools during building design and investigations of moisture related damage. Dvelopment work was undertaken within the framework of the whole building simulation tool, ESPr, to improve modelling of transient heat and moisture transfer processes, including building material moisture buffering; and occupant related moisture generating activities. Static hygrothermal conditions commonly used to derive material properties raises concern over accurate representation of the hygrothermal response of building materials when exposed to dynamic whole building scenarios. This issue was addressed by improving the modelling of the response of porous building materials exposed to short duration, high intensity moisture loading conditions. Using an empirical verification approach, the range of material moisture properties adopted in ESP-r has been expanded to model the hygrothermal response of moisture buffering materials exposed to these conditions.

Convective transfer coefficients are regularly applied to model heat and moisture exchange processes at the surface of porous building materials. These are derived from existing empirical correlations with air velocity, meaning spatial and temporal effects are usually not accounted for. Convective mass transfer coefficients are often calculated using convective heat transfer coefficients without fulfilling the conditions under which the heat and mass transfer analogy is valid for. One such moisture exchange process, where these coefficients are applied, is drying. Its underlying complexity is due to the interrelated heat, air and moisture transfer flows occurring at the interfacial region, and the influence of the material properties on the rate of moisture transfer from within a material to its surface. The existing ESP-r model was developed to improve the accuracy and treatment of the different stages of drying associated with this hygrothermal phenomena.

Acknowledgments

Firstly, I would like to express my gratitude to both of my supervisors, Dr Nick Kelly and Dr Paul Strachan. Their support and guidance throughout the duration of this research has helped me greatly in completing this thesis.

My thanks also go to the students and staff at ESRU (both past and present) who have given me valuable support, advice and a listening ear during this time: Simon Borg, Giorgos Kokogiannakis, James Ure, Amos Madhlopa, Willie Maruwo, Aizaz Samuel, Jon Hand and Antonis Maitos.

I would also like to thank Dr Paul Baker, with whom I have been working with at Glasgow Caledonian University over the past two years. I am very grateful for the time he has afforded me during this period to complete the writing of this thesis, for the indepth discussions that have helped to guide this work, and also for the experimental work carried out, the results of which have fuelled this research.

I acknowledge the Engineering and Physical Sciences Research Council for their funding of this research.

I wish to thank my family and friends. I am extremely grateful for the patience, understanding and the support they have shown me throughout my time at university and whilst doing this research. My sincere thanks go to Dr Brian Lambkin and Dr Kay Muhr for the time they spent reading chapters and providing comments, which helped me make it over the final hurdles in the writing up process.

Most importantly, I wish to express my warmest thanks to my partner Magdalen, and daughter Màiri. None of what has been achieved would have been possible had it not been for their unwavering understanding, encouragement and love.
I dedicate this thesis to them.

List of symbols

A	Area of exposed surface	m_2
ac/h	Volumetric flow rate measured in room air changes per hour	ac/h
a	Regression analysis constant	[-]
B_e	Energy boundary conditions	[-]
B_m	Moisture boundary conditions	[-]
b	Regression analysis constant	[-]
C_p	Specific heat capacity	J/ kg.K
c	Solute concentration	
d_b	Thickness of active buffering layer	m
d_p	Effective moisture penetration depth	m
E	Energy coefficient matrix	[-]
ev	Evaporation rate	kg/ s
e_h	Evaporative history coefficient	[-]
G_{buf}	Moisture exchange rate between room air and moisture buffering layer	kg/ s
D_e	Effective diffusion coefficient	m^2/ s
D_h	Hydraulic diameter	m
D_m	Molecular diffusion coefficient	m^2/ s
D_{aw}	Binary diffusion coefficient of air and water	m^2/ s
D_s	Superficial diffusion coefficient	m^2/ s
D_f	Liquid conduction coefficient	kg/ m.s
D□	Drying rate	kg/m^2.s
G(t)	Moisture uptake over the period of moisture flux	kg/ m^2
G_{vp}	Internal moisture generation rate	kg/ s
g/ h	Moisture production rate	g/ h
g_w	Moisture flux	kg/ m^2.s
h_c	Convective heat transfer coefficient	W/ m^2.K
h_m	Convective mass transfer coeffiient	s/ m
h_{vap}	Latent heat of evaporation	J/ kg

j	Moisture flux	kg/ m^2.s
k	Thermal conductivity of air	W/ m.K
K	Unsaturated hydraulic conductivity	Kg/ m.s.Pa
l	Length of moisture particle trajectory	m
Le	Lewis number = $\frac{h}{\rho C}$	
$MBV_{practical}$	Practical Moisture Buffer Value	g/ m^2.%RH
MBV_{ideal}	Ideal moisture buffer value	kg/ m^2.%RH
M_{H2O}	Molecular weight of water	kg/ mol
M	Multiplication factor for the rooms moisture buffering capacity	[-]
m	Mass	kg
m_{air}	Mass of air	kg
m_e	Evaporated mass of moisture	kg
m_i	Initial mass of moisture at material surface	kg
m	Regression analysis constant	[-]
N	Air exchange rate	1/ h
n	Regression analysis constant	[-]
Nu	Nusselt number = $\frac{cDh}{k}h$	
P_c	Capillary suction pressure	Pa
$p_{v,sat}$	Saturated vapour pressure	Pa
p_{vi}	Vapour pressure of indoor air	Pa
p_{ve}	Vapour pressure of external air	Pa
p_{vb}	Vapour pressure in moisture buffering layer	Pa
p_b	Barometric pressure	N/ m^2
Pr	Prandtl number = $\frac{\nu}{\alpha}$	
q_v	Mass flux of vapour flow	kg/ m^2.s
$q_{c,w}$	Convective heat flux at the wall	W/ m^2
R	Effective resistance	s/ m
R_{in}	Indoor volumetric air flow rate	m^3/ s
Re	Reynolds number = $\frac{\rho UD}{\mu}$	
R_s	Surface resistance	s/ m

R_v	Gas constant of water vapour	J/ kg.K
r	Radius of capillary tube	m
s_d	Standard diffusion thickness	m
Sc	Schmidt number = $\frac{\mu}{\rho D}$	
St	Stanton number = $\frac{h}{\rho u C_p}$	
T_b	Temperature in moisture buffering layer	K
T_i	Internal temperature of enclosure	K
T	Absolute temperature	K
t	Time period	s
t_1	First point of reflection	s
t_2	Second point of reflection	s
u_h	Gravimetric moisture content	kg /kg
u	Air flow velocity	m /s
V_v	Volume of void space	m^3
V_s	Volume of solid	m^3
v	Specific volume of enclosure	m^3
x	Depth at which moisture content measurement is taken	m
Y	Mass fraction	kg/ kg
Z	Mole fraction at the material surface	mol/ mol
Z_i	Vapour resistance of construction material	m^2.s.Pa/ kg

Greek symbols

□	Correction factor	[-]
□	Convective surface mass transfer coefficient	s/ m
□$_l$	Vapour permeance	kg/ m^2.s.Pa
□$_a$	Vapour permeability of stagnant air	kg/ m.s.Pa
□	Water vapour permeability	s
□	Porosity	mm^3/ mm^3
□	Relative humidity	%RH
□	Thermal conductivity	W/ m.K

□-profile	Profile developed when Boltzmann conditions are met (a boundary condition that is initially at uniform moisture content).	[-]
□	Dynamic viscosity	kg/ m.s
□	Contact angle	□
□	Density	kg/ m^3
□	Surface tension of liquid	N/ m
□	Tortuosity	[-]
□	Moisture capacity of moisture buffering layer	kg/ m^3
□	Humidity ratio	kg/ kg

Subscripts

a; air	Air
air, in	Air inside
air, out	Air outside
i	Internal
l	liquid
nw	Non-wetting phase
o	Outside
P	Pressure driving potential (primary)
ref	Reference point
s; surf	surface
sat	saturation
v	Vapour phase
w	water
w	Wetting phase
y	Driving potential

Superscripts

c	Secondary driving potential
i	Node label
j	Node label
n	Present time row of current time step
n+1	Future time row of current time step

n	exponent
□	Temperature driving potential (secondary)

Introduction

Chapter overview

This thesis aims to advance the modelling of indoor moisture transfer processes within the context of whole building simulation, using the simulation package ESP-r. It does this by seeking to accurately model the impact of the moisture buffering behaviour associated with hygroscopic porous building materials in the building envelope and by developing the treatment of surface evaporation from indoor moisture sources within the modelling capabilities of ESP-r. In order to demonstrate the need for this work and to show how it fits within current research the importance of controlling moisture in buildings is first discussed. The importance of moisture buffering in controlling moisture levels is then described before finally presenting the case for the use of computer modelling in assessing moisture buffering, as well as certain shortcomings in current modelling capabilities. A summary overview of the thesis chapters is then presented, explaining the specific aims and methodology of this thesis, which offers some significant advances in the moisture modelling capabilities of ESP-r.

1.1 Moisture in the indoor building environment

Moisture is considered to be one of the most destructive elements in the built environment (De Freitas et al, 1996). For this reason, addressing the potential causes of moisture related damage appearing in the building, prior to its construction and during its service life, is critical. Determining the causes of moisture related damage however, is difficult due to the range of interrelated and complex hygrothermal transfer processes occurring in the built environment over varying time and spatial resolutions. It is important to consider the origins of the moisture when designing solutions for moisture control in the building, which include moisture storage in the construction, outdoor climate conditions, and indoor moisture generation.

1.1.1 Moisture storage in the construction

The moisture present in the building environment can originate from as early as the construction phase of a building, where a considerable quantity may already exist in the materials used. Firstly, this can be the result of the inherent moisture storing capacity of porous building materials, and secondly as a consequence of building design defects, such as improper drainage of groundwater (Lstiburek, 2001), which could also lead to the physical properties of the materials changing. The former is a characteristic reported in a wide range of hygroscopic porous building materials (Rode et al, 2007) and is discussed further in section 1.2. The stored moisture in the building envelope however, must be removed to ensure acceptable levels of initial moisture content in the construction are achieved (Hall et al, 1986). One reason for this is to ensure the calculated thermal performance of the building envelope design is not hindered by excess moisture in the building fabric. In the same way that building materials exhibit temperature dependent behaviour, the moisture content of a building material will also influence the thermal properties of the construction material. This relationship is acknowledged when the thermal conductivity of insulating material components is considered. A higher moisture content will lead to increased thermal conductivity and thus reduce the effectiveness of insulation and consequently the building energy efficiency (Al-Homoud, 2005).

1.1.2 Outdoor climate conditions

The outdoor climate is another prominent factor influencing the moisture conditions of the indoor air and the building envelope fabric. Air exchange between the indoor and outdoor climate takes place through leakage paths in building constructions with a low level of airtightness, resulting in moisture exchange between the two environments. The air change rate inside the building will also affect the moisture distribution both within a room and across multiple zones in addition to the temperature and moisture content differences between the inside and outside of the building. Induced air density variation across the building is the product of the disparity in the

hygrothermal conditions observed within the indoor air and at the surface of building materials.

Seasonal effects are also observed as moisture stored during the summer period is released from the porous building materials in the winter, due to lower outdoor air temperatures and moisture content, which create thermal and pressure gradients between the indoor and outdoor climate (Wyrwal and Marynowicz, 2002). Additionally, wind-driven rain (WDR) is one of the most important outdoor sources of moisture that can impact on the hygrothermal performance and durability of the building facades. Potentially damaging consequences can arise from prolonged wetting and eventual saturation of the affected surfaces (Trechsel et al, 2009), which can be in the form of water penetration and long term interstitial condensation as a result of insufficient drying following a wetting period; frost damage; and structural cracking caused by thermal and moisture gradients across the material (Blocken and Carmeliet, 2004). Prolonged accumulation of moisture in the building fabric can inevitably lead to a serious deterioration of the building envelope performance and the degradation of the affected structural components (Sanders C, 1988). A sign of this structural degradation can be the presence of surface mould, which is discussed in section 1.1.4.

1.1.3 Indoor moisture generation

Occupant related moisture-generating activity, e.g. showering, cooking and clothes drying is also responsible for a significant quantity of moisture introduced to the indoor air, with values as high as 20 kg/day having been reported in some climates (Tariku et al, 2010).

Studies have highlighted the intrinsic link that exists between the duration and intensity of moisture production activities taking place in the indoor environment and the resulting hygrothermal response of building materials exposed to these conditions (Ge, 2014). This has also placed emphasis on assessing the hygrothermal interaction between the moisture absorbent materials in the building envelope exposed to dynamic, short term moisture production schemes and not focusing solely on long term material exposure to moisture, where satisfactory levels of accuracy in material moisture performance assessment are already established.

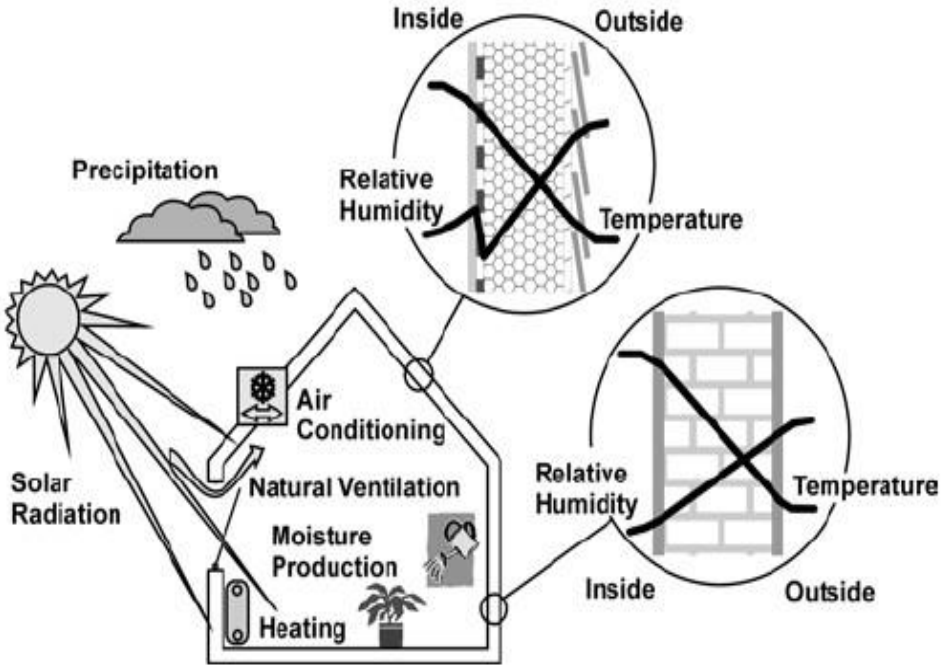

Figure 1.0 Coupling concepts for the simultaneous treatment of hygrothermal factors influencing indoor conditions (Künzel et al, 2003).

1.1.4 Moisture and Mould growth

A strong relationship exists between a building's design and the health and comfort of its occupants, particularly in the case of indoor air quality. Consideration of the intrinsic link between indoor air quality and the well-being of occupants is gradually becoming a more recognised feature of building design practice (Meadow et al, 2014), driven by the knowledge that has been gained on the potential health risks associated with exposure to indoor air pollutants found in the form of particulates, gases (Jones, 1999) and allergens. One of the main producers of allergens in the domestic environment is mould – which is also an indicator of elevated levels of moisture in the indoor building environment (Haverinen, 2001).

Provided there is sufficient water activity (A_w), a term used to describe the effective water concentration in a substrate, mould has the capacity to grow on virtually any substrate including glass, paint, plastics and textiles, materials which are widely used in the majority of building construction types and everyday objects found in the indoor environment, such as furniture (Miller, 1992).

Figure 1.1 Evidence of mould growth behind vinyl wallpaper covering (Lstiburek, 2001).

Studies of indoor air quality have identified several mould types, *Penicillium*, *Fusarium*, *Aspergillus* and *Cladosporium* to name a few, linked to symptoms of poor health in occupants (Daisey et al, 2003). The causal relationship between mould spores and the effects on occupant health is highly complex due to the array of factors influencing this problem, including occupant related activity; biological and toxicological emissions; the outdoor climate conditions; the building construction; and the methods used to manage the air supplied and extracted, to and from the building (Sherman et al, 2011). Therefore further investigation is required to continue to improve our knowledge.

Nevertheless, strong evidence exists to suggest that long-term moisture accumulation in buildings and the resulting exposure to mould produces adverse health effects in occupants. *Stachybotrys* was the most prevalent mould identified in housing that was linked to both several symptoms and diseases, such as colds and flu, respiratory infections and asthma, being suffered by the adult and child occupants (Husman, 1996). Studies using the relative humidity (RH) to represent the moisture present in the indoor environment showed levels surpassing the 60%RH bound would instigate the proliferation of mould and release of fungal spores from colony forming units (CFU) (Wolkoff et al, 2007), the spread of which would enhance the probability of viral infection (Hersoug, 2005). In the UK alone, 5.4 million people have been diagnosed with asthma, 31% of those having the condition triggered by mould (Allergy UK. 2011).

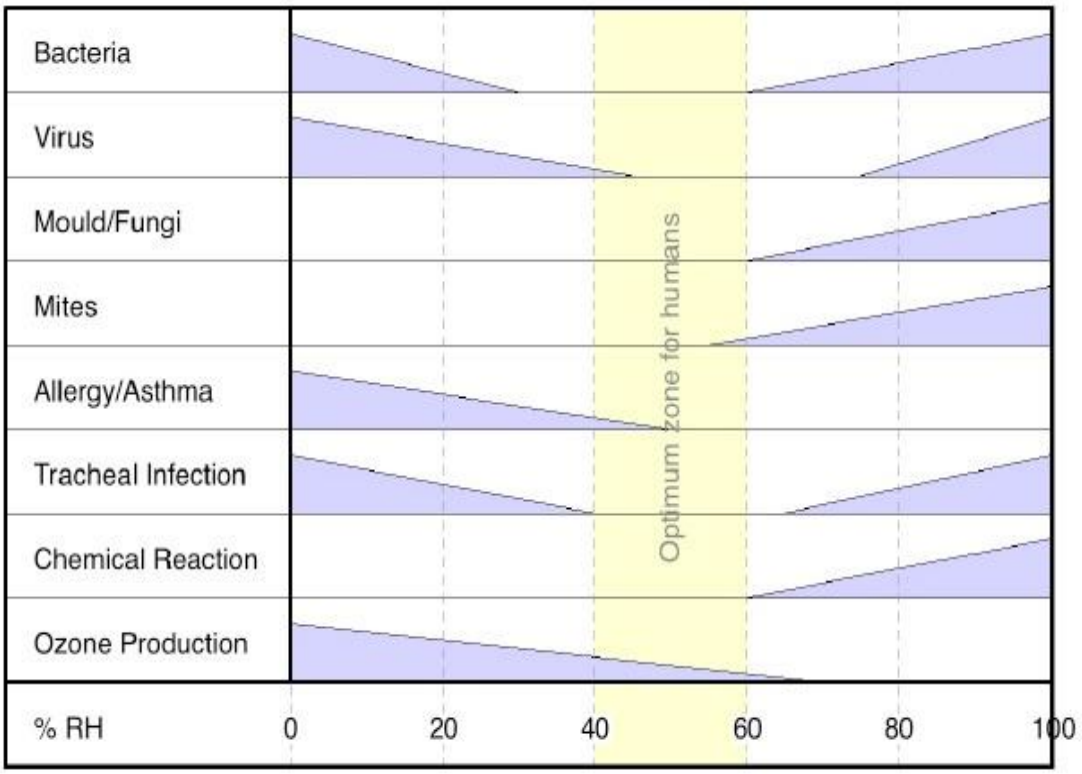

Figure 1.2 Indirect health effects of relative humidity in the indoor environment (Arundel et al, 1986).

1.1.5 Building design with moisture in mind

Focus on indoor air quality in the field of building physics has grown in recent years and there is increasing demand for building regulations authorities to improve their understanding on this subject given the strong links to occupant comfort and health. Emphasis on the issue of indoor air quality within the UK building regulations has been largely overlooked however, and is instead directed on improving building energy efficiency and heat retention through increased air-tightness, which reduces the ingress of moisture (from the outdoor air) through the building envelope by filling gaps in the construction to lower the air permeability of the fabric; and by improving the levels of insulation in the building envelope construction.

With respect to indoor ventilation, the UK building regulations include recommended minimum air exchange rates whereby 'fresh' outdoor air is supplied by natural ventilation (usually through trickle vents or by opening windows); mechanical ventilation schemes, mainly in the form of extraction fans (Laverge et al, 2011), or as a combination of the two, in order to 'dilute' the indoor air and remove moisture from areas in the building where it is produced in high quantities, which are specified as the kitchen and the bathroom (Parliamentary office of Science and Technology (POST), 2010). However, statutory standards in the UK building regulations do not provide an effective solution when considering occupant related activities such as that of passive indoor drying of laundry. On a typical laundry day, 30% of the moisture in the indoor air

will be attributable to the clothes drying process for a family with two children an assuming two laundry loads being dried on the same day (Menon and Porteous, 2011).

Despite the regulations being designed for both existing and new housing stock in the UK, the likelihood is that the recommendations will only be applied in new housing developments. Yet a significant proportion of existing housing is already displaying signs of moisture related damage. In Scotland for example, 15.2% of homes in the current housing stock (approximately 2.8 million) are affected by damp and/or condensation (Scottish Housing Conditions Survey, 2012: 79-80). Introducing mechanical systems to control increased levels of indoor moisture is not particularly suited to small, lowdensity interiors, such as houses (Cerolini et al, 2009), and in light of the research highlighting the inadequate provision of space in new housing stock (Robert-Hughes, 2011), the issue of indoor air quality is likely to be further exacerbated. There is therefore a real need to identify and develop a suitable balance between the measures being implemented to improve building energy efficiency (i.e. increased airtightness) and maintenance of comfortable and healthy levels of indoor air quality.

1.2 Moisture buffering: an additional method of moisture control

With emphasis on the reduction of energy consumption in the built environment, and increasing awareness over the impact of housing design on indoor air quality (Dimitroulopoulou, 2012**)**, hygroscopic, porous building materials have been identified as an additional means of moderating the indoor relative humidity. A positive effect has been identified in a range of materials (Osanyintola and Simonson, 2006) commonly found in the building construction that can help to moderate the indoor relative humidity by as much as 35%RH (Simonson et al, 2002), and thus help to prevent the conditions that give rise to problems such as mould growth. The extent to which this moisture buffering takes place and the resultant impact on indoor relative humidity conditions is influenced by a number of hygrothermal processes and building parameters, which include:

- the indoor and outdoor boundary conditions, which will influence thermal and moisture related transfer processes occurring both within the material and at its exposed surfaces;
- the airflow conditions inside the building resulting from intentional means of ventilation and/ or air infiltration through leakage paths that consequently influence the indoor temperature profile and distribution of moisture within the building;
- the use of the building i.e. the level of occupancy, and moisture sources;
- building operational systems such as heating and cooling.

As a result of the interrelated and transient nature of the physical processes described above, it becomes clear that the indoor hygrothermal conditions created are both dynamic and highly complex. Quantification of the interaction that takes place between the moisture buffering materials present in the indoor environment and the indoor air therefore requires a solution that is able to integrate this variable behaviour in a holistic, time dependent manner. An available means by which the complexity of this environment can be analysed is through the use of building simulation.

1.3 Modelling the hygrothermal material performance

The need to model the indoor hygrothermal conditions of a building is driven by the range of heat, air and moisture transfer processes arising from the topics listed above. Building computer simulation tools e.g. WUFI Plus (www.wufi.de), HAMBASE (http://archbps1.campus.tue.nl/bpswiki/index.php/Hamlab), ESP-r (Clarke JA, 2001), can provide the capability to carry out this process to varying degrees of complexity. These include the modelling of the moisture storage capacity of building materials using either lumped models or detailed descriptions of the heat and moisture transfer process taking place through the material, which allows for the determination of the moisture content. This sorptive behaviour of the material can be described using the wellestablished sorption isotherm, where the calculated moisture content is a function of the relative humidity and temperature conditions when in equilibrium with the surrounding boundary conditions (Ramos and de Freitas, 2012).

As moisture penetrates into the material pore domain, three primary mechanisms related to moisture transfer within the hygroscopic material dominate: (1) absorption, (2) condensation and (3) capillary motion (De Freitas et al, 1996). There are models that can quantify this change in phase and the transfer process associated linked to this behaviour. This enables phenomena including hysteresis effects and pore-scale moisture migration to be numerically modelled. There is significant mathematical difficulty however, in incorporating these micro-scale phenomena into a macro-scale predictive tool to improve the accuracy of the moisture transfer processes being modelled, which has resulted in the development and use of averaging techniques such as the representative elementary volume method (Whitaker, 1977) and the use of constitutive relations for porous media systems that describe the relevant movement (Chen and Shi, 2005).

Hygrothermal material properties are required to relate the balance equations forming the mathematical model to the physical interaction (Miller et al, 1998). To this end, building research continues to use (in the main) phenomenological macroscopic models that analyse HAM transfer processes observed in the indoor environment and relate them to each other by adopting moisture and temperature dependent transport coefficients (Mendes and Philippi, 2005), derived experimentally. There are simplified numerical models adopted in building simulation however, which do not take this

interdependency into account, and therefore do not accurately represent the transient effect of the materials moisture buffering capacity.

This static representation of hygrothermal conditions is also encountered during the experimental process, where steady state and isothermal conditions are applied to determine the sorption isotherm and the moisture permeability of a material. Given the non-linear nature of material properties, uncertainty arising in measured data produced under these conditions will be transferred into the simulation tools that adopt the derived properties and apply them to model dynamic conditions. This raises the issue of the reliability of simulation predictions. Compromises also have to be made between the accuracy of a modelling outcome and the complexity of the system it is modelling. This involves making simplifying assumptions, as is the case for modelling heat and moisture transfer conditions at the interfacial region. These conditions are highly coupled with the process of drying, which has been referred to already in the context of domestic clothes drying and highlighted the extent to which this process may contribute to reducing the indoor air quality. Absence of the drying process associated with this practice therefore, would mean the indoor hygrothermal environment is not being modelled adequately. Furthering the modelling of material components and the moisture production processes described will require verifying and developing the moisture modelling capabilities of whole building simulation tools.

1.4 Research objectives and methodology

Significant effort continues to be made in addressing heat and mass transfer modelling deficiencies existing within whole building simulation tools. An initial modelling verification study presented in Chapter 5 will highlight the range of results produced using different modelling tools when modelling the same test cases, and hence the challenge that remains in improving the accuracy of heat and moisture transfer modelling. Review of the available literature in this field has helped to identify the uncertainty surrounding material moisture properties derived experimentally and hence the consequential impact this might have on modelling of the moisture transfer process in porous building materials, a topic presented in Chapter 3. Additionally, the incorporation of simplifying assumptions for surface transfer phenomena and the use of empirical correlations to represent coupled heat and moisture transfer processes remains an area under development. Literature presented in Chapter 4 also highlights the complexity of the transfer processes taking place at the interfacial region, and the common use of the heat and mass transfer analogy to overcome this, despite being derived under different hygrothermal boundary conditions. The need to advance the modelling of this boundary layer problem is critical in determining accurate characterisation and quantification of combined heat and moisture transfer processes such as drying. The aim of this research therefore is to advance the modelling of indoor

moisture transfer processes, in light of the existing issues described above, within the context of dynamic whole building simulation.

The following objectives have been identified in order to achieve this:

- accurately model the impact of the moisture buffering behaviour associated with hygroscopic porous building materials in the building envelope.
- develop the representation of surface evaporation from indoor moisture sources.

These objectives will be realised by using the moisture modelling framework found in the integrated whole building simulation tool ESP-r, which is widely used in the field of building science. The steps taken to deliver these objectives include an initial verification of the existing moisture transfer model employed in ESP-r. This will involve conducting a series of simulation test cases varying in complexity, in order to compare ESP-r predictions with analytical solutions and numerical results produced by other building simulation tools. Following this, the ESP-r model will be applied to simulate the impact of a range of building parameters, including hygroscopic building materials and the air exchange rate, on the indoor relative humidity conditions to help identify the factors displaying significant influence under realistic climatic conditions. Furthermore, empirical verification studies will be conducted to assess the modelling capabilities of ESP-r's moisture transfer model, to address the issue of reliability when applying standard material moisture properties to model the hygrothermal response to dynamic indoor climate conditions; and modelling of the passive indoor drying process of porous materials, in particular laundry items.

ESP-r provides a platform from which to model a range of building parameters and hygrothermal processes including occupancy and its associated heat and moisture gains; natural and mechanical means of ventilation; convective heat and mass transfer processes; the outdoor hygrothermal climate conditions, which have been described in section 1.1. The ability to model the interdependencies existing between the building parameters mentioned in section 1.2, during whole building performance analysis, is an added advantage of this modelling approach.

ESP-r is capable of modelling the moisture buffering effect associated with hygroscopic, porous building material, enabling the verification, development and expansion of the range of available material moisture properties in ESP-r. This will address the issues raised in section 1.3 of furthering the accurate modelling of hygrothermal material performance. The surface evaporation model in ESP-r will be developed to treat the specific process of clothes drying more accurately. The developed model will incorporate an initial moisture content of the item being modelled and different evaporation rate calculations to address the issue of surface boundary conditions raised in section 1.3.

The use of simplified numerical models to determine the moisture buffering potential of building materials is reviewed in Chapter 2, highlighting the aspects of these approaches that do not enable dynamic hygrothermal modelling of material moisture performance. This chapter also includes a more in-depth review of the factors influencing the moisture buffering performance of materials, including a sub-section on materials. The range of properties derived for use in the quantification of material moisture performance is presented in Chapter 3, in the process identifying those that are applied in ESP-r. This includes a review of the measurement procedures adopted in the building sector and by the building physics community; and emphasis will be on their associated drawbacks.

The development of numerical modelling of hygrothermal processes in the building environment is given in Chapter 4. A review of ESP-r's integrated moisture modelling methodology will be given, including the treatment of convective surface transfer properties and their significance in modelling the drying process.

The initial verification cases conducted to assess ESP-r's current moisture modelling capabilities are presented in Chapter 5, which is followed by an overview of a study applying the current moisture transfer solver in ESP-r to model and assess the influence of multiple building parameters, including airtightness, moisture loading, insulation and outdoor climate conditions on moisture buffering. Further empirical verification studies are then presented. Firstly, the assessment of using standard material moisture properties to model the hygrothermal material response to dynamic moisture loading conditions is given. The second study focused on the modelling of a clothes drying experiment. Chapter 6 presents the development work that was undertaken to improve the modelling capability of the simulation tool in response to the findings produced from the verification work presented in the previous chapter. Finally, in Chapter 7 conclusions are drawn and recommendations for future work are made.

Moisture buffering and performance analysis

Chapter Overview

This chapter sets out evidence for the impact of hygroscopic material on internal relative humidity and discusses the techniques used to quantitatively and qualitatively analyse moisture buffering performance. It highlights the importance of understanding the role that moisture buffering effects have in helping to passively control the indoor air humidity experienced under dynamic indoor environmental conditions. The transfer of this knowledge into whole building simulation is discussed.

2.0 Introduction

Issues surrounding IAQ, particularly the on-going effort to reduce energy consumption in housing and the potential hazards associated with poor moisture management, have been explored in Chapter 1. The issue of moisture management has become critical in furthering the service life of buildings. This is as a result of excessive indoor moisture generation rates, which are mainly due to the presence of occupants and their indoor activities. The ability to evaluate available means of indoor moisture moderation in the indoor building environment is a key topic covered in this chapter, with the main focus being on the role hygroscopic building materials play in helping to control the indoor air moisture content. A review of the key design features of the building envelope is presented with regard to the incorporation of moisture buffering material, covering areas such as the location of the material, the quantity and material type.

Evidence in Chapter 1 suggested that all three issues (IAQ, energy consumption and moisture management) should be assessed as part of an integrated whole building modelling approach in order to predict the resulting indoor building environment conditions. This would entail an integrated analysis of the coupled nature of the various HAM (heat, air and moisture) processes taking place around the building. The interaction between the indoor air and the building envelope however, is ignored or lacks comprehensive analysis in most moisture models (Tariku et al, 2010). This is despite the fact that approximately one third of the moisture generated inside a room may be absorbed by moisture buffering materials. A percentage of this stored moisture will, at some stage, be released back into the indoor air, thus adding to the air moisture content. This complex behaviour necessitates a moisture analysis model that determines the combined effect of these dynamic processes.

An overview of the qualitative and quantitative techniques developed for building material moisture performance analysis is presented in sections 2.1 and 2.2, highlighting the associated drawbacks of each method when considering their application to a whole building HAM transfer scenarios. Section 2.3 will review a number of factors influencing the hygrothermal performance of porous building materials and hence the impact on their moisture buffering capacity. Finally, section 2.4 will provide a summary of the information that has been presented in this chapter.

2.1 Analysing Moisture Buffering Performance

2.1.1 Qualitative Analysis

The moisture buffering potential can be classified into three distinct categories. These are shown in the figure below.

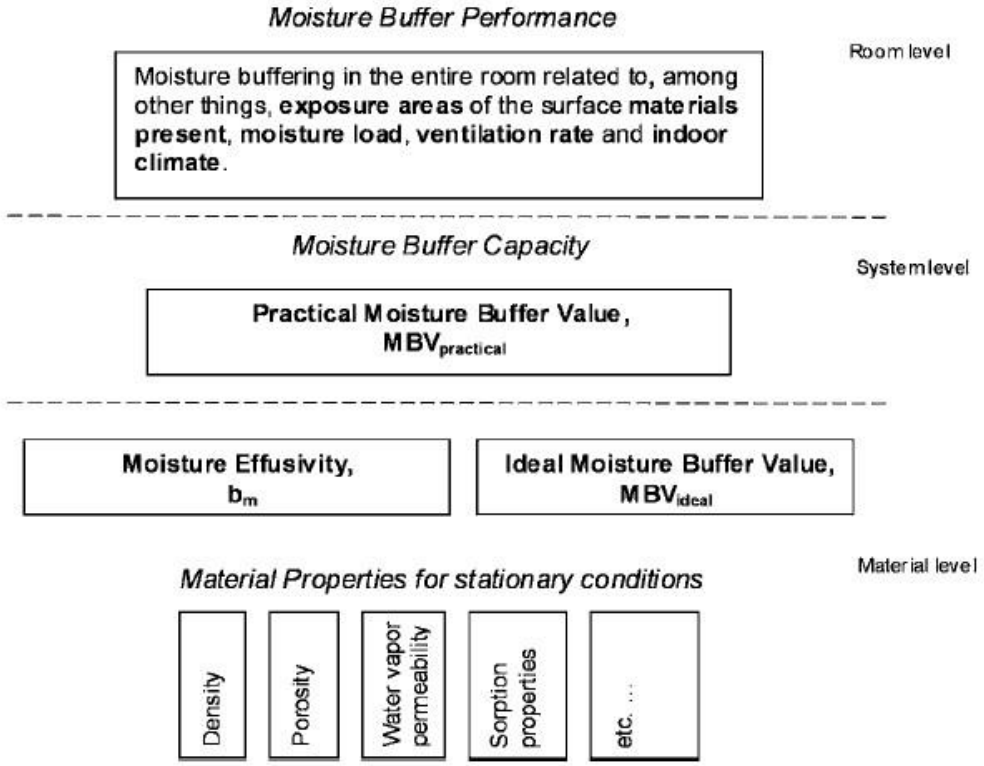

Figure 2.0 Moisture Buffering phenomena divided into three specific levels (Svennberg, 2006).

The first category is identified as 'material level' characterisation, which involves developing standard properties for the material such as density, porosity, moisture permeability and functions representing sorption behaviour. Additional methodologies that have recently been developed to characterise the moisture buffering potential of individual finishing materials found in furnishings and different material combinations in the building enclosure, such as the Moisture Effusivity (Rode et al, 2007), which describes the rate of moisture transfer across the surface of a material when the surface relative humidity changes, are also included in this level. The second category labelled 'system level', represents the moisture buffering performance of a single material or combination derived using an experimental approach, in the form of a single practical Moisture Buffer Value ($MBV_{practical}$) ($g/m^2.\%RH$). This form of single element material characterisation provides a quick and simple method of comparing the moisture buffering performance of individual materials. The final category called 'room level', enables an assessment of the combined moisture buffering potential of a room that accounts for the total number of hygroscopic elements found within that space (Li Y et al, 2012). The protocol used to measure the moisture buffering potential together with the relevant methods required for superimposing these schemes into the building domain, will be described in section 2.2.4.

2.1.2 Quantitative Analysis

Quantitative characterisation is an invaluable practice to undertake given the emphasis is on calculating the transient and dynamic heat and mass transfer processes occurring simultaneously at the surfaces of all hygroscopic elements found in the enclosure. Several other physical phenomena should be noted when analysing the migration of moisture both at an exposed surface and within the material itself. Some of these include the time duration and intensity of moisture cycles, surface transfer coefficients, material structure and the material thickness, fundamental parameters in several of the moisture buffering characterisation schemes developed (Janssen H and Roels S, 2009).

2.2 Characterisation techniques

Three of the most widely acknowledged methods used to determine the moisture buffering performance of a building enclosure are the Effective Moisture Penetration Depth (EMPD), the Effective Capacitance (EC) model and more recently the Moisture Buffer Value (MBV) concept, an assessment protocol developed during the Nordtest project (Rode et al, 2005).

2.2.1 Effective Moisture Penetration Depth (EMPD) model

The Effective Moisture Penetration Depth model (EMPD) characterises the hygrothermal performance of moisture buffering materials based on the effective moisture penetration depth calculation, where only the surface finishes that provide any form of moisture buffering potential are included when calculating the total hygric inertia of a room enclosure. It is defined as the distance from the material surface to the point where the amplitude and phase response for the effective cyclic moisture concentration, located in the active layer at the effective depth, is 1% of the surface vapour pressure (Yang X et al, 2012).

The key assumption made in this method is that the moisture buffering only takes place within a thin layer of the exposed surface. The effective moisture penetration depth calculation, applied in this model, requires a comprehensive collection of material properties to represent the multi-material components and finishes found within the enclosure. These include the vapour permeability and moisture capacity that, once calculated, are assumed constant, independent of fluctuations in the relative humidity. In reality, the relative humidity of the indoor air will vary between low levels of humidity ≈30%RH, up to humidity levels in excess of 80%RH. However, the lack of interdependency between relative humidity and the relevant moisture properties used in this model has not prevented reasonable agreement from being achieved between calculated and measured results in some studies (Steeman H J et al, 2009). The equations used to calculate the resulting buffering effect are shown below:

$$d_b = a \cdot d_p = a\sqrt{\frac{t_p \cdot \delta_v \cdot p_{v,sat}(T_b)}{\rho \cdot \xi}}$$

Equation (2.0)

The term d_b (m) is the resultant thickness of the active buffering layer. The d_p is the effective moisture penetration depth, which relates to the active buffering layer by using a correction factor a (-). This factor accounts for the possibility that the actual layer thickness might be smaller than the effective moisture penetration depth (Janssen H and Roels S, 2009). The d_b term can then be substituted into the equation below that calculates the resulting moisture exchange between the indoor air and the room enclosure.

$$G_{buf} = A.\frac{p_{vi} - p_{vb}}{\frac{1}{\beta} + \frac{d_b}{2\delta_v}} \quad A \cdot \frac{d_b \cdot \rho \cdot \xi \cdot p_{vb}}{t \cdot p_{v,sat}(T_b)}$$

Equation (2.1)

The units for the remainder of the parameters presented in Equation (2.0) and Equation (2.1) are as follows:

G_{buf} = moisture exchange rate between room air and moisture buffering layer (kg/s)
A = Area of exposed surface area (m^2)
β = convective mass transfer coefficient (s/m)
δ_v= vapour permeability (s) t_p = time
period (s) δ_v= vapour permeability (s) $p_{v,sat}$
= saturated vapour pressure (Pa) p_{vi} =
vapour pressure of indoor air (Pa) p_{vb} =
vapour pressure in buffering layer (Pa)
T_b = temperature in the moisture buffering layer (K)
ξ = moisture capacity of the moisture buffering layer (kg/m^3)

A lumped modelling approach is assumed when solving the moisture exchange between the material surface and the adjacent indoor air environment, by identifying key physical processes taking place and simplifying them due to their inherent complexity. The moisture diffusion coefficient, D (m^2/s), is assumed constant and the moisture transfer occurs under isothermal conditions.

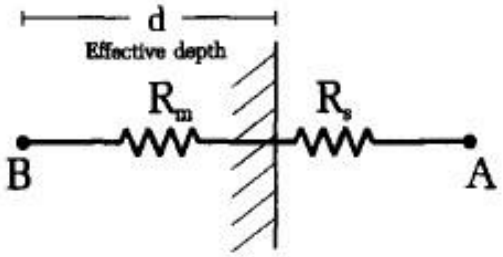

Figure 2.1 One-sided model (Cunningham MJ, 1992).

The total moisture content in the one-sided case, shown in Figure 2.1, is derived from a uniform moisture content distributed across the material to a depth of two times the magnitude of the effective moisture penetration depth. Two nodes, A and B, represent the external moisture content driving force and the lumped moisture content at a depth equal to the effective moisture penetration depth, respectively. The resistance at the surface boundary layer of the material is denoted R_S and the additional resistance provided by the material structure is labelled R_m.

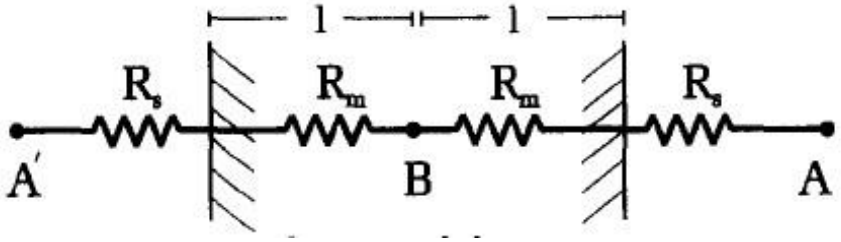

Figure 2.2 Two-sided model (Cunningham MJ, 1992).

Figure 2.2 represents the underlying lumped model for the two sided case, where moisture exchange occurs on both sides of the building envelope. The moisture content is derived as a lumped value distributed across the entire thickness (*2l*) of the material structure, where two combined resistances in series (R_m + R_s) obstruct the flow of moisture between nodes A, A' and through the material (Cunningham M J, 1992).

A serious disadvantage associated with this particular model is the required calculation of the total surface area available for moisture exchange. This is achievable when considering the exposed building envelope surfaces, such as vertical walls and ceilings. However, the situation becomes more complicated when individual elements such as furniture and textiles within the enclosure are included in this calculation. Furthermore, over reliance on the moisture penetration depth is another factor which poses more problems in this methodology. This property can only be calculated using the moisture storage capacity and moisture permeability of the material. Determining values of these two properties is both time consuming, due to the extended periods that

hygroscopic material requires to reach equilibrium, and also labour intensive. However, by allowing the material to reach its equilibrium state, the reliability of the experimental procedure is improved due to potential effects such as hysteresis being accounted for.

Hysteresis is commonly described from an empirical standpoint, using weighted values of the moisture capacity or functions of the absorption and desorption curve (Carmeliet J et al, 2005). These do not have identical functions and form a hysteresis loop. The process refers to the phenomenon that, at the same relative humidity, the material undergoes a different degree of saturation depending on its moisture loading history (Derluyn H et al, 2012). The process is strongly influenced by the physical properties of the material that exist at the microscopic scale, including pore size distribution and total porosity (Kwiatkowski J et al, 2009). For most porous materials, the concentration of moisture stored also depends upon the ambient relative humidity conditions of the environment in contact with the material. Accounting for the transient nature of these conditions is deemed highly important. By disregarding these variations at the boundary level, the accuracy of sorption hysteresis measurements can be reduced by 30-35% (Johannesson B and Janz M, 2009). Several theoretical and analytical models have been developed to analyse the significance of hysteretic phenomena and these are discussed in further detail in Chapter 4.

Nonetheless, the EMPD approach does highlight important factors, including the sensitivity of material performance in relation to changing indoor humidity and boundary conditions. It also highlights the significance of representing the resulting internal moisture transfer behaviour of the hygroscopic building material and at the interface between the indoor air and the building material, through the use of experimentally derived material moisture properties. Drawbacks include the extended time duration of measurement procedures used to derive the necessary material moisture properties and subsequently; the increased computational time required to calculate the moisture transfer rate for each surface; and the uncertainty in calculating the effective moisture penetration depth when considering moisture transfer through multi-layered building envelope construction (Janssen H and Roels S 2009).

2.2.2 Effective Resistance Model

The effective resistance model (ER) provides insight into the amount of resistance that will be experienced during moisture transfer into and out of a porous material (Cunningham M J, 1992). This quantity is essentially the equivalent of the effective moisture penetration depth i.e. the peak moisture concentration at the effective depth will have a corresponding resistance associated with that moisture cycle. Effective resistance is calculated using the following formula:

$$R = \frac{d}{R_S}$$

$$D$$

Equation (2.2)

R = effective Resistance (s/m) d = effective penetration depth (m)

D = diffusion coefficient (m^2/s)

R_s = surface resistance (s/m)

This again is a lumped approximation where the entire moisture content of the hygroscopic material is focused at one point and transfers into and out of the material at the rate allowed by the effective vapour resistance (Cunningham M J, 1988).

2.2.3 Effective Capacitance Model

The effective capacitance (EC) model presumes that the moisture concentration in the active layer of the absorbing material is in equilibrium with the moisture content of the air in contact with its surface (Vereecken E et al, 2009). This is proportional to the hygric inertia of the room enclosure. The resultant moisture buffering capacity calculated for the building envelope material can be added to the whole air mass balance of the enclosure. In a room where the air is well mixed, such that air temperature, humidity and vapour pressure are equal across the entire air volume (a condition presumed in the wide range of building simulation tools), the air mass balance can be calculated using equation 2.3 presented below:

$$\frac{V}{R_v T_i}\frac{\Delta p_{vi}}{\Delta t} = (p_{ve} - p_{vi})\frac{nV}{3600 R_v T_i} - G_{vp} - G_{buf}$$

Equation (2.3)

A second more simplified method is available that characterises the moisture buffering capacity of the building envelope using a multiplication factor M, which is also a qualitative representation of the moisture buffering capacity of the entire room enclosure. This, however, is not accepted as a reliable indicator due to its consideration of the materials moisture capacity only and neglect of other properties such as the vapour permeability (Janssen H and Roels S 2009). The total air mass balance can now be seen in equation 2.4, where the moisture buffering capacity of the enclosure has been substituted using the multiplication factor M.

$$\frac{V}{R_v T_i}\frac{\Delta p_{vi}}{\Delta t} = (p_{ve} - p_{vi})\frac{nV}{3600 R_v T_i} - G_{vp}$$

$$M = \frac{V}{R_v T_i} \cdot \frac{\Delta t}{3600 R_v T_i}$$

Equation (2.4)

where,

V = volume of enclosure (m^3)

R_v = gas constant of water vapour (J/kg.K)

T_i = internal temperature (K) P_{vi} = internal vapour pressure (Pa) t = time (s)

p_{ve} = external vapour pressure (Pa) n = air exchange rate (1/h)

G_{vp} = internal moisture generation rate (kg/s)

G_{buf} = moisture exchange between room air and hygroscopic material (kg/s)

M = multiplication factor for the rooms moisture buffering capacity (-)

2.2.4 Moisture Buffer Value (MBV)

The Moisture Buffer Value (MBV) is used to characterise the hygrothermal performance of hygroscopic materials and was designed as part of the NordTest Project (Rode et al, 2005). It represents the amount of moisture uptake or release in a material when it is exposed to repeated daily variations in relative humidity between two given levels and under constant ambient temperature conditions. The mass of moisture absorbed or desorbed by the material by the exposed surface over the range of humidity levels produces a resultant MBV (kg/m².%RH). Theoretically, it can be equated to the moisture effusivity of the material, a property used to quantify the ability of a half-infinite homogeneous slab to absorb or release moisture due to a surface pressure gradient and the square root of time, in the form of an 'ideal' MBV (MBV_{ideal}). It can be calculated as follows (Woloszyn M and Rode C, 2007):

$$b_m = \sqrt{\frac{p \cdot \delta_0 \cdot \xi}{p_s}}$$

Equation (2.5)

b_m = moisture effusivity (kg/m².Pa.$s^{1/2}$)

δ_p = vapour permeability (kg/m.s.Pa)

ρ_0 = density of solid (kg/m^3)

ξ = moisture capacity (kg/kg)

p_s = saturation water vapour pressure (Pa)

The moisture effusivity however, does not account for fluctuations in the indoor relative humidity conditions, finite surface mass transfer coefficients; fintite thicknesses of multiple materials; and is not designed for multidimensional features (Janssen H and Roels S 2009). The 'idealised' conditions i.e. steady state and isothermal, seldom exist however, and therefore the relationship with the buffering property calculated is only an approximation (Rode et al, 2007).

Two MBV's can be defined. Firstly, a practical MBV ($MBV_{practical}$) is determined experimentally, where a sample specimen is subjected to scheduled block periods of fluctuating environmental conditions inside a climate chamber. The normal case is a periodic exposure of 8 hrs at 75%RH and 16 hrs at 33%RH, the size of this interval being 42%RH. The resultant value is a direct measurement of the mass of moisture released and absorbed by the sample during the exposure time. Secondly, an ideal value can be calculated called the MBV_{ideal}. Fourier analysis enables the surface mass flux to be calculated based on variable surface conditions produced during a period of high humidity followed by a period of low humidity, and with respect to the time that has elapsed. The combined moisture absorbed and released is determined numerically by integrating the mass flux at the surface, as shown in equation 2.6:

$$G(t) = \int_0^t g(t)\,dt = b_m \cdot \delta_p \cdot \frac{\sqrt{t_p}}{h(a)}$$

Equation (2.6)

where h(α) is calculated is follows:

$$h(\alpha) = \frac{2}{\pi} \sum_{n=1}^{0.535} \frac{\sin^2(n\pi\alpha)}{n^{3/2}} \approx 2.252\alpha(1-\alpha)$$

Equation (2.7)

α represents a fraction of the total time period during which the material sample is exposed to a high value of relative humidity. The total $\sqrt{t_p}$ moisture exchange at

the surface is normalised with respect to the humidity variations thus producing the resultant MBV_{ideal}. A proportionality exists between the MBV_{ideal} and the moisture effusivity multiplied by the square root of the time period, as mentioned earlier, which is included in the ideal (MBV_{ideal}) or theoretical definition of the Moisture Buffer Value (Rode C et al, 2007): $G(t)$

$$MBV_{ideal} = \frac{G(t)}{0.00568 \cdot p_s \cdot b_m \cdot \Delta\varphi}$$

Equation (2.8)

G(t) = moisture uptake over the period of moisture flux (kg/m^2)

p_s = saturation water vapour pressure (Pa) b_m = moisture effusivity (kg/m^2.Pa.s$^{1/2}$) t_p = time period (s$^{1/2}$)

$\Delta\varphi$ = change in relative humidity (%)

The difference between the two MBV values is the manner in which the air surface resistance is accounted for. The internal material resistance to moisture transfer is identified as the primary force obstructing the flow of moisture from inside the material to the surface in these methodologies and so assuming the ideal MBV as a reasonable approximation for the practical value would generally be accepted. This, however, has been disproved by studies comparing measured values to calculated ideal MBV's, found to be approximately three times larger than the practical MBV (Abadie M O and Mendonca K C, 2009). The influence of surface conditions plays a far greater part in determining the buffering potential of a hygroscopic material and the negligible effect assumed in this methodology is not entirely reliable. Accepted values for the convective surface mass transfer coefficient and resistance are used, 2.0 x 10^{-8} kg.m^2.s/Pa and 5.0 x 10^7 Pa/kg.m^2.s respectively, in an environment where the ambient air flow velocity is approximated as 0.1 m/s (Rode C et al, 2007).

A case involving a semi-infinite material body subjected to non-symmetrical fluctuations of moisture concentration, with the aim of relating the practical MBV to standard material properties, has not been developed widely. This has meant that adaptation of the method for a whole building simulation, enabling investigation of its performance at room level, remains relatively unexplored (Abadie M O and Mendonca K C, 2009). The MBV provides an efficient method for inter-material comparison based on hygrothermal performance, classifying the resultant moisture behaviour in terms of the concentration of moisture absorbed and released during a cyclic loading scheme. Obtaining MBV's for a larger range of common building materials would also provide further benefit to building practitioners who do not have access to measurement equipment (Goto Y, 2012). However, the static environmental conditions used in the experimental process, from which the MBV is extrapolated, do not reflect the dynamic

conditions the material will be exposed to in a realistic setting i.e. variable occupancy and occupant behaviour and subject to internal climatic changes caused by ventilation. Deficiencies are also highlighted when other material properties are considered, factors such as surface finishes that interfere with the vapour resistance of the material and furthermore, physical phenomena impacting on the overall buffering process, most notably hysteresis (Delgado J M P Q et al, 2006), which should be implicit in the assessment procedure.

2.3 Factors influencing Moisture Buffering performance

2.3.1 Moisture production schemes

In addition to the increased time required to obtain numerous material properties to model the hygrothermal behaviour observed at the fluid-solid interface (Steeman HJ et al, 2009), drawbacks also arise when focus turns onto the duration of the moisture production cycles and the variability of the concentration of moisture produced over the course of the production period. Studies focusing on indoor moisture production schemes, have shown that a correlation exists between moisture loading of the indoor air and material moisture buffering performance. Long duration and high intensity schemes result in increased rates of absorption in hygroscopic materials. Specific investigations, looking into the moisture behaviour of wood panelling, produced results highlighting an increase in moisture absorption during an 8hr period of moisture injection when the rate of moisture injection was increased from 42 g/h to 58 g/h (Li Y et al, 2012). This difference was observed under constant temperature and ventilation conditions, with the latter being monitored further during a sensitivity analysis to assess the combined effect of varying moisture generation regimes and ventilation rates. The table below presents a range of moisture related activities observed in the indoor environment with their associated moisture release rates and total moisture released.

Source		**Release**
Humans	light activity (g/h)	30-60
	Medium activity (g/h)	120-200
	Hard work (g/h)	200-300
Bathroom	Bath (15 min, g)	60

Shower (15 min, g)		660
Breakfast preparation for 4 people (g)		160 to 270
Lunch preparation for 4 people (g)		250 to 320
Dinner preparation for 4 people (g)		550 to 720
Breakfast dish washing for 4 people (g)		100
Lunch dish washing for 4 people (g)		70
Dinner dish washing for 4 people (g)		310
Simmering pot (diam.=15 cm, 10 min)(g)		60
Boiling pot (diam.=15 cm, 10 min)(g)		260
Potted flowers		5-10
Potted plants		7-15
Drying laundry	Already spin-dried	20-200
	Dripping-wet	100-500
	Non-vented drier	2130 to 2900

Table 2.0 Total moisture and moisture release rates associated with a range of indoor environment activities (Kumaran K and Sanders CH, 2007).

Procedures designed to determine the hygrothermal response of materials exposed to cyclic step change moisture conditions have shown greater accuracy when focusing on long duration moisture productions schemes. This has led to questions being raised over the adequacy of existing moisture generation models in modelling shorter term occupant related moisture release (Emmerich SJ et al, 2002). The use of trial and error to determine moisture generation rates within integrated building heat, air and moisture transfer analysis highlights the need for better representation of indoor moisture related occupant activity within building simulation (Lu X, 2003).

Attempts have been made to develop new methods that determine the moisture buffering potential of materials exposed to shorter moisture production schedules using existing sorption measurement techniques. The proposed MBV_{1h} method does not require additional measurement results or material properties, in contrast to the Effective Moisture Penetration Depth (EMPD) and Effective Capacitance (EC) models; and derives the moisture response potential of the material from the moisture accumulated after the desired moisture production period through the use of the following equation, which also applies a weighing factor:

$$MBV^{*} \square\square\square MBV_{8h} \square(1\square\square)\square MBV_{1h}$$

Equation (2.9)

where □□is the weighting factor and MBV* is the production adaptive Moisture Buffer Value (g/m².%RH). The weighting factor is classified using the following time intervals:

- 0h < production interval ≤ 2h: □□= 0
- 2h < production interval ≤ 6h: □□= 0.5
- 6h < production interval ≤ 10h: □□= 1

Simulations adopting this strategy indicate that reasonable agreement can be achieved between measured and predicted values (Janssen H and Roels S, 2009). The figure below illustrates the concept of the production adaptive moisture buffering potential described above. The two curves represent two samples of differing thickness (10cm and 1cm), being exposed to 8hr of high humidity (75%RH) followed by a 16hr period of low humidity (33%RH). The moisture accumulated (kg/m²) by the either material, as indicated by the y-axis, is the product of the change in relative humidity and the MBV of the material i.e. □RH□MBV, over the desired moisture production period. The moisture accumulated over a shorter moisture production period e.g. 1hr, is taken as 1/8 of the moisture absorbed by either of the materials tested over that period. Using this approach requires no additional material moisture properties

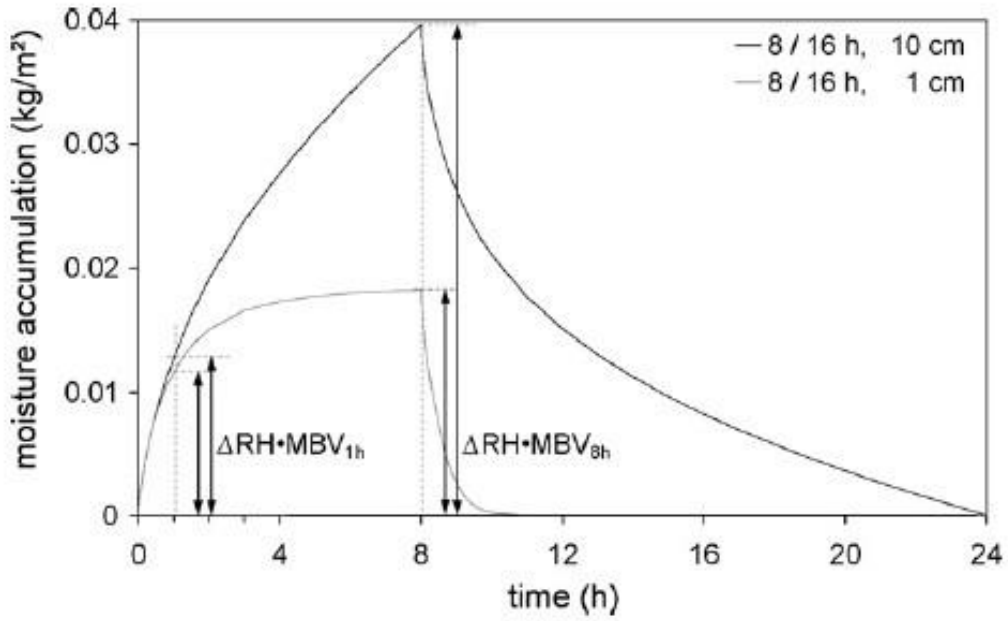

Figure 2.3 Determination of the $MBV_{1h/8h}$ characterisation parameter (Janssen H and Roels S, 2009).

Few studies however, have focused specifically on the relationship between different moisture load profiles and the resulting response of a range of materials. Measurement procedures generally apply idealised moisture conditions when assessing the moisture performance of hygroscopic materials and it is therefore accepted that better representation of realistic moisture production regimes is required if the

agreement between measured and simulated hygrothermal behaviour is to be improved (Janssen H and Roels S, 2009)

Given the varied response times of different hygroscopic porous materials to indoor air moisture loading conditions, a behaviour primarily governed by the moisture permeability and moisture sorption properties, applying realistic, more dynamic moisture loading cycles during measurement procedures will provide further insight into hygroscopic porous material moisture response characteristics and how to optimise their inherent moisture buffering potential in their application. This type of study was conducted by (Ge H et al, 2014). It investigated the impact of moisture load profiles and the moisture loading history on the moisture buffering performance of different materials. Their analysis involved dividing ten hygroscopic materials into three groups whereby the first group consisted of materials with a high moisture capacity but low moisture permeability e.g. wood panelling and oriented strand board; the second group of materials contained low moisture capacity and a high moisture permeability e.g. uncoated gypsum board; and finally the third set of materials possessed both high moisture capacity and moisture permeability e.g. wood fibre board. The sorption and moisture permeability properties of the selected materials were calculated using the following expressions taken from (Kumaran MK, 2004):

$$w = w_{sat}\left[1-\left(-m\ln(RH)\right)^{n}\right]^{\frac{1-n}{n}}$$

Equation (2.10)

where w_{sat} is the saturation moisture content (kg/m^3); m and n are coefficients taken from regression analysis.

$$\mu = \frac{1}{b}\, a\, e^{c\cdot RH}$$

Equation (2.11)

μ is the vapour diffusion resistance factor and a, b and c are coefficients derived from curve fitting.

The assessment procedure involved exposing each group to both long (10 hr) and short (1-2 hr) moisture generation periods, with a step change from 33%RH up to 75%RH for the daily cycles of long and short moisture loading periods. Results showed that materials in the first and second groups produced similar moisture buffering responses to the long moisture loading periods. Under the shorter moisture production

cycles however, the materials in the first group displayed lower levels of moisture buffering in comparison to the second group, results reflecting the contrast in the moisture permeability of the two sets of materials. The third group produced high moisture buffering potential during both of the generation regimes, due to its high moisture capacity and moisture permeability.

For all ten materials studied, the derived theoretical moisture buffering capacity results showed good agreement with the calculated moisture effusivity values (the rate of moisture transfer over the surface of the material when subjected to changes in relative humidity) under the short duration moisture exposure periods, whereas the correlation between these two parameters decreased when the moisture loading period was increased, which was possibly due to the finite thickness of the materials and thus the penetration depth exceeding the thickness of the material sample used during the test. The relationship between the moisture buffering capacity and the moisture effusivity was derived using idealised conditions during this study, and are described as follows:

1. the thickness of the material sample exceeds the penetration depth resulting from daily relative humidity variation and can therefore be described as semiinfinite.
2. the non-linear nature of the material properties is negligible.
3. resistance to moisture transfer at the material surface is negligible in comparison to the diffusion resistance inherent within the pore structure of the material

These conditions though are rarely reproduced during experimental procedures (Rode C et al, 2007). Therefore the relationship can only approximate the material's response to the relative humidity conditions. The potential for numerical uncertainty was highlighted in results obtained from the study, when comparison of the penetration depth between two of the materials was made. Under realistic conditions, the predicted moisture buffering capacity of an uncoated gypsum board is 40-45% less than that derived under ideal conditions for both the long and short term moisture production periods, whereas this difference is reduced to 10% for a wood panel sample. This difference was mainly due to the thickness of the samples tested being and whether this was less than the penetration depth. For the uncoated gypsum board, a sample thickness of 13mm was used compared to a 1% penetration depth of 103mm (the depth at which the amplitude of the moisture content variation is only 1% of the variation on the material surface (Peuhkuri R et al, 2005); and for the wood panel a sample thickness and effective penetration depth of 18mm and 4.5mm was reported, respectively. It was identified that an inverse relationship existed between the effective penetration depth and the time required for either an equilibrium moisture content to be established in a material

subjected to step-changes in moisture loading conditions or a stable moisture buffering cycle to be reached under cyclic moisture loading across the sample range.

The importance of this particular aspect of the moisture performance of the indoor environment is further highlighted in section 2.3.5 where comparison is made between the moisture accumulation of different materials exposed to long and short term moisture generation schemes; and the influence of their associated moisture transfer properties on the resultant hygrothermal response.

2.3.2 Surface finishes

It is highly common for a surface coating to be applied to an internal surface lining material and numerous surface finish types are applied to the exposed materials lining the interior and exterior walls of building envelopes. These include wallpapers, latex paint, oil surface treatments, acrylic paints, whitewash and almost impermeable enamel paints (Svennberg K, 2006). The paints are composed of pigments, binders and fillers diluted by water. An array of elements, including carbon, aluminium and sodium, are also found in water based paints. The area of hygroscopic material available for moisture absorption is significantly reduced as a result of increased surface resistance, which in turn will impact on its active buffering of indoor humidity (Hameury S, 2005). A study on the effect of the application of paint to hygroscopic materials lining internal walls (acrylic, latex and vinyl) found that the increased vapour resistance produced by the surface coating reduced the materials' buffering potential by as much as 50%, although the majority of this increased resistance was due to the primer applied prior to the paint layer (Ramos N M M et al, 2010). The distribution of the coating onto the material surfaces has also been linked to the performance of hygroscopic material. A 30% reduction in the concentration of binder in the paint in addition to a heterogeneous distribution of pigment and filler across the material surface has been shown to increase the permeability of the coating layer by a factor of 3, as seen in the figure below. Accompanying permeability studies and scanning electron microscopy have produced images showing the increased surface porosity is due to a decrease in the binder concentration (Topcuoglu O et al, 2006).

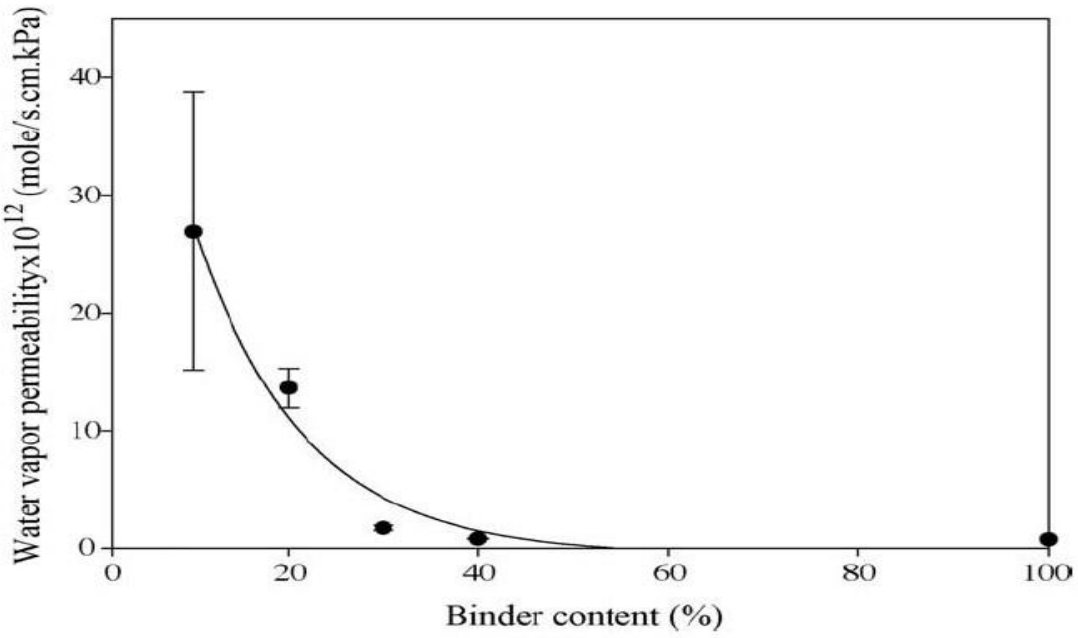

Figure 2.4 Water vapour permeability of paint layer as a function of binder concentration.

2.3.3 Influence of the airflow conditions

It has been shown that indoor relative humidity can be moderated as a result of the air change rate and flow of air over material surfaces. Natural air infiltration as a result of poor air tightness in the building envelope fabric and other air leakage points in indoor spaces can result with an energy penalty. This is due to the increased demand placed on space heating and adequate mechanical ventilation when being operated to maintain comfortable indoor environmental conditions. This relationship between building air tightness and energy demand was shown in a study comparing two typical detached houses with varying air change rates and an installed infiltration heat recovery (IHR) system. The case with a typical building leakage rate of 3.9 ac/h for a timber framed construction, showed the infiltration to account for about 15-30% of the total space heating and ventilation demand. A leakier (10 ac/h) building was also studied and produced a corresponding value of between 30-50% of the total demand (Jokisalu J et al, 2009). Solutions to improve building energy performance by accounting for the management of indoor air conditions have been presented in studies such as that by (Woloszyn M et al, 2009). In this particular case, promising outcomes have been achieved using RH sensitive ventilation systems. This involved the monitoring of changes in indoor RH in order to adapt future ventilation rates. Results from their simulations showed that the mean ventilation rate could be reduced by up to 40% during the cold season and generate energy savings of up to 17%. However, during milder climate periods the energy savings were much lower at only 2%, mainly due to the higher moisture content of the outdoor air being brought into the building being modelled.

The detrimental impact associated with the mismanagement of ventilation, poor insulation and inadequate heating regimes has also been observed in homes of lower

income. By limiting heating to occupied spaces only, the combined effect of increased indoor air moisture content produced by occupant activities such as cooking, will increase the likelihood of surface condensation and the deterioration of the building fabric, mould growth and damp over an extended period of time in the colder regions of the indoor building environment (Riffat S B et al, 1989). Instances of mould growth can be seen in the pictures below.

Figure 2.5 Formation of mould as a result of surface condensation (Curtis R, 2007).

Figure 2.6 Swelling and cracking of a non-permeable paint (Curtis R, 2007).

The demand for adequate indoor air management to help balance energy performance and indoor air quality highlights the importance of this building design issue and the significance of adopting a holistic view of the indoor environment.

2.3.4 Location and quantity

It is known that indoor hygroscopic surfaces are capable of absorbing more than a third of airborne moisture (Plathner P et al, 1998). Studies have shown that with the addition of hygroscopic fabrics a greater moisture buffering capacity is achieved in comparison to unfurnished spaces and independent of the ventilation rate. This is down to the increased surface area available for moisture exchange (Yang X et al, 2012). The link between the moisture buffering potential of a room and the location of materials present in its construction is not as clear. One study using a test chamber to measure the effects of various building factors including ventilation rate and material quantity on the air relative humidity, also produced inconclusive results with respect to the location of the hygrothermal materials tested (Yoshino H et al, 2009) When comparing their experimental data to predicted results taken from various building simulation tools, the biggest differences were observed when there was no ventilation and hygroscopic material lined the floor. It was said that due to poor air mixing in the room under the applied airflow conditions, the rise of water vapour to the ceiling of the chamber would make the available moisture buffering effect redundant. It was also noticed that the amount of moisture buffering that took place was more closely related to the quantity of hygroscopic material available as opposed to its location and that the overall buffering effect could be more greatly influenced by moisture distribution in the test chamber, again highlighting the significance of air movement.

2.3.5 Materials

A wide range of materials exhibit the ability to absorb, store and release moisture. The common properties amongst these materials that allow them to facilitate moisture buffering are their inherent moisture permeability and storage capacity. These properties vary under the influence of transient boundary conditions, further necessitating the use of a dynamic analytical methodology. The experimental methodologies used to determine the hygrothermal material properties of individual material samples are discussed in greater depth in Chapter 4.

Studies investigating the moisture buffering performance of wooden panelling, porous wood fibre board and cellulose insulation, have produced results indicating a reduction in peak relative humidity values ranging from 20-35% under the effect of varying levels of ventilation (0.1, 0.5 and 1 ac/h) and warm and humid outdoor conditions (Osanyintola O F and Simonson C J, 2006). The variability in moisture buffering

performance observed between different materials found in building construction, as a result of their hygroscopic properties, has also been brought to the fore in experimental investigations. Another study investigated the moisture response of uncoated gypsum board, which has a low moisture capacity and high vapour permeability (defined by a vapour diffusion resistance factor between 4 and 6) and wood panelling, which possesses a high moisture capacity (44 kg/m^3.%RH) as a result of changes in the ambient relative humidity, and inversely a low vapour permeability (Yang X et al, 2012). Over a 10hr moisture generation period, the uncoated gypsum board absorbed 226g of moisture compared to 236g for the wood panelling, but the amplitude of the response was greater in terms of the depth to which the moisture migrated within the uncoated gypsum board, due to its lower diffusion resistance to moisture transfer. In contrast, the moisture absorbed by the wood panelling was retained in a thinner layer at the exposed surface due to a decrease in vapour permeability. The same materials were also subjected to a 2hr period of humidification, this time resulting in very different responses. In Figure 2.8, case 3 and case 17 highlight the difference in effect of the moisture permeability of these two materials.

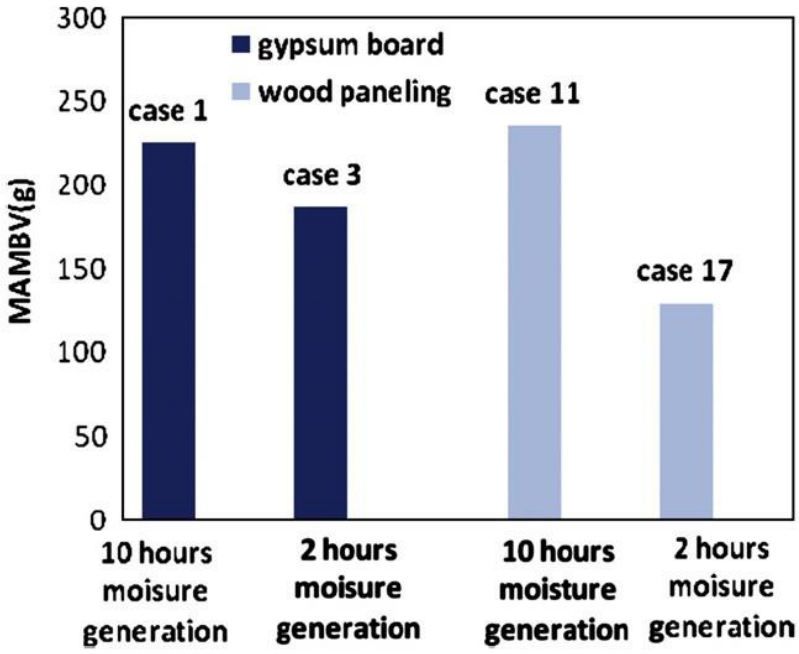

Figure 2.7 Maximum accumulated moisture buffering values (MAMBV) for different moisture generation rates (Yang X et al, 2012).

The higher resistance to moisture transfer associated with the wood panelling explains the lower mass of moisture accumulated during the 2hr period of moisture injection compared to the uncoated gypsum board. The rate of moisture diffusion in wooden construction products has also been linked to their orientation, where in the transverse direction moisture penetration over daily humidity cycles was recorded in the order of

1mm (Padfield T, 1998). The depth to which moisture will penetrate the porous structure of a hygroscopic material, referred to as the active thickness, will vary significantly for different materials over periods of varying humidification. This material characteristic has been recognised to have an influence on the overall moisture transfer rate calculated during experimental procedures. Osanyintola OF et al (2006), found it becomes critical to consider the difference in sample thicknesses as well as other variables used in experimentation, such as the moisture production regime, when intercomparison of the moisture buffering performance of sample materials taken from different testing facilities is conducted. The diagram below shows the relationship between different test sample thicknesses on the moisture buffering capacity of plywood with respect to a range of surface convective heat transfer coefficients.

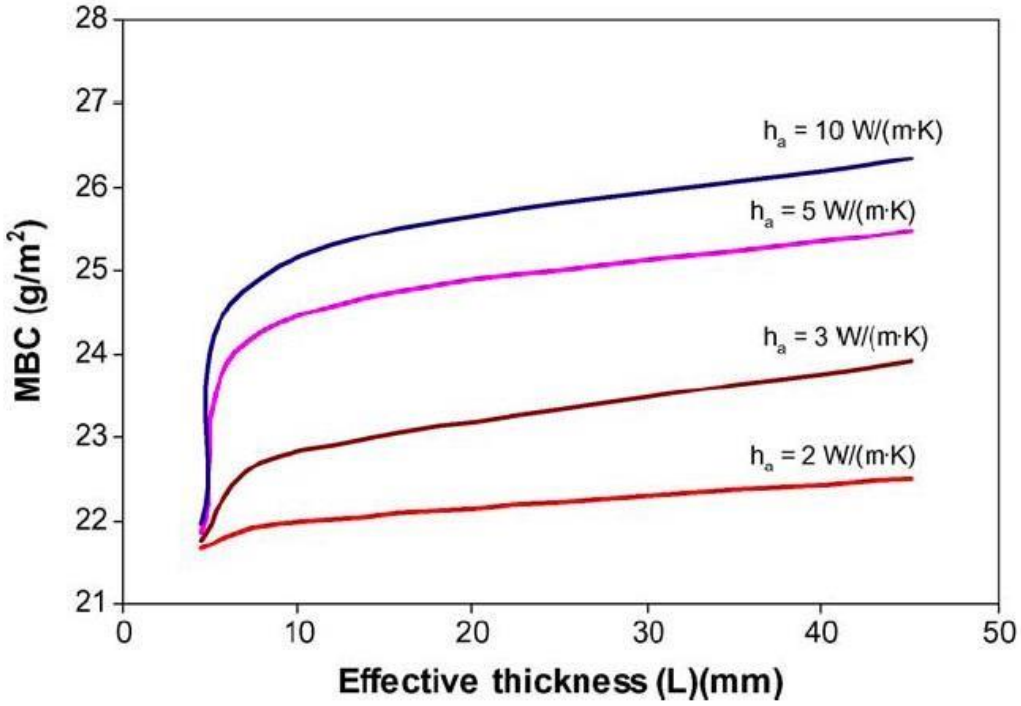

Figure 2.8 Effect of the effective penetration depth and the surface transfer coefficient on the moisture buffering capacity of spruce plywood (Osanyintola OF et al, 2006).

The positive effect of hygroscopic materials on reducing indoor relative humidity was identified in a further study by (Kunzel H M et al, 2005). A series of simulations were performed on a test building subjected to diurnal fluctuations of internal sensible heat gains and moisture concentrations representing occupied and unoccupied periods. The test room was exposed to an external climate where air temperature ranged between 20 and 40°C and the external relative humidity oscillated between 30 and 100%RH. Intermaterial comparison was made using walls lined with plaster in one room and aluminium lined walls in the adjacent test zone. Throughout the period of simulation, the indoor humidity in the room with plastered walls did not exceed 70%RH whereas the zone lined with a vapour impermeable material experienced humidity levels of 80%RH.

Based on the evidence presented, the fundamental impact of hygroscopic building material can be seen to play a positive role in helping to damp excessive accumulation of moisture in the indoor environment. This outcome highlights the necessity for including quantified assessment of the associated moisture buffering potential in dynamic, whole building HAM transfer, in order to improve the impact of the predicted results in building design practice (Rode C et al, 2004).

2.4 Chapter summary

This chapter has provided insight into the moisture buffering ability inherent in hygroscopic materials found in building construction. It has also highlighted the level of sensitivity that exists between this material characteristic and a range of building parameters. To accurately assess the hygrothermal performance of hygroscopic material lining a room enclosure, the dynamic and interrelated nature of HAM transfer processes taking place between the indoor air and the surface of these materials needs to be addressed, taking into account important factors such as the variable indoor climate conditions, surface transfer parameters and material properties.

The available methods used to assess the hygrothermal behaviour of hygroscopic material, both quantitatively and qualitatively, have been reviewed. The methods looked at include the Effective Moisture Penetration Depth (EMPD) and an equivalent approach called Effective Resistance (ER) model. Significant drawbacks with these approaches have been identified, including the increased computational time required when solving numerically, the extended time needed to measure material moisture properties, and the steady state conditions imposed during these analyses. Omission of key material properties, especially moisture permeability, from the Effective Capacitance (EC) assessment, whereby only the moisture capacity is used to determine the moisture buffering effect of the building envelope material, is also detrimental to result accuracy.

As mentioned above, the simplification of the indoor climate conditions is an aspect that requires further attention. The NordTest protocol described in section 2.2.4, delivers a parameter known as the Moisture Buffer Value (MBV). This material characterisation is determined under constant thermal conditions and cyclical moisture loading conditions, the latter of which is seen as a limitation to this method. Given the evidence that has been presented, the value of using a dynamic, whole building simulation tool is strongly supported.

This approach has therefore been adopted in the work presented in this thesis. The integrated whole building simulation tool ESP-r was used as the platform from which to conduct an investigation into the modelling issues that have been discussed in this chapter. In light of this, the initial step taken in this work was to carry out a verification of the moisture modelling domain implemented in ESP-r. This was done in order to ascertain the current capabilities of the tool, with respect to combined heat and moisture transfer modelling, and thus to identify the modelling areas requiring further development. A set of verification exercises is presented in Chapter 5 which addressed the research objectives set out, especially the suitability of hygrothermal material properties when used to model dynamic indoor moisture conditions.

The subject of moisture property data, as implemented in moisture modelling approaches, will now form the focus of the following chapter. Detail will be given

regarding the experimental techniques available to measure the hygrothermal material response.

Moisture Property Data

Chapter Overview

There is growing need for accurate and reliable representation of moisture transfer characteristics in porous building materials, fuelled by the increasing awareness and focus surrounding the impact of moisture in the indoor building environment. This chapter introduces the moisture transfer measurement procedures used by both the building sector and the field of building science and explores why there is uncertainty about the characterisation of how materials respond to the hygrothermal conditions to which they are exposed. An assessment of the suitability of applying the derived forms of material property data in building simulation tools is then offered.

3.0 Introduction

This chapter introduces the measurement techniques used to monitor the behaviour of moisture in building materials and provides an overview of common material moisture property data derived from measurement procedures. Sections 3.1 and 3.2 include overviews of the various data measurement procedures used by the professional building sector and by the building science research community, highlighting the benefits and disadvantages of these methods. From the data acquisition methods described in the previous two sections, section 3.3 covers the topic of hygrothermal material properties, focusing on how these are derived and on the analytical expressions used to represent the monitored moisture behaviour. At the end of this section, a discussion on the applicability of these derived properties in combined heat, air and mass transfer modelling is presented. The existing moisture transfer functions currently used in the dynamic building simulation software ESP-r are also identified. In section 3.4, an evaluation of the quality and reliability of the measurement procedures described earlier on in this chapter is given. The focus of this section is to describe the boundary conditions used during measurement tests and how the fundamental heat, air and mass transfer processes are accounted for when deciding on the driving potential activating moisture transfer. This final point is particularly important when considering the number of physical variables that are to be included in a dynamic computer simulation.

Predicting the migration of moisture through a porous material is a difficult process, as was discussed in Chapter 2. One of the factors impeding progress in this area is the unreliability of the empirical data used to determine analytical expressions that represent the materials hygrothermal behaviour. Underlying issues such as the complexity of experimental arrangement and repeatability of measurement techniques influence the accuracy and reliability of the recorded data. As already highlighted in Chapter 2, the slow speed of moisture transport in porous media, necessitating long experimental periods, also raises concerns over measurement accuracy (Galbraith et al, 1998).

As was described in Chapter 2, quantitative analysis methods for predicting the migration of moisture through a porous material require the use of material moisture transfer properties. As modelling of moisture migration in the building environment has developed as a key component of whole building computer simulation, so demand for moisture property data has grown rapidly. This form of analysis provides a malleable platform for developing a realistic impression of the buildings hygrothermal behaviour, taking into account the influence of multiple parameters simultaneously. Continued advancement of modelling algorithms which predict the combined effect of heat, air and mass transfer in hygroscopic building material requires the incorporation of appropriate

material property data, which will account for transient and fluctuating hygrothermal material behaviour. Applying this improved data to simulation software will help in designing building environments with consideration being given to risks related to moisture, such as interstitial condensation and poor indoor air quality. This will also help to diagnose the nature and origin of building defects that may be encountered during the service life of buildings.

There is a need for obtaining material data from measurement procedures that take into account a number of environmental conditions and features observed in and around the building environment. Some of these features include:

- non-isothermal conditions
- surface transfer phenomena
- increased selection of materials used for furnishings and textiles
- transmission of moisture from sources and emission processes
- a wider range of driving forces, such as wind
- liquid transfer

By incorporating these building phenomena into the measurement procedure, users of the resultant data will have an improved knowledge of its origin and hence be better informed if the data is to be applied in a building simulation environment.

3.1 Moisture Property measurement

The method used to obtain material moisture property data will vary depending on the application and the level of accuracy required. At present the development in moisture content measurement techniques has been mainly in the field of soil science (Stafford J V, 1988). Applying the measuring equipment and approaches developed in this field for use in the building environment will be beneficial for both building professionals and building scientists.

3.1.1 Techniques used in the building profession

In the building sector, being able to measure the moisture content of building material in situ can significantly aid the process of building surveying of specific building attributes, short to long term monitoring, inspecting material integrity and supplying damage limitation solutions (Philipson M C et al, 2007). To this end, measurement methods employed by the building sector should provide reliable results, be time effective and relatively simple to perform on site. Some of the frequently used techniques for on=site moisture measurement are shown in Table 3.0 on the following page, accompanied by comments on the associated advantages and disadvantages of each technique.

		Comments	
Technique	*Intervention needed*		
Drilling techniques	Requires hole to be drilled for each measurement		
Electrical techniques	Non-destructive, usually surface contact only		
Proxy materials	Can be destructive (cores used) or nondestructive (materials placed in surface contact).		
Environmental monitoring	Non-destructive		
Thermographic imaging	Non-destructive		
Type of measurement			
Absolute moisture content measurements possible; Can measure profiles			
Measures surface (or near surface conditions); Rapid measurements possible. Relative moisture content measurements only, unless calibrated.			
Allows monitoring of long term trends of the relative moisture content; Instant readings are not possible; Measurement limited to point of contact between proxy material and substrate.			
		Allows monitoring of long term trends in relative surface moisture content; Instant readings are not possible	
		Allows measurement of surface characteristics to identify extent of moisture problems. Evaluation of moisture content not possible.	
		Time consuming; Not suitable for monitoring; Allows chemical analysis	
		Contact problems with some materials; Presence of salts, metallic or magnetic materials near measurement point can cause error.	

Unsuitable for monitoring rapidly fluctuating materials; Sampling material can deteriorate; Minimal equipment needed between readings.	Absolute moisture content measurements only possible with complex calibration. Requires experience to use and interpret correctly; Requires knowledge of underlying structure for correct interpretation.

Table 3.0: Overview of common field measurements techniques used in commercial building sector (Philipson M C et al, 2007).

Drilling techniques

By drilling into a masonry or cement based wall, a sample of the material can be extracted and its moisture content measured. This measurement is done gravimetrically by recording the sample weight before and after it has been oven dried. Samples can be extracted progressively from different depths, enabling a moisture profile through the building material to be developed.

Alternatively, using a carbide meter can reduce the time required to determine the moisture content of the materials. This involves placing the sample into a sealed container and exposing it to a calcium carbide concentration.

$$CaC_2 + 2H_2O \rightarrow Ca(OH)_2 + C_2H_2$$

The amount of moisture stored in the material will be proportional to the volume of acetylene gas released into the container as a result of the chemical reaction between the moisture and calcium carbide. The rise in pressure inside the container is indicative of the presence of acetylene.

The drawbacks of using a drilling method to extract the material are that:

- heat generated from drilling equipment can influence moisture content
- it is an invasive procedure, which can cause further damage
- the technique does not allow for long term monitoring
- if only a small sample can be obtained, the moisture gradient across the entire structure cannot be accurately represented
- a finely divided sample will have a more rapid rate of moisture loss due to the inverse proportionality between drying and the square root of the sample thickness (Waters E H, 1965)

Electrical measurement procedures

The relationship between the inherent electrical properties of porous material and its stored moisture content enables electrical devices to be used in assessing the stored moisture content. The measurement is made by observing an equivalent change in electrical resistivity, impedance or in the dielectric constant of the material when the measuring device comes into contact with the material, which is then translated into a reading for moisture content. For this method to be effective, it is important that the instrumentation used to measure the moisture content is designed appropriately with significant attention given to electrical material properties.

Potential measurement difficulties linked to this approach include the effect of salt concentrations found in the material. Studies have shown that the resistivity of concrete may vary by 40% due to changes in the salt concentration observed in pores (Wormald & Britch, 1969). This suggests that the electrical property being monitored may be influenced by other factors in addition to moisture fluxes. Furthermore, commercially available devices are generally built and calibrated for one select material, such as timber or concrete. Although comparative measurements can be obtained for other materials, the downside is that the same level of accuracy cannot be expected without further calibration.

Proxy material testing

This form of moisture content measurement requires placing a sample material in hydraulic contact with the building substrate. Over a period of time, the sample will reach hygric equilibrium with the surrounding material. During this time, the sample can be removed periodically and weighed to assess the relative moisture content of the building fabric without the need for excessive data measuring and processing equipment. It is important to select a sampling material that has similar moisture transport properties to that of the building material, in order to compare the performance of the two.

Environmental monitoring

Relative humidity conditions at the surface of a building material can be measured and used to determine the moisture content of the building material through use of its sorption isotherm function. As already described in Chapter 2, this function can be used to calculate the equilibrium moisture content of a material at a given relative humidity. The limitation of this method is that it is only able to give an approximate indication of what the absolute moisture content of the material may be as it does not take into account the internal material phenomena influencing moisture transfer, which is discussed in Chapter 4, thus significantly reducing the reliability of any predictions being made. This procedure may be more effective when monitoring is carried out over an extended time period, where the influence of hysteresis and capillary flow are included.

Thermal techniques

The moisture content present in a porous building material can impact its thermal properties (Ludwig N et al, 2004). In general, most building materials will absorb a small amount of water due to the limited pore space available for water ingress. Where air voids in the pore structure are fully saturated with water, approximately 1020% of the

available pore space (Gayo E et al, 1996), the thermal capacity and conductivity can be increased.

Thermographic imaging can be used to detect variations in material surface temperature using an infrared (IR) scanning device. The results provide an indication of the extent of moisture related damage at the surface of a material, however, an alternative method to evaluate the moisture conditions within the material pore structure is required.

3.1.2 Factors influencing measurement results

The majority of the techniques that have been listed are indirect, meaning the measured output is dependent on a change in the material's moisture content. Interpreting the final measured outcome will therefore require considering additional factors, such as:

- the effect of additional substances present in the material, such as salt, also need to be taken into consideration when analysing the measured data as this may interfere with the accuracy of the procedure.
- the state of the moisture within the pore structure of the material, which can exist as a gas, liquid and solid. The potential for misinterpretation of the measured moisture content arises. The range of techniques available do not all account for this phase variation and therefore discrepancies may arise between the different measuring devices.
- the effective depth at which the measurement is made may be dependent on the test technique being used (Dill M J, 2000).

3.2 Measurement techniques devised for building physics

In contrast to the methods used in the professional building sector, the building research community has striven towards developing whole building computer simulation models in order to analyse the impact of combined heat, air and mass transfer in building materials that do not necessarily require direct field measurement data. Instead, material moisture properties required by this type of analysis are determined using laboratory based testing and then integrated into the whole building model. By using laboratory-based techniques, a higher level of accuracy is expected. This is done through calibration of measuring equipment designed for specific investigations on selected materials and by testing sample materials with known design attributes, such as pore geometry and stated dimension, enabling further study on the effects of porosity and tortuosity on moisture transfer. Another advantage of the laboratory environment is the ability to precondition the material sample, so as to assess moisture behaviour in a material when an initial moisture content is present. This last point can be important when investigating physical phenomena such as hysteresis (Philipson M C et al, 2007).

Some of the widely used measurement techniques are discussed below.

Nuclear Magnetic Resonance (NMR) spectroscopy

This is a direct method of measuring the moisture content of a porous material. The technique is based on the angular momentum induced in positively charged atoms in the material and the resultant magnetic moment produced. Within an external magnetic field of constant strength, the hydrogen nuclei act like dipole magnets. The magnetic moment associated with these atoms produces two proton energy levels that correspond to their orientation with respect to the applied external magnetic field, either in parallel or in opposition. The moment of the dipole magnets is manipulated by adjusting the proton energy levels. This variation in energy is achieved by alternating the magnetic field strength, at right angles to the field. The level of change is proportional to the concentration of hydrogen nuclei in the material, which in this case are found in the form of the water stored in the material. A key benefit of this method is its ability to measure the moisture content present in different states i.e. chemically bound, physically bound and free liquid (Philipson M C et al, 2007). This method can also measure a change in moisture distribution and report on diffusion coefficients (Dill M J, 2000).

TDR – Time domain reflectometry

Significant potential for moisture measurement has been identified in the development of the TDR method. Moisture content measurement carried out using the TDR method is non-destructive and continuous, monitoring the average volumetric moisture content by means of dielectric measurement. During the measurement process, a TDR pulse is guided through a probe inserted in the material. The velocity of this signal is related to the speed of light in a vacuum (constant) and the dielectric constant of the surrounding dielectric media. When a change in electrical impedance is encountered, part of the signal will be reflected back towards the original source. This reflection can be plotted as voltage against time. The time lapse and the magnitude of the reflected signal can be used to determine properties such as the dielectric constant, which is strongly influenced by the moisture content of the surrounding material. The TDR method is particularly sensitive to moisture due to the higher dielectric constant of water compared to typical building materials. The relationship between signal velocity, time, the dielectric constant is expressed using the following equation (Roels S et al, 2004):

$$\sqrt{\varepsilon_a} = \frac{c}{2l(t_2 - t_1)}$$

Equation (3.1)

where ε_a is the dielectric constant (-), c is the velocity of the electromagnetic wave in free space (m/s), l is the length of the inserted probe (m) and t_1 and t_2 are the points of

reflection (s). A mixing law approach has been developed by Tinga et al (Tinga W R et al, 1973) to account for the various moisture phases and physical properties of porous building materials when calculating the dielectric constant. This is shown in the equation below:

$$\varepsilon_a = \left[\theta\varepsilon_w^{\alpha} + (1-\theta)\varepsilon_s^{\alpha} + (\theta - \theta)\varepsilon_a^{\alpha}\right]^{1/\alpha}$$

Equation (3.2)

where θ and θ are the volumetric water content (kg/m^3) and the porosity θ (mm^3/mm^3) respectively, the subscripts w, s and a represent the dielectric constant in the water, solid and air phases and θ refers to a geometry factor accounting for the orientation of the imposed electrical field, calculated using empirically measured data and a least square minimisation technique (Roels S et al, 2004).

The successful application of this method however, is dependent on certain challenges being overcome. Firstly, given that the time period between transmission and reflection of the initial TDR pulse is of the order of nanoseconds, highly accurate measurement of the time lapse is necessary for reliable data to be produced. The difficulty is heightened when applied to building materials that may have a dense structure. Secondly, careful installation of the sensor is key to obtaining optimised results, as air gaps between the sensor and the contact material may interfere with the measuring device.

Dual Probe

The dual probe technique is a measuring approach that has emerged from the field of soil science. There is significant potential for this method to be applied to moisture content measurement in building materials. With knowledge of the volumetric heat capacity of dry soil (θC_p), the moisture content can be determined by monitoring the temperature rise of the soil when an electrical charge is applied to a heating needle positioned in the soil. Applying this method to a building environment scenario requires careful calibration of the dual probe heating needle for the selected material. Proceeding from the principle that the heat capacity of water remains constant at 4187 J/kg.K, the moisture content of a material can be determined using the following relationship:

$$w = \frac{\theta C_p \theta\theta_0 C_0}{4187}$$

Equation (3.3)

where w is the volumetric moisture content (kg/m^3) and ρC_p and $\rho_0 C_0$ are the measured volumetric heat capacities of soil and the dry material respectively, calculated using data output from the probe.

The advantages of this measuring approach are the relative insensitivity it has to the presence of salt in the material and secondly, the ability to accurately measure fluctuations in moisture content even when the volumetric heat capacity of the dry material is not known. However, a number of sources of error exist that require further experimental investigation. Some of these include a lack of sensitivity to the effect of the heat input on moisture migration, fit for purpose probe dimensions, errors in the measured change in temperature (arising from poor contact between probe and material) and the error originating from incorrect assumptions made regarding the homogeneity of the building material being tested (Philipson M C et al, 2007).

Radiation attenuation techniques

Microwave absorption systems require the alignment of a transmitter and receiver on either side of a material sample. A pulse of radiation is then fired at the sample and the level of wave attenuation can be equated to the amount of moisture present in the material. The high frequency of this pulse has the potential to reduce the influence of salt present in the material on the final reading. However, this approach is considered impractical for certain cases where alignment of the transmitter and receiver is not possible.

The same technique can be conducted using gamma-rays, which involves observing the interaction between photons, the solid material matrix and moisture. The attenuation of photon concentrations can be correlated to the moisture content present in the material using Beer's attenuation law (IEA Annex 41, 2008)

The techniques described can provide important insight into the transient nature of moisture transfer in hygroscopic materials along with providing data that is manipulated to determine material properties. This is done through multiple regression analysis that can provide a mathematical interpretation of the data in the form of transport coefficients for a specified material property, as a function of the moisture conditions. The representative equation of the characteristic curve can then be used to predict the behaviour of the material. Some of these properties are discussed in the following section.

3.3 Hygrothermal Material Properties

3.3.1 Moisture Permeability

A common technique used to measure vapour transmission through building materials is the cup test. This technique provides two resultant values for the materials permeability. Firstly, the dry cup method provides the permeance or vapour

permeability of a material sample at an average RH of 25% (with RH ranging between 0 and 50%), whereas the wet cup test can be used to deliver the same properties when the sample is maintained at an average RH of 75% (where RH ranges between 50% and 100%) (Kumaran M K, 1998). The total moisture flow rate, i.e. the combined vapour and liquid flow, which takes place through a material sample for a stated vapour pressure difference across the sample and under isothermal conditions, is measured. Consequently, under these environmental conditions, their application is limited to isothermal cases. Differentiation between the two fluid phases has not been developed for an unsaturated flow measurement technique and so the total moisture flux through the material is measured (Galbraith G H et al, 1998). The total moisture transfer (j_{total}), can be determined by summing the fluxes of the individual moisture phases i.e. vapour (j_v) and liquid (j_l), as shown in the equation below:

$$j_{total} = j_v + j_l$$

Equation (3.4)

where the moisture flux in the vapour phase j_v (kg/m^2.s) is defined using Fick's first law of vapour diffusion that correlates mass flow with a concentration gradient and expresses the rate of transfer per unit area under steady state conditions, as shown in the following formula:

$$j_v = D_e \frac{dC}{dx}$$

Equation (3.5)

In this equation, D_e (m^2/s) represents an effective diffusion coefficient and dC/dx is the solute concentration gradient (usually vapour pressure in the case of vapour diffusion). The effective diffusion coefficient describes the diffusion of vapour through a porous material and is calculated as follows:

$$D_e = \frac{D_m \cdot \cdot}{\cdot}$$

Equation (3.6)

Here, D_m is a molecular diffusion coefficient (m^2/s), ..is the effective porosity, ..is the constrictivity factor that relates the solute diameter to the pore diameter and ..is the tortuosity (-).

The measurement process involves sealing the material to the mouth of an impermeable cup, which is filled with distilled water, a saturated salt solution or a desiccant in order to regulate the internal pressure. The cup is then positioned in an

environmental chamber, where a constant vapour pressure is maintained across the sample. Once equilibrium has been attained, the moisture flow can be determined from the progressive change in cup mass over time. The material's vapour permeability can be calculated using the following equation:

$$j = \frac{\delta_p (p_{vi} - p_{vo})}{l}$$

Equation (3.7)

where j equals the total mass flux through the material (kg/m^2.s), δ_p is the vapour permeability of the sample (kg/m.s.Pa), l equals the thickness of the sample (m) and p_{vi} and p_{vo} equate to the vapour pressures (N/m^2) inside and outside of the cup, respectively.

The resultant vapour permeability is therefore an average value as it is a product of the moisture conditions on either side of the test sample (Galbraith G H et al, 1997). This technique is widely employed although there are differences in the recommended cup design, the vapour pressure regulator used and the environmental chamber conditions (Galbraith G H et al, 1998).

3.3.2 Vapour Permeance

For membranes and composite materials, an analogous property called the vapour permeance can be adopted, utilising the data collected from the cup test method. The equation is shown below: J_v

$$\Lambda_l = \frac{}{A \cdot \Delta p}$$

Equation (3.8)

Vapour permeance is represented by Λ_l (kg/m^2.s.Pa), A is the cross sectional area (m^2) of the sample and Δp (Pa) signifies the pressure difference across the sample. The vapour permeance is defined as the ratio between the density of the vapour flow rate and the magnitude of the vapour pressure difference across two flat parallel bounding surfaces under steady state conditions.

3.3.3 Vapour diffusion resistance factor

The vapour permeability of a material can also be incorporated into an equation that determines the vapour diffusion resistance factor μ (-). The relationship is shown here, where δ_a (kg/m.s.Pa) represents the vapour permeability for stagnant air.

$$\mu = \frac{\delta_a}{}$$

$$\mu_p$$

Equation (3.9)

The variable μ is defined as the ratio between the vapour permeability of stagnant air and that of the material, when subject to identical hygrothermal settings i.e. the same temperature and vapour pressure boundary conditions. Drawing on experimental measurement, the equation below can be used to represent this material property:

$$\phi = \frac{1}{b.\exp(a\phi_c)}$$

Equation (3.10)

where a, b and c are coefficients obtained from regression analysis and ϕ is the relative humidity.

Properties of air are influential factors determining moisture transfer into and out of a material at the surface boundary. One such parameter is the moisture permeability of stagnant air (μ_a), which is used to calculate the vapour diffusion resistance factor discussed above. It can be applied as a constant in building simulation, where a value of the order 10^{-10} has been suggested (Kumaran M K, 1998). ESP-r currently adopts this approach, assigning a value of 1.89923×10^{-10}. Various studies have produced correlation equations for this property (Kumaran M K, 1998), that relate the effect of temperature and pressure on the diffusion coefficient, thus in keeping with the aim of modelling the dynamic nature of moisture transfer. Using Equation 3.11, the coefficient as a function of temperature can be calculated:

$$\mu_a(T) = \frac{D^{aw}(T)}{R_v T}$$

Equation (3.11)

where D_{aw} (m^2/s) is the binary diffusion coefficient of air, R_v (J/kg.K) is the ideal gas constant for water vapour and T (K) is the air temperature. Achieving reasonable experimental results for the vapour permeability of stagnant air is difficult due to experimental complexity and therefore theoretical approaches are applied (Kumaran M K, 1998).

In the building physics community and in many of the European standards, a widely used approach for determining the binary vapour diffusion coefficient of air is the semi-empirical correlation equation derived by Schirmer (Schirmer, 1938, quoted in

Descamps 1996). This equation is as follows and is a function of temperature and pressure:

$$D_{aw} = 2.3 \times 10^{-5} \left(\frac{P_0}{P_L}\right)\left(\frac{T}{273}\right)^{1.81}$$

Equation (3.12)

where 2.3×10^{-5} is the reference value for the diffusion coefficient of vapour in air (m^2/s), P_0 is the standard atmospheric pressure (101,325 Pa), P_L is the ambient pressure (equal to the sum of the atmospheric pressure and the vapour pressure (Eitelberger & Hofstetter, 2011), T is the ambient temperature and 273 represents the standard temperature (K). Several other empirical expressions developed for this property appear in available literature and are shown below:

Sherwood

$$D = \frac{0.926 \times 10^{-3} \left(T^{2.5}\right)}{p_b \left(T - 245\right)}$$

Equation (3.13)

De Vries

$$D = 2.17 \times 10^{-5} \left(\frac{T}{273.15}\right)^{1.88} \left(\frac{101323}{p_b}\right)$$

Equation (3.14)

Krischer

$$D = 2.39 \times 10^{-5} \left(\frac{T}{273.15}\right)^{2.3} \left(\frac{101323}{p_b}\right)$$

Equation (3.15)

where p_b represents the barometric pressure (N/m^2) (Galbraith GH et al, 1997).

Other key variables influencing mass transfer at the boundary layer and necessary for improving the predicted results of hygrothermal performance simulation, include the convective surface transfer coefficient, air velocity and surface roughness.

The importance of these variables will be discussed further in Chapter 4.

3.3.4 Standard vapour diffusion thickness

An alternative property used to quantify the moisture transfer resistance in building materials is the standard vapour diffusion thickness s_d (m). In contrast to the □value, this term is measured as a function of the air layer thickness analogous to the distance moisture will travel within the material. The equation used to calculate this property is shown below:

$$s_d \square\square d$$

Equation (3.16)

where d (m) is the material thickness.

There are several reasons why this metric is preferred to the vapour diffusion resistance factor. These include:

1. the difficulty associated with taking measurements from materials that are inaccessible or have a non-uniform thickness
2. thin composite layers such as vapour barriers
3. layered composite surfaces e.g. masonry work
4. surface damage including cracks and leaks increase the difficulty in defining the vapour transfer potential. In this scenario, the diffusion thickness is referred to as the equivalent diffusion thickness. However, in calculating this redefined property the building material is assumed to be dry at the initial construction stage, whereas in reality the moisture content of the building material will not be zero. This is the result of chemical processes and wind-driven rain, which will result in moisture penetrating the substrate (Hens H S L C, 2007).

3.3.5 Absorption and desorption isotherm functions

As already mentioned in Chapter 2, the moisture content of a porous material will reach an equilibrium based on the conditions the material is exposed to. This relationship can be described by using the sorption isotherm function (or isotherm) for a given hygroscopic material. Figures 3.0 and 3.1 below, display the range of isotherm functions that have been developed for the absorption of various vapours and gases in porous material and the stages of moisture transfer in relation to relative humidity, respectively. The isotherm function can be used to express both the absorptive and desorptive processes that occur.

In the case of absorption, the procedure adopted to determine the behaviour of the hygroscopic material involves using a dry sample specimen. Under isothermal

conditions, the dried specimen is placed in a series of test environments where the relative humidity is increased incrementally. The sample is weighed once it has reached an equilibrium mass under the specified moisture conditions. This equilibrium moisture content can then be calculated and the absorption isotherm plotted. When measuring the desorption process, a sample is conditioned to near enough a completely saturated state (approximately 100% RH). Again under isothermal conditions, the sample is placed in consecutive test environments of decreasing RH levels. Periodic weighing of the sample will eventually indicate when an equilibrium moisture content has been achieved.

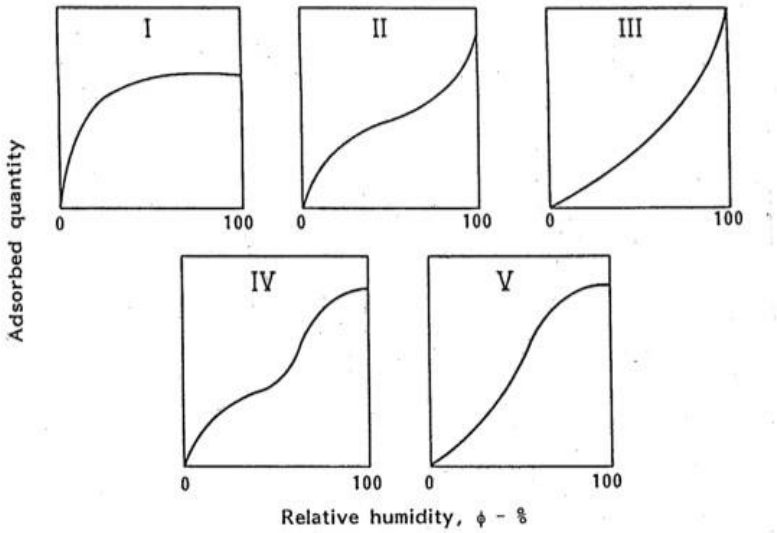

Figure 3.0 Shapes used to represent the sorption isotherm (Hansen K K, 1986).

The first two images in Figure 3.0 represent the most commonly observed forms of the sorption isotherm. An S-shaped curve is almost always produced during monitoring of moisture transfer in porous building material for both the absorption and desorption processes. The different phases of moisture flow observed in a material, which occur as a result of the effects boundary and internal conditions bring about, are presented in Figure 3.1.

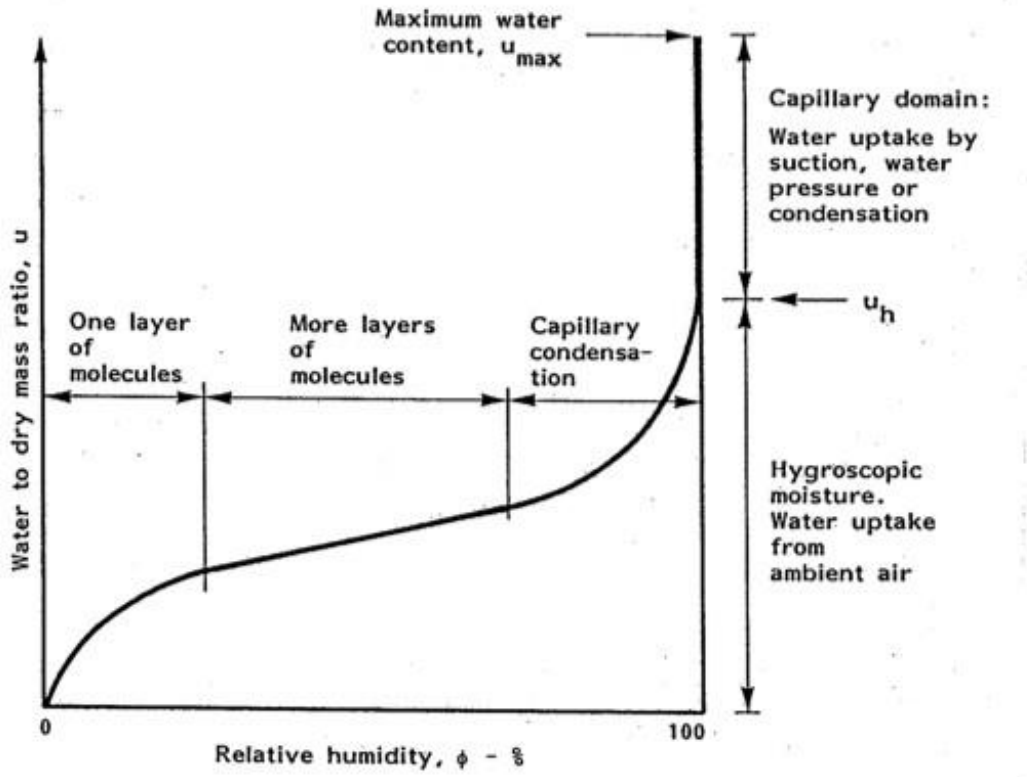

Figure 3.1 Stages of the equilibrium moisture curve in a porous material (Hansen K K, 1986).

The moisture content calculated can be expressed either as a ratio between the condensed mass of moisture and the mass of dry material (u: kg/kg), the mass of moisture per unit volume of dry material (w: kg/m^3) or as the volume of condensed moisture per unit volume of dry material (θ: m^3/m^3) (Trechsel H R, 2001). Although no one equation is universal, there are various mathematical expressions available to calculate the moisture content of a building material (Hens, 2007). Some of these are shown below:

$$\frac{\theta \cdot w}{A_2} \qquad A_2 \cdot \theta \qquad A_3 \quad 0 \cdot \theta \cdot 1 \qquad {}_1\theta \cdot$$

Equation (3.17)

$$u \cdot u_h \cdot 1.0 \cdot \theta^{\frac{1.0}{n}} \qquad 0 \cdot \theta \cdot 1 \qquad \theta \qquad \ln\theta \cdot \theta \qquad A \cdot \theta$$

Equation (3.18)

where A is a material coefficient derived experimentally, n is a fixed empirical exponent and u_h is the maximum hygroscopically bound water by adsorption.

The first of these functions is the BET function that has been developed using the Langmuir theory. It states that the adsorption isotherm can be determined by a series of simultaneous Langmuir adsorption isotherms (shown below) composed of single molecular layers. The second of these equations is known as the Hansen equation and is used in ESP-r's moisture modelling domain (Hansen K K, 1986). In order to apply this equation in ESP-r's moisture solver, the three values for A, n and u_h are required. The specific material coefficients found in the Hansen equation (A and n) can be determined experimentally but will differ in relation to the moisture transfer process taking place i.e. absorption and desorption.

The following is the empirical equation, known as the Langmuir Isotherm:

$$u = \frac{a\,b}{1+b}$$

Equation (3.19)

where a is the moisture content absorbed in one complete monolayer and b is a coefficient proportional to the temperature.

Although the shape of the wetting and drying processes are similar, a higher residual moisture content is observed during the desorption phase in comparison to the absorption process at the same relative humidity due to the hysteresis effect that is described in further detail in Chapter 4. This is a result of the moisture transfer resistance brought about by the pore structure of the material. Similarly, the effect of temperature on the equilibrium moisture content will influence the position and shape of the sorption isotherm. This can be seen at higher temperatures, which will induce higher energy levels in the water molecules and therefore easier movement (Hansen K K, 1986). Modelling this phenomenon in dynamic computer simulation is still a problematic feature of building physics research as the complete nature of the process has yet to be fully understood (Kwiatkowski J et al, 2009).

The hygrothermal properties that have been discussed here are widely used in building simulation programmes. There are, however, a number of other properties that can be derived empirically and integrated into a moisture modelling environment. These

include moisture diffusivity, water absorption coefficient, heat capacity and thermal conductivity of materials as functions of moisture content and air permeability as a function of total pressure difference across a building material. Therefore, the accuracy and reliability of the measurement procedures are highly important components for the sustained development and improvement of moisture modelling in building simulation software. The effectiveness of experimental procedures and the choice of appropriate driving potentials used to form empirically sourced hygrothermal functions will be covered in the following section.

3.4. Impact of driving potentials on moisture transfer

A central issue in moisture transfer analysis of building construction is the dependable measurement of moisture transport processes taking place within building material and the choice of suitable driving potentials dictating the moisture flow. Some of the driving potentials used to analyse moisture flow, which will be reviewed in Chapter 4, include the concentration of water vapour (ρ_v), vapour pressure (p), temperature (T), capillary pressure (P_c), moisture content by volume (w) and relative humidity (□), although no consensus exists on which of these driving forces is the most appropriate (Peuhkuri R et al, 2008). Several of the experimental procedures used to determine the moisture transfer properties of building material are generally carried out under isothermal conditions, thus neglecting the effect of temperature, but the applied to non-isothermal modelling conditions. This measurement condition is based on the premise that the effect of temperature gradients across a porous building material on the rate of vapour diffusion is negligible, and that vapour pressure is the primary driving force behind vapour diffusion (Baker P H et al, 2009).

In the building physics community, the issue of thermally induced moisture transfer, in particular, is a highly disputed one, with some research suggesting that thermal diffusion does have a significant influence on moisture transfer (Kumaran M K, 1987**)** and other research findings proposing that the effect of temperature is negligible (Galbraith G H et al, 2008). The difficulty of measuring non-isothermal moisture transport processes, however, limits the inclusion of properties obtained under this dynamic setting in building simulation models. Further data is necessary to derive additional thermal diffusion properties required by the analytical models i.e. measuring temperature profiles requires installing thermocouples at various points across the sample (potentially interfering with the pore structure). Qin et al proposed a method including a temperature gradient coefficient □ (kg/m^3.K) to determine the moisture flow (Qin et al, 2008). This parameter is the quotient between the thermal diffusion coefficient and the moisture diffusion coefficient, which can be obtained experimentally. Both isothermal and non-isothermal measurements were required, from which vapour

concentration, temperature and vapour flow were measured and calculated, respectively. The mass flux would then be determined using the following calculation:

$$j_v = -\delta_p \nabla p_v = -\delta_p R_v T \nabla \varphi_v - \delta_p R_v \varphi_v \nabla T$$

$$= -D_\varphi \nabla \varphi_v - \delta D_\varphi \nabla T$$

Equation (3.20)

where δ_p is the material vapour permeability, p_v is the vapour pressure (Pa), φ_v is the density of vapour (kg/m^3), R_v is the gas constant for vapour (J/kg.K), D is the diffusion coefficient of vapour (m^2/s) and T is the temperature (K). Calculating this parameter adds further complication to the moisture modelling process by increasing the amount of data and hygrothermal properties required. In contrast, the vapour pressure difference across a material sample is far simpler to determine. This results in a mass flux equation as follows:

$$j_v = j_p = -\delta_p \nabla p_v$$

Equation (3.21)

As is the case in the majority of building applications, the vapour pressure gradient across the building envelope is usually greater than the observed temperature gradient; and is far simpler to determine. Even in circumstances where the temperature difference is considerable, the resultant influence on moisture flow remains negligible, a result indicating inaccuracy arising in the measurement procedure as opposed to an actual thermal effect. This supports the conclusion that thermal diffusion is negligible as the thermal diffusion effect is determined from the ratio between temperature and vapour pressure differences. It can therefore be cautiously assumed that the vapour pressure is the primary driving force behind vapour diffusion in porous material, for both isothermal and non-isothermal conditions (Janssen H, 2011).

3.4.1 Reliability of measurement procedures

During empirical investigation, several variables are measured in order to develop analytical expressions and to derive hygrothermal material properties for application to computer simulation. The range of variables available to study, including temperature, vapour pressure, boundary layer air flow velocity, mass and time, all have associated measurement uncertainties based on the accuracy of the measuring instruments being used and the complexity of the procedure conducted.

The uncertainty level of the measured data obtained will depend upon the instrumentation used. However, the combined effect of the various measurement uncertainties associated with the data used to derive hygrothermal properties, such as vapour permeability, will be far greater e.g. an uncertainty of 28% was observed in an experimental procedure assessing the vapour permeability of aerated concrete (Kumaran M K, 2006). The uncertainty is strongly linked to the structural heterogeneity observed in porous building materials, the lack of transient boundary conditions used during measuring procedures and the limited availability of benchmark cases (Roels S et al, 2010).

The transient conditions mentioned are in the form of diurnal fluctuations of relative humidity in the indoor building environment, which are the result of a number of dynamic convective heat, air and mass transfer processes occurring at different temporal and spatial resolutions. Examples of these include both the sorption processes and convective drying. When assessing the hygrothermal conditions observed at the surface boundary of hygroscopic building materials, several variables influencing these conditions, including the air flow velocity, the reference temperature of the indoor air and that at the boundary layer; and the surface relative humidity are incorporated into studies of the material response during the experimental phase. Studies have shown that there is significant uncertainty arising from standard test procedures used to measure the sorption characteristics of building materials at relative humidity values exceeding 80% RH; and the vapour permeability performance of coated materials (Roels S et al, 2010). Conducting direct comparison of the measured data is difficult to perform due to measurements being taken from different locations in the sample material and at varying time steps. A Boltzmann transformation is applied to quantify the scale of the differences observed between measurement procedures (Roels S et al, 2004). This method involves plotting the moisture content against a □-profile, which is derived using the following expression.

$$\square\square \; xt\square^{1/2}$$

Equation (3.22)

where x is the depth at which the measurement is taken (m) and t is the time elapsed between each data point measured (s). If the Boltzmann conditions are satisfied i.e. a constant boundary condition applied to a semi-infinite homogeneous medium, initially at a uniform moisture content, then the moisture content profiles obtained from each respective measuring technique will lie on a single □-profile (Roels S et al, 2004).

This issue of reliability, when incorporating these empirically derived moisture properties into building simulation, is therefore raised. The extent of the variability in derived moisture properties, even for different samples of the same type of material, is a

common observation when comparison is made between different laboratories. This uncertainty is strongly linked to a lack of benchmark cases; limited use of transient boundary conditions in measurement procedures, including the magnitude and rate of moisture production; and the effect of complex physical structure of porous building materials on moisture transfer processes, which has led to dynamically simplified approaches being used to determine material properties.

3.5 Chapter summary

This chapter has provided an overview of the various measurement techniques used to assess moisture transfer in porous building materials, both in the building profession and the building science research community. It has been shown that a number of empirically derived hygrothermal material properties are available to use in building simulation models, describing various characteristics of tested materials, including their moisture permeability and sorption behaviour. The reliability of the material moisture properties when applied to whole building dynamic simulation tools however, has been brought into question. This is in part as a result of potential inaccuracies arising during experimental procedures, which are consequently carried forward into the numerical calculations by incorporating the derived material moisture properties in the solution. The use of simplified measurement conditions, i.e. long duration moisture exposure schemes and isothermal, steady state conditions, is a standard of material moisture property measurement. This presents an additional drawback in that the transient indoor environmental conditions observed in reality are not replicated in the experimental setting. Applying these hygrothermal material properties to building

simulation models that aim to replicate realistic indoor climatic conditions and hygrothermal material performance therefore, introduces significant uncertainty in the modelling predictions.

As a result of the observations made in this chapter, the verification work presented in Chapter 5 was extended to assess the suitability of the hygrothermal material properties used in ESP-r to model short term, high moisture loading schedules. This involved measuring the rate of moisture uptake and release from two sample materials experimentally and comparing the measured resultant surface moisture flux arising during the applied cyclic moisture loading scheme with the result modelled using ESP-r. The level of agreement between measured and predicted results would help to assess how well the material moisture property data and numerical modelling approach used by the tool were modelling the surface heat and moisture transfer processes.

The following chapter gives an overview of heat, air and moisture transfer modelling within porous media. This includes a review of the physical forces driving moisture transfer, drawing particular focus on material characteristics and surface transfer boundary conditions. A detailed section presents how these processes are represented in moisture modelling theory and hence numerical modelling approaches, and then a review of the moisture modelling methodology adopted in the whole building simulation tool ESP-r is presented.

CHAPTER 4

Modelling Moisture Transfer in Porous Media

Chapter overview

The complexity associated with accurate representation of moisture transfer both in air and within hygroscopic building materials was discussed in the preceding chapter. It highlighted the uncertainties surrounding the accurate measurement and derivation of material moisture properties, and identified the need for an integrated modelling approach when assessing the hygrothermal performance of a building. With this in mind, an overview of the numerical approaches adopting these properties to model HAM transfer processes is provided in this chapter. Additionally, the integrated whole building simulation tool ESP-r, which has provided the platform for the simulation work conducted during the course of this research is explored. The focus is primarily on

the existing integrated and coupled moisture modelling domain. Aspects of the surface transfer phenomena influencing the modelling of the hygrothermal performance of the building material, such as the boundary conditions and the surface transfer coefficients, are examined.

4.0 Introduction

Designing buildings that provide the desired indoor environmental conditions, retain material durability, and meet energy performance standards is a challenge that requires assessment of the combined effect of transient heat and air transfer processes. The response has been the development of numerical modelling methods capable of simulating the range and variability of the indoor hygrothermal environment, with emphasis on spatial and temporal variations observed during HAM (Heat, Air and Moisture) transfer processes. Developing a mathematical approach to model these conditions however, requires identification of relevant energy and mass balance equations, selecting appropriate driving forces dictating the moisture transfer, and using appropriate performance characterisation criteria, the latter having been described previously in Chapter 3. Further aspects to consider would include building assembly and material surface details e.g. material fracturing, ageing and the influence of chemical components (Rouchier et al, 2012); and the initial state of the materials before installation (Osanyintola et al, 2006), but these will not be discussed here.

It soon becomes apparent that when the full range of modelling scales and moisture transport processes are considered, a major computational challenge develops. It therefore becomes necessary to apply simplifying assumptions to reduce the level of numerical complexity, by considering the parameters influencing the overall model accuracy (Miller et al, 1998).

In order to overcome the modelling challenge developed in the context of a dynamic moisture transfer assessment, the important parameters to be considered are:

1. indoor air conditions;
2. material moisture transfer properties, including moisture permeability; and
3. surface boundary conditions critical in the analysis of interfacial moisture flow.

The first of these parameters infers the transient effects of moisture brought into the indoor environment through natural infiltration, the indoor moisture generating activities taking place, and the moisture buffering phenomenon associated with moisture absorbent materials. Parameter two listed above is essential in determining the response of building materials exposed to varying temperature and relative humidity conditions and their moisture storage capability. Finally, surface boundary conditions are deemed critical for moisture transfer analysis, both at exposed material surfaces and at contact points between different materials in the building envelope construction, which will include phenomena such as surface evaporation and interstitial condensation, respectively.

4.1 Complexity surrounding Moisture Transfer Modelling

Concerns were raised in Chapter 2 over the material moisture flow assessment methods, including the Effective Moisture Penetration Depth (EMPD), and the Moisture Buffer Value (MBV). These concerns were primarily in relation to their limitations when used to evaluate more complex and dynamic indoor environmental scenarios. Numerous mathematical approaches have been formulated, which interpret the complex and dynamic hygrothermal behaviour of porous material, utilising a number of different driving potentials, material properties and choice of transfer mechanisms (Li et al, 2009). Much of the research carried out in this field still adopts macroscopic scale modelling of the building material, relating thermodynamic forces to moisture fluxes through moisture and temperature dependent transport coefficients (Mendes and Philippi, 2005). Challenges persist in a wide range of modelling areas, meaning a realistic representation of thermal and moisture behaviour patterns remains difficult to replicate. The following subsections present an overview of difficulties underlying this process.

4.1.1 Boundary conditions

The variability observed in indoor air conditions is influenced by heat and moisture exchanges taking place at the point of contact between the building envelope fabric and the indoor air. Accurate representation of conditions at various locations in a building space and over variable time periods, including those at material surfaces and within the material pore structure, are difficult to repeat experimentally. However, these

conditions are deemed highly necessary and important in developing dependable hygrothermal models that provide reliable performance evaluations (Janssen et al, 2007) due to their impact on energy performance and indoor air quality (Singh, 2001). As a result of the transient indoor environmental conditions experienced, monitoring of the materials moisture storage and enthalpic variations would help to provide a more holistic understanding of a materials response when exposed to dynamic boundary conditions. At present, the moisture content of a porous material is calculated using the developed sorption isotherm that does not take into account changes in moisture phase and features of moisture transport occurring at different scales.

4.1.2 Impact of moisture on thermal performance

Research has shown both the influence and neutral effect of temperature on moisture transfer (Janssen 2011). When considering the reverse, namely the impact of moisture content on thermal behaviour, it is generally accepted that building energy models ignore the influence of moisture on thermal transport and capacitance properties of building materials, relevant to the local heating and cooling effects generated within pore spaces in the material structure, due to moisture phase change (Mendes et al, 2003). The resulting enthalpy of the moisture phase change within these spaces however, creates a local heat source (or a sink in the case of surface evaporation); and is either stored or released, during the accumulation (condensation) or drying (evaporation) phases respectively. The *heat pipe* effect created, as a result of moisture transfer, is responsible for increasing the conduction of heat. As already discussed in section 3.1.1, moisture present in the building material pores at the micro-scale is known to increase the associated thermal conductivity of the material, which also results in an increased material heat capacity. For this reason, it is important to implement a thermal conductivity function that accounts for the influence of moisture present in the material at the pore scale (Woloszyn and Rode, 2008).

The approach taken in building energy models reduces the accuracy of predictions by not considering the associated impact on sensible and latent heating loads in the final calculation (Tariku et al 2010). This highlights the specific need for modelling aspects of heat and moisture related phenomena within the pore spaces.

4.1.3 Space Domain discretisation

The complexity of multiphase moisture transfer processes and the inherent heterogeneity of building material composition, together, create a difficult problem requiring solution during accurate simulation of multiphase subsurface transport phenomena. Random pore geometry and pore size in materials and their resulting effect on vapour diffusion and liquid transfer in the building material will influence the amount and rate of moisture distribution within construction materials.

The influence of the spatial discretisation scheme on the resultant accuracy of coupled heat and moisture transfer predictions is widely recognised. Adopting the appropriate gridding approach will depend on the shape of the material domain being modelled and therefore the use of a non-uniform mesh may become necessary. This is frequently the case in building envelope structures where the large variation in size and shape of this environment requires a balancing between the type of gridding approach used and the predictive capability of the model. The non-linear, complex nature of the combined heat and moisture transfer taking place through the material domain and at the surface boundary requires the modelling solution to remain stable throughout the simulation. This has been recognised in validation exercises undertaken to benchmark the influence of thin paint layers (0.1mm) applied to the internal surface of the building envelope. By treating these as additional porous material layers in the construction, inaccuracies between measured and predicted performance have arisen as a result of grid size selection and the implementation of material properties (James et al, 2010). It is therefore preferable to apply the fewest number of nodes in each layer of the building envelope construction, thus reducing the number of gridlines required without detracting from the accuracy level needed for the case being studied; and in doing so decreasing the computational time required to solve the problem (Burch, 1997).

The potential for numerical error also appears when using sets of differential equations as part of the control volume method. This approach calculates material properties and environmental variables and solves by reaching a point of convergence based on preceding and future results. An inherent memory effect develops, as has been detected when applying this procedure, resulting in a cumulative error effect being carried over into proceeding solution time steps. This can strongly influence the level of accuracy achieved by the simulation and supports the need for an appropriate choice of spatial discretisation (Carmeliet, 1992).

Given the variation in the heat and moisture transfer processes occurring at the material surface boundary, the discretisation scheme becomes an increasingly critical component of the numerical modelling solution. The sensitivity of the spatial discretisation scheme to the numerical model, in particular when considering the transfer problem as a coupled process, will increase. This is due to the difference in the rates of heat and moisture transfer processes taking place, both independently and when combined, which may result in different optimal grid sizing being used for each of the phenomena; and in part due to steady state hygrothermal conditions seldom existing at the interface between the air and a porous material. A similar sensitivity arises when dealing with the modelling of heat and moisture transfer at the intersecting points of different materials in the building envelope construction, caused by the introduction of an expansion factor applied within a single material layer, in one direction. This creates a non-symmetrical grid distribution through the material and between different layers

in the construction and may cause significant solution inaccuracies at the point of contact between two different materials that respond differently to the imposed hygrothermal conditions (Galbraith et al, 2001). Four main categories of grid sizing used in whole building modelling approaches are presented in the table below and classified in terms of their application, advantages and limitations:

Granularity	Advantages	Limitations	Applications
Very fine	• detailed representation of Temperature, Concentration and velocity fields • represent stratification, details of thermal bridges and weak points	• detail of geometry required • high computational time required • speed and convergence dependent on solver	• coupled HAM transfer in critical locations • calculating global properties for coarser models e.g. surface coefficients • steady state and dynamic short period conditions
Fine	• good representation of heterogeneous volumes • Computing time	• Requires use of adapted empirical laws for critical points (driving flows for air) • Air zonal modelling with fixed mesh not adapted for transient conditions	• Detailed behaviour of single or group of rooms in dynamic conditions • 2D computations of the building envelope
Intermediate	• relatively fast • representing complex building, with thermally different zones	• Can not represent non-uniformity of air conditions in single zone • Can not represent thermal bridging	Adapted to whole building dynamics, computation of energy and mean indoor climate
Coarse	• Fast • Good estimations of energy use in simple buildings	• Not adapted to complex buildings • Unable to assess conditions within building envelope	Adapted to dynamic simulations of energy and mean indoor climate in simple buildings or in a single zone

Table 4.0 Outline of advantages, limitations and applications of common discretisation schemes (Woloszyn M and Rode C, 2008).

Galbraith et al, (2001) introduced a two-way expansion method in an attempt to improve the accuracy of numerical solutions for heat and mass transfer in a group of porous building materials. Based on the premise that most commonly available simulation models for heat and moisture transfer in the building environment adopt the one-way expansion method, the study was designed to allow comparison between different space

discretisation schemes, in order to determine their effectiveness when aligned with a simulation model implementing the Control Volume Method, which will be discussed later in this chapter. Figure 4.0 below displays the space discretisation schemes selected:

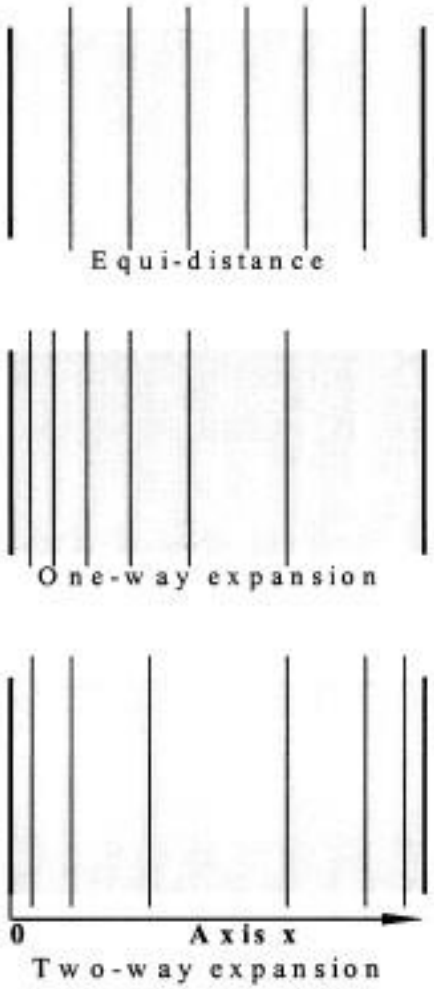

Figure 4.0 Space discretisation schemes (Galbraith et al, 2001).

The results from the study revealed a strong interdependency between the numerical solutions and found the two-way expansion method to produce similar accuracy to that achieved using the finer grid, although this was achieved with a reduction in the number of grid divisions and hence the computation time required. Attention was also drawn to the increased variation and time duration associated with the moisture transport across the samples tested by making comparison to the observed heat transfer process through the tested materials.

The following section describes the moisture transfer processes taking place in porous media and the approaches used to integrate them into building performance analysis.

4.2 Moisture phase and transport processes

Moisture transport processes are referred to as flows of water vapour-air mixtures, liquid and dissolved solids through materials and the building construction (Hens 2007). Moisture found in building materials is either a vapour, liquid or solid (in the form of ice) and depends on the prevailing environmental conditions. The transport processes occur predominantly in the vapour and liquid phases or as a combination of the two. This variability introduces significant difficulty during measurement and modelling of the resultant hygrothermal behaviour. This is partly due to the range of phase interaction that occurs between fluid-fluid and fluid-solid interfaces that are key variables in governing many flow and transport processes (Al-Raoush and Willson, 2005).

In the vapour phase, moisture transport processes are commonly known as water vapour diffusion and effusion (also known as Knudsen diffusion), which traditionally use the vapour pressure as the driving potential. For the liquid phase, the transfer mechanisms are known as capillary suction, Soret effect and surface diffusion (Peuhkuri et al, 2008). These commonly use the pore moisture pressure (capillary suction pressure) as the transfer potential (Belarbi et al, 2008). Table 4.1 below presents the various transfer mechanisms with their associated driving forces.

Vapour Transfer	Gas Diffusion Molecular transport (Effusion) Solution Diffusion Convection	Vapour pressure, temperature, total pressure difference
Liquid Transfer	Capillary conduction Surface diffusion Seepage flow Hydraulic flow Electrokinesis Osmosis	Capillary pressure Relative humidity Gravity Total pressure difference Electrical fields Ion concentration

Table 4.1 Transfer mechanisms and relevant driving forces (Kunzel,1995).

4.2.1 Vapour transport

Convective and diffusive processes are used to classify moisture migration in the vapour phase (De Freitas et al, 1996). The convective moisture transfer is a result of air movement within the material or at its exposed surfaces. The resultant change in vapour concentration is equivalent to the product of the total air flux and concentration of vapour in the gaseous mixture. Quantifying this process is made difficult due to the

nature of the (i) dynamic air flow conditions; (ii) convection taking place; and (iii) variable boundary conditions present at the surface and within the building envelope material (Pedersen, 1990). Point (iii) will be further elaborated upon in Chapter 5, in the context of modelling moisture sources and the effect of surface boundary conditions on moisture transfer.

When considering diffusive processes, Fick's law describes the flow of vapour in still air and can be used to determine the rate of vapour diffusion under isothermal conditions, as shown in the equation below:

$$q_v = -D_v \nabla X$$

Equation (4.0)

where q_v is the mass flux rate of the vapour flow (kg/m².s), D_v is the diffusion coefficient of vapour in air (m²/s) and X is the vapour concentration (kg/m³). The mass flux rate will be proportional to the vapour pressure gradient across the material and its moisture permeability. Further to this, the total flux will be inversely proportional to the thickness of the material.

$$\delta D_v \frac{M q_v}{RT} \nabla P_v$$

Equation (4.1)

M is the molar weight of water (0.018kg/mol), R is the universal gas constant (8.314J/mol.K), T is the temperature and P_v is the vapour pressure (Pa). The rate of diffusion is equated to that in still air by a resistance that corresponds to the volume fraction of air filled open pores (ξ) and a tortuosity factor (a). This is presented in the following expression:

$$\xi a \delta D_v \frac{M q_v}{RT} \nabla P_v$$

Equation (4.2)

The resistance is denoted by the symbol μ, which is equivalent to $1/(\xi a)$. Introducing this factor into the mass flux calculation results in the following function:

$$q_v = \frac{D_v M P_v}{RT}$$

Equation (4.3)

$D_v M$ / RT

The moisture permeability of a material (kg/m.s.Pa) is analogous to , which further alters the final version of the mass flux equation.

Vapour diffusion in porous material has minimal impact on performance when pore diameters are smaller than that of the water vapour particle (measured in the region of 0.27nm). The more pronounced effects are observed when moisture transfer takes place in pores greater than 2nm (Swirska-Perkowska 2011). The types of diffusion that can take place include:

- **Volumetric** – where diffusion takes place in pores with a diameter greater than that of the mean free path of the vapour particles
- **Knudsen effect** – also known as effusion, this form of diffusion occurs in pores relatively small in size and when the mean free path of the vapour particles is still larger than the pore diameter. The rate of mass transfer is dependent on the frequency of collisions between the vapour particles and the pore walls as this occurs more frequently than the collisions between water vapour molecules
- **Superficial** – the result of a thin layer of water vapour particles adsorbed at a pore wall that forms a liquid film. A local equilibrium is achieved between liquid and vapour moisture phases, creating a local concentration gradient that induces a superficial diffusive flux, which can be determined using the following expression:

$$j_s = -D_s \frac{\partial c_s}{\partial}$$

Equation (4.4)

where is equal to the density of the material (kg/m^3), is the material porosity (m^3/m^3), D_s is the superficial diffusion coefficient

(m^2/s) and c_s is the mass concentration of the superficial moisture (kg/kg) (Swirska-Perkowska 2011).

The level of interconnectivity between pore spaces and their size, will determine the available number of sorption sites in a porous medium. The moisture absorption taking place within these sites can consist of multilayer absorption and capillary condensation, with the resulting moisture content a product of the hygrothermal conditions observed in the available sorption locations (Derluyn et al, 2012). At a moisture content less than critical, the potential for a condensate to form decreases (Harmathy, 1969). This means that the possibility of liquid moisture migration due to capillary forces is reduced, if not completely stopped. Beyond this critical point, usually in high humidity environments and in regions where a large temperature gradient exists, condensed moisture accumulates to form wetted regions within a pore that initiates liquid moisture migration across the moisture content gradient created by surface tension forces (Wyrwal and Marynowicz, 2002). At this point, the available sites for vapour diffusion are reduced resulting from a rise in the number of connected liquidfilled pores. A more detailed outline of the liquid transfer process is now described.

4.2.2 Liquid Transport

The transition from low to high relative humidity produces a rapid increase in moisture permeability of a porous material, initiating the formation of capillary condensation and thus leading to liquid moisture migration. This phase can be defined in terms of the pore size and relative humidity, as shown by the Kelvin equation below.

$$\ln(\square) \square\square \frac{2\square\square}{rRT}$$

Equation (4.5)

where $\square$= surface tension of liquid (N/m), $\square\square$= specific volume (m^3/kg), r = radius of capillary (m), R = gas constant of water vapour (J/kg.K) and T = absolute temperature (Galbraith and Mclean RC, 1990). Some of the first moisture models to consider capillary flow effects were developed by Luikov and Philip and De Vries, both of which are described in section 4.5 of this chapter.

Two transport processes are used to define the flow of liquid moisture in a porous material. The first involves liquid transport occurring under the influence of a suction pressure or a force in the capillary region causing infiltration flow. This type of transport takes place across the hygroscopic sorption region until free water saturation is achieved and equilibrium is reached. Once saturation is achieved within the capillary region, supersaturation of the capillaries will follow. Liquid flow in this physical state will

be driven by diffusion under a temperature gradient or by suction forces resulting from external pressures (Chen and Shi 2005). The second mode of liquid transport is by surface diffusion caused by the adsorption and desorption processes.

The Darcy theory for laminar flow in capillary tubes (generally accepted as moisture flow under the effect of suction pressure) relates directly to suction flow in building materials.

$$g_w = -K \frac{\partial P^c}{\partial x}$$

Equation (4.6)

g_w representing the moisture flux (kg/m^2.s) and K equal to the unsaturated hydraulic conductivity (kg/m.s.Pa) of the porous material (which is influenced by temperature as liquid viscosity decreases with rising temperature and the conductivity is inversely proportional to the viscosity). The potential for hydraulic conductivity varies widely as the available pore capacity for transport increases in accordance with the increasing moisture content, signifying the strong relationship between the two variables (Pedersen 1990). The relationship between the hydraulic potential and conductivity can be described using the following expressions.

$$K = K_s \left(\frac{\psi_s}{\psi} \right)^{2.75}$$

Equation (4.7)

where ψ_s is the saturated hydraulic potential (m), ψ is the hydraulic potential and K_s is the saturated hydraulic conductivity (m/s) (Clapp and Hornberger 1978).

In contrast to the aforementioned equation for liquid flux, the following expression can be used to derive the transport of liquid through a capillary network, accounting for the additional effect of gravity on the flow:

$$\overline{q_w} = -D_u \frac{\partial u}{\partial x} - D_{Ph} \frac{\partial \overline{P}_h}{\partial x} + \rho_w g K_{Ph}$$

$$\frac{\partial u}{\partial x}$$

Equation (4.8)

q_w representing the mass flux rate of liquid (kg/m^2.s), $D_{\square}$ is the liquid coefficient (kg/m.s), g is the acceleration due to gravity (m/s^2), $\square_w$ is the density of water (kg/m^3), $\square\square$is the relative humidity and u is the liquid moisture content. Suction forces generally have a much stronger effect than that of gravity on liquid transfer, such that with the exception of almost saturated materials gravity can be neglected (Woloszyn and Rode 2008). The capillary suction pressure P_c (Pa) linked to this type of capillary liquid flow can be calculated using the Laplace equation shown below:

$$P_c \square P_{nw} \square P_w \square \frac{}{2\square \cos\square r}$$

Equation (4.9)

where P_{nw} and P_w are the non-wetting and wetting phase pressures, $\square$ is the surface tension of water (value of 72.75x10^{-3} N/m taken at 20 degrees centigrade), r is the radius of the capillary tube (m) and $\square\square$is the contact or wetting angle (degrees) (Al-Raoush and Willson 2005). This property can be substituted into Kelvin's Law when using the continuum approach to determine capillary suction pressure in isotropic, homogeneous and nondeformable media, as shown in the following expression:

$$\ln(\square) \square \frac{\square\square\square\square\square P_c\square\square\square}{\square\square\square_l R_u T\square\square}$$

Equation (4.10)

where R_u is the gas constant for water vapour (J/kg.K), $\square_l$ is the density of liquid water (kg/m^3),and the temperature T is measured in degrees Kelvin (Carmeliet et al, 1999).

Alternative liquid transport coefficients have been developed in relation to specific moisture transfer potentials. These include the moisture diffusivity D_w (m^2/s), the liquid conduction coefficient D_f (kg/m.s) and as already mentioned, the hydraulic conductivity $K_{\square}$ (m/s). In reality however, the calculated transport coefficient for liquid flow will change very rapidly from one time step to another as the rate of diffusivity varies in relation to moisture content (Karagiozis 2001). Experimental studies have shown the

strong dependency that exists between moisture content and the material moisture transfer properties, the level of capillary saturation and hysteresis effects (Carmeliet et al, 1999). This is where the strong hysteresis phenomena between the uptake and release of moisture have been associated with porous materials comprised of a large pore-size range and complex pore geometry. This issue is discussed further in section 4.5.

4.2.3 Air Transport

Airflow in a building originates from a range of sources. These include the air movement through the building envelope due to the air permeability of certain construction materials; leakage points in the building construction; joints in the building structure; cracks formed in building surfaces adjoined to the external environment; and mechanical ventilation schemes. This passage of air will influence the rate of air movement in the indoor environment, which is also determined by the combination of buoyancy forces in non-isothermal conditions (natural convection) that are dependent on the variability of the air density (a property strongly dependent on moisture content and temperature fluctuations). Additional inter-zonal air pressure differences, induced by wind, fans, or the stack effect, will contribute to the air flow present in the indoor environment (Woloszyn M and Rode C, 2008).

Both temperature and relative humidity distributions within the building envelope construction itself are known to be affected by the rate of air movement, significantly influencing the local hygrothermal conditions (Li et al, 2012). This increases the spatial resolution required in the modelling process. Figure 4.1 below represents the sources of air leakage in a building:

Figure 4.1 Diagram indicating the main air leakage points in a building (d'Ambrosio et al, 2012).

Some of these are considered within whole building HAM simulation. Existing airflow simulation tools modelling both room and whole building scenarios, and CFD (Computational Fluid Dynamics) software, are able to produce reasonable representations of airflow networks between the indoor and external environment. In some cases, the presence of moisture in the airflow is also accounted for through the use of HAM transfer models.

The incorporation of HAM modelling into either BES (Building Energy Simulation) models or CFD tools, depending on the type of application being aimed at, is featuring more widely in building design using simulation. A more detailed analysis of the hygrothermal interaction between the indoor air and the building envelope or indoor objects can be achieved in this manner, bringing about significant advantages, such as 3D representations of the indoor temperature, and surface moisture flux and air velocity distributions at the interfacial region (at the point between air and porous material surfaces) (Van Belleghem, 2011). There is also potential to conduct specific air flow field studies on particular zones and objects within a building using this method. Application of this coupled analysis procedure however, is limited in part due to the excessive computational time required when solving energy, mass and momentum conservation equations for each control volume being simulated; and secondly by the lack of data available for validation purposes (Van Belleghem et al, 2010). To this end, a more general method used in building simulation to solve the overall air mass balance inside a building, including the energy and moisture transfer processes discussed previously, involves analysing the air mass and momentum conservation equations. A basic form of the mass conservation equation, referred to as the continuity equations, calculating the rate of change in the mass of the air, is shown below (Woloszyn M and Rode C, 2008):

$$\frac{dm_{air}}{dt} = \rho_{air,in} R_{in} - \rho_{air,out} R_{out}$$

Equation (4.11)

Here m_{air} is the mass of air (kg), ρ_{air} is the density of air (kg/m^3) and R is the volumetric airflow rate (m^3/s). This form of the conservation equation is applied for both the air and building envelope control volumes being modelled.

It is common practice within a wide range of building simulation tools to calculate this total air mass balance at a single node assuming well-mixed zonal air conditions. A well-mixed air zonal model, using specific assumptions for the boundary conditions and uniform properties for the indoor air, will provide a prediction of the average indoor environmental conditions and hygrothermal performance of the building envelope.

These predictions do not provide an indication of the true nature and extent of hygrothermal interaction between zones or at internal wall surfaces, meaning evaluation of local thermal comfort and risk of moisture related damage to materials is not fully assessed (Steeman et al, 2009).

The sensitive nature of air flow properties and the variable hygrothermal behaviour observed across numerous locations in a building environment i.e. indoor air, interfacial region at both internal and external surfaces, and intra-material pore structure connectivity, has resulted in a variety of approaches, ranging in complexity, developed to numerically model this within a building simulation domain. A review of these methods is provided in (Delgado et al, 2013). In addition to the increased processing time and limited validated examples available mentioned previously, a further difficulty associated with airflow phenomena is their accurate measurement.
This stems from reasons including:

- the multiple driving forces involved with each process,
- the rapidly changing boundary conditions, resulting in the use of fixed conditions for ease of simulation e.g. well-mixed indoor air with uniform properties; and transfer analogies when analysing surface transfer behaviour such as convective drying
- localised transfer processes i.e. micro-climates formed within the indoor environment and within the building construction material.

The importance of accurate representation of local transfer site boundary conditions in the field of hygrothermal material performance assessment has already been discussed in Chapter 2. The practical difficulties associated with accurate acquisition of experimental data in situ leads to the use of generic property data in building simulation models. This brings up concern over the reliability of simulation predictions when conducting assessments of indoor air quality and thus the suitability of using analogies to determine surface mass transfer.

4.3 Heat and mass transfer analogy

The use of convective transfer coefficients therefore continues to be the commonly used approach when modelling the hygrothermal behaviour at the interfacial region. The coefficients relate the convective heat and moisture fluxes normal to the surface of the wall to the difference between the temperature or vapour pressure gradient at the wall, respectively, and then either a reference temperature or vapour pressure. By assuming there is continuity of the temperature; the humidity in the gaseous phase; and the flux densities normal to the interfacial region, the heat and mass transfer flows can be obtained by coupling the governing equations describing the transport processes in both the solid and fluid media (Masmoudi and Prat, 1991). These relations

are presented in the example equations shown below for both the heat and moisture transfer coefficients:

$$h_c = \frac{q_{c,w}}{T_w - T_{ref}}$$

Equation (4.12)

$$h_m = \frac{g_{c,w}}{p_{v,w} - p_{v,ref}}$$

Equation (4.13)

For Equation (4.12), the units for h_c are W/m^2.K; $q_{c,w}$ is the convective heat flux (W/m^2); and T is the temperature (K), for the wall and the reference point, denoted by *w* and *ref*; h_m (s/m) is the convective mass transfer coefficient; $g_{c,w}$ is the convective mass flux (kg/m^2.s); and *p* is the vapour pressure (Pa) at the wall and the reference point, denoted by *w* and *ref* in Equation (4.13).

The transfer analogy was originally developed for forced boundary layer flow over flat plates or inside tubes (Colburn, 1933). The first reported observations of the analogous behaviour portrayed by heat and momentum transfer were those of Reynolds. The analogy was derived from results indicating the frictional resistance to fluid transport in conduits, allowing for the quantitative analogy between the two transport phenomena to be deduced (Welty et al, 2001). The relationship between the heat transfer and the frictional resistance in the boundary layer is derived from laminar forced flow over a surface, where no drag is present and therefore the Prandtl number, representing the relationship between heat and momentum transfer as shown in the equation below, is equal to one.

$$\mathrm{Pr} = \frac{\nu}{\alpha} = \frac{\mu C_p}{k}$$

Equation (4.14)

where ν (m^2/s) is the kinematic viscosity; α (m^2/s) is the thermal diffusivity; C_p (J/kg.K) the specific heat capacity; ρ (kg/m^3) and k (W/m.K) the density and thermal

conductivity, respectively. The analogy can also be applied to cases of mass transfer when the Schmidt number, calculated using Equation (4.15), is also equal to one.

$$Sc = \frac{\mu}{\rho D}$$

Equation (4.15)

μ represents the dynamic viscosity (kg/m.s); and D symbolises the mass diffusivity (m^2/s). Prandtl also developed an analogy between the mass and momentum transfer that accounted for the turbulent core and the laminar sublayer in the boundary layer equations (Welty et al, 2001). In contrast to this approach, the Reynolds analogy was later adapted through the application of experimental data. This resulted in a simple modification being made to the analogy for the cases where the Pr and Sc numbers were not unity. A j factor was defined for both the heat and mass transfer as follows:

$$j_H = St\mathrm{Pr}^{2/3} = C_f/2$$

Equation (4.16)

$$j_m = St_m Sc^{2/3} = C_f/2$$

Equation (4.17)

where j_H and j_m are the heat and mass transfer factors, respectively; St and St_m are the Stanton numbers for heat and mass transfer, where the second Stanton number uses the subscript letter m to represent the mass transfer; and C_f to represent the skin friction coefficient. By combining these two equations, the final Chilton-Colburn analogy is as follows (Steeman et al, 2009), where Le is the Lewis number.

$$\frac{St}{St_m} = \frac{h_c}{C_p h_{m_c}} Le^{2/3}$$

Equation (4.18)

This relationship is also presented using the format described by (Threlkeld 1998):

$$h_c = K_y C_p (Sc/\mathrm{Pr})^{1-n}$$

Equation (4.19)

where K_y represents the mass transfer coefficient with respect to a driving potential y; and n is an exponent, which typically adopts the value 1/3 based on experimental data. The driving forces commonly used when analysing surface evaporation and moisture transfer through a porous material is the difference in vapour density at the interface and in the gas free stream; and the difference in the mass fractions. Certain conditions are required when using either of these variables. A constant vapour density should be assumed when relating this driving force to the mass transfer coefficient otherwise a dependency on ambient hygrothermal conditions such as the temperature and relative humidity will form. If this is the case, a mass transfer coefficient determined under the same dynamic conditions would be necessary. Relating the mass fraction to the mass transfer coefficient therefore is recommended to prevent this potential interdependency from appearing.

Other driving potentials include the molar density and molar fraction, and the specific humidity of air, which is typically used for problems involving humidification and dehumidification of steam-air mixtures. The following are different forms of the analogy with respect to the driving potential (Webb 1990).

$$h_c / C_p Le^{2/3} = K_y = MK_{\rho} = K = pMK_p = K_w/(1 + y)^2$$

Equation (4.20)

where the mass transfer coefficients presented in Equation (4.20) are, in order of appearance, based on the molecular weight M of the gas mixture (kg/mol); the mass density of the mixture (kg/m^3); the partial pressure of the gas mixture (Pa); and finally the specific humidity of the air (kg steam/kg dry air). Assuming that Fick's Law for diffusion is valid and the air-porous material interface is semi-permeable, the mass transfer coefficient can be used to calculate the mass flux at this fluid-solid junction using the following equations:

$$h_{mY}(Y_s - Y_\infty) = g = \left| \frac{D\, dY}{1 - Y_s\, dn} \right|_{n=0}$$

Equation (4.21)

$$h_m = \frac{(\rho_{v,s} - \rho_{v,\infty})\, g \left| \frac{D\, d\rho_v}{1 - Y_s}\, dn \right|_{n=0}}$$

Equation (4.22)

$$h_m = \frac{(P_{v,s} - P_{v,\infty})\, g \left| \frac{1}{R_v T} \frac{D\, dP_v}{1 - Z_s}\, dn \right|_{n=0}}$$

Equation (4.23)

$$h_m = \frac{(Z_s - Z_\infty)\, g \left| \frac{P\, D\, dZ}{R_v T} \right|_{n=0}}{1 - Z_s}$$

Equation (4.24)

the variable *Y* representing the mass fraction (kg/kg) as the driving force at the surface and free stream points, denoted by the subscripts *s* and ∞; *g* is the mass flux (kg/m².s); *D* is the mass diffusion coefficient (m²/s); and n is the direction of the normal (m); ρ_v is the density of vapour (kg/m³) at the surface and the free stream; *P* is the vapour pressure at the surface and free stream; R_v is the specific gas constant of vapour (J/kg.K); *T* is the temperature (K); *Z* is the mole fraction (mol/mol) at the material surface and in the free stream.

Various forms of the heat and mass transfer analogy have been developed, with contrasting limitations and levels of application. The assumption made for the use of these developed analogies was that they were applicable to forced convective flow conditions over a solid surface. In this case, the velocity field would be calculated using the momentum boundary conditions and any variations in the fluid density considered as having an insignificant impact on the flow profile across the boundary layer. These conditions however, are not generally met in the indoor environment due to the presence of heat and moisture sources. The conditions cannot be assumed constant as variable air density will induce buoyancy effects and subsequently interfere with the air velocity profile across the surface boundary. The majority of the air flow regimes in the indoor building environment predominantly take the form of natural convection where the air velocity is less than 0.2m/s (Worch, 2004). They may also take the form of a mixture of both turbulent and natural convection regimes, and hence create an additional source

term in the momentum boundary equation. This is a characteristic feature of natural convection (Steeman et al, 2009). Changes in the airflow profile at the air-porous material interface will influence the rate of moisture transport, a relationship that was studied by (Mortensen et al, 2005). The aim of the study was to determine the surface convective transfer coefficients as a function of the surface airflow velocity. Comparison between measured and predicted surface resistances showed the numerically derived values were underestimated when using the Lewis relation. The difference was reduced as the airflow velocity was increased, simultaneously raising the value of the convective heat transfer coefficient, by way of the relationships shown below (Hagentoft, 2001):

$$h_c = 6.4 + 4u \qquad u < 5\ m/s$$

Equation (4.25)

$$h_c = 7.41 u^{0.78} \qquad u > 5\ m/s$$

Equation (4.26)

where u is the air flow velocity (m/s) and h_c is the convective heat transfer coefficient (W/m^2.K). However, the air flow velocities to be expected near the surface of internal walls will be quite small, indicating that this type of error may result in inaccurate predictions of the moisture transfer rate. This outcome was deemed to be insignificant if materials with a high vapour diffusion resistance were considered (Mortensen et al, 2005). This however, is not the case in a realistic building envelope construction, where permeable hygroscopic building material accounts for significant reductions in indoor relative humidity. In addition, the increased surface roughness of some materials used in the building construction increase the specific surface area available for moisture exchange. This has been shown to enhance the ability of individual water molecules to transfer to and from a material and the air in contact with the material surface and was observed over a range of air velocities (Worch, 2004).

Another study highlighted the significance of the relationship between the convective heat transfer coefficient and the airflow velocity in the surface boundary layer (Steskens et al, 2008). It was found that by assuming a constant convective heat transfer coefficient, the accuracy of the heat, air and mass transfer predictions could be reduced; and by discounting the variable local conditions in a room, simulation predictions could miss the potential risk of mould problems. The significance of the dynamic coupling of the heat and mass transfer involved with the convective drying process observed at the interface between the air and a porous building material is discussed in the following section.

4.3.1 The drying process

Research into the physics of material drying and moisture transfer exchange with porous building materials indicates the vapour pressure difference is widely used as the primary driving force of the associated mass transfer processes. Findings however, have shown that this relation is only applicable to isobaric systems and should be adjusted by the total pressure when used under variable air pressure (Steskens et al, 2008). One of the first studies conducted on the drying of solids deduced that the process could be divided into two mechanisms. Initially, a diffusion based transfer of moisture occurs from the interior of the solid to the outer surface of the material. This is followed by a second stage involving the evaporation of moisture from the surface of the solid (Whitaker, 1977). The diffusion was based on the equation shown below:

$$\frac{\partial C}{\partial t} = D\left(\frac{\partial^2 C}{\partial x_2}\right)$$

Equation (4.27)

where C represents the moisture content present in the medium and D is a parameter determined experimentally. It was later found, however, that this diffusion theory of liquid could not be applied to all porous media and other relevant phenomena such as moisture in the vapour and heat transfer became apparent in further study of the drying process. Clear indications were observed that surface tension effects could not be ignored in the study of liquid motion in unsaturated porous media (Gardner and Widtsoe, 1920 cited in Whitaker 1977: 215-232). Also capillary action was an important component of the liquid transfer process during the drying of porous material (Comings EW et al, 1934). Definitive evidence proved that the diffusion equation could be used to model the latter stages of drying (Haines WB, 1927 cited in Whitaker 1977: 264-290). By this means moisture transport owing to capillary action is reduced and the dominant methods driving the transfer are convection and vapour diffusion.

One of the many areas of interest in convective heat and mass transfer processes is its relationship with indoor hygrothermal analysis and the resulting influence on indoor air quality and comfort, moisture buffering and energy consumption (Hensen JLM et al. 2012). To assess the impact of convective drying on the indoor environment, numerical models have been developed to simulate the associated behaviour. These models generally integrate convective heat and mass transfer coefficients that in the main relate heat and moisture fluxes to changes in temperature and vapour pressure. This simplified approach is adopted to avoid explicit modelling of the complex and varying surface boundary conditions observed at the air-porous material interface. This

is discussed in greater depth in a subsequent section on moisture transfer at the interfacial region. The different stages of the drying process are presented in the figure below:

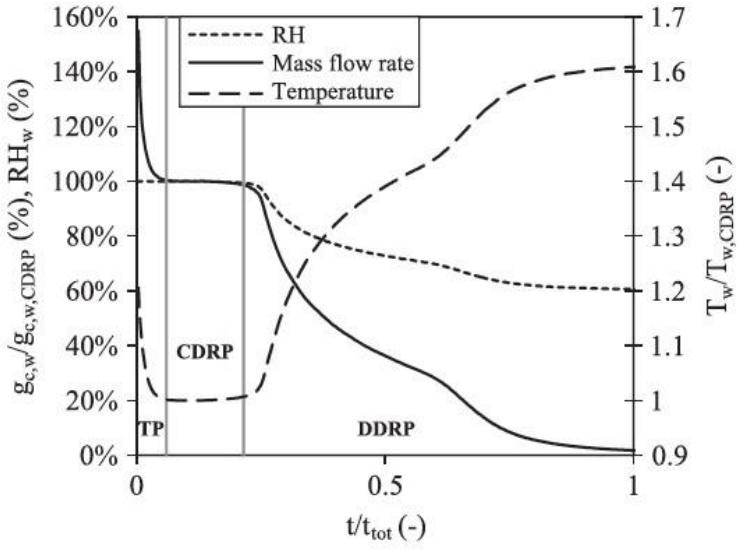

Figure 4.2 Stages of a porous material drying process (Defraeye et al, 2012).

After an initial transition period (TP in the figure above), when sufficient moisture is present in the material, the porous medium approaches the wet bulb temperature. The higher the initial temperature, the greater the drying rate. Once the temperature of the material becomes uniform over the whole cross section, the material will undergo a constant drying rate period (CDRP in the figure above). The drying rate is then proportional to the heat being supplied and represented by Equation (4.28) below (Nasrallah SB et al, 1988):

$$D_\tau = \frac{\alpha}{\Delta h_{vap}} (T_\infty - T)$$

Equation (4.28)

where D_τ (kg/m^2.s) is the drying rate, α (W/m^2.K) is the convective heat transfer coefficient, Δh_{vap} is the latent heat of evaporation (J/kg), and the difference between the ambient and the equilibrium temperature, the latter referring to the temperature in the porous medium when the drying rate becomes stable, is calculated. Evaporation from the surface of the material during the constant drying rate period is dependent on the flow

of air over the material surface although and on the supply of moisture to the surface from within the material; processes accounted for in several moisture modelling techniques (Janssen H et al, 2007). Once the moisture at the interface between the material and the air in contact with its surface reduces, a decreasing drying rate period (DDRP in the figure above) is reached, whereby the dry outer layer of the material is seen as an additional layer of resistance to liquid transfer, alongside the boundary layer resistance. At this point, the rate of drying is dominated by vapour diffusion through the porous material.

4.4 Moisture Transfer driving potentials

The presence of a potential gradient across a material will determine both the strength of the transfer process and the resultant flow rate from a region of high to low concentration. Each, however, is limited in its application. For example, the vapour pressure is only relevant for vapour diffusion, and hence is not used as the sole driving force. The common design of multilayered building envelope construction gives rise to the issue of discontinuity at material interfaces, which further complicates the calculation process. This also creates difficulty in using the capillary suction pressure as the driving potential, since in practice there are drawbacks to being able to measure this directly (Qin 2009). In the past, several moisture transport models were developed to use a discontinuous transfer potential. In this instance, the moisture content would be calculated at the interface between two materials. Implementing the moisture content as the driving potential requires analysis of the flux variations present at different intersecting points between materials, necessitating a mass balance calculation to be conducted iteratively at these points. The advantage of this approach is that the moisture content can be applied directly to calculate the liquid diffusivity (Karagiozis, 2001). Another potential is the relative humidity that remains continuous across the material assembly, although this is not a direct driver of moisture transfer.

The proportionality existing between the rate of moisture flow and the driving potential density gradient is generally determined experimentally. In spite of the available range of driving forces and relevant transport parameters considered, consensus on the most suitable choice of driving potential to best describe the moisture transfer phenomena is yet to be reached. The drawback in achieving a complete understanding lies primarily in the field of experimentation. Difficulty exists in identifying the individual transfer processes occurring during different moisture phases. Also, the same complexity is experienced when measuring moisture movement under non-isothermal conditions, where temperature dependent transfer coefficients cannot be easily quantified, thus limiting their application to simulation (Peuhkuri et al, 2008). This can be addressed by implementing continuous driving potentials such as vapour pressure, relative humidity, suction pressure and chemical potential, which reduce the

required computation time and formulation of governing equations (Karagiozis 2001). The fundamental characteristics and physics of moisture transfer processes in and around porous materials have now been reviewed. The next section discusses the application of this knowledge with reference to moisture transfer taking place in the pore domain of a material. This includes a review of moisture behaviour in the pore domain, providing detail regarding interstitial evaporation and condensation processes occurring at the microscopic level in porous building materials and the interaction between pore spaces. It also includes the development of the relevant moisture material characteristics applied in building simulation tools.

4.5 Influence of pore geometry on moisture transfer

A porous material is composed of a solid phase containing void spaces that are evenly or irregularly distributed throughout the medium. The pores, also known as sorption sites, can be isolated or interconnected. This multilevel composition requires classification of the pore structure i.e. a granular or fractured formation, consolidated or unconsolidated mechanical properties (the difference resulting from the level of connectivity between pores) (Coutelieris and Delgado 2012). Detailed monitoring of the heat, air and mass transfer processes occurring at the pore scale has been highlighted as a critical part of improving numerical predictions (by increasing accuracy) and the assessment of building material moisture performance over the course of its useful life (Adan and Brocken, 2003). Over time, the response of a material to the surrounding boundary conditions will vary, resulting in changes to its physical structure and hence its response to moisture. These responses include fracturing caused by thermal and moisture content fluctuations, the latter leading to hysteretic phenomena caused by repeated sorption cycles induced by capillary suction effects that are considered one of the main transfer mechanisms of moisture transport (Derluyn H et al, 2012). To this end, increased interest is being shown towards the physical processes taking place at the pore-scale, including multiphase moisture flow.

The accuracy of the hygrothermal models developed is dependent on reliable experimental derivation of moisture transfer coefficients representing the materials used in the building construction. The limitations in our understanding of the complex range of transport mechanisms, physical systems and coupled dynamics of the internal material structure therefore requires continual development of measurement techniques to improve numerical modelling of these phenomena. Generally, moisture transfer within pore spaces is represented in modelling by focusing on particular aspects of the pore structure. One such aspect is the porosity □□(mm^3/mm^3), which is considered to be one of the most difficult to incorporate into an analytical procedure with sufficient accuracy (Nikitsin VI and Backiel-Brzozowska, 2013). The porosity is used to

characterise the pore structure (representing the ratio of the volume of void spaces to the total volume of a porous medium) (Massey, 2006):

$$\varepsilon = \frac{Volume\,of\,voids}{Volume\,of\,voids + Volume\,of\,solids} = \frac{V_v}{V_v + V_s}$$

Equation (4.29)

Additional parameters detailing pore size distribution and pore morphology, including geometric properties such as pore shape and volume and topological properties e.g. pore interconnectivity, are also investigated. This area of microstructural material characterisation however, is still lacking (Raimondo et al, 2007). The following section describes available methods used to model moisture transfer at the pore scale.

4.5.1 Modelling HAM transfer processes at the pore scale

A wide range of numerical models have been developed with varying degrees of detail to investigate HAM transfer processes at the pore scale. Existing models include simplified parallel capillary models, network modelling (Fatt I, 1956) and multilayer adsorption modelling. These provide a systematic approach towards defining parametric relationships between multiphase flow and the physical nature of the porous domain and for estimating interfacial sorption phenomena (Al-Raoush and Willson 2005). It is important to be able to construct models that account for the heterogeneity of the pore geometry as this is a common attribute of a vast number of building materials.

In the main, advanced theoretical models solve the heat, mass and momentum transfer balance equations for a porous building material using the continuum approach. This models the porous medium as a homogeneous and isotropic system of continuum media, adopting volume-averaging techniques to solve for each system component. Translating the results obtained under these conditions for use in micro-scale analysis of moisture behaviour is an area still undergoing development, especially in areas where repeated wetting and drying phases occur and the associated dynamics measured in the pore structure require understanding e.g. formation of dry and wet patches (known as clusters) at intersection points between different materials in the building envelope. Several experimental studies have reported the formation of dry patches during drying of capillary porous material, indicating the large scale of heterogeneity present in the liquid phase distribution (Maneval and Whitaker S, 1988). This type of result highlights the importance of developing alternative modelling approaches to the continuum model that are able to simulate the variability in moisture flow within porous materials and could also be used to study the mass transfer behaviour at interfaces between a material and external air flows (Laurindo and Prat 1996). Some of the modelling techniques

developed to account for the various micro-phenomena observed, in the context of building simulation, are discussed below.

4.5.2 Pore Network modelling

Developing modelling techniques that replicate the behaviour of moisture in porous building material is an area that has been the subject of numerous studies. A number of processes, for instance drying, take place within this environment. The drying processes occurring are generally categorised using the effective diffusion coefficient and the porous material is considered as a continuum. By adopting the continuum approach, the effective diffusion coefficient property is applied once it is determined experimentally. Values for this property will vary depending on the material; although the conditions under which it is obtained remain constant during measurement e.g. temperature, surface air velocities. Relying on this empirical approach to define the drying characteristics of materials does not provide detailed information on the behaviour of moisture within pores that may vary in size and shape and hence will influence the moisture transfer process. It is deemed preferable to determine structural models of the materials pore pathways, which account for geometrical and topological variations. These types of models can then be combined with the relevant transport equations necessary to carry out numerical analysis of mass flow processes through porous media. Pore network models were designed for this purpose and are used to analyse moisture flow, for both fluid phases, through porous material (Prachayawarakorn et al, 2008). The first use of pore network modelling to represent multiphase flow in porous material was by Fatt in the 1950's. Figure 4.3 below presents the approach used to model the pore network within a porous material.

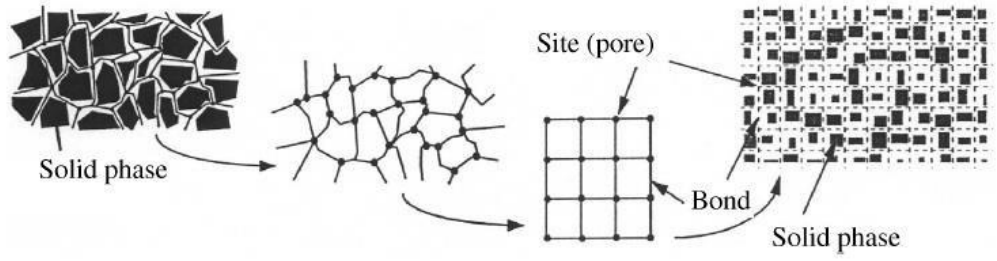

Figure 4.3 Modelling of a pore structure using a network of sites and bonds (Prat, 2002).

The method developed by Fatt included the two main modes of moisture transport within pore spaces, i.e. as a result of a materials hygroscopicity and through capillary effects, the second of which is deemed to be a more 'simplified' example, to be used in the development of more complex models representing a wider range of moisture transfer processes (Prat, 2002). These models were based on a continuum approach where

phenomenological characteristics of the pore domain were represented by lumped transport coefficients, derived from experimentation.

During the 1980's, the percolation theory was used to describe multiphase flow properties at the pore scale. Pore scale displacement mechanisms for both the ingress and drainage processes were observed directly in micromodel experiments and then incorporated into three dimensional network models. By adjusting certain parameters understood to impact on pore scale moisture behaviour, experimental data could be matched with model predictions and the trends in performance could be explained in terms of pore scale phenomena. The predictive capability of these models however, was limited to simple systems that consisted of closely packed spheres (e.g. glass beads and sand particles) and the focus was concentrated on two phase flow in water wet media. Attention shifted from research into percolation models and simplified pore scale geometries, as it was believed further enhancement in the predictive capability of any model would require improving the representation of a whole range of flow and transport phenomena in porous media.

Traditional network models represent the void spaces in a porous material by employing a regular two or three-dimensional lattice of wide pores connected by narrower throats. A modelled pore space would contain a single phase and its size would not be spatially correlated, whereas a real pore system can potentially exhibit three phases in a single pore, have a random topology and have correlated pore sizes. Determining the level of detail necessary in representing the pore geometry is a critical aspect of pore scale modelling and achieving accurate predictions of macroscopic properties (Blunt 2001). The use of empirically sourced transfer coefficients in determining macroscopic properties such as the capillary tortuosity □(m/m), which can be used as a numerical representation of the pore geometry:

$$\square\square = \frac{l}{L}$$

Equation (4.30)

where l (m) is the mean length of moisture particle trajectory and L (m) is the thickness of the materials, also presents a significant disadvantage as there is a limited number of materials for which this information is available to use in the aforementioned modelling approaches and thus limits its application in simulation (Nikitsin VI and BackielBrzozowska, 2013).

The numerical approaches used to compute pore space properties can be divided into two main categories. The first is direct simulation, where the governing equations of

flow and transport are determined on the image produced from imaging techniques. The second is the use of a network modelling approach to translate an image of the pore structure into a topological representation, from which the relevant displacement and transport equations can be solved. This is considered the most computationally efficient and successful in predicting multiphase flow in the pore domain (Blunt, 2013).

The outlook on pore-scale modelling has changed yet again however, with current models available not being limited to two phase flow processes. More complex geometries can be modelled, which has enhanced the holistic approach in predictive modelling and a wider range of phenomena can now be explored, including the effects of wettability, three phase flow, mass transfer between phases and hysteresis effects.

4.5.3 Effects of hygroscopicity and hysteresis on moisture transfer

Porous building material has the inherent ability to store moisture, which can be defined in the form of relative humidity or a capillary pressure. These two properties are interchangeable when used in the Kelvin equation (Equation 4.5), which allows the moisture storage function to be expressed with relation to either. A reasonable illustration of the moisture storage behaviour over the entire hygroscopic range can be produced using this equation. From the figure below, the moisture retention characteristics become apparent as functions of the two moisture potentials. Knowledge of these moisture storage capabilities is important for developing transient moisture transfer calculation tools.

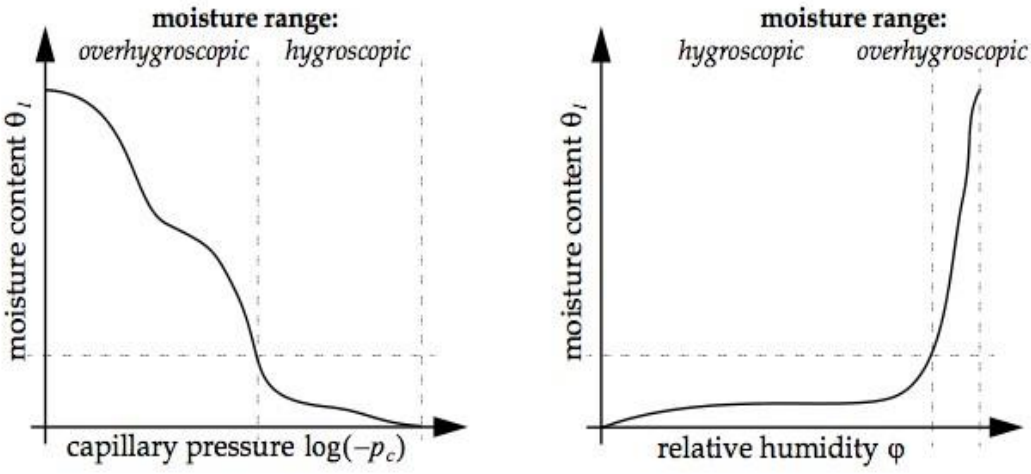

Figure 4.4 Moisture storage characteristics as functions of capillary pressure and relative humidity (Scheffler, 2008).

A range of moisture transfer processes will occur over the hygroscopic range. From a completely dry state, a material will absorb moisture at low relative humidity values, resulting in a thin single layer of water molecules becoming bound to the inner surfaces of the material pores. As the relative humidity increases, the amount of bound water will increase, so that the moisture begins to condense within the pores, eventually

reaching the point of capillary saturation, causing the larger voids of the material to be filled. At this stage, capillary flow becomes the predominant method of describing the moisture flow. If on the exposed surface of the material there exists a lower relative humidity, moisture will migrate towards the lower potential under capillary forces and will then evaporate to and from the surface, creating a state of dynamic equilibrium. This will also result in some hysteresis originating from dynamic uptake and release of moisture.

Moisture hysteresis refers to the recognised phenomenon that at the same relative humidity, a material undergoes a different level of moisture saturation or moisture content uptake relative to the moisture loading experienced (Derluyn et al, 2012). Variable moisture behaviour can be the cause of a range of hysteretic effects, some of which are described below:

- ink bottle effect, i.e. larger pores are connected to the pore matrix via small pores and thus remain liquid filled until the smaller pores have emptied
- air trapped inside the pore system cannot exit the material as a result of the liquid filled pores
- changing contact angles for advancing and receding liquid in a capillary. Experiments have shown that the pore shape can greatly influence the drying time of a porous medium with drying times varying over periods exceeding two decades depending on the pore shape. For a given contact angle, the drying time significantly increases relative to the number of sides in a pore. The sensitivity to the contact angle can be seen in the figure below. This suggests that a modification of the contact angle for a given porous medium can lead to significant changes in the drying kinetics further illustrating the significance of film flows on overall drying rates. This effect is presented in Figure 4.5 below, where □□is the contact angle (°), N is the number of sides in the pore being modelled, t_D is the drying time (s) and t_{Dref} is the reference drying time (s):

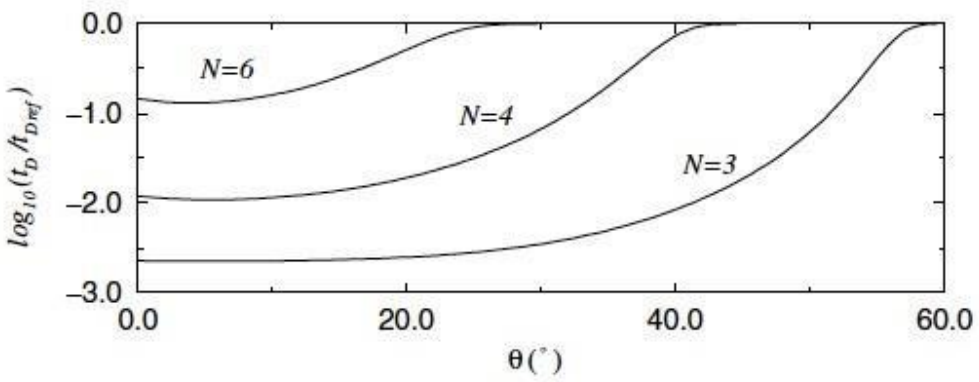

Figure 4.5 Evolution of the drying time of a porous materials as a function of the contact angle (Prat, 2007) physical or chemical variations to the pore system due to the presence of water e.g. shrinkage and swelling, chemical reactions.

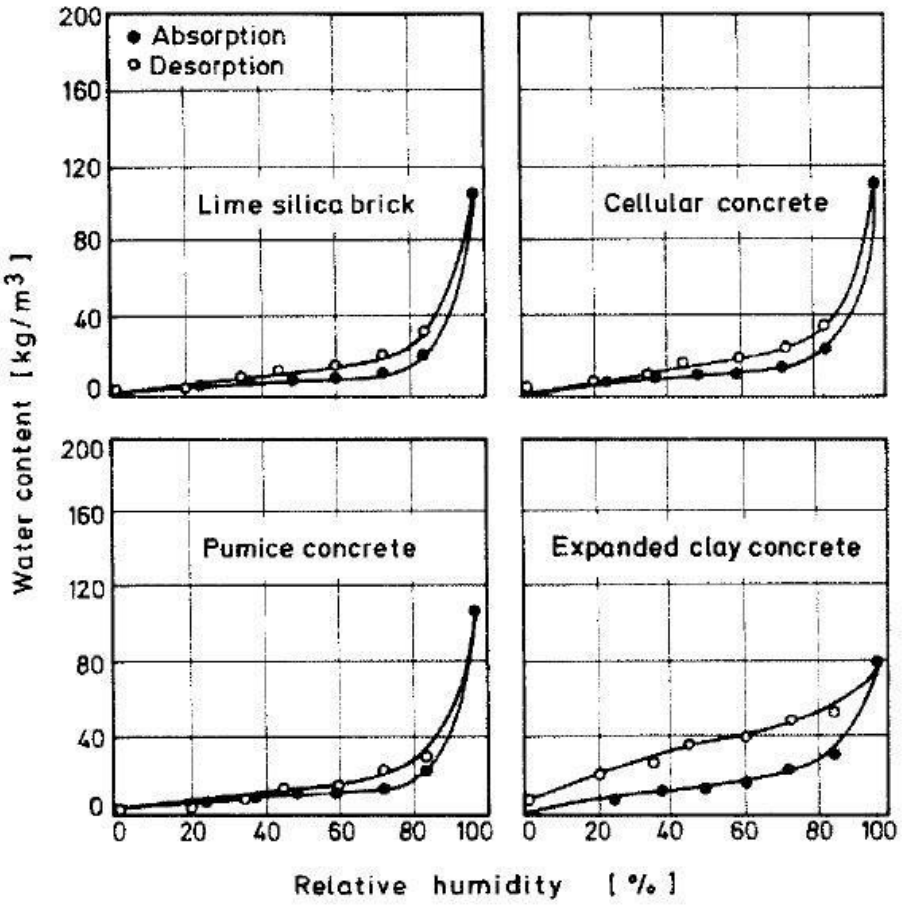

Figure 4.6 Absorption and desorption isotherms for a range of common building materials (Kunzel 1994).

As seen in Figure 4.6, the hysteresis effect observed between the absorption and desorption phases is not that significant for some of the materials and in general, the absorption isotherm could be considered adequate in modelling the moisture storage characteristics of a building material (Kunzel 1994). By using a capillary pressure curve, it is possible to view the amount of hysteresis resulting from the wetting and drying phases a material will undergo. Results from experimentation reported in one study discovered the magnitude of the hysteresis loop observed to be material dependent (Molenda, 1992). The effect was shown to be more significant when measuring the capillary pressure curve for sand fill in comparison to aerated concrete; and the reason for this is that the majority of mineral based building materials have a significantly larger pore diameter size and hence less variation is noticed in the suction pressure curve (Krus M, Moisture Transport and Storage Coefficients of Porous Mineral Building Materials, Theoretical Principles and New Test Methods, 1995 (English version published in 1996), Report based on PhD Thesis).

Another study found from comparing resultant data with and without the consideration of hysteretic effects that accurate representation of the moisture storage performance could be calculated by using an average of the absorption and desorption isotherms during extended periods of wetting or drying, given the uncertainties surrounding determining sorption parameters (Pedersen, 1990). The more likely scenario of diurnal variations in indoor moisture conditions was highlighted however, indicating the resultant moisture content of the materials, exposed to this type of indoor environment, will follow a path between the absorption and desorption isotherms, thus supporting the incorporation of both functions within a modelling context. Figure 4.7 below presents the results comparing the results for calculations neglecting and including hysteresis effects for one of the material tested.

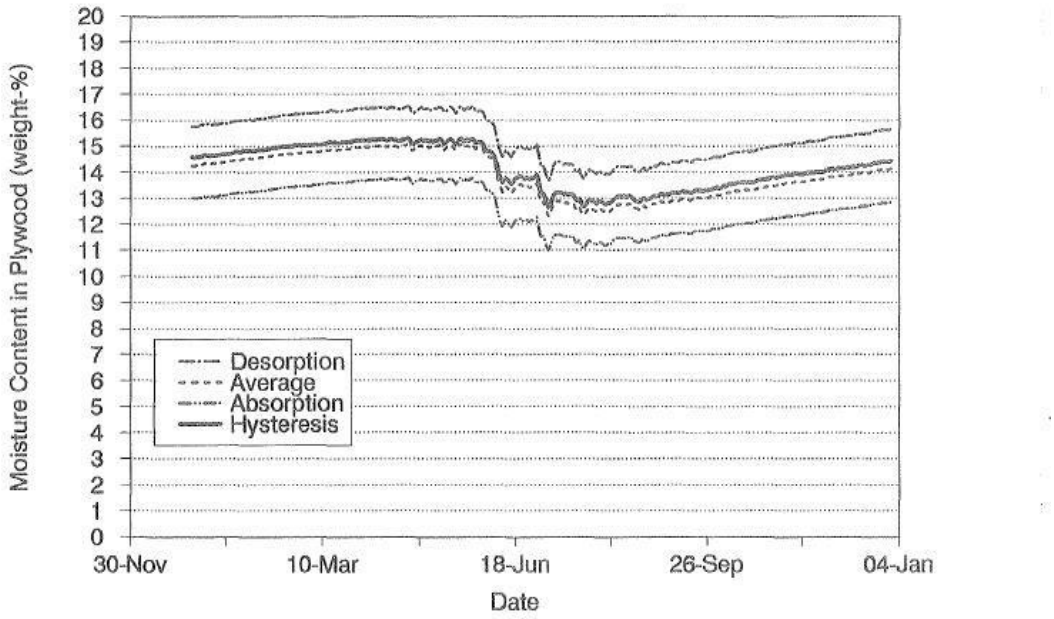

Figure 4.7 Moisture content of plywood a function of time for calculations using the absorption isotherm; the desorption isotherm; the average of the absorption and desorption isotherms; and finally the calculation with hysteresis (Pedersen 1990).

This result was also verified in a study conducted by Kwiatkowski et al (Kwiatkowski et al, 2009). Their investigation demonstrated the influence of sorption hysteresis effects on water vapour transport in porous building materials. A series of simulations were conducted using four model variations to represent the material moisture transfer properties. These included a model that accounted for hysteresis effects, a second model variant that used the sorption isotherm to replicate the dependency between relative humidity and the material moisture content, thirdly the desorption isotherm alone was applied and finally the average of both the sorption and desorption isotherms was introduced to simulate this relationship. Results showed the difference in simulation predictions could be as much as 20% when comparing the models with and without consideration of hysteresis. More precise results were obtained

when using the average of the adsorption and desorption isotherms. However, for strong variations in boundary conditions, this model was not well suited. The rate of moisture release from the material being modelled, into the indoor air, was greater than that of the model accounting for hysteresis effects. By neglecting hysteresis effects it was assumed that the moisture buffering capacity of the materials would be overestimated due to inaccurate representation of the dynamic behaviour of the material, which could potentially lead to the oversight of risks such as mould growth and condensation. Figure 4.8 below presents the model predictions, firstly under steady state conditions and secondly in a realistic setting with a variable climate and moisture loading.

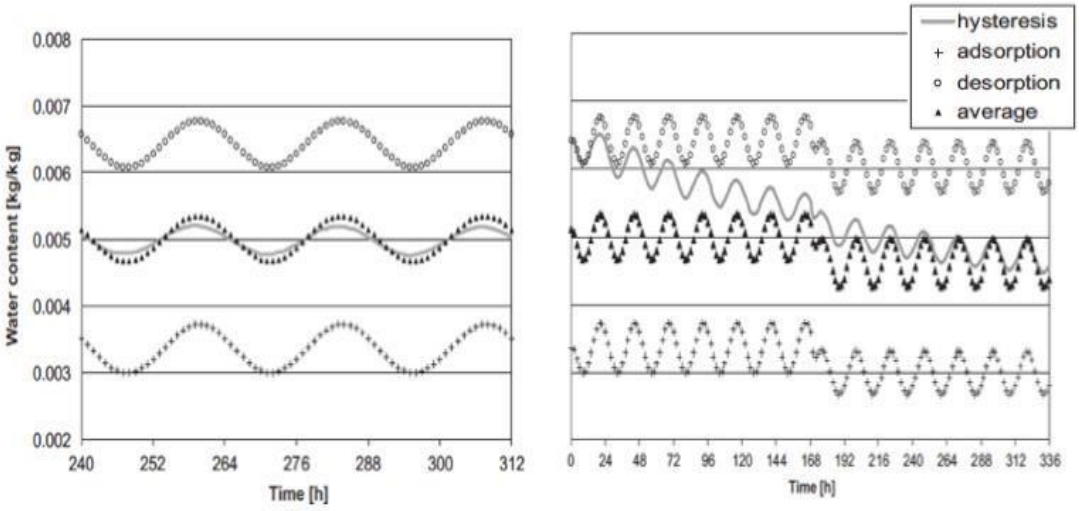

Figure 4.8 Predictions of moisture content in Gypsum Plasterboard (t=12.5mm) from four model variants under steady state conditions (left); and in a realistic setting with variable climate and moisture loading (right).

A short overview of the approaches adopted in combined heat and moisture transfer modelling is provided in the following section.

4.6 Developed and applied HAM Transfer theory

4.6.1 Combined heat and mass transfer

Early models developed to investigate the movement of moisture in porous building material include the Luikov (Pandey et al, 1999) and Phillip and De Vries (De Vries DA, 1987) methods. The general structure of these models involves a system of partial differential equations (PDE's) that incorporate the thermodynamic behaviour of irreversible processes. In the Luikov model, this system of equations is non-linear due to the nature of transport coefficients and thermal properties used, which are functions of both moisture content and temperature (Pandey et al, 1999). Derivation of the moisture and thermal diffusion coefficient properties required by the model is difficult as a result of the interrelated effects of heat and moisture transfer, which are hard to isolate and determine independently within an experimental setting given they are both dependent on the two driving potentials simultaneously. The model describes both vapour and liquid transfer driven by the total moisture concentration gradient and the thermal gradient; and the assumption is made that molecular and molar transfer of air, vapour and liquid moisture transfer occur simultaneously within the porous domain. One of the main advantages of the Luikov model is that the mathematical structure provides exact solutions to many modelling scenarios, which allows for the accuracy of approximate or numerical solutions to be evaluated (Qin, 2009).

The Philip and De Vries approach to developing theoretical expressions for moisture and thermal diffusivity at the macroscopic level, involves linking the two selected driving potentials, mentioned in the previous paragraph, to the relevant constituent equations that would account for the combined heat and mass transfer effect in the material. The moisture potential and hydraulic conductivity of the porous medium, in addition to the thermal conductivity, are then associated with their respective dependencies on volumetric moisture content and temperature (De Vries, 1987). The approach does not take into consideration processes such as boiling, freezing or thawing of moisture and further limitations of the method are that:

- the material structure is considered at the macroscopic scale, where the structure of the porous domain is homogeneous and isotropic.
- the theory does not apply to materials that are experiencing movement as a result of shrinking and swelling, which can ultimately lead to the weakening of the material structure, fracturing and a decrease in durability.
- the moisture potential with respect to the moisture content does not take into account the effect of hysteresis.

- finally, the influence of surface transfer phenomena at the interface between the porous medium and moisture in the liquid phase are not accounted for. Additionally, the Knudsen effects in the gaseous phase are not included.

The Luikov and Philip and De Vries methods are widely used for determining coupled heat and moisture transfer in porous building material. Both temperature and the moisture concentration gradient are used as the driving potentials however, using these parameters in a building simulation environment introduces difficulties in their application to non-isothermal moisture transfer scenarios in porous materials. These include the discontinuity of the moisture content profile in multilayered and multimaterial building envelope construction. The non-uniformity frequently seen in construction brings about changes in material hygrothermal properties and induces material interface phenomena that interrupt the flow of moisture.

A more recent development in the field of combined heat, air and moisture transfer is the Glaser method, which was initially used to determine the vapour pressure distribution across constructions by graphical means. Its function was to estimate the amount of condensate accumulated during the colder winter period and equally to determine the mass of water vapour evaporated over the summer. The method was designed using Fick's theory of mass diffusion (in the form of vapour) under steady state conditions and with constant material properties applied to the construction materials. The mass flux through a layer in a construction is calculated using the following expression:

$$g_{v,i} = \delta_i \frac{\Delta p_i}{\Delta x_i} = \frac{\Delta p_i}{Z_i}$$

Equation (4.31)

where $g_{v,i}$ represents the vapour flux through the construction layer denoted by i. δ(kg/m.s.Pa) is the vapour permeability of the construction material, Δp (Pa) and Δx (m) are the change in partial vapour pressure and space coordinate in the material layer respectively and finally Z (m^2.s.Pa/kg) denotes the vapour resistance of the construction material (Pedersen 1992). Significant drawbacks exist in this method, however. Firstly, the moisture content distribution within the porous medium is calculated under steady state conditions, which results in instantaneous moisture variations. The hygroscopicity of the material is ignored, resulting in the vapour pressure fluctuations relating to the saturation conditions only or alternatively being dependent on changes in boundary conditions and the distribution of vapour resistances. This type of behaviour is not readily observed in reality, highlighting the importance of using the relationship between

vapour pressure and material moisture content, described by the sorption isotherm, to account for the dynamic nature of mass transfer and hygrothermal material properties. Secondly, the method does not include the potential for liquid transfer, therefore omitting the possible phase changes that may occur within the material (Ficker, 2003).

Finally, the climatic and internal boundary conditions are assigned fixed set points, depending on the season being analysed, which can be seen in the corresponding building standard DIN 4108 for this methodology. This approach misrepresents the true nature of the transient climate conditions experienced by a building and can therefore produce inaccurate predictions of interstitial condensation and evaporation. In order to achieve more realistic predictions of the conditions found in the building envelope, a more detailed set of time varying climate data would be required, thus increasing the level of computation required. Modelling these physical aspects at the level of detail necessary to achieve a fully realistic model however, is not possible (Hens, 2007).

4.6.2 Numerical modelling in Building Simulation

Different numerical approaches exist to perform a range of coupled hygrothermal process modelling in building simulation tools under differing spatially and temporal resolutions. This section provides a brief overview of the structuring and primary methodologies adopted by building simulation tools to model this hygrothermal behaviour in porous building material.

Unlike the available analytical techniques that provide exact solutions to a specified problem within a designated system, numerical models are far more suited to the field of whole building simulation, in the main, due to the array of problem handling capabilities available. The structure of a numerical model can be described as a three stage process whereby the system is initially discretised (in the spatial and temporal domains); secondly there is the introduction of a set of nodal points with assigned equation sets originating from governing partial differential equations for the respective physical domain being investigated; and which are then calculated simultaneously to determine the distribution and magnitude of state variables in the final stage of the numerical modelling analysis. These are approximations determined using the truncated Taylor series expansion or by application of conservation principles to small control volumes, of which further detail can be found in a number of references that includes (Clarke JA, 2001). An example of the latter approach is that of continuum modelling. This widely used method in the field of moisture transfer modelling represents a simplified version of heat and mass transfer characteristics and properties in the porous domain. This method adopts a phenomenological approach to represent the complex microscopic geometry and properties of porous media, using transfer coefficients derived experimentally from macroscopic scale balance equations. Three basic assumptions are made when outlining the mathematical description of heterogeneous material systems:

- hygrothermal and physical properties of the porous medium can be associated with numerical field variables that are spatially defined using representative elementary volumes (REV's). This volume averaging technique transforms the geometric and physical properties from the microscopic to the macroscopic scale that complies with the continuum modelling approach.

- microscopic mass transfer phenomena are modelled using equivalent mass transfer equations based on the numerical field variables, as stated above

- numerical field variables' temporal and spatial dependency is represented in the form of differential balance equations for mass, momentum and energy (Descamps, 1996).

Further techniques available for space discretisation in building simulation are described below and are classified as either explicit (solving equations at the following time step with values acquired from the previous time step) or implicit (meaning the equations are solved at each time step) in terms of the temporal discretisation, They include the:

- Finite Difference Method that is used to solve diffusion based phenomena e.g. heat conduction, vapour, liquid and/or air flow processes, for one, two and threedimensional systems. The principle of the method is to transform the developed partial differential equation describing the rate of change of a driving potential into a finite difference based system of equations. In the case of HAM transfer across a layer in a building envelope construction, a series of grid points are positioned through the cross section of each layer. The transfer rate through the material is then determined at each of these designated points.
- Finite Control Volume Method is similar to the Finite Difference method described. This method allows variable application of gridding positions that can, helping to focus computer processing demand at points of greater influence e.g. interfacial surfaces. The same principle applies to the time step resolution such that the computational effort is greater when rapidly changing processes take place.

- Finite Element Method (FEM), which is provides a flexible solution to partial differential equations. The main benefit associated with FEM is its ability to apply unstructured gridding patterns, meaning multidimensional problems can be solved for areas of non-uniform geometry. The governing mathematical equations are solved for each finite element specified in the gridding geometry by integrating the relevant equation across the control volume. The diagram below illustrates the variation in the mesh geometry that can be applied using FEM:

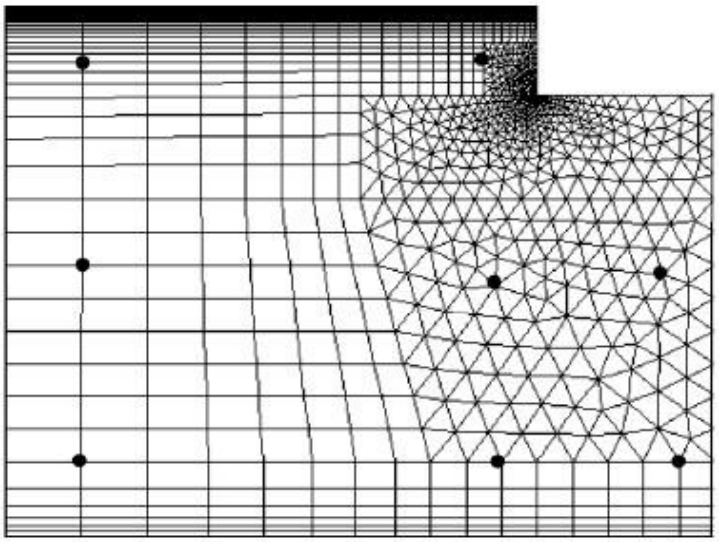

Figure 4.9 Image of an example numerical mesh developed for FEM analysis.

The applicability of FEM in building physics at present however, is limited to specific components and areas surrounding a building and has not been used for whole building simulation due to the increased computing capacity required (Woloszyn and Rode, 2008).

- Transfer Function Method and the Response Factor. The main objectives of these approaches are to calculate transient heat conduction problems and relate this performance to the thermal conditions of a building; and secondly to deduce the effect of the resultant thermal conditions on building energy consumption. Neither method is usually applied to calculate the hygrothermal behaviour of building material in a wall. This is partly the consequence of the methods inability to manage nonlinear transport phenomena and hence the highly coupled and nonlinear moisture transfer characteristics make it unsuitable in this field.

Having discussed key aspects of the numerical modelling approaches applied in building simulation tools, the following section introduces the methodology adopted by the dynamic whole building integrated simulation tool called ESP-r. This tool was selected to conduct the simulation based constituents of this research, due to the wide range of physical systems incorporated into the modelling domain, including combined heat, air and mass transfer.

4.7 Introduction to ESP-r

This section will provide an overview of the existing mathematical framework implemented in ESP-r to model the movement of moisture in building materials, taking into account the coupled nature of heat, air and mass transfer processes; and its integration into a whole building dynamic simulation environment.

4.7.1 ESP-r approach to moisture modelling

The ESP-r building simulation system uses an integrated modelling approach to solve a range of building performance related processes. These processes include heat transfer, interzonal air transfer, electricity flows, solar processes, plant and energy systems and finally moisture transfer. Mathematical models have been produced for each of these domains and are combined in ESP-r to form a unified representation of the building and its environmental control systems (Clarke J A, 2001). Partitioning of the mathematical solvers brings about the benefit of optimised computation times when calculating the resultant behaviour of the various building domains. The interrelated nature of some of the domains also requires communicating information between the relevant solvers using a time-step approach, allowing for their coupled solution.

The following subsections describe the integrated components of ESP-r's modelling solution for combined heat, air and moisture transfer.

4.7.1.1 Heat Transfer model

ESP-r partitions the solution procedure for each of the physical domains modelling combined heat, air and moisture transfer. A finite difference methodology based on a control volume heat balance is applied to calculate the thermal conditions of the building, where all inherent energy flows are considered. Three principal steps outline this approach whereby (1) the building is discretised to represent several building components including air volumes, opaque and transparent materials, plant components and solid-fluid interfaces using finite difference nodes positioned in each of these components; (2) a heat balance is calculated for each of these nodes, approximating the governing partial differential equations and linking the resultant heat flows between nodes over space and time; (3) a simultaneous analysis is performed on the associated equations to predict the thermal conditions of each node and the thermal interaction between nodes for a given point in time (Beausoleil-Morrison I, 2000).

As mentioned previously in this chapter, the airflow conditions of the indoor environment are strongly dependent on the thermal state of the building, where stack pressure effects induce buoyancy forces across indoor building spaces and across the building envelope as a result of temperature differences. This results in the coupling of the thermal air point nodes and the designated airflow network nodes allowing data to be passed between each solver at each time-step. Results from the thermal domain are used to determine the temperatures at airflow network nodes that in turn will influence the buoyancy driven flow. External boundary conditions, including air temperature and wind speed, are also considered when carrying out the mass balance equations for the airflow network. The results equate to the infiltration and inter-zonal air transfer parameters used to determine the heat balance for each air node in the thermal domain

that in turn influence the solution of the heat transfer model. The following subsection briefly describes the multi-zone airflow network model found in ESP-r. It is presented primarily as a means of providing a context for the use of airflow network modelling when addressing moisture transfer in a multi-zone environment.

4.7.1.2 Air Transfer model

The importance of inter-zonal air movement and the interaction between the indoor and outdoor environments is widely recognised within the context of whole building moisture flow modelling (El Diasty R, 1993). These processes can influence the transfer of contaminants between indoor spaces and the potential for condensation e.g. in air leakage paths. To this end, various multi-zone models have been developed to assess the induced flow distribution, an example of which is COMIS (IEA Annex 23 Final Report, 1996). The airflow network model implemented in ESP-r is based on four principles taken from the work by (Cockroft J P, 1979), and are as follows:

1. the discretisation scheme applies a single air node to each air volume and air handling system within the building. The external conditions surrounding the building can also be represented using an air node;
2. a range of components including doors, windows, ducts, fans and supply vents are modelled with their associated pressure drops through leakage paths or through the building envelope fabric;
3. the components are linked through connections to generate the perceived flow network; and
4. the mass balance at each node identified in the flow network is calculated, producing nodal pressures and the rate of flow between each component. The flow rate between linked components is a function of pressure differences across the connection.

The components designated in the model relate the airflow rate at a connection with the pressure difference observed across the connection. ESP-r can model a number of components including leakage points created by cracks, open windows and open doors. From the data provided at the air nodes and the relevant connections, a mass balance is then calculated every simulation time step for each node, displayed in the following equation:

$$\sum_{j=1}^{n} f(\Delta P_{ij})$$

Equation (4.32)

where ΔP is the pressure difference observed between nodes *i* and *j*; and n relates the number of nodes connected to node *i* (Beausoleil-Morrison I, 2000).

It becomes apparent that detailed information relating to the building features modelled in this approach is required. This information is not regularly available and given the complex interaction between the components described, uncertainty may arise in modelling predictions (Plathner P et al, 2002). For this reason, the airflow network model found in ESP-r was not applied during the course of this research.

4.7.1.3 Moisture Transfer model

Analysis of moisture in buildings requires consideration of both the behaviour of moisture in the indoor air and its interaction with hygroscopic material found in the building environment. Modelling the movement of moisture in porous building material involves incorporating several physical and material properties. Detailed representation of properties, which exist at the microscopic scale, increases the difficulty of an already highly complicated task. The heterogeneous nature of pore structures described, a result of varying pore distribution, pore size and tortuosity of flow paths in the material, further heightens the level of complexity faced in achieving accurate representation of the material in a building simulation environment.

With this in mind, the use of a representative control volume approach, as already described in this chapter, is implemented in ESP-r, whereby bulk properties are allocated to the user specified control volumes alongside variables of state, including temperature and vapour pressure. The coupled mass and energy conservation equations are then assigned to the control volumes that are assumed homogeneous and isotropic. Applying this assumption to adjoining surfaces of different building material layers comprising the building envelope construction mitigates the impact of the non-linear behaviour associated with moisture flow under these conditions. Three additional principal assumptions are made in ESP-r's integrated mathematical model, which are (1) that vapour and liquid flows are slow enough to allow thermodynamic equilibrium between phases; (2) that filtration flow due to to total pressure differences between the indoor and outdoor environments is negligible (Galbraith, 1992); and (3) while liquid flow and capillary condensation are considered in the moisture equations, the associated enthalpies are combined and estimated from the vapour-specific enthalpy alone, with heat absorption and dissipation resulting from phase change assumed to occur at saturation (Clarke, 2013).

The established mass flow model applied in ESP-r is as follows for the moisture source term (Clarke, 2001):

$$\Delta(P/P)$$

$$\rho_o \frac{\partial}{\partial t}\left(\frac{\partial P}{\partial \varphi}\right) = \frac{\partial}{\partial x}\left(D_{\varphi P}\frac{\partial P}{\partial x}\right) + \frac{\partial}{\partial x}\left(D_{\varphi T}\frac{\partial T}{\partial x}\right) + S$$

Equation (4.33)

where ρ is the density (kg/m^3), *o* and *l* denote the solid medium and the liquid components respectively, φ (kg/kg) is the moisture storage capacity of the medium, *P* (Pa) is the partial water vapour pressure, P_s is the saturation vapour pressure (Pa), δ (kg/m.s.Pa) is the moisture permeability of the material, *D* (kg/m^2.s.K) is a thermal diffusion coefficient and S is a moisture source term (kg/m^3.s). P and q represent the vapour pressure and temperature driving potentials used in ESP-r's moisture flow model. In the equation above, the primary driving potential is given as the subscript.

The moisture storage capacity for the specified control volumes is evaluated at each moisture node applied to each construction layer. This includes the interfacial regions, where there is contact between adjacent layers and is calculated as follows:

$$\rho_i \varphi_i = \frac{\sum_{i=1}^{N} (\rho_o)_i x_i \varphi_i}{\sum_{i=1}^{N} (\rho_o)_i x_i}$$

Equation (4.34)

where N represents the number of materials in the control volume (N=2 for a one dimensional simulation).

For the energy component of the model, the implemented algorithm is shown here:

$$\rho_o (c_o \varphi c_v g_v) \varphi c_l \rho_l \frac{\partial t}{\partial \tau} = h_v \rho_v \frac{\partial t_v}{\partial x} + h_l \rho_l \frac{\partial t_l}{\partial x} \rho_l \frac{\partial}{\partial x}\left(h_{x_s} J_v\right) + q$$

Equation (4.35)

c representing the specific heat capacity (J/kg.K), g is the moisture content (kg/kg), the thermal conductivity λ (W/m.K) is treated as a constant material property, J_v is the vapour mass flux (kg/m^2.s), *q* is a heat source (W/m^3) and h is the enthalpy for vapour, liquid and the moisture flux sources. The subscripts v and s represent vapour and moisture source terms. The moisture flux term J_v is determined based on an existing Lewis relation that interprets the convective mass transfer coefficient (s/m) as a function of the convective heat transfer coefficient (W/m^{2}K). This method was proposed in IEA Annex 14 (IEA. 1991.). The prescribed method is shown below in equation 4.36.

$$h_m = \frac{h_c}{C_p R_a \rho_a} Le^{0.67}$$

Equation (4.36)

where h_m is the convective mass transfer coefficient, h_c the convective heat transfer coefficient, C_p the specific heat capacity (J/kg.K), R_a the specific gas constant (J/kg.K), θ representing temperature in degrees Celsius, ρ_a the density of air and *Le* the Lewis number, which is given a value of 0.79 in ESP-r. Several methods are available to calculate the convective mass transfer coefficient, and further reading on the subject of the Lewis number can be found in (Webb 1990). This is a significant topic in keeping with the main context of the outlined objectives of this research and will be discussed in greater detail in Chapter 6. The convective heat transfer coefficient values are calculated in ESP-r using the well-mixed air assumption with surface specific convection coefficients for internal surfaces. This approach however, does not adapt to account for variability in indoor air flow regimes and hence the potential for changing boundary conditions in the indoor environment (Beausoleil-Morrison I, 2000). The influence of surface boundary conditions is well documented in the field of HAM modelling in porous building material. Given the relationship used in ESP-r to calculate the convective mass transfer coefficient, the need for accurate representation of the level of interaction between heat and moisture flows at solid-fluid interfaces becomes critical.

As already mentioned in point (3) previously, the enthalpy associated with moisture phase change is calculated using the specific enthalpy of the vapour phase only and this is due to insufficient availability of data for the separate phases. The assumption applied in the energy equation is that the resultant heat generated during phase change occurs at saturation. Evaporation, capillary condensation and liquid flow components of moisture flow are both considered in the ESP-r model, which requires an additional equation to determine the occurrence of these processes in the assigned building envelope control volumes.

Finally, combining the coupled equations provides a solution at each control volume for the dependent variables of pressure, temperature and liquid density under the influence of changing heat and mass transfer boundary conditions; and resolved within the interconnected domain scheme of the whole building simulation. The finite difference approximation method used for a one dimensional moisture transfer environment is presented below.

$$a_{in\square 1}P_{in\square 1}\square\sum_{j\square 1}^{2}a_{nj\square 1}P_{jn\square 1}\square(m_l)_{ni\square 1}\square\square\square tS_{in\square 1}$$

$$\square\ a_{in}P_{in}\square\sum_{j\square 1}^{2}a_{nj}P_{jn}\square(m_l)_{ni}\square(1\square\square)\square tS_{in}$$

$$\sum_{j=1}^{2} b_{nj}(\rho_{nj}\,\delta\delta_{in}) - \sum_{j=1}^{2} b_{nj-1}(\rho_{nj-1}\,\delta\delta_{in-1}) \qquad \Delta X_{j-i}$$

and

$$a_{nj-1} = \frac{(\delta_{\delta p})_{nj\delta\delta 1i} A\Delta t}{\Delta X_{j-i}},$$

$$a_{nj-1} = \frac{(1-\delta\delta)(\delta^{\delta})^{n} \quad A}{\Delta X_{j-i}}$$

$$a_{nj} = \frac{\delta_{P} \qquad j-i}{\delta^{t}},$$

$$a_{ik} = \frac{\delta_{ki}\,\delta\delta a_{iik} V_{-1}}{\delta\, a_{ik-1}},$$

$$b_{nj-1} = \frac{(P_s)\,\delta\,(D_{-P})_{nj\delta\delta 1i} A\Delta t}{\delta\, \Delta X_{j-i}},$$

$$b_{nj} = \frac{(1-\delta\delta)(D^{P})^{n} \quad A}{\delta_{j-i}\,\delta^{t}},$$

$$m_{ik} = V_{lk},$$

$$S_{ik} = Vs_{ik},$$

Equation (4.37)

where A (m^2), V (m^3) and ΔX (m) are quantities representative of the control volume; and the superscripts *n* and *n+1* are the present and future time rows of the current time step. The moisture storage capacity $\delta\delta$ used in the above equations is the differential of the moisture content function (known as the Hansen equation) that has been described already in Chapter 3 to quantify the concentration of moisture present in a heterogeneous control volume in a material layer. This value is based on either the average of the absorption and desorption isotherm curves or the absorption isotherm on its own in ESP-r, thus not incorporating the potential for hysteresis effects. The other material property involved in the control volume solution is the moisture permeability of a material. This property has already been reviewed in Chapter 3, whereby the resultant value is determined by dividing a constant moisture permeability value for air

by a relative humidity dependent vapour diffusion resistance factor. Uncertainty over the reliability of material properties used in building simulation has been discussed in the previous chapter and reviewed here in relation to pore scale modelling and hysteresis effects. This issue will be extended in Chapter 6, which presents an investigation into the hygrothermal performance of hygroscopic material exposed to intensive moisture loading conditions that involved a comparative study between measured behaviour and simulation predictions.

Finally, coupling of the moisture and energy equations discussed to solve for a desired system is presented as follows:

□□E □□□□□□□□□□B_e□□
□□□□□□ □□□ □□ □□
□□M□□□□P□□□□B_m□□

Equation (4.38)

where E and M represent the energy and moisture coefficient matrices, respectively; □□and P are the temperature and vapour pressure vectors; and B_e and B_m are the energy and moisture boundary conditions, respectively. Further insight into the development and structure of this method can be found in (Nakhi 1995).

4.8 Chapter summary

An overview of several issues arising when attempting to numerically model the hygrothermal performance of a building has been provided in this chapter. Emphasis was initially placed on outlining the interrelated characteristics of heat and mass transfer processes occurring in and around porous building materials, including the interdependencies of driving potentials, types of heat and mass flow observed, both at the solid-fluid interface and those in the pore domain, which introduced phenomena including phase change and resultant hysteresis effects. The latter was discussed in more detail, by outlining the importance of available pore scale modelling techniques from which a greater level of accuracy could be achieved in building simulation, through adaptation of standard models such as the continuum space model, to include information relating to micro-scale phenomena. Experimentally based studies, reported in the chapter, highlighted the significance of hysteresis effects within specific material types, supporting the need to investigate this issue further within the scope of this research.

This chapter also introduced the numerical approaches used to model hygrothermal behaviour in the porous material and indoor air domains. A brief overview of the development of heat and mass transfer modelling was provided initially before

focusing more closely on the methods applied in contemporary building simulation tools. This included discussion on the spatial and temporal discretisation procedures used and insight into the necessary techniques used to simplify the application of material properties and characteristics of the pore environment into the mathematical framework. The modelling methodology implemented in the building simulation tool ESP-r was then described. More specifically, the approaches taken to model combined heat, air and mass transfer in the indoor air and the building construction were described; and the method in which the coupling of the energy and moisture domains are included in the solution process of an integrated whole building analysis. This section also highlighted the assumptions made in ESP-r regarding the material properties and calculation of surface transfer properties implemented in the modelling procedure, of which both have been identified as influencing the accuracy of simulation results.

To this end, it was important to assess the predictive capability of ESP-r in modelling heat, air and moisture transfer processes taking place in the indoor building environment. This was done through a set of verification and application exercises which are presented in the following chapter. In addition, reporting of the outcomes obtained from these validation exercises is also provided.

CHAPTER 5

Verification and Application of ESP-r moisture modelling domain

Chapter Overview

This chapter presents the process by which the integrated moisture modelling domain of the building simulation tool ESP-r was verified and applied. The uncertainty that exists over the output of hygrothermal building modelling analysis has dictated the

need for further performance development of both the experimental and numerical assessment approaches taken, as was discussed in the previous chapter. The results presented in this chapter are taken from a series of hygrothermal modelling test cases used to assess the current capabilities of the moisture model employed in ESP-r under a range of indoor environmental conditions. From these results, it was shown that significant uncertainty remained in modelling predictions for more complex building scenarios by comparing ESP-r modelling predictions to other tools; and that the current ESP-r approaches used in modelling the dynamic hygrothermal response of building materials and the drying process would require further development work, which is subsequently reported in Chapter 6.

5.0 Introduction

A range of building simulation tools are available to model a number of coupled heat, air and moisture transfer processes observed in the indoor air and through the building fabric (Woloszyn et al, 2008). There is still, however, a growing need to improve and develop reliable and accurate modelling of the hygrothermal behaviour observed in the indoor environment. There are three main concerns with existing simulation tools which need to be addressed:

- the suitability of hygrothermal material properties used when modelling realistic indoor conditions, described in section 3.4.1;
- consideration of the hygrothermal impact associated with changing boundary conditions on heat, air and moisture transfer, as discussed in section 4.7.1.3; and
- the dynamic nature of transfer processes taking place within the building envelope, as was described in section 4.5.3.

The work presented in this chapter, and the subsequent development work included in Chapter 6, has been carried out with the aim of addressing these issues. The current moisture model found within the whole building simulation tool ESP-r was used as the

platform upon which the necessary development work was implemented. The methodology adopted a combination of empirical validation work and a series of comparative testing techniques, as described in (Judkoff R. and Neymark J, 1995).

This chapter presents the developmental work carried out in three stages. The first of these includes an initial series of moisture modelling test cases, presented in sections 5.1 to 5.6, which were used to examine the existing moisture modelling capabilities of ESP-r. The test cases were taken from a recent International Energy Agency (IEA) (Woloszyn et al, 2008) project and were chosen due to the wide range of modelling scenarios they introduced, including multiple material building envelope constructions and dynamic indoor and outdoor climatic conditions, enabling a broad overview and verification of the moisture modelling capabilities of ESP-r. The specific cases looked at were chosen due to the availability of analytical and numerical results that allowed intermodel and analytical comparison to be made between the different moisture modelling approaches adopted. Gaining consensus, however, on the dominant factors influencing the performance of the integrated moisture model was made difficult, as a result of the multi-variable and dynamic nature of some of the test cases. Further consideration of this issue is found in section 5.7 and is presented in the form of the outcomes taken from a recent project undertaken to investigate the impact of indoor laundry drying on indoor moisture conditions, air quality, and energy use. This involved the application of ESP-r's moisture model, in order to assess the impact of a wide number of building operation related factors on the indoor humidity conditions. Using this approach helped to identify particular areas in the modelling approach, where further investigation was required. The specific areas identified are presented in sections 5.8 and 5.9, which focus on the dynamic modelling of the response of hygroscopic building materials exposed to short duration moisture loading conditions; and the evaporation process associated with material drying, respectively.

Section 5.8 presents the second stage of the verification work carried out, with the principal aim of comparing ESP-r moisture model predictions to results produced from a controlled laboratory experiment. The emphasis was on the reliability of material moisture property data applied in a moisture modelling context and the influence of this data on numerical predictions. Evidence was presented in section 3.4 of Chapter 3, outlining the uncertainty stemming from experimentally derived material moisture properties. This uncertainty is, in part, due to the difficulty associated with replicating the range of transient variables, recognised in the building environment to influence the hygrothermal response of a material, in an experimental setting. Given the significance of the impact of moisture buffering materials on the indoor moisture conditions, and the variation in the response of hygroscopic building materials to moisture generating activities observed inside buildings i.e. occupant related moisture generating activity, as was highlighted in section 5.7, it was important to undertake this form of empirical

verification. (Janssen H et al, 2009) stated that idealised moisture conditions are generally applied when assessing the moisture performance of hygroscopic materials. Yet, it is deemed necessary to represent realistic moisture production regimes if the agreement between measured and simulated hygrothermal material performance is to be enhanced. The laboratory experiment referred to therefore, was designed to assess the suitability of the material moisture property data being used in ESP-r; and involved modelling the hygrothermal response of two sample materials exposed to a short duration moisture loading scheme in a controlled experimental facility.

The final verification case presented in section 5.9 involves the modelling of the moisture loss rate associated with the passive indoor drying of clothes. This is a practice frequently used in UK social housing and is a common cause of unsatisfactory indoor air quality (Porteous CDA et al, 2012). In order to investigate the effectiveness of moisture modelling solutions used to model this practice, further empirical verification of ESP-r's current approach adopted to quantify the evaporation rate from a wet surface was carried out. This involved using measured data collected from an indoor clothes drying experiment conducted in a real home environment. The mass of the items drying was recorded and then compared to the simulation outcomes in order to verify the modelling process.

5.1 Verification Methodology

The initial component of the verification approach involved the use of hygrothermal modelling exercises designed as part of the International Energy Agency Annex 41. These exercises were part of a methodology created for assessing the current use of heat, air and moisture modelling tools with the hope of introducing new developments in the form of new models or extensions to existing tools (Woloszyn et al, 2008). A selection of the test exercises were applied to assess the performance of the current ESP-r heat, air and moisture transfer model, the results from which are presented in sections 5.1 through to section 5.6.

The exercises incorporate a range of environmental conditions resulting from varying air flow conditions and moisture production schemes used in each case. Emphasis was also on examining the influence of the moisture buffering potential associated with hygroscopic materials located in the building envelope construction. The level of accuracy achieved in the predictions is quantified by drawing comparison between ESP-r predictions and:

- available measured data for the chosen tests;
- analytical results; and
- simulation outcomes provided by other HAM models.

The test case presented below provided opportunity to compare the numerical predictions made using ESP-r with other existing HAM simulation models for a range of environmental conditions and building envelope constructions.

5.2 Test case 1

5.2.1 Objective

This exercise focused on the analysis of moisture conditions observed in the building envelope construction and the indoor environment. Three variations of the model were examined to investigate the influence of different building parameters including the building material properties, the external climate and indoor climate control on indoor moisture conditions. This test was undertaken in order to examine the current state of ESP-r's moisture modelling methodology. Simulation results provided by partners of the IEA Annex 41 enabled intermodel comparison to be made in support of this initial inquiry of the existing approaches adopted in ESP-r's moisture model; helping to highlight potential areas requiring additional attention.

5.2.2 Model Outline

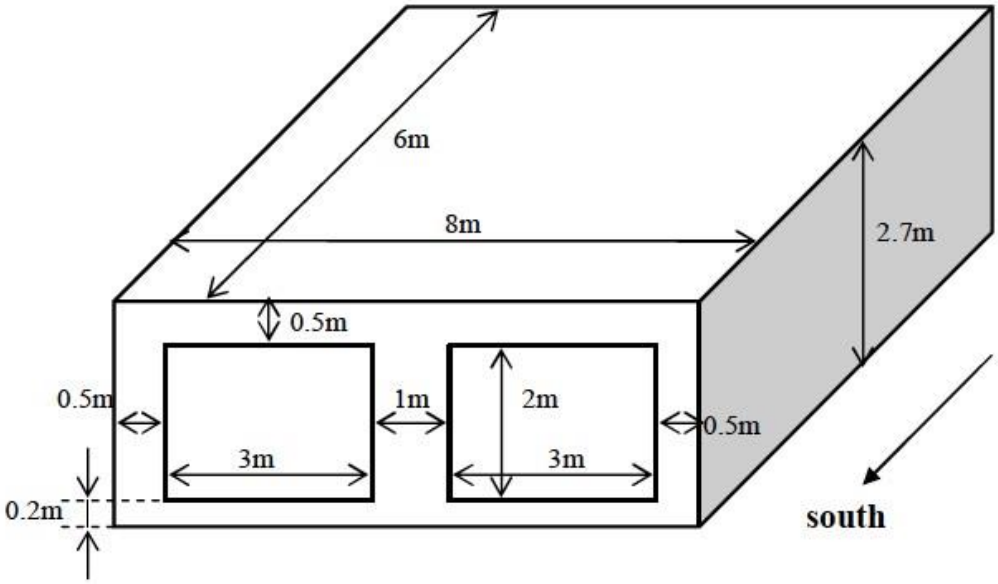

Figure 5.0 Image of building modelled in Test Case 1.

Details were given in the exercise outline regarding the buildings use. A brief overview of these is given below:

- the glazed area of the building was south facing and a constant ground temperature of 10°C was specified
- an internal sensible heat gain of 200W was included in all three variants of the case models
- an internal moisture gain of 500 g/h was activated between the hours of 09:00 and 17:00 every day and the ventilation rate in the building is maintained at 0.5 ac/h.

A range of materials was used in the building envelope constructions. The hygrothermal properties applied in ESP-r's moisture model are outlined as follows in Table 5.1**.**

Material Name	**Sorption Isotherm Data**			**Moisture Permeability**		
	U_h	A	n	a	b	c
Wood Panels	0.463	0.283	0.106	7.7E-11	-	-
Fibreglass quilt	0.02	0.007	0.01	1.58E-10	-	-
Cellulose Insulation	0.229	0.018	0.025	1.3E-10	-	-
Wood Siding	0.463	0.283	0.106	7.7E-11	-	-
Timber Flooring	0.463	0.283	0.106	7.7E-11	-	-
Insulation	0.02	0.007	0.01	1.58E-10	-	-
Roof deck	0.336	0.153	0.085	3.4E-12	-	-
Concrete Block	0.079	0.051	0.017	6.8E-03	8.21E-05	5.66
Foam Insulation						
Concrete Slab	0.079	0.051	0.017	6.8E-03	8.21E-05	5.66
Plasterboard (9mm)	57.4	28.92	28.26	$(1.68+0.0124*RH)x10^{-11}$		
Plasterboard (12mm)	57.4	28.92	28.26	$(1.78+0.018*RH)x10^{-11}$		

Table 5.1 Hygric Material properties (IEA Annex 24 Final Report, 1996) Sorption data represents coefficients produced from regression analysis. All sorption data has the unit kg/kg except for Plasterboard that uses kg/m^3.

5.2.3 Methodology

A series of models were developed and designed according to the specification given above. Cases 600_0A and 600_0B were first solved analytically with fixed outdoor boundary conditions of 10°C and 42 RH%; and the indoor air temperature was maintained at 20°C. Additionally, for Case 600_0A, solar gains were discounted from the modelling solution and the internal wall surfaces were clad with a moisture impermeable material. The latter condition was changed for the model 600_0B, as the internal wall

surfaces were made permeable and hence moisture transfer taking place between the air and the internal lining material feasible. The indoor thermal conditions were maintained between 20 and 27°C, and an air change rate of 0.5 ac/hr was maintained.

5.2.4 Outcomes from Test Case 1 simulations

The graphs below present the predictions produced by the building simulation tools used during the modelling of this exercise and the results achieved when modelling the same case using ESP-r. The tools being compared to ESP-r include Clim2000, HAMTools, BSim, Wufi+, Xam, EnergyPlus, PowerDomus, IDA ICE, TRNSYS ITT, DELPHIN, BUILTOPT-VIE, 1DHAV and SPARK. The individual results produced by the additional tools used to carry out these cases have not been highlighted in the graphs presented as this information was not made available.

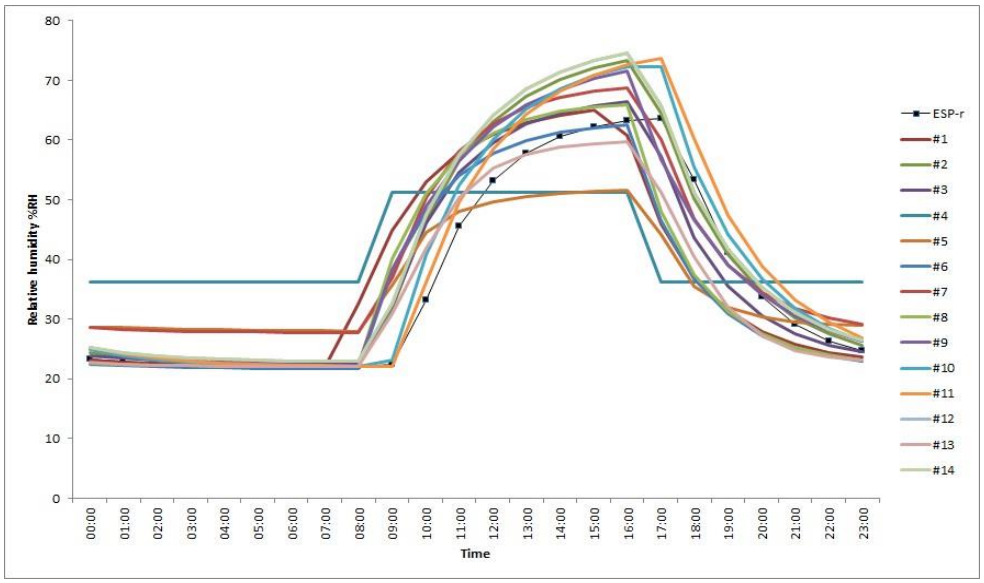

Figure 5.1 600_0A – Analytical case; Isothermal conditions with moisture tight construction surfaces (comparison between ESP-r predictions and other building simulation tools).

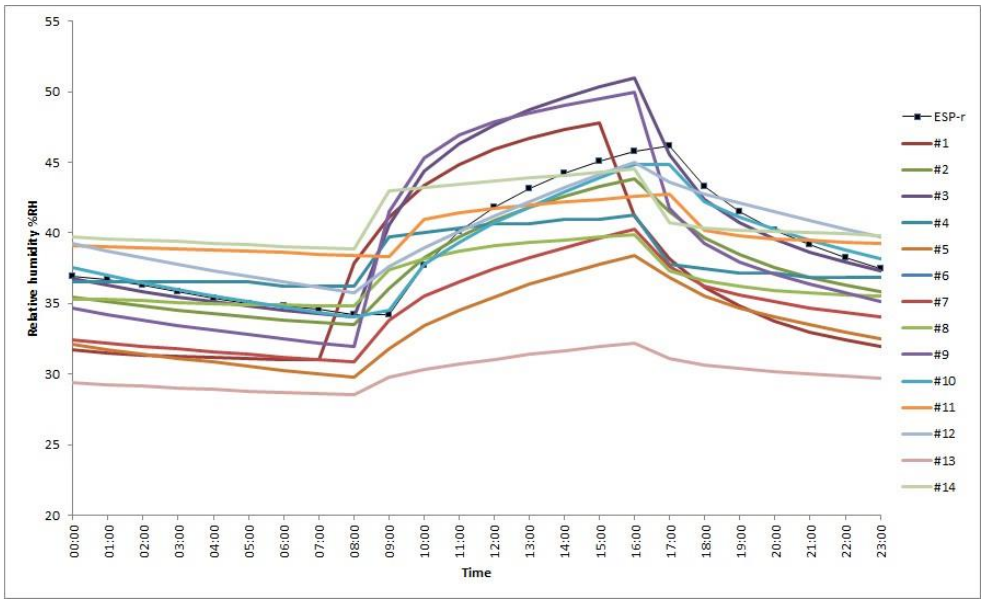

Figure 5.2 600_0B – Analytical case; Isothermal conditions with moisture permeable construction surfaces.

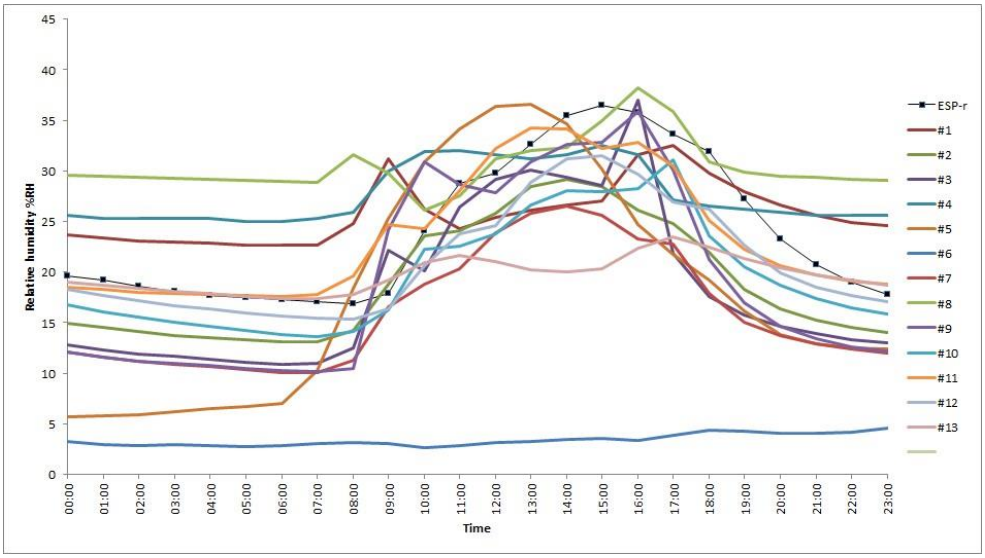

Figure 5.3 600_Open – Lightweight structure with moisture permeable construction surfaces (sample simulation period: January 4th).

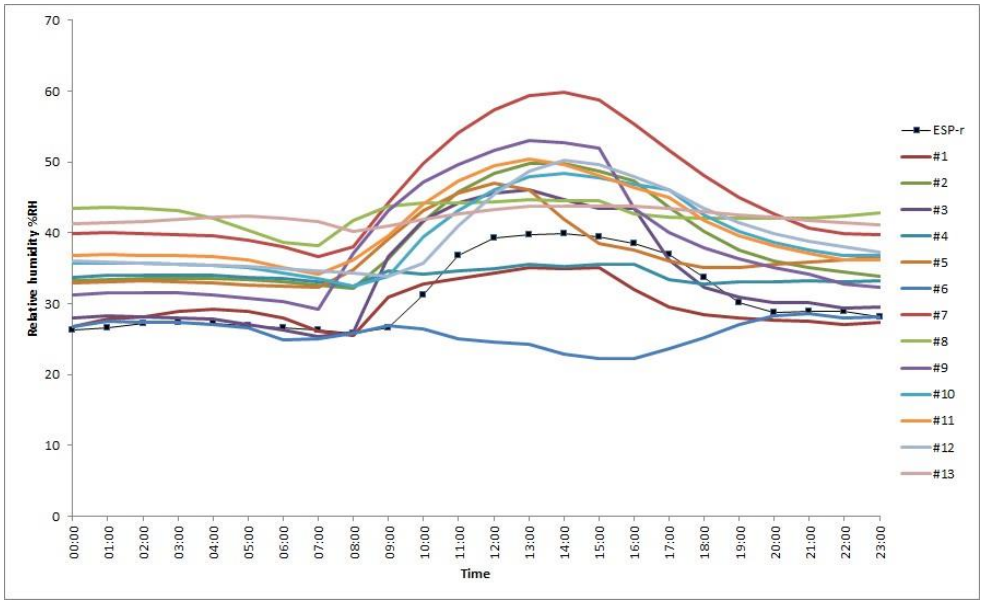

Figure 5.4 600_Open – Lightweight structure with moisture permeable construction surfaces (sample simulation period: July 27th).

The wide range of results produced by current available HAM simulation tools adopted to carry out these modelling exercises illustrates the need for improving modelling accuracy. Further explanation of the variation is provided in the following section.

5.2.5 Discussion

The inter-model comparisons presented in Figure's 5.1, 5.2, 5.3 and 5.4 highlight the wide range of results being produced by different modelling approaches used to solve the same test cases; and the reduction required in the margin of error. In both of the analytical cases looked at, ESP-r's modelling predictions lie within the range of results produced, both in terms of magnitude and the profile of the relative humidity calculated. However, as the model specification became increasingly more complicated in the latter case (600_Open) modelled, where non-isothermal conditions were applied through the use of a heating system; and a real outdoor climate was introduced, the level of variation in predictions also increased. This indicated the need to further improve the modelling of more complex indoor building environments in the context of heat and moisture transfer and to develop the consensus over the modelling of material moisture properties.

5.3 Test Case 1A

5.3.1 Objective

This exercise is a variation of the initial Test Case 1, which uses a simplified approach in terms of the boundary conditions and introduces new material properties.

5.3.2 Model Outline

Two cases were proposed that can be solved using both numerical and analytical solutions. The modelling outlines for the two cases are described as follows:

1. **Case_0A –** Isothermal exposure where both internal and external temperatures are set at 20°C. The internal surfaces of the building are kept vapour tight.

2. **Case_0B –** Similar isothermal conditions applies as in Case_0A. Internal construction surfaces are now assumed open to moisture transfer.

Further editions made to the model specification are presented below:

- The altitude is 0m.
- Building envelope construction is made of monolithic aerated concrete
- Vapour tight membranes are applied on the exterior surface of the construction (and the interior in Case_0A), preventing loss of moisture through the building walls from the internal environment.
- The exposure is completely isothermal.
- The building has no windows.
- The outside and initial conditions are stated as 20°C and 30% RH (relative humidity). These are also the initial conditions of the materials in the building envelope construction.
- The building is assumed to be floating (i.e. no ground).

Details of the thermal and physical material properties are specified in Table 5.2 and are applied to all surfaces of the model.

	□ **W/mK**	t **m**	□ **kg/m³**	C_p **J/kg.K**	□□**%**	U **W/m².K Int Surf**	U **W/m².K Ext Surf**
Aerated Concrete	**0.18**	**0.15**	**650**	**840**	**76**	**8.29**	**29.30**

Table 5.2 Thermal Property data for Aerated Concrete.

Information regarding the hygrothermal behaviour of the aerated concrete was applied using the following vapour diffusion resistance and moisture content data shown below:

1. Moisture Permeability

$$\square\square \quad \frac{1}{0.116 \quad 6.28 \quad 10^{\square 3} \exp^{4.19\square}} \qquad \square \quad \square \quad \square$$

Equation (5.0)

2. Moisture Content (kg/m³)

$$\square\square \quad \ln\square\ \square\square\square_1 \frac{1}{99.}$$
$$\square\square\ 300\square\square 1.0\ \square\_\_\_\_\_\square\square$$
$$\square\square \quad 0.0011\square\square$$

Equation (5.1)

where the units for □□are kg/m.s.Pa; and *u* represents the gravimetric moisture content (kg/m³) and□□ is the relative humidity**.**

5.3.3 Methodology

The simulations carried out included the use of a moisture injection strategy similar to that used in the original Test Case 1. Between 09:00 and 17:00 every day, moisture is injected at a constant rate of 0.5 kg/h. In order to apply this to the model, the rate was converted into a latent gain and then incorporated into the operational details of the model. Out with these hours, there was no additional moisture gain and heat gains were ignored, meaning the effect of solar gains was also excluded. As previously mentioned, the internal surfaces of the model in Case_0A were clad with a vapour impermeable material. The initial and boundary conditions used in Case_0B are identical to Case_0A however, the potential for moisture transfer through the building wall fabric is accounted for in Case_0B in the form of diffusion; which also considered a convective surface resistance to moisture transfer of 5.0×10^7 Pa.m².s/kg for the entire construction.

5.3.4 Outcomes from Test Case 1A simulations

The additional results displayed in the figures below were produced by the institutions participating in Subtask 1: Common Exercises component of IEA Annex 41.

The building simulation tools used by the institutions include HAM-Tools, BSim, Wufi+, Xam, PowerDomus, NPI, IDA ICE, DELPHIN TRNSYS ITT, HAMBase, BUILTOPT-VIE, EnergyPlus TRNSYS and TRNSYS SPARK.

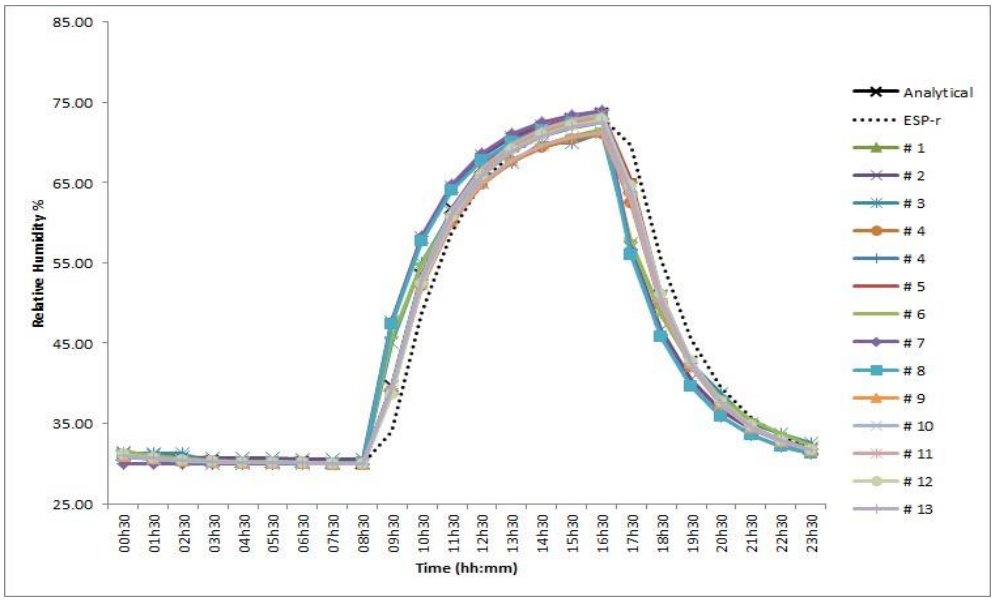

Figure 5.5 Analytical Test Case 1A_0A – Comparison between analytical solution and relative humidity predictions produced by ESP-r and other building simulation tool results.

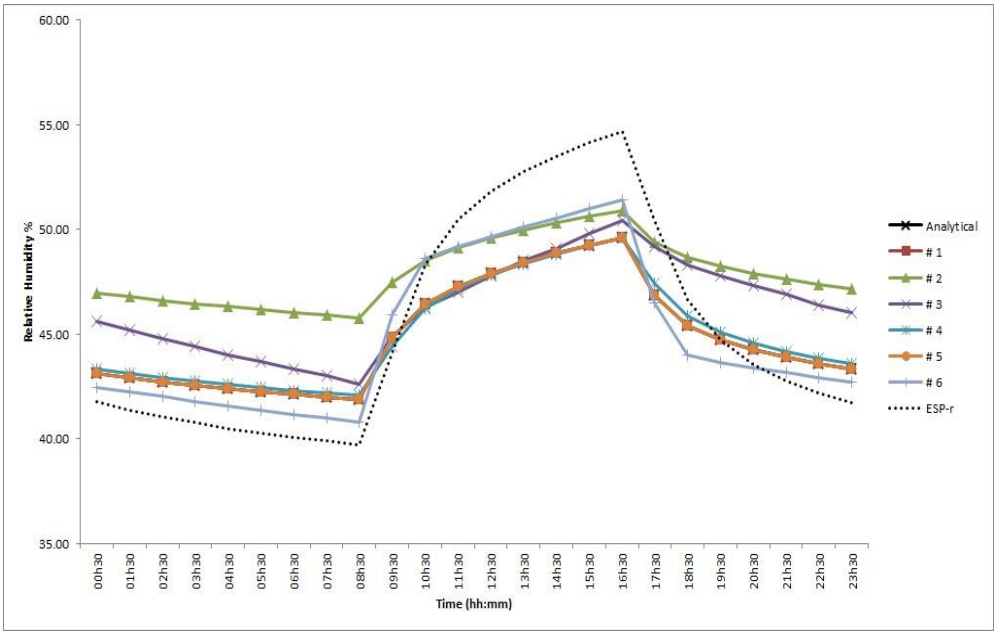

Figure 5.6 Analytical Test Case 1A_0B **-** Comparison between analytical solution and relative humidity predictions produced by ESP-r and other building simulation tool results.

As these graphs show, the impact of introducing moisture permeable building materials to the construction is significant, yet interpretation of the comparison and cause of the discrepancy between results produced by the different tools, especially when modelling the moisture buffering effect of building materials, remains challenging.

5.3.5 Discussion

Under isothermal conditions and using a vapour tight fabric on the interior lining of the building envelope, the ESP-r model is capable of predicting indoor humidity conditions with reasonable agreement to the analytical result. By not taking into account the hygrothermal interaction between the building envelope fabric and the indoor air, all other building simulation tools are also able to achieve good agreement with the analytical result in terms of the indoor air relative humidity, as can be seen in Figure 5.5. Reasonable agreement is seen when comparing ESP-r's predictions to results produced using alternative building simulation tools with HAM modelling capabilities. The range of predictions is similar with respect to magnitude and the overall profile. This outcome however, was not repeated when the moisture absorption properties of the building envelope material are included in the solution. Figure 5.6 presents the significant variation between all of the predictions, including ESP-r's, compared to the analytical solution. Although the predicted relative humidity conditions are similar with respect to the profile of the hygrothermal processes being modelled, the wide distribution of results emphasises the need to further investigate the modelling approach used when simulating the hygrothermal performance of hygroscopic building material. Test Case 1B develops this idea by investigating the impact of using more realistic environmental conditions on the modelled performance of hygroscopic building material.

5.4 Test Case 1B

5.4.1 Objective

This case adopted the simple model already specified in Test Case 1A and focused the simulation analysis on the hygrothermal performance of the indoor air and the building envelope under more realistic environmental settings. The results presented in the figures provided in section 5.4.4 are taken from the simulations carried out by the same institutions already mentioned in section 5.3.

5.4.2 Model Outline

The location used was Copenhagen (altitude: 5m, latitude: 55°37' north, longitude: 12°40' east) and the building model retains the monolithic aerated concrete construction with every surface, including the floor, subject to the same outdoor boundary conditions. Additionally, no surface coatings or membranes are applied to any face. The tables below present the material properties and hygrothermal conditions modelled.

Thickness **(m)**	0.15
Inside surface area of walls **(m^2)**	75.6
Inside surface area of roof **(m^2)**	48.0
Inside surface area of floor **(m^2)**	48.0

Internal surface resistance for heat transfer **(m^2.K/W)**	0.121
External surface resistance for heat transfer **(m^2.K/W)**	0.034
Dry density **(kg/m^3)**	600
Dry heat capacity **(J/kg.K)**	840
Dry thermal conductivity **(W/m.K)**	0.18
Initial temperature of construction and indoor air **(°C)**	20
Initial relative humidity of constructions and indoor air **(%RH)**	80

Table 5.3 Thermal and physical properties of Aerated concrete.

Internal convective surface resistance for vapour transfer **(Pa.m^2.s/kg)**	5.0×10^7
External convective surface resistance for vapour transfer **(Pa.m^2.s/kg)**	1.6×10^7

Table 5.4 Surface Transfer Properties used for Aerated Concrete.

The following hygrothermal property functions were provided as part of the exercise. The derived coefficient values entered into the ESP-r moisture model for moisture permeability were 0.116, 0.00628 and 4.19 as shown in Equation 5.2 below; and for the sorption isotherm function, the values u_h = 300, A = 0.0011 and n = 1.99 were taken from Equation 5.3.

Moisture Permeability (kg/m.s.Pa)

$$\square\square\ 0.176\ \square 10^{\square 9}.\square 0.116\square 0.00628\exp\square 4.19\square\square\square$$

Equation (5.2)

Moisture Content (kg/m^3)

$$\square\square \quad \ln\square\ \square\square\square_1{}^{\frac{1}{99.}}$$
$$\square\square\ 300\square\square 1.0\ \square\_\_\_\_\_\square\square$$
$$\square\square \quad 0.0011\square\square$$

Equation (5.3)

5.4.3 Methodology

A series of modelling scenarios were defined to investigate the impact of the realistic climate conditions on indoor relative humidity predictions, which included:

1. maintaining an indoor temperature of 20°C and neglecting external radiation. A constant indoor temperature was suggested in order for deviations in moisture calculations to be revealed.

2. control of indoor temperature in the range 20 to 27°C and again excluding external radiation. This was deemed a more realistic representation of indoor climate conditions.

3. a similar temperature control range as in scenario 2 but now including the addition of solar and long wave radiation effects through the windows and on external opaque surfaces.

5.4.4 Outcomes from Test Case 1B simulations

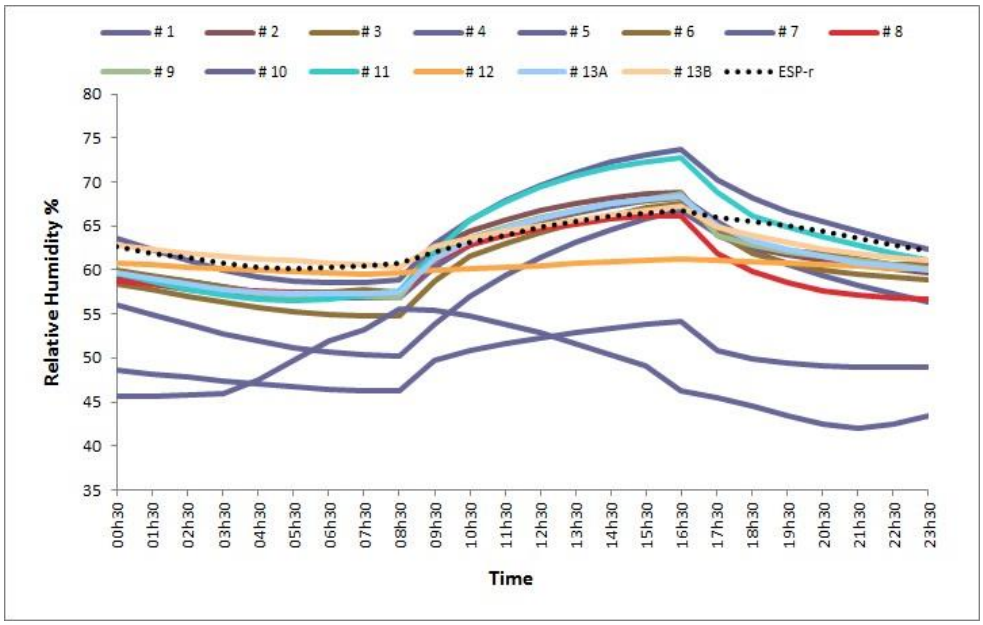

Figure 5.7 Indoor temperature is kept constant at 20°C; and no solar radiation is included.

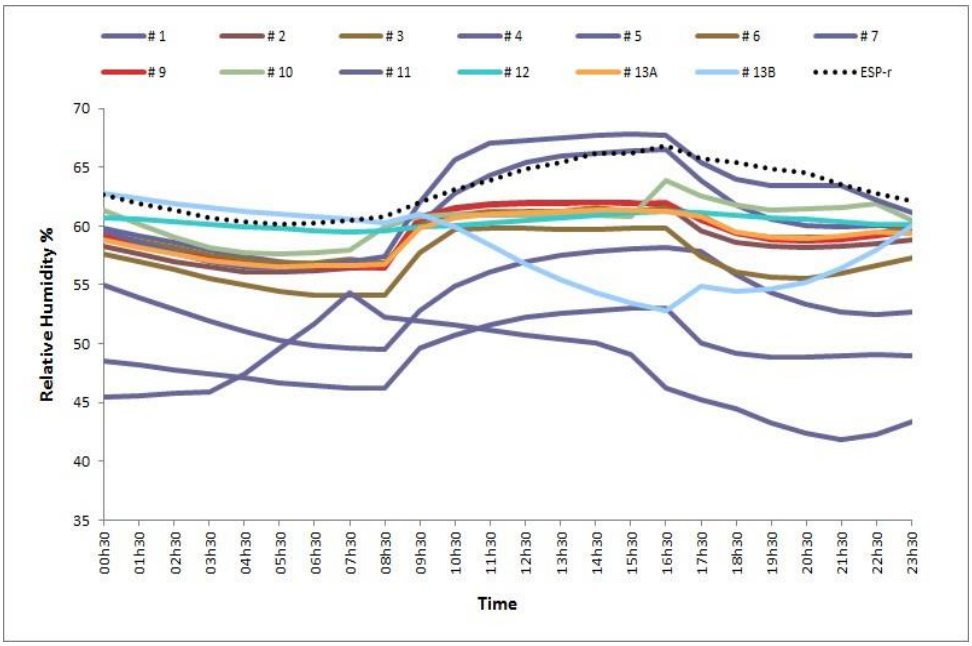

Figure 5.8 Indoor temperature fluctuates between 20 and 27°C; and no solar radiation was considered.

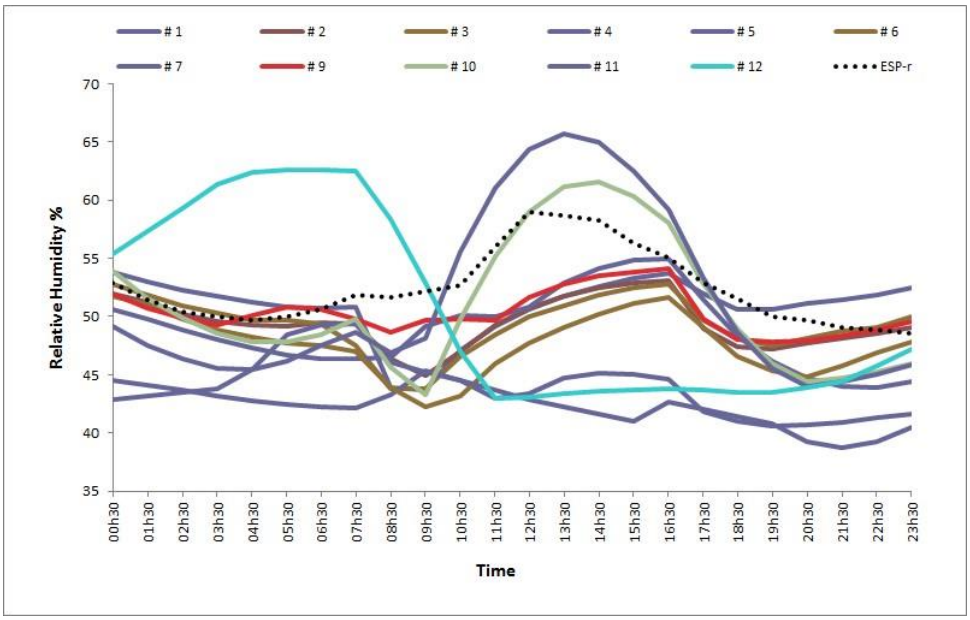

Figure 5.9 More realistic case where indoor temperature fluctuates between 20°C and 27°C; and solar and long wave radiation is considered.

As in Test Case 1, the wide distribution in the simulation results highlights the difficulty associated with interpreting the comparison between different moisture modelling tools and therefore the accuracy of the approaches adopted.

5.4.5 Discussion

This exercise involved the simulation of a moisture permeable construction exposed to varied environmental conditions. An isothermal case, followed by two cases with an applied temperature control range was modelled. Solar gains were ignored only

in one of the cases and a constant ventilation rate was applied across all three. A fixed sensible heat gain was also applied in all three cases. Comparison between ESP-r predictions for the three test cases and solutions provided by alternative building simulation software capable of heat, air and mass transfer modelling showed a large degree of variation exists in outcomes, although ESP-r predictions were seen to lie within the upper and lower boundaries of the results. These findings further highlighted the differences in modelling approaches being used with respect to the incorporation of material moisture properties and the influence of variable outdoor climate conditions on the indoor environment; and hence the uncertainty surrounding moisture modelling predictions. Results from all three case models emphasised the need for more detailed analysis of the approaches used to solve combined heat and moisture transfer processes taking place when more complex climate conditions are introduced. As already observed in Test Case 1A, the importance of accurate integration of hygrothermal material properties into the numerical modelling procedure remains a key factor. The impact of hygroscopic building materials on indoor moisture conditions was further examined in Test Case 2. Given the modelling uncertainty that has arisen when variable boundary conditions have been used, as in Test Case 1B, simplified environmental conditions and a scheduled moisture production scheme were applied.

5.5 Test Case 2

5.5.1 Objective

In order to propose and design suitable indoor environmental control methods for residential spaces, it is important to investigate the influence of both the ventilation rate in an indoor space and the impact of hygroscopic building materials. This test case was designed to look at the influence of both of these building parameters on indoor humidity conditions. Using results of an experiment carried out in an environmental test chamber called THU Test room (Yoshino H et al, 2008), an empirical validation was conducted by applying the building simulation tool ESP-r to model the original empirical study, in order to assess the level of agreement between measured and predicted data.

5.5.2 Model Outline

Each of the experiments consisted of a preconditioning period to ensure the ambient conditions in the test chamber were set at 20°C and 50 RH%. Following this, a 6-hour period of humidification was activated before returning to the initial environmental conditions for a period of 12 hours. This moisture production profile is displayed in the figure below. A target moisture injection rate of 20 g/h was applied in the chamber by heating two water reservoirs with an electric element.

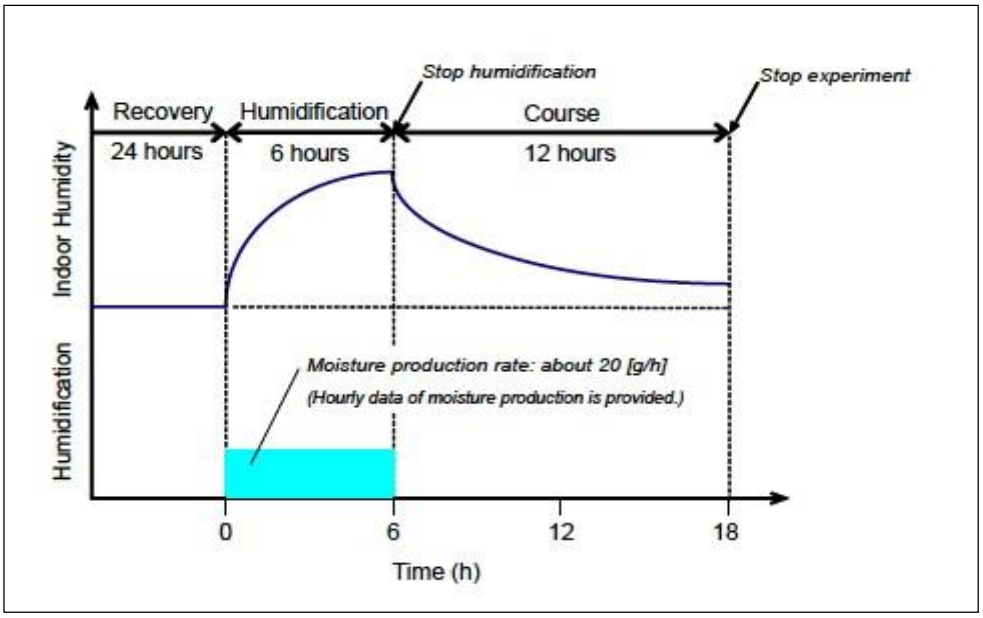

Figure 5.10 Schedule of humidification in test chamber (Yoshino H et al, 2008)

The target ventilation rates, locations of hygroscopic building materials installed in the chamber and the associated hygrothermal material properties are shown in the tables below.

Case	**Ventilation rate (ac/h)**	**Location of Moisture Buffering material**
Case 1-1	0	3 sides of walls, ceiling and floor
Case 1-2	1.0	
Case 1-3	5.0	

Table 5.5 Cases focusing upon influence of ventilation rate.

Case	**Ventilation rate (ac/h)**	**Location of Moisture Buffering material**
Case 2-1	1.0	All walls, ceiling and floor
Case 2-2		Floor
Case 2-3		One side of walls
Case 2-4		3 sides of walls
Case 2-5		Ceiling
Case 2-6		None

Table 5.6 Cases focusing upon location and quantity of moisture buffering material.

Material	t **m**	□ **kg/m³**	□□□ **m³/m³**	C_p **J/kgK**	□□□ **W/mK**	□ **dry**	W_{80} **kg/m³**	W_f **kg/m³**

Polystyrene	0.1	30	0.95	1500	0.04	50	0	0
Aluminium	$1x10^{-4}$	-	-	-	-	$2x10^{8}$	0	0
Gypsum Board	0.0125	850	0.65	850	0.2	8.3	6.3	400
Vinyl sheet	$2x10^{-4}$	-	-	-	-	1605	0	0

Table 5.7 Hygrothermal Properties for model construction (provided in the IEA Annex 41 exercise overview).

The focus of cases 1-1 to 1-3, outlined in Table 5.5, was to investigate the impact of different ventilation rates on the moisture conditions within the test chamber, whereas cases 2-1 to 2-6 (displayed in Table 5.6) turned the attention of the investigation onto the impact of the location and number of moisture permeable and impermeable building materials on absolute humidity within the chamber. The multilayered material construction of the chamber walls is illustrated in Table 5.7, where the Vinyl sheet was applied to create the moisture impermeable internal wall lining necessary in case 2-6. Application of the defined test conditions is described further in the methodology.

5.5.3 Methodology

The investigation focused, initially, on testing the influence of the ventilation rate, before the impact of the location and quantity of hygroscopic building material within the modelled environmental chamber was looked at. ESP-r was able to model the range of ventilation rates in the test case by setting a defined air change rate; and modelled the hygrothermal behaviour of the required materials using derived moisture transfer coefficients for both the moisture permeability and the sorption isotherm functions. The moisture production profile described was reproduced in the simulation by calculating an equivalent latent gain using Equation 5.4. This was coupled with a sensible heat gain produced as a result of the heating element and defined as part of the operational details of the model.

$$Q = m \cdot h_{fg}$$

Equation (5.4)

where Q represented the Total Energy (W), m the mass flow rate (kg/s) and h_{fg} the energy resulting from phase change.

5.5.4 Outcomes from Test Case 2 simulations

The results presented are for the cases where empirical data was available to compare with ESP-r modelling predictions.

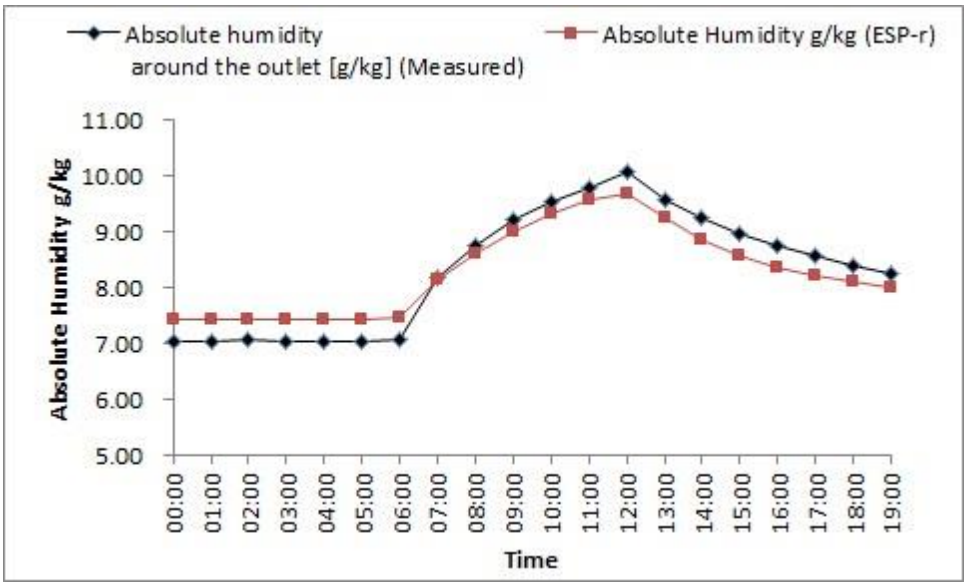

Figure 5.11 Ventilation rate is 1.0 ac/hr and all construction surfaces are moisture permeable [Case 1-2 and Case 2-1].

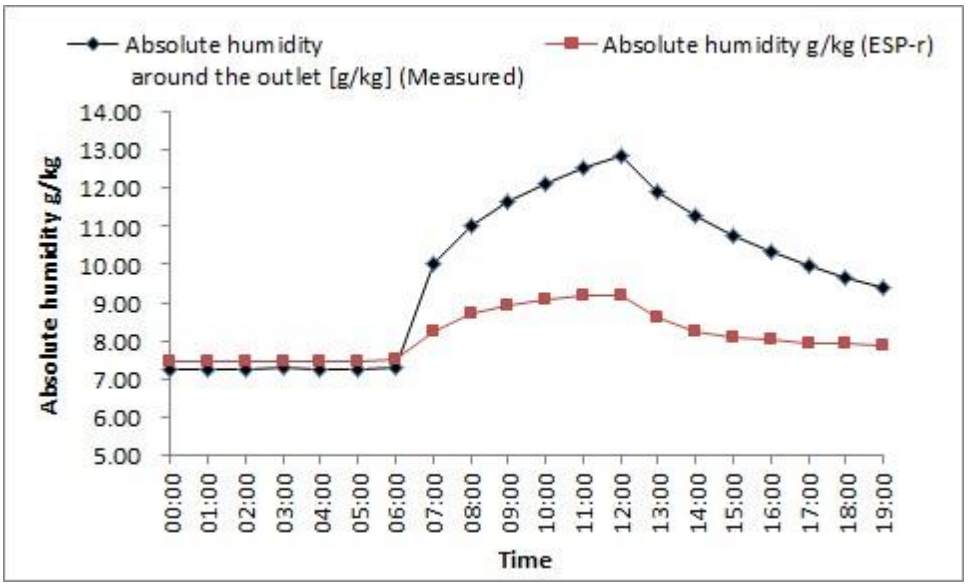

Figure 5.12 Ventilation rate is 1.0 ac/hr and only the floor has moisture permeable construction [Case 2-2].

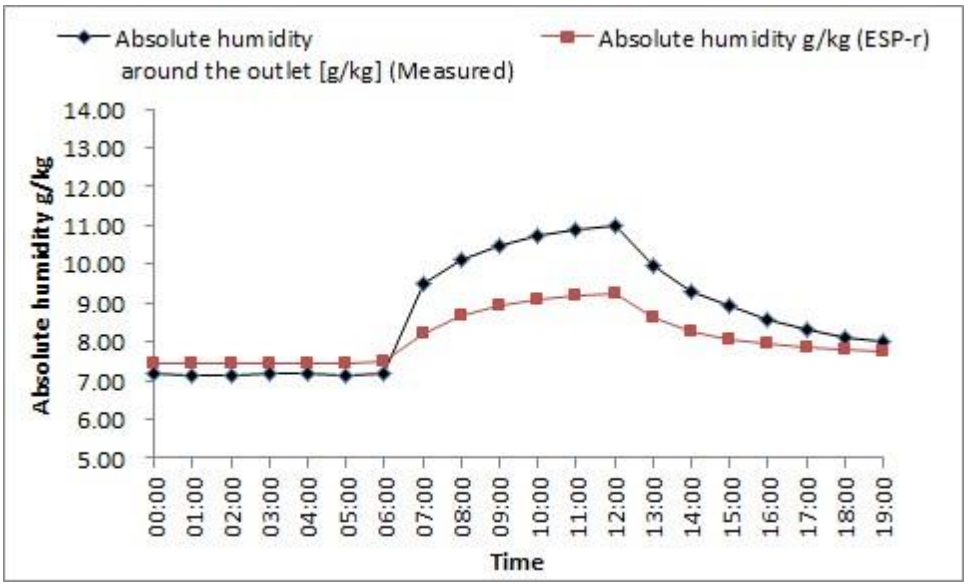

Figure 5.13 Ventilation rate is 1.0 ac/hr and only one wall has moisture permeable construction [Case 2-3].

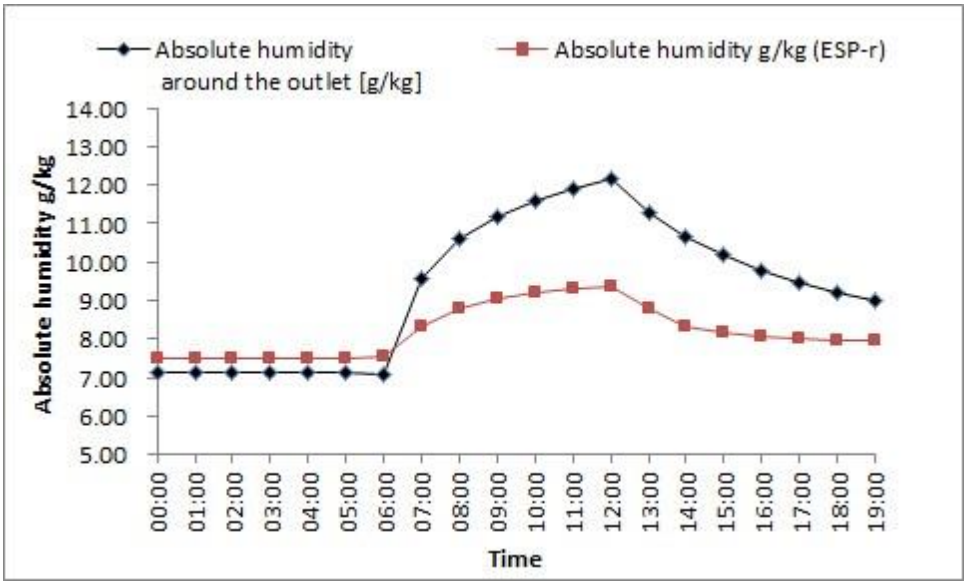

Figure 5.14 Ventilation rate is 1.0 ac/hr and only the ceiling has moisture permeable construction [Case 2-5].

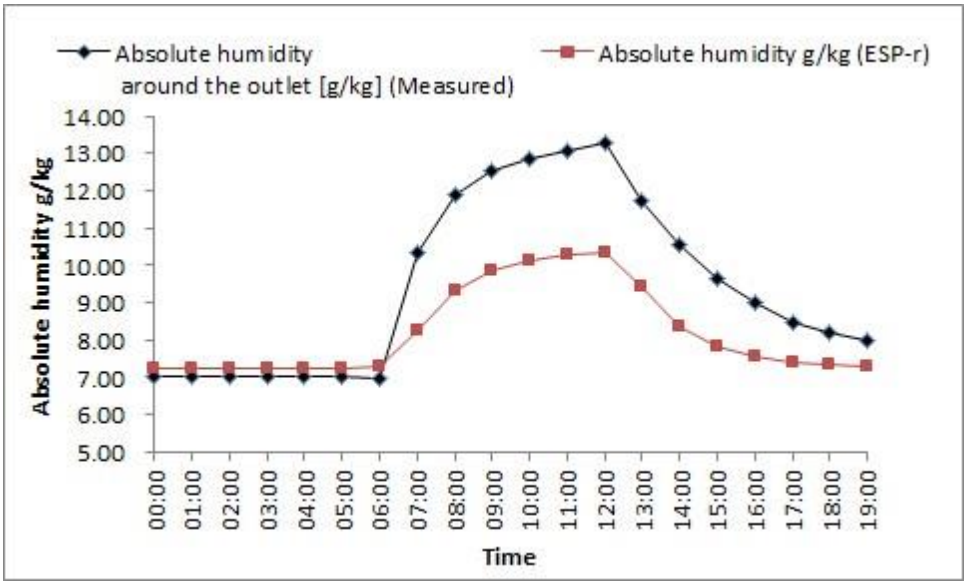

Figure 5.15 Ventilation rate is 1.0 ac/hr and all surfaces are impermeable to moisture [Case 2-6].

The same basic pattern emerges when comparison of results is made, in all but one of the graphs presented above. Issues related to the level of agreement achieved between measured and predicted absolute humidity is discussed in the following section.

5.5.5 Discussion

Reasonable agreement between predicted and empirical data was achieved in Case 1-2 and Case 2-1, where all surfaces in the chamber were lined with moisture permeable material. There was a significant difference between predicted and experimental results for Cases 2-2 to Case 2-6, as the location and quantity of moisture permeable material was varied. The greatest difference was seen in Case 2-2 where only the floor provided the potential for moisture buffering in the walls of the chamber. Modelling predictions for all the cases assessing the impact of material quantity and orientation were similar in magnitude and underestimated the peak absolute humidity within the chamber. This indicated that neither the location nor the quantity of hygroscopic building material were the most influential factors in determining the final air mass balance calculation. A more detailed representation of the airflow characteristics inside the chamber would be required, as this was shown to have a greater influence on the modelled humidity conditions in the chamber. This could help to improve interpretation of the boundary conditions, in particular at the chamber wall surfaces, and therefore increase understanding of the interaction between indoor air moisture and the surrounding internal surfaces of the chamber.

Given the two test cases that have gone before in sections 5.1 to 5.5, a third test case was undertaken to develop the overall investigation into the modelling of the effect of moisture buffering materials within a more complex and dynamic multi-zone building environment. A combination of attributes from the previous test cases have been

incorporated into the model, including multilayered construction and variable climatic settings, with the addition of surface finish coatings. The underlying aim is to assess the accuracy of the moisture modelling approach being implemented when compared to measured data.

5.6 Test Case 3

5.6.1 Objective

The exercise was designed to observe the extent to which the moisture buffering effect of common building materials positioned at the internal faces of the building envelope construction influence the indoor humidity conditions. The level of agreement between predicted and empirical results forms the basis for the assessment of the suitability of the modelling approach.

5.6.2 Model Outline

A model connecting a series of zones with individually specified indoor climates and boundary conditions was constructed. Focus was placed on two of the zones being modelled, the Reference room and the Test room, which are identical in geometry. Different material finishes were applied to the internal surfaces of the building envelope. Each of the three steps of the modelling procedure varied the orientation and the total wall surface area with an applied moisture absorbent material. The results would provide insight into the accuracy of the modelling approach used to determine indoor climate conditions in the scenarios outlined in Table 5.8.

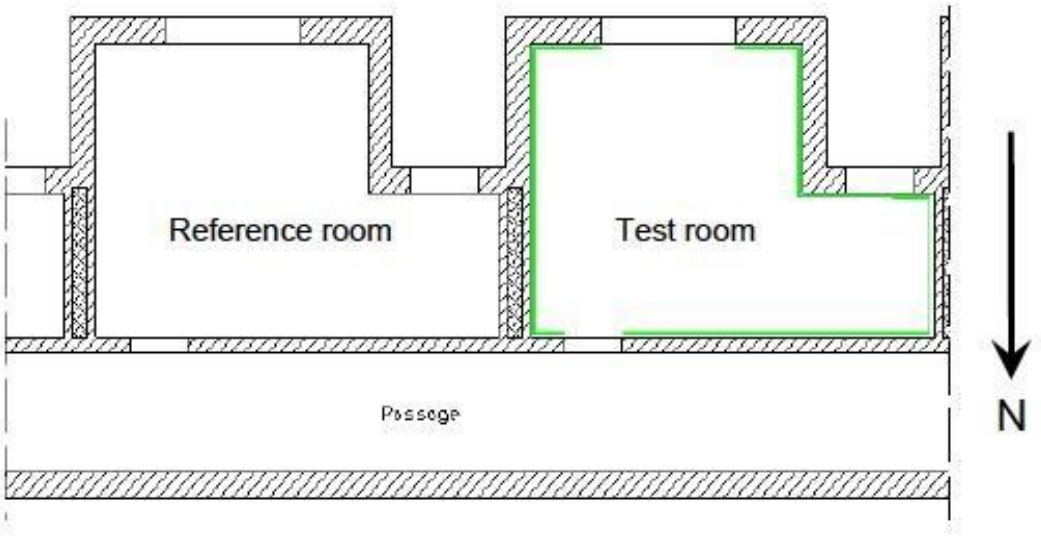

Figure 5.16 Overview of zonal floor plan (Lengsfeld K, 2008).

The indoor air temperature in both Reference and Test Room was maintained at 20^0C using a basic heating controller system with a maximum power output specified at 1kW.

Due to surface defects and natural leakage through joints in a buildings construction, the rooms were sealed using masking tape to limit the ingress of airflow. A ventilation system was applied to the Reference and Test Room's following tracer gas tests that were carried out to calculate the air change rate during operational hours. The results indicated an air change rate of 0.63 ac/hr in the Reference room; and 0.66 ac/hr in the Test Room.

The moisture production schedule shown below in Figure 5.17 has been designed to represent a four person household. This has been applied to both rooms and the diurnal pattern is described as follows:

1. Between 00:00 and 06:00, a basic production rate of 0.025 kg/hr is assumed analogous to pets and general items such as plants;
2. Between 06:00 and 08:00, the rate increases to 0.4 kg/hr to account for human activities such as showering and washing that would be taking place during these hours;
3. The basic rate of 0.025 kg/hr is resumed after the periods of occupation;
4. A longer moisture production period of 6hrs becomes active between 16:00 and 22:00, which represents activities such cooking or drying laundry.

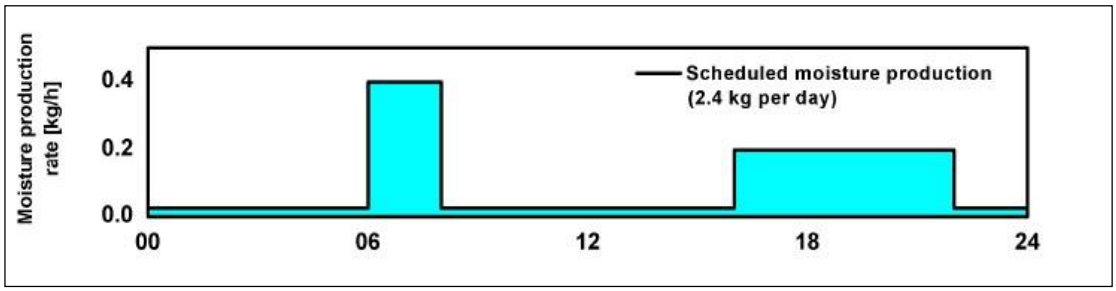

Figure 5.17 Moisture production schedule (representative of daily occupied periods) (Lengsfeld K, 2008).

The boundary conditions were varied at different locations around the building. At the South-facing wall, the external boundary conditions were represented by the Holzkirchen climate. An additional climate was applied specifically to the North facing section of the building and in the region above the ceilings of both zones. The ground temperature was specified as 2˚C on average and was assigned to the model using a ground temperature profile facility available in ESP-r. Figure 5.18 is an image of the model produced during an ESP-r session.

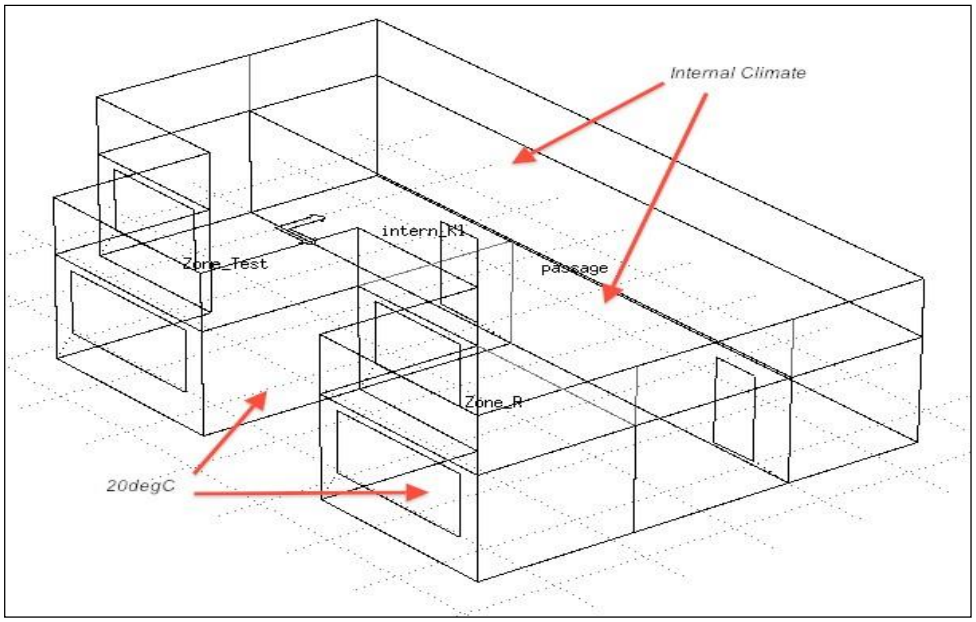

Figure 5.18 Screen shot of ESP-r model.

The radiative surface properties and the total surface resistance coefficients for the ceiling, floor and both inside and outside walls was provided in the exercise specification as shown below. This caused confusion with respect to which values to model. For this reason, the surface heat transfer coefficients used in the model were calculated by using the default buoyancy driven setting in ESP-r. The radiation properties applied to surfaces in the model were as follows:

- Internal opaque surfaces (emissivity and absorption)
  - Long wave: 0.9
  - Short wave: 0.4
- External surfaces (emissivity and absorption)
  - Long wave: 0.9
  - Short wave: 0.4

The convective heat transfer coefficients applied to the different surfaces of the model are given below:

- Outside walls
  - Internal surface: 8 $W/m^2.K$
  - External surface: 18 $W/m^2.K$

- Inside walls
  - Internal surface: 8 $W/m^2.K$
  - External surface: 8 $W/m^2.K$

- Ceiling
  - Internal surface: 8 W/m^2.K
  - External surface: 8 W/m^2.K

- Floor
  - Internal surface: 8 W/m^2.K
  - External surface: 99 W/m^2.K

5.6.3 Methodology

Table 5.8 below displays the series of steps taken in the modelling study in order to address the impact of hygroscopic building material. A gradual application of the Gypsum Board into different internal surface locations enabled the analysis of the materials performance to be assessed.

Step 1 was used to compare the impact of a coated moisture absorptive surface applied in a Reference Room to a Test Room with impermeable wall surfaces on indoor relative humidity conditions. The simulation procedure was adapted in Step 2 to include an uncoated moisture permeable material in the internal lining of the walls of the Test Room, enabling comparison to be drawn between the relative humidity conditions achieved under these design circumstances and those observed when the internal surfaces are painted.

Finally, the simulation for Step 3 involved all of the surfaces in the Reference Room remaining finished with painted gypsum plaster however, the Test Room was now finished with uncoated Gypsum Board on all surfaces, including walls and the ceiling. This approach was based on assessing the effect of the quantity of moisture buffering material present in a room as opposed to its location, as was the case in Step 2. The outdoor climate of Holzkirchen (Germany) was used in each of the steps.

	Step 1	**Step 2**	**Step 3**
Simulation period	17.1.2005 – 2.2.2005	14.2.2006- 20.3.2006	27.3.2006- 22.4.2006
Reference Room	Painted gypsum plaster	Painted gypsum plaster	Painted gypsum plaster

Test Room	Aluminium foil	Gypsum boards on the walls	Gypsum boards on ceiling and walls
Temperature and moisture load	20^0C / 2.4 kg/day	20^0C / 2.4 kg/day	20^0C / 2.4 kg/day

Table 5.8 Outline of simulations undertaken.

An overview of the results for each of the outlined steps is provided in the following sections.

5.6.4 Outcomes from Test Case 3 simulations

5.6.4.1 Step 1

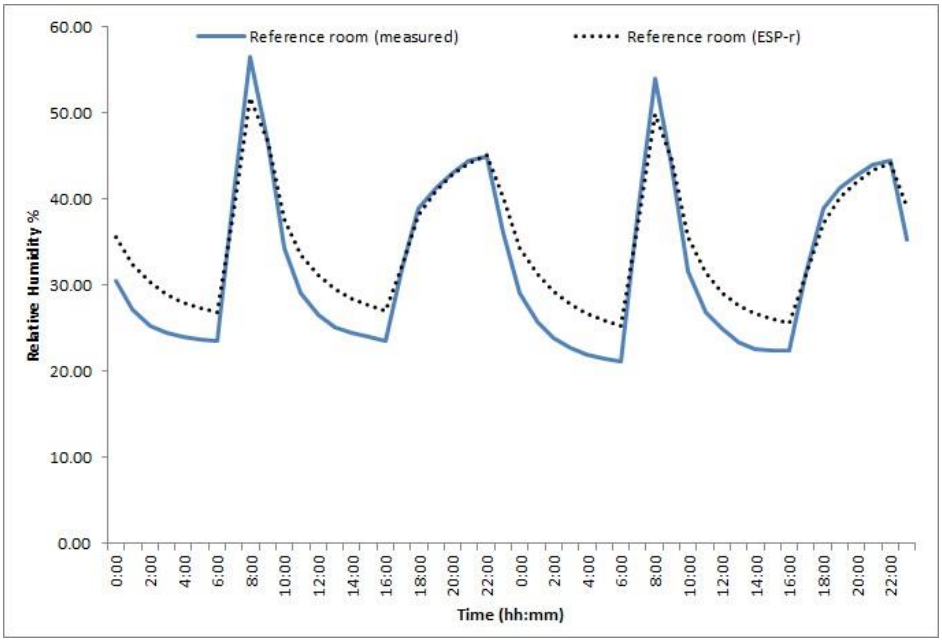

Figure 5.19 Modelling of coated gypsum plaster in Reference Room (25.1.2005 – 26.1.2005) Comparison between measured and predicted results.

Figure 5.19 shows the relative humidity obtained from measured data and from the results obtained using ESP-r simulations over a selected period of two days. There is reasonable agreement, in terms of the peak humidity, in both sets of results. The level of agreement between predicted and measured decreases however, after the moisture injection period has ceased. A slower rate of decay (between 08:00 and 16:00; and 22:00 and 06:00) in the simulation, results in the predicted minimum relative humidity being greater than that, which has been measured. On average, the difference was 12.6% across the simulation period. This also has the added effect of producing a higher average humidity over the whole simulation period when compared to the measured data.

The results displayed in Figure 5.20 compare the relative humidity conditions predicted by ESP-r for the Test Room to the measured data. There is reasonable agreement between the two sets of results both in terms of peak and average relative humidity. When comparing the relative humidity conditions in the two rooms, it can be seen that the effect of the paint layer in the Reference Room is similar to that of the impermeable surface i.e. aluminium foil, being used in the Test Room.

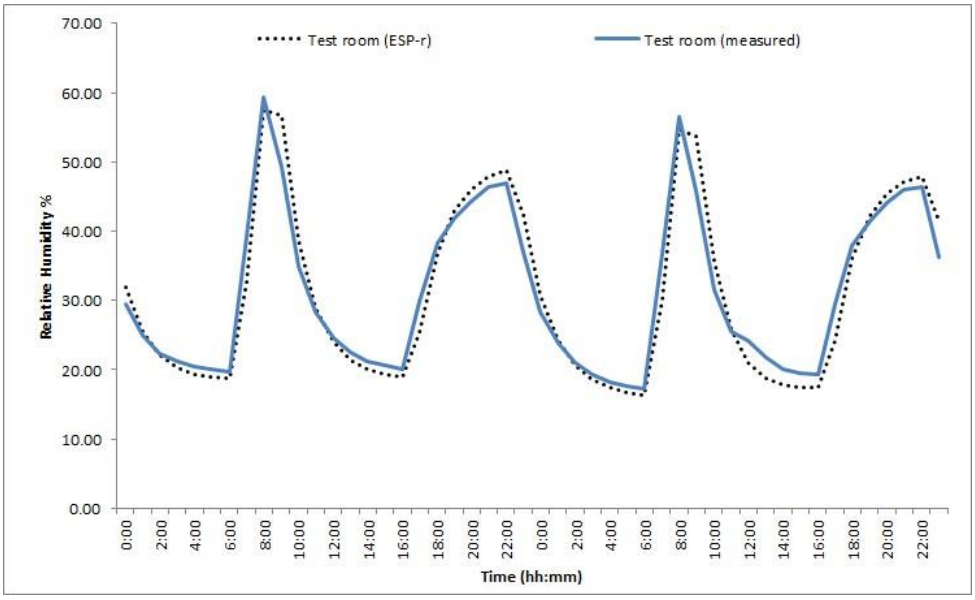

Figure 5.20 Modelling of impermeable surfaces in Test Room (25.1.2005 – 26.1.2005) Comparison between predicted and measured relative humidity in the Test room.

Having completed the first step of the series of simulations, it was necessary to proceed to the second stage that would highlight the effect of introducing moisture permeable materials at the internal surface wall lining of the Test Room.

5.6.4.2 Step 2

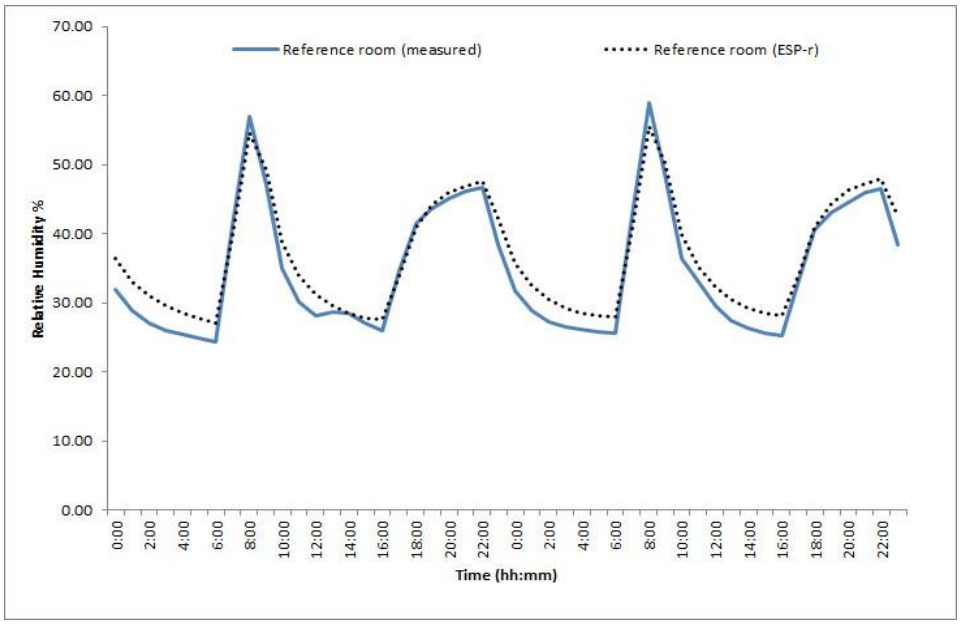

Figure 5.21 Modelling of painted gypsum plaster in Reference Room (17.2.2005 – 18.2.2005) Comparison between measured and predicted results.

Figure 5.21 displays the relative humidity performance inside the Reference Room over a selected two-day period in winter. Reasonable agreement in peak and average relative humidity values was achieved. The peak and average relative humidity values decrease significantly in the Test Room however, as is shown in Figure 5.22. By using uncoated gypsum plasterboard to line the internal wall surfaces, the additional moisture buffering capacity being provided is evident; and the total range of the relative humidity (maximum – minimum) is reduced.

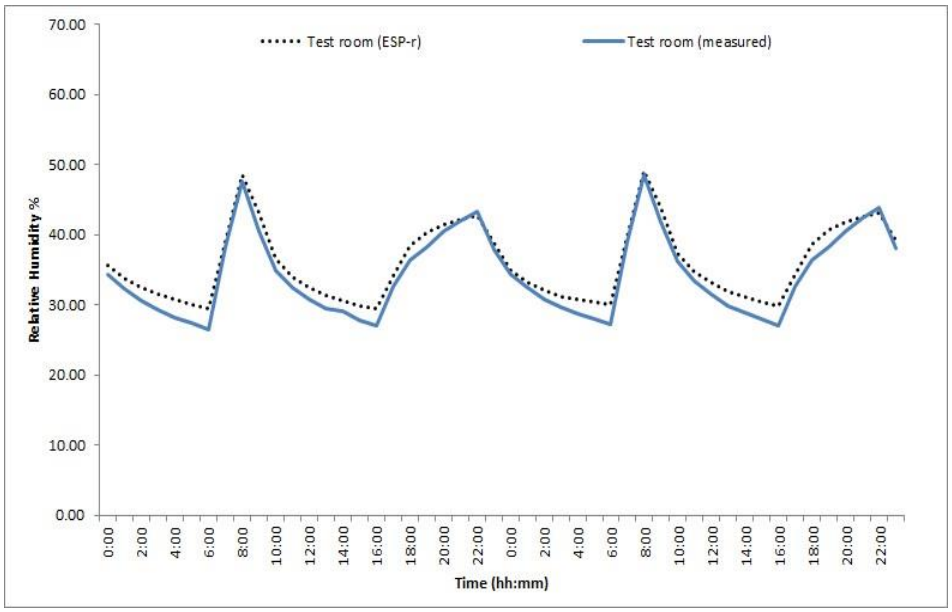

Figure 5.22 Modelling of gypsum board on the walls of the Test Room (17.2.2005 – 18.2.2005) Comparison between predicted and measured relative humidity in the Test room.

Following on from Step 2, simulation of the effect of multiple hygroscopic materials lining the internal wall surfaces of the Test Room was undertaken in Step 3.

5.6.4.3 Step 3

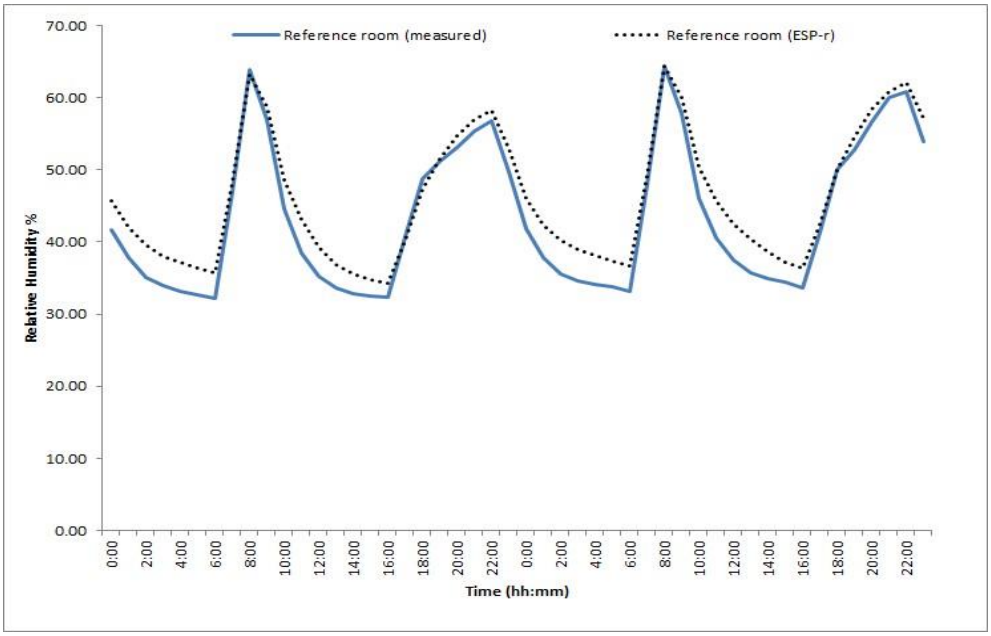

Figure 5.23 Modelling of painted gypsum plaster in Reference Room (4.4.2005 – 5.4.2005) Comparison between measured and predicted results.

Results from Step 3 for the Reference Room show similar indoor moisture performance characteristics to that seen in Steps 1 and 2. On average, peak relative humidity values were underestimated by 0.3%RH after the first moisture injection period (06:00 – 08:00); and overestimated by 2%RH during the second moisture injection period (16:00 - 22:00). An overestimation of the relative humidity, following each moisture injection period, indicated a reduced rate of moisture absorption - a pattern in behaviour that was also observed in the Test Room.

The resulting difference between the predicted and measured peak and average relative humidity values in the Test Room was even greater, as is shown in Figure 5.24. Simulation predictions produced an overestimation of the base relative humidity values, with an average difference of 8.2%RH between predicted and measured data. Over the course of the whole simulation period (26 days), the average predicted relative humidity was 5.7%RH greater than the average of the measured data.

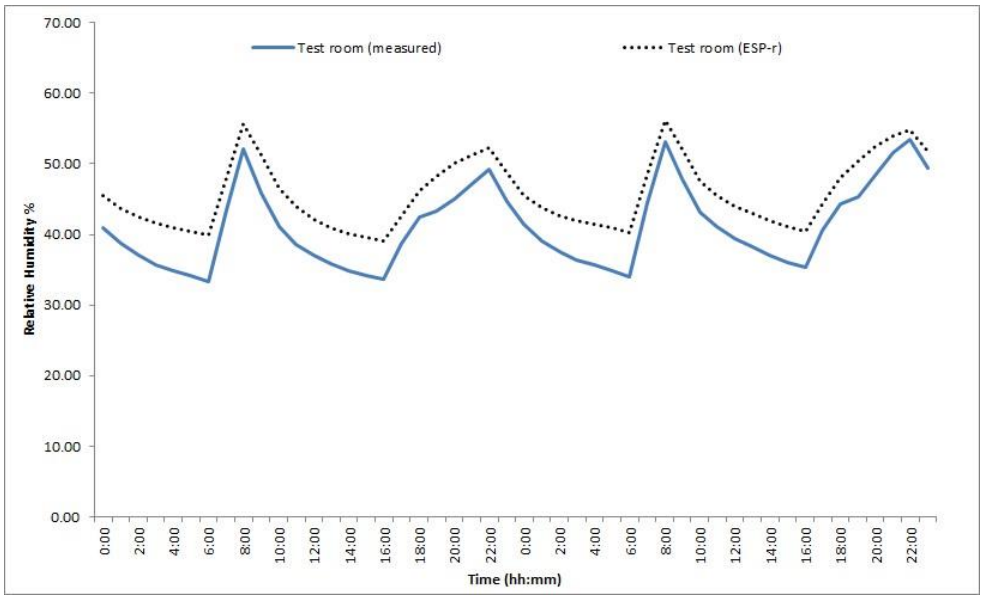

Figure 5.24 Modelling of gypsum board on all walls and ceiling in the Test Room (4.4.2005 – 5.4.2005) Comparison between predicted and measured relative humidity in the Test Room.

As was the case in Step 2, moisture permeable surfaces in the Test Room helped to reduce peak and average relative humidity values. In terms of the total range of the relative humidity in the Test Room i.e. the difference between the maximum and minimum relative humidity, there was no significant difference observed by having an additional moisture absorbent material at the internal surface of the ceiling. However, the predicted average relative humidity in Step 3 was higher than that produced in Step 2. This shift could be attributed to increased seasonal air moisture content being ventilated into the room from the external environment.

5.6.5 Discussion

Results have shown that the moisture buffering potential of moisture absorbent materials is reduced when a layer of paint is applied to an exposed material surface. This reduced absorption rate was prominent in the Reference Room, following each moisture injection period; and resulted in a higher relative humidity being predicted. In order to address this difference, further investigation of the modelling of the absorption and desorption processes; and moisture permeability specifically of thin layers is required in order to provide insight into the suitability of the modelling approach currently adopted in ESP-r. ESP-r uses empirically derived coefficients taken from published catalogues to represent the moisture properties of the materials being modelled. These are applied in ESP-r's existing sorption isotherm and moisture permeability functions, which are called during the simulation process to calculate the moisture content and moisture permeability of a material at a predefined moisture node in a material layer. The single function for the sorption isotherm can be assumed analogous to the average of the absorption and desorption curves, in cases where measured data is available for both of these processes. When this data is not available however, the absorption isotherm data is assumed as the default function. With respect to calculating moisture permeability, the default equation used by ESP-r that requires three empirically derived coefficients, is not always represented in material catalogues. Alternative values given in the form of the standard diffusion thickness or the vapour diffusion resistance factor are adapted therefore to fit this existing format.

For the steps where a paint layer was not applied on the internal wall lining material (Step 2 and Step 3), the effect was to produce a greater reduction in both the peak and average relative humidity values over the simulation period; and to decrease the total range between maximum and minimum relative humidity. As can be seen in the results produced in Step 2 and Step 3, there is also reasonable agreement achieved between predicted and measured values of peak humidity. In addition, the profile of the predicted relative humidity values in these steps follows that of the measured data.

5.6.6 Summary of Test case outcomes

Throughout the series of modelling test cases presented, a range of boundary conditions and building constructions have been applied. Reasonable agreement has been achieved between the modelling predictions and analytical results consistently when simplified building constructions i.e. monolithic construction or vapour tight surfaces; and isothermal conditions were used, as was observed in Test Case 1A. The deviations between the numerical and analytical results coincided with the introduction of dynamic environmental conditions and the increased application of hygroscopic material properties in multilayered building envelope construction.

The wider distribution of results seen in Test Case's 1 and 1B could not be explained simply as a response to the changes made to boundary conditions. Significant differences were observed between the results of the various modelling tools used (including ESP-r) and the analytical results, even when constant indoor temperature conditions were used. This was also observed in Test Case 2, where differences between numerical and measured relative humidity data (designed to test the impact of varying the number and location of hygroscopic surfaces within a climate chamber indoor moisture conditions) arose despite the isothermal conditions applied. Possible causes of the differences in Test Case 2 were linked to potential uncertainty in the experimentation procedure itself, and the possibility of variable surface boundary conditions influenced by the airflow characteristics of the chamber. This was recognised when minimal variation in the predicted values of absolute humidity occurred in the different experimental permutations.

The impact of the moisture absorbing potential of different materials on indoor relative humidity conditions was significant, however, in Test Case 3. This case reaffirmed the need for accurate representation of the characteristics of moisture permeable construction, including thin layers. This was highlighted in Step 3 where ESPr predictions were seen to overestimate the indoor relative humidity. The potential cause of the discrepancy was attributed to ESP-r's use of the absorption isotherm to represent both absorption and desorption of moisture to and from a material, respectively. From the range of test cases conducted, it was difficult to find consensus on the cause of the differences between analytical and numerical results; and measured and numerical results. This was, in the main, due to the challenges posed by the associated complexity of the interrelated nature of the transfer processes occurring, which contributed to the difficulty of identifying specific transport effects or physical factors responsible for the range of hygrothermal behaviour observed in the test cases conducted. In light of the summary conclusions drawn in this section, a further investigation of the coupled heat, air and moisture modelling capabilities of ESP-r, within the context of a recent project (discussed in Chapter 1), was conducted and is described in the following section.

5.7 Applying ESP-r's moisture model to assess impact of indoor clothes drying

Application of ESP-r's moisture modelling facility in this project was an opportunity to gain further insight into the modelling of specific factors affecting the hygrothermal performance of the indoor environment. In doing this, the challenge of separating the transport effects influencing moisture transfer between the indoor air and hygroscopic building materials, as stated in section 5.6.6, could be addressed.

The project was designed to investigate the impact of occupant related moisture generation on the indoor environment. The specific moisture generating activity identified is the passive indoor drying of laundry. This has become a prominent feature

of occupant behaviour in social housing, resulting in elevated levels of indoor air moisture. The primary reasons for this type of laundry drying behaviour being adopted are minimal provision of secure and convenient outdoor spaces; and poor outdoor weather. Studies have shown a correlation between low-income families and high laundering loads, a consequence of high occupation intensity over daily and weekly periods (Porteous et al, 2012). Figure 5.25 presents vapour pressure values calculated using monitored indoor relative humidity and temperature data collected from housing case studies used in the project. Therefore, the risk of elevated indoor moisture levels exceeding recommended thresholds for the proliferation of allergens such as dust mites, (Platts-Mills et al, 1989) is clearly evident.

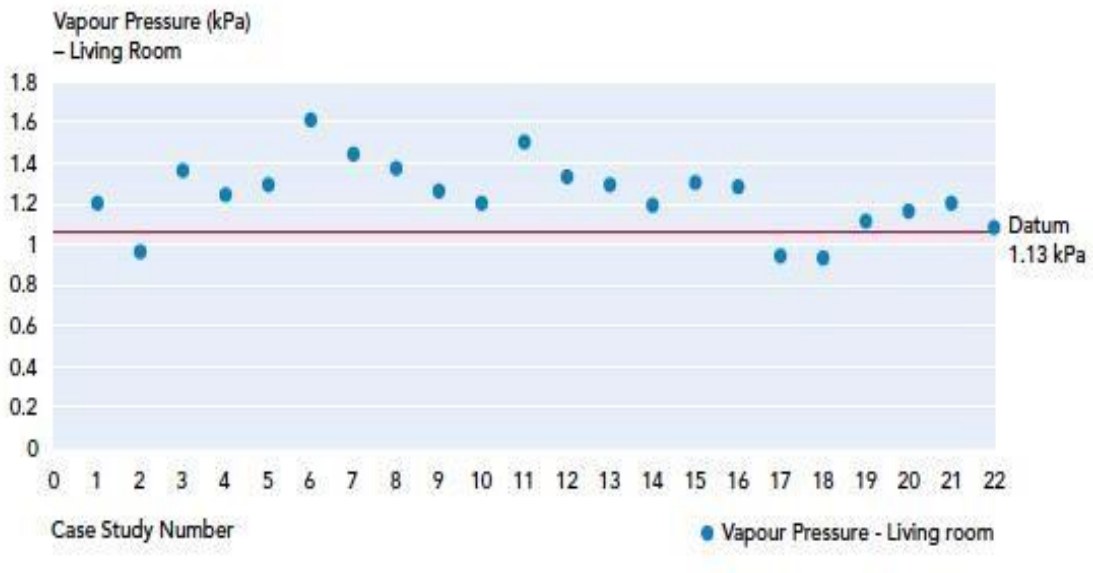

Figure 5.25 Comparison of average vapour pressures measured in living rooms of case study sites and the recommended vapour pressure threshold for dust mites (Porteous et al, 2012).

Three primary objectives were devised for the project and are as follows:

1. To evaluate significant environmental impacts of domestic laundering by firstly surveying the laundry habits across a wide demographic of Glasgow residents with the aim of identifying:
    a. the sum of energy use and CO_2 emissions resulting from the means used;
    b. the balance between energy efficiency and good indoor air quality in relation to drying; and
    c. negative effects on the indoor environment including the potential for condensation and risk to occupant health;

2. Investigate the influence of hygroscopic internal wall material for its ability to provide a moisture buffering capacity for elevated levels of indoor relative humidity. This required adding to the existing knowledge base of transient, hygrothermal properties of relevant materials, surface finishes and furniture fabrics, found in social housing; and to perform laboratory experiments based on scenarios derived from housing survey results to provide suitable data for ESP-r model validation; and

3. Generate a theoretical framework to enhance the modelling of moisture transfer.

The first of these objectives was set to help develop and improve initial understanding of occupant related clothes drying practises. The second objective was devised to assist in the acquisition of moisture property data for existing and new hygroscopic materials and to provide a means for validating the approaches taken to enhance the framework of ESP-r's moisture model against measured data, as stated in the third objective. The following section provides an outline of the initial series of multiple parameter tests devised in response to the information about occupant clothes drying behaviour obtained during the housing survey.

5.7.1 Outline of multiple parameter testing

A series of multiple parameter tests were conducted using the moisture modelling platform provided by ESP-r. A more detailed description of ESP-r's modelling structure has already been given in section 4.7 of Chapter 4. A primary focus for these tests was to identify which building parameters had the most significant impact on the indoor moisture conditions. From the original housing survey, the parameters selected for the analysis included the moisture loading; infiltration rates; internal wall surface lining materials, including materials both permeable and impermeable to moisture transfer; insulation levels in the building envelope construction; and the impact of the external climate. The table below presents the different parameters, from which a range of combinations were tested.

Building Type (insulation)	Infiltration (ach^{-1})	Moisture Generation	Materials and finishes	Occupancy and heating	Climate
Poor insulation	Poor (1.5)		Vinyl wallpaper		

		Light		Light and intermittent	Dundee
Well insulated	Good (0.6)	Heavy	Uncoated Gypsum plasterboard	High and continuous	London
Passive House insulation levels	MHVR (Passive House only)		Clayboard		

Table 5.9 Parameter combinations considered in the study.

5.7.1.1 Model description

The building setting for these tests was a semi-detached dwelling including a living room and sleeping space, with the aim of developing a model that was thermodynamically relevant to the building type as opposed to placing emphasis on its architectural merit. The materials selected for lining of the inside walls of the building envelope were both representative of common social housing installations observed during the field work and material designed with focus on its moisture sorption properties. These included Vinyl wallpaper and Uncoated Gypsum Plasterboard listed in the table above and a product known as Claytec (www.claytec.de), a composite material constructed using reed, hessian and clay that is a heavier and thicker alternative to Gypsum Plasterboard. Additional components included in the analysis were:

- the level of insulation applied to the building envelope. Three levels were defined including 'poor', 'good' and Passive House standard, with U-values ranging from 1.3 to 0.14 $W/m^2.K$ for each type of wall construction, respectively;
- the occupancy profiles being modelled were outlined as continuous for a family of four and an elderly couple and then an intermittent pattern for a working couple;
- the infiltration rates being used to represent housing construction that was either reasonably air tight with 0.6 $achr^{-1}$ or leaky with 1.5 $achr^{-1}$
- a moisture loading schedule designed for the purpose of this investigation was based on clothes drying experiments carried out at a home and monitored on an hourly basis for a total period of 7-8 hours. A 'heavy' wash load composed of 10 items and a light load (6 items) were modelled.

As mentioned in the second point above, the models were designed to include heat gains in keeping with different levels of occupancy. The heating strategies implemented in the

model were used to reflect the occupancy patterns described. Outside of these hours, the heating would be turned off. Table 5.10 displays the schedules applied. As mentioned in the fourth point above, the process of laundry drying was modelled in the living space and was based on the aggregated sum of various items of clothing being hung up to dry. The moisture loading was represented in the ESP-r model as an hourly latent gain step change. The schedule for the 'heavy' and 'light' wash loads modelled is presented in Table 5.11.

Occupancy pattern	**Heating schedule (hours in use)**	**Heating schedule (temperature setting)**
High occupancy (family)	0700-0000	21^0C
Low occupancy constant use (elderly)	0700-0000	21^0C
Intermittent occupancy (working couple)	0700-0900; 1600-0000	21^0C

Table 5.10 Heating schedules applied to the different occupancy regimes.

Moisture Load	**Moisture injection period**	**Days laundry drying takes place**
Light	1000-1700	Weekdays; Saturday
Frequent washing	1000-1700; 1900-0200	Weekdays; Saturday; Sunday

Table 5.11 Laundry drying schedule.

Based on the schedules outlined in the tables above, a series of multiple parameter modelling studies were carried out, the results of which are described in the following sections.

5.7.2 Outcomes from multiple parameter testing

An overview of the impact of each of the building parameters tested over the summer and winter simulation periods is presented in this section. The results plotted in Figure's 5.26, 5.27, 5.28 and 5.29 represent the absolute change in the mean and peak indoor relative humidity conditions predicted in the living space. The key in the graphs defines this absolute change in terms of a maximum (greatest) and an average change. For example, the greatest change in mean relative humidity (see Figure 5.26) in the living space was approximately 12%RH during the summer when testing the impact of

moisture buffering materials. This value is the resulting change in mean relative humidity when Clayboard, as opposed to Vinyl Wallpaper, is used to line the internal wall surfaces. The results highlight the importance of the moisture buffering effect associated with the materials tested, particularly during the summer period where the resultant change in mean relative humidity is comparable to that achieved through varying the moisture loading scheme and the level of infiltration.

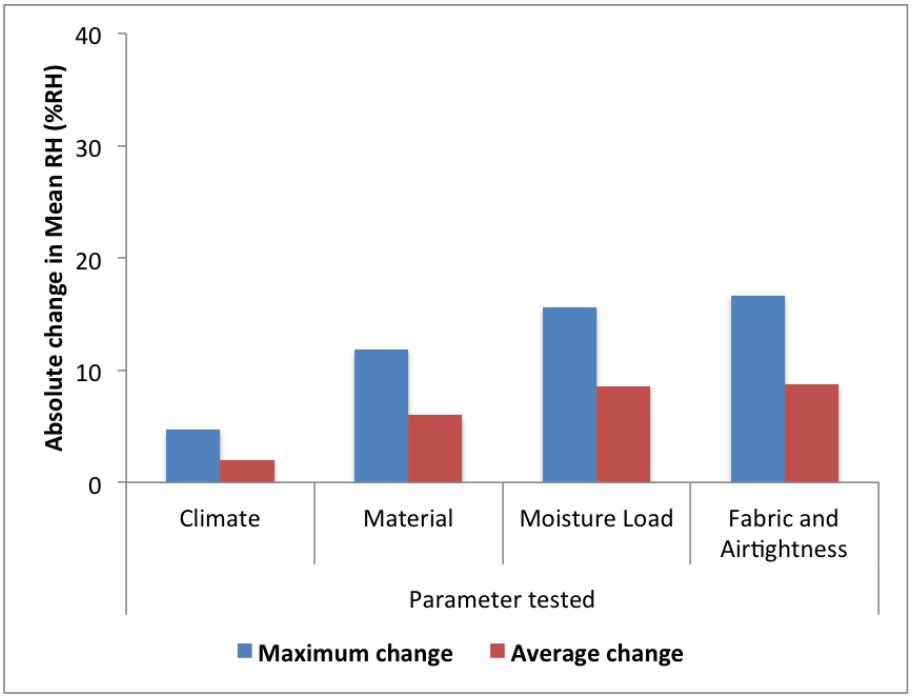

Figure 5.26 Maximum and average absolute change in Mean relative humidity in the Living space due to parameter tested (Summer period).

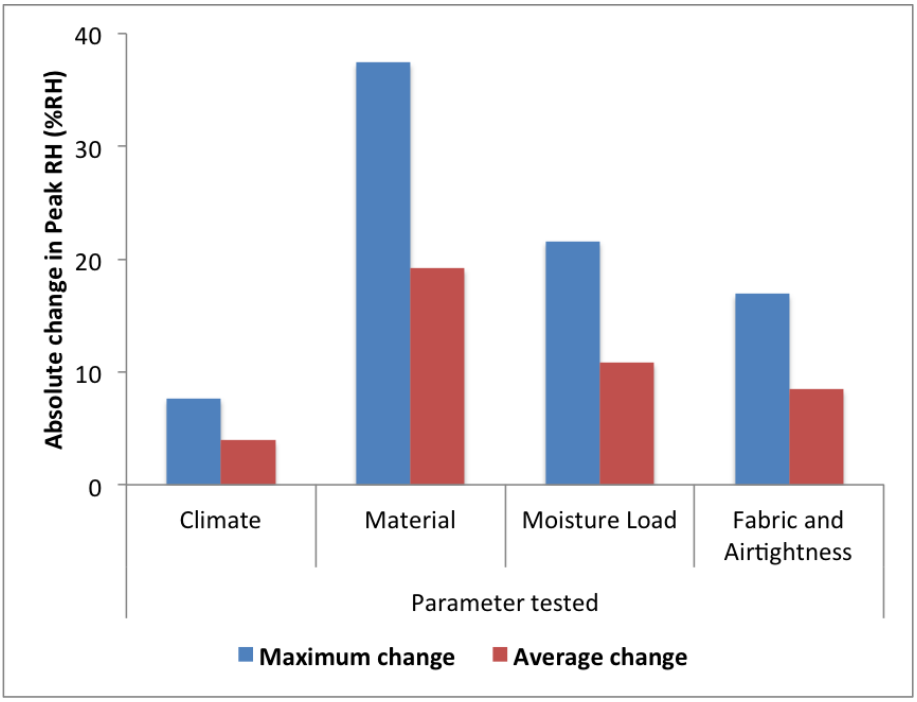

Figure 5.27 Maximum and average absolute change in Peak relative humidity in the Living space due to parameter tested (Summer period).

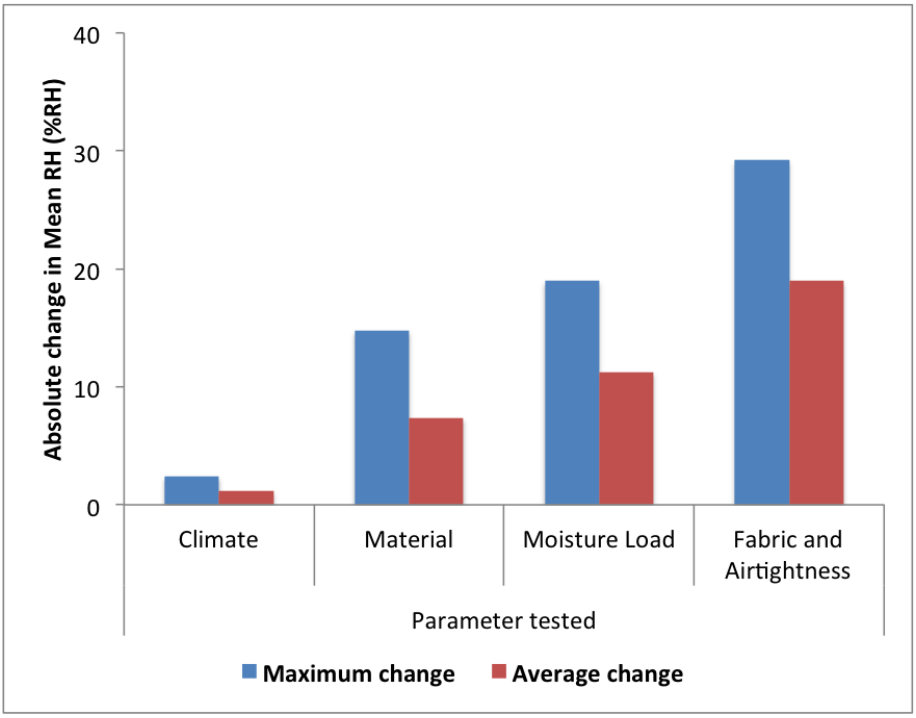

Figure 5.28 Maximum and average absolute change in Mean relative humidity in the Living space due to parameter tested (Winter period).

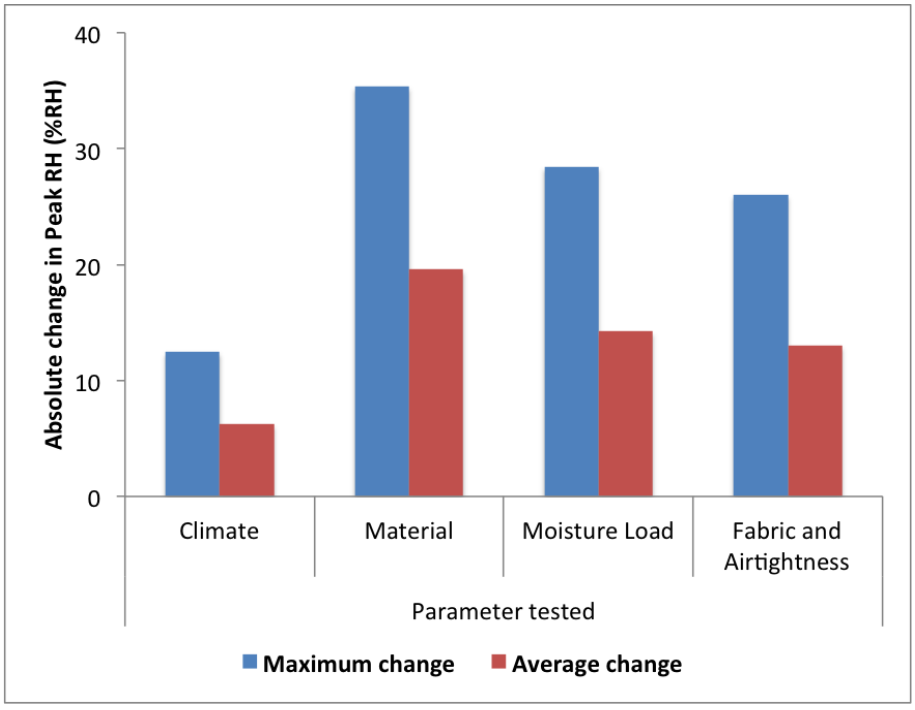

Figure 5.29 Maximum and average absolute change in Peak relative humidity in the Living space due to parameter tested (Winter period).

The impact of moisture loading and increased airtightness on the mean relative humidity was of more benefit during the winter period. This was also the case when the quality of

the building fabric was improved, as seen in Figure 5.28, due to the effect of elevated indoor air temperatures helping to manage relative humidity. The magnitude of the change in peak relative humidity during summer and winter simulations however, was still considerably greater when significant areas of hygroscopic building material is used to line the internal wall surfaces.

Figure's 5.30 and 5.31 provide examples of the impact different materials applied to the internal wall surfaces had on the mean and peak indoor relative humidity. Simulations over a winter and summer period are presented, where a low infiltration level (0.6 ac/hr) and light moisture loading conditions were applied. The moisture absorbing capacity of the Gypsum Plasterboard and Clayboard was reflected in significantly reduced peak relative humidity values in comparison to the results produced by the same model using an impermeable material to line the internal wall surfaces, such as Vinyl wallpaper.

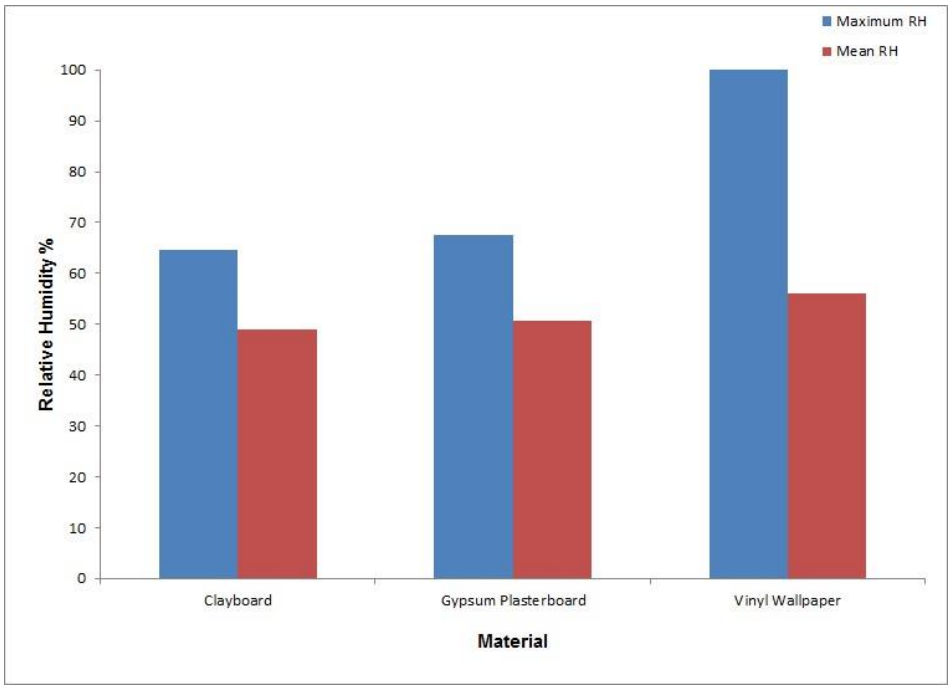

Figure 5.30 Week simulation over winter period; Low infiltration levels and light moisture loading.

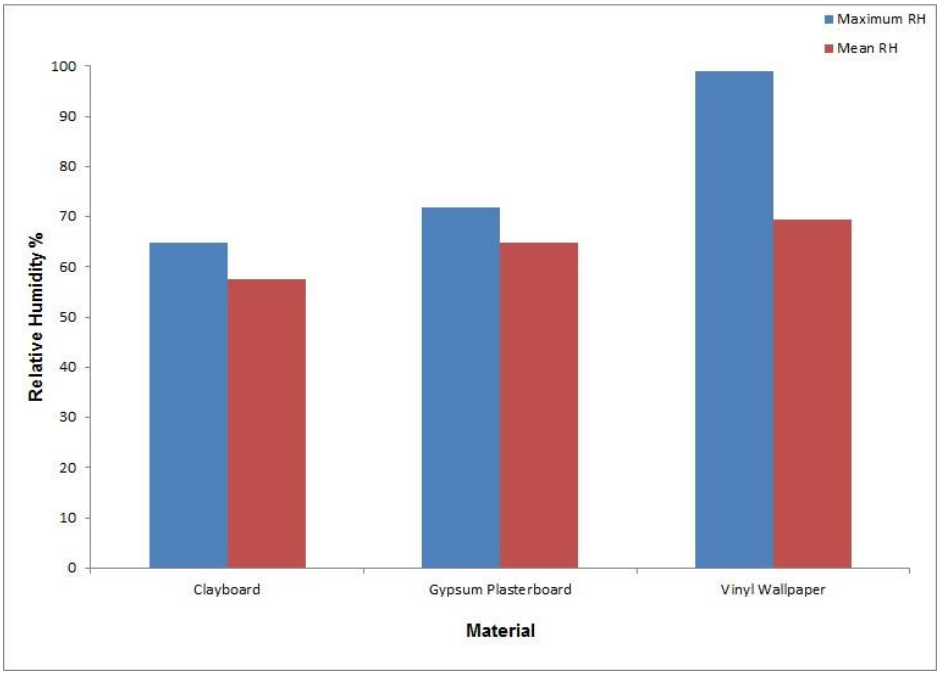

Figure 5.31 Week simulation over summer period; Low infiltration levels and light moisture loading.

A summary of the outcomes taken from the parametric analysis is provided in the following section.

5.7.3 Summary of multiple parameter analysis

The results indicated the significant impact moisture permeable surfaces can have on indoor relative humidity levels. The effect of the increased moisture capacity of the Clayboard was more pronounced during the summer period compared to the performance of the Gypsum Plasterboard, with further reductions to the mean and maximum relative humidity in the range of 2-7%, as is shown in Figure 5.31. Moisture entering the indoor environment by way of infiltration and in combination with a heavy moisture loading scheme, was seen to reduce the benefit of using moisture absorbent materials. Despite being a dedicated moisture absorbing material, the Clayboard performance did not differ greatly from the standard hygroscopic building material (Gypsum Plasterboard) used in these tests.

Given the similar performance of the two moisture permeable materials used in these modelling exercises when exposed to the elevated indoor moisture conditions further verification of ESP-r's ability to accurately model this variable moisture transfer scenario was proposed. In light of this observation, the hygrothermal interaction between moisture permeable materials and dynamic moisture loading schemes now forms the basis for the modelling verification study presented in the following section.

5.8 Verification study of short duration, high moisture loading

Experiments have the advantage of providing results tailored to a specific problem. As already discussed in Chapter 3, the reliability and accuracy of experimental

procedures used to determine hygrothermal material properties has been questioned (Kumaran MK, 2006), along with the suitability of the mathematical methods integrated into whole building simulation tools to model the dynamic indoor environmental conditions. This has been put down mainly due to the lack of sufficient validated benchmark cases (James C et al, 2010). The steady state environmental conditions widely used in the experimental process, from which material properties are extrapolated, do not accurately reflect the dynamic conditions likely to be observed in a realistic building setting.

This study was designed in order to address this issue, by assessing the suitability of moisture related material properties applied in building simulation to model this dynamic hygrothermal interaction through the use of an empirical verification approach.

By conducting short duration, high moisture loading experiments to assess the hygrothermal response of sample materials, the predictive capability of ESP-r's integrated moisture modelling domain could also be assessed by modelling the same experimental procedure. ESP-r employs a specific set of material moisture property data and transfer parameters, including the convective mass transfer coefficient (calculated using a heat and mass transfer analogy) into the numerical analysis. The moisture permeability and sorption isotherm material moisture property data for an assumed homogeneous, isotropic material was adopted when ESP-r is solves the moisture flow model in one dimension. Populating and solving these equations in ESP-r's modelling approach is done by applying material property data found in existing materials databases. These data sets are questioned in terms of their overall suitability, due to difficulties including the lack of uniformity in the applied measurement techniques. The process of experimentation can also be time consuming to prepare and results carry a level of uncertainty. Introducing this uncertainty into ESP-r's numerical modelling could consequently give rise to potential errors in the numerical predictions.

The empirical validation approach undertaken in this study provided a platform for a quantitative comparison to be made between measured and predicted resultant data and was seen as a way to verify the accuracy of the solution (Neale et al, 2007). The outcomes were used to analyse the suitability of the current modelling methodology applied in ESP-r. The following section provides details of the experimental and numerical procedures used to carry out the empirical validation.

5.8.1 Methodology

The Gintronic GraviTest environmental test chamber, with an internal volume of 0.015m^3 (images of the equipment used are presented in Figures 5.33 and 5.34), was used during the experimental phase of the investigation. This instrument provided a high precision mass balance and a programming facility for controlling the supply of hygrothermally conditioned air, allowing for accurate measurement of the materials

response under realistic time and moisture conditions; a vitally important attribute of reliably quantifying the material response (Janssen et al, 2009).

Two sample material specimens (i) Gypsum Plasterboard with a matt paint surface finish (PGP) and (ii) Clayboard (CB) ('Claytec' as named by manufacturer), were selected (a further description of the materials is provided in section 5.8.2). An image of the complexity of the Clayboard composition is shown in Figure 5.32. The samples were exposed to a relative humidity range of 50-90%RH for a period of 2 hours. This moisture loading regime was applied to represent a high level of occupant related moisture generating activity, such as those presented in Table 2.0 in Chapter 2. The mass of each sample was recorded at 10min intervals. Relative humidity and temperature within the material samples were not measured. The environmental conditions inside the chamber were maintained at:

- a constant air temperature of 23 °C
- a constant rate of air supply with a flow velocity of 0.5 m/s
- an air change rate of 13 ac/h was used in order to ensure the required RH profile produced during the experimental process was repeated in the model
- 50% RH before and after a 2 hour period of moisture injection to achieve 90% RH.

Figure 5.32 Image of the clay, reed and hessian composition of Clay board **(www.womersleys.co.uk/acatalog/Building_Products_2_6.html)**.

The air temperature within the chamber was set to 23 °C as this is a standard reference value used in several moisture measurement experimentation procedures, such as the NordTest protocol (Rode C et al, 2005) and the Japanese Industrial Standard (JIS A 14701). The thicknesses of the sample materials tested were kept the same as those applied in practice. The painted gypsum plasterboard had a thickness of 12.5mm and a surface area of 0.0025m^2; the Clayboard used had a thickness of 20mm and a surface area of 0.0014m^2. Maintaining the thickness of the sample, as used in practice, is suggested in

the NordTest experimental protocol, the JIS procedure and the Draft International Standard (DIS 24353) (Roels S et al, 2006).

The exact surface convective boundary conditions of the material specimens were not measured and so it was assumed that the air in the chamber could be characterised by the well-mixed air conditions assumed in the model. This implied uniformity of relative humidity and temperature conditions throughout the chamber and across the surface of the material samples. A laminar air flow across the samples was assumed for the model and a convective heat transfer coefficient value of 2.3 W/m^2.K was calculated using an expression for airflow through a square duct (Incropera FP et al, 2002), which was then set as a constant in the ESP-r model. The function used to determine the heat transfer coefficient involved the use of Nusselt numbers derived for laminar flow in ducts and over a flat plate with a fixed temperature (Neale et al 2007), as shown below. Given the importance of this issue in dynamic processes such as convective drying and material moisture loading (Defraeye et al 2012) a range of duct sizes was tested, as the exact geometry of the air inlet into the chamber was unknown. Due to the strong influence of the velocity of air moving over a porous material surface (Mortensen 2005), a sensitivity analysis was conducted to investigate the impact of different convective heat transfer coefficients on the modelled mass transfer rate.

$$Nu_{Dh} = \frac{h_c D_h}{k}$$

Equation (5.5)

where D_h is the hydraulic diameter (m) and k it the thermal conductivity of air (W/m.K). The Reynolds number was also calculated, in order to confirm that the flow of air over the surface of the two samples could be characterised as laminar, by using the following equation:

$$Re_x = \frac{\rho U \rho D_h}{\mu}$$

Equation (5.6)

where *u* is the free stream air velocity (m/s) and μ is the dynamic viscosity of air at the specified temperature (kg/m.s). A resultant value of 21.4 was calculated, indicating a laminar air flow (Peeters et al, 2011).

Figure 5.33 Measurement equipment (left); Environmental test chamber (right).

Figure 5.34 Image of sample loading method in test chamber (image taken from www.gintronic-instruments.com).

An insight into the reasons for testing the two materials selected is given in the section below.

5.8.2 Material selection

The reason for choosing to test painted Gypsum Plasterboard was in order to represent a standard building envelope construction material used in UK housing design. The painted finish was also selected in order to determine if the hygrothermal material properties derived for coated materials are able to adequately model the associated impact on moisture transfer. The Clayboard was identified as a new building material composed of organic materials, including clay, reed and hessian. The design philosophy behind this material product is aimed at providing an alternative to plasterboard without reducing the associated levels of thermal and hygric performance. It is thought to be especially suitable for high comfort; low energy buildings (www.claytec.de).

The hygric and thermophysical properties for each of the two materials are presented in the tables below.

Material	**Density (kg/m³)**	**Specific Heat Capacity (J/kg.K)**	**Thermal Conductivity (W/m.K)**	**Thickness (mm)**
Painted Gypsum Plasterboard (CGP)	690	750	0.3	12.5
Clayboard (CB)	1438	1500	0.5	20

Table 5.9 Thermophysical properties for Painted Gypsum Plasterboard and Claytec Clayboard.

Material	**U_h**	**A**	**n**
Painted Gypsum Plasterboard (CGP)	21.4	2.65e-2	1.54
Clayboard (CB)	944.0	2.70e-3	1.54

Table 5.10 Transfer coefficients used for calculating the moisture content using the absorption isotherm function.

The moisture permeability data for each of the two items was represented by a constant vapour diffusion resistance factor. A value of 4 was used for the Clayboard and a value of 7 was used for the painted plasterboard (Baker P H, 2014).

5.8.2.1 Material moisture property data

Using ESP-r's integrated moisture modelling module as part of a whole building dynamic simulation, requires a moisture property data file to be created and implemented in the model. For each moisture permeable surface identified in the building model, the file will contain corresponding transfer coefficients, derived from regression analysis, for both the sorption isotherm and the moisture permeability. An overview of the numerical analysis used in ESP-r to model the behaviour of the hygroscopic materials can be found in section 4.7 of Chapter 4 and by reading (Nakhi, 1995). The basic functions used in the model are the Hansen equation (Equation 5.7), which determines the moisture content of the material; and the moisture permeability function (Equation 5.8) calculated in relation to the vapour diffusion resistance factor as a function of the relative humidity.

□1.0

□□ ln□□□ $\overline{n}$

u □ u_h□□1.0 □ □□ 0 □□□1

□□ A □□

Equation (5.7)

Important to note, is that the modelling of the moisture absorption and desorption phases in a material in ESP-r is carried out by using either the average of the two processes or by using the absorption isotherm alone. During the investigation, the absorption isotherm for the two materials tested was determined using a standard procedure for absorption. Steady state material properties were therefore produced using this method and are presented in the figure below.

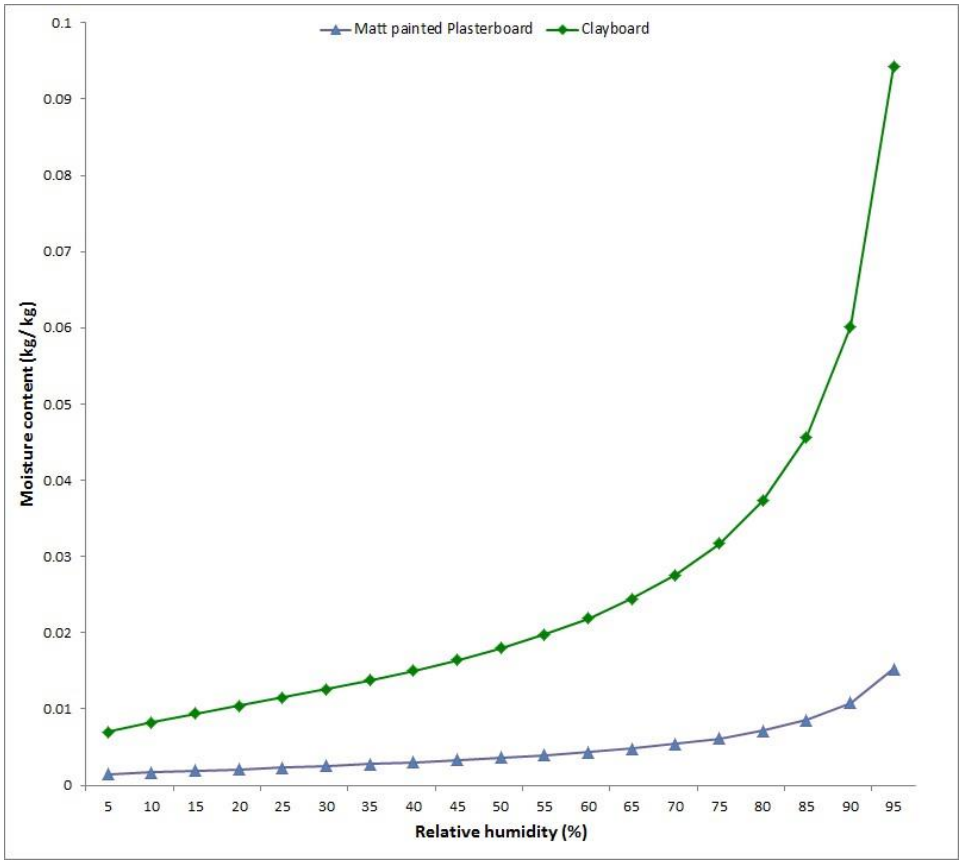

Figure 5.35 Clayboard and Painted Gypsum Plasterboard absorption test results with Hansen equation fitted.

The standard method used to calculate the moisture permeability of a material in ESP-r involves Equation 5.8 where the moisture permeability of stagnant air □$_a$ (kg/m.s.Pa) is divided by the vapour diffusion resistance factor □.

□$_a$

□$_p$ □

□

Equation (5.8)

where the vapour diffusion resistance factor is calculated as follows:

$$\mu = \frac{1}{b \exp(a \cdot c)}$$

Equation (5.9)

The next section presents a comparison of the results produced using the existing modelling methodology applied in ESP-r with the laboratory measured data.

5.8.3 Comparison between experimental data and ESP-r results

The results presented in Figures 5.36 and 5.37 compare the surface moisture flux predictions produced by ESP-r and the measured data obtained from the laboratory experiment. The surface moisture flux was calculated by multiplying the convective mass transfer coefficient by the vapour pressure gradient between the surface of the sample and the indoor air.

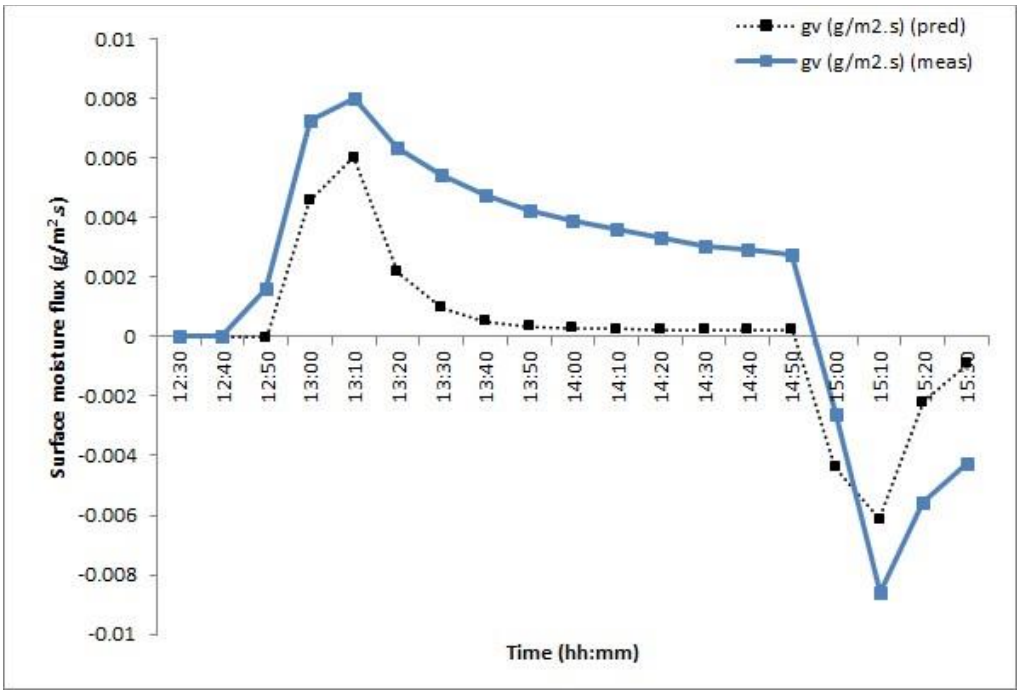

Figure 5.36 Surface moisture flux comparison between experimental data and ESP-r predictions for painted plasterboard.

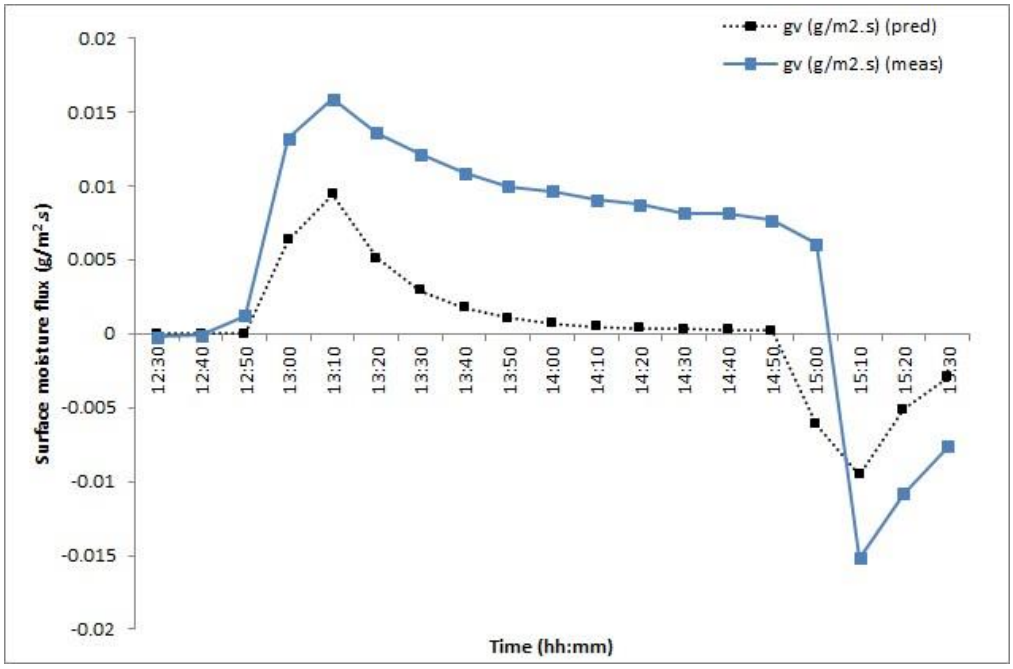

Figure 5.37 Surface moisture flux comparison between experimental data and ESP-r predictions for Clayboard.

The poor level of agreement indicated by these graphs is summarised in the following section.

5.8.4 Summary of moisture loading study

A poor level of agreement was achieved between predicted and measured data for both of the materials looked at in this investigation. During the initial step change in relative humidity, where the moisture level in the chamber was increased from 5090%RH, the vapour pressure gradient was the primary driving force behind the initial moisture transfer at the surface. This material response was repeated in the predicted results as the relative humidity fell from 90 to 50%RH at the end of the moisture loading period. However, during the period where relative humidity was maintained at a constant 90%, the predicted surface moisture flux decreased, indicating the rate of moisture transfer was not being accurately modelled. Further investigation of this modelling process is presented in Chapter 6, in order to determine if improved performance could be achieved. In particular, the uncertainty over the moisture transfer property representing the moisture permeability of the samples was addressed in the development work presented in Chapter 6.

The emphasis on moisture production in relation to indoor sources is continued in the following section, which presents a verification study focusing on the moisture released during the clothes drying process. Using data collected from a clothes drying experiment, comparison between the measured values and those predicted using ESPr's evaporative surface model was made. As stated in section 5.7, the second objective of this project was to carry out laboratory tests in order to aid the verification of ESP-r's existing moisture modelling framework. As will be discussed in Chapter 6, this form of empirical testing

has supported the development work that has been undertaken to enhance the existing moisture modelling framework.

5.9 Verification study of surface evaporation

With indoor moisture generation rates being reported as high as 20 kg/day in some climates (Tariku et al, 2010), an investigation into the modelling of moisture generating processes in the context of whole building heat and moisture transfer analysis was conducted. The focus of the study was specifically on the indoor drying of laundry and to identify if the approach taken in ESP-r to model the moisture release rate of passive drying of domestic laundry was suitable. This investigation was in keeping with the subject of the project presented in section 5.7, designed to investigate the impact of domestic drying of laundry on the indoor environment.

An empirical validation was conducted to determine the suitability of the evaporation model used in ESP-r. Particular focus was on the moisture evaporation rate at the surface of the clothing items and being able to predict this behaviour within reasonable agreement to the measured data. In this investigation, a homogeneous pore structure was assumed for the clothing material.

5.9.1 Methodology for modelling of surface evaporation

Review of the drying process revealed the modelling of the mass transfer rate associated with evaporative processes usually involves the use of a mass transfer coefficient and multiplying this by a driving force and the area of the surface (A_s) considered. This is the approach taken in ESP-r (as shown in Equation 5.10) where the humidity ratio (kg/kg) is the driving force in the process and a simplified Lewis relation is used to determine the mass transfer coefficient, as shown below:

$$ev = h_c A_s(\omega_{surf} - \omega_{air})/C_p$$

Equation (5.10)

where *ev* is the evaporation rate (kg/s); ω is the humidity ratio (kg/kg) at the surface of the material and the air, denoted by the subscripts *surf* and *air*. The heat transfer coefficients are calculated in ESP-r based on buoyancy forces created at each modelled surface within a model as a result of temperature differences between the internal surfaces and the indoor air.

The drying process was investigated by modelling the moisture release from clothing items being dried passively on a clothes airer within a real home environment. The relative humidity and temperature were measured and recorded at 1-minute intervals at three different points on the airer. The surrounding ambient relative

humidity and temperature were also measured and were found to be reasonably steady over the duration of the measurement period. During the drying period of the clothing being monitored, the mass of each item was measured and recorded every 1 to 2 hours. The clothing items modelled were assumed initially saturated, thus discounting the effects of the different stages of the drying process and equally the modes of moisture transfer taking place through the pore network of the clothing. The moisture properties of the clothing items were not measured as part of this investigation either and so each item was modelled as a single surface within a whole building model. In total, there were six items of clothing (a towel, two t-shirt's, jeans, a shirt and a facecloth) being monitored.

Based on the in situ measured data for relative humidity and temperature, mean values for the ambient indoor environmental conditions were applied in the ESP-r model and set as constants at 67%RH and 23˚C, respectively and maintained by applying ESPr's basic controller heating model. The simulations were also conducted using ESP-r's default internal convection model where the convection coefficients are calculated in relation to buoyancy effects arising from temperature differences between the indoor air and the modelled building surfaces. Simulations were performed using a 15mins time step. Finally, the air change rate was applied and maintained at a constant 0.5 ac/hr.

5.9.2 Results from surface evaporation modelling

The current surface evaporation model is capable of calculating the evaporative rate and the associated heat loss associated with a saturated surface. An initial simulation was conducted using ESP-r's existing evaporative surface model for two of the clothing items measured during the experimental procedure. The graphs below illustrate the resultant difference between the rate of surface evaporation observed during the measurement period and that produced by the model.

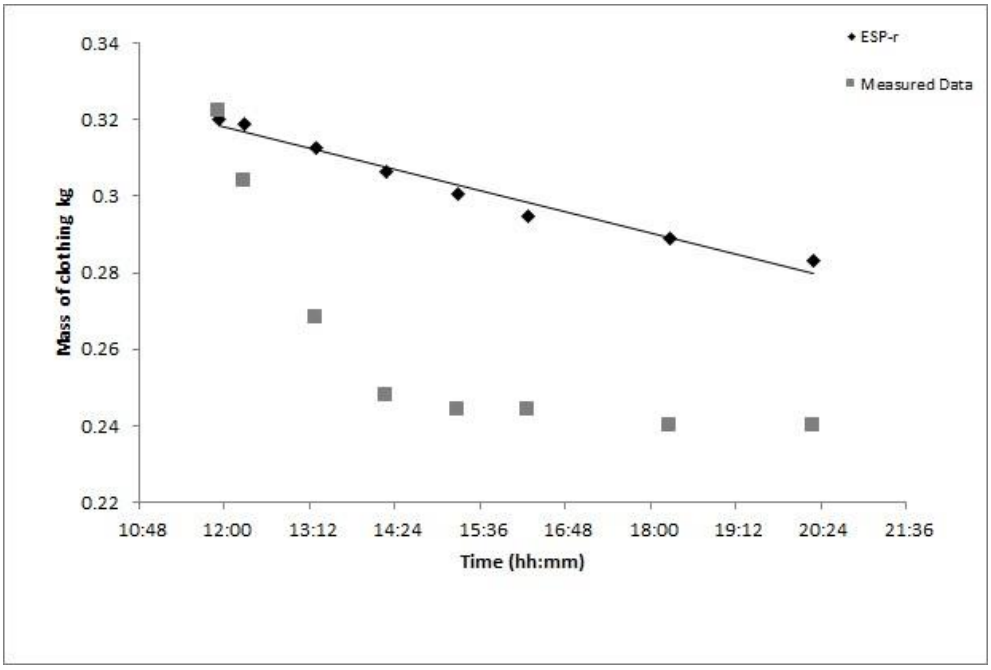

Figure 5.38 Measured versus predicted mass loss rate of linen shirt.

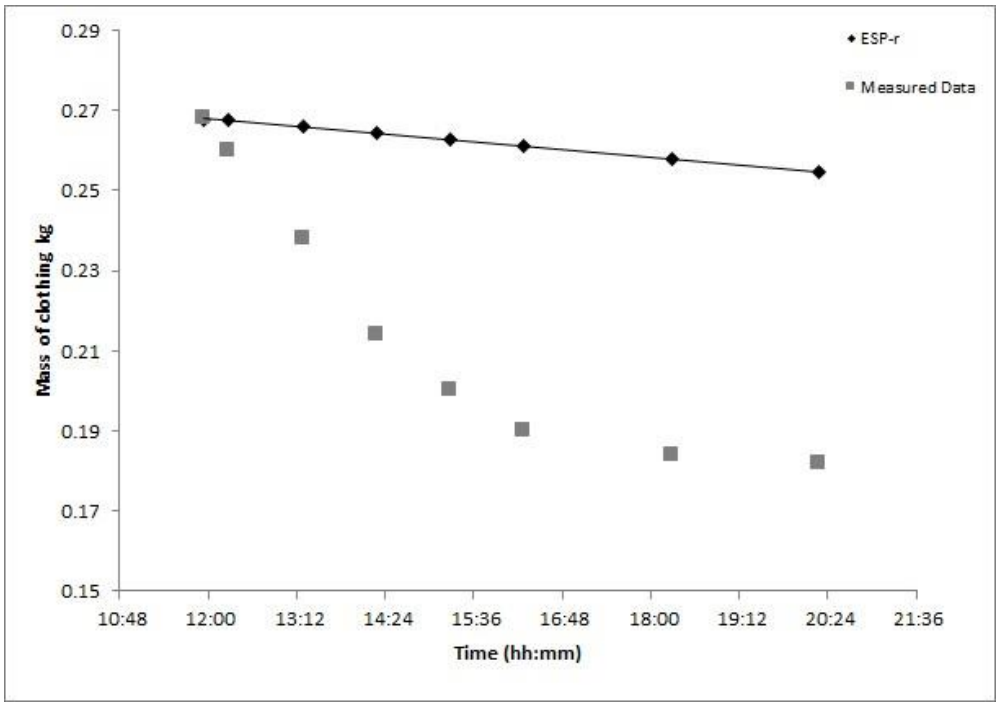

Figure 5.39 Measured versus predicted mass loss rate of t-shirt.

A summary of the surface evaporation results comparison is provided in the next section.

5.9.3 Summary of surface evaporation study

The resultant evaporation rate from the clothing was being modelled as a linear process in ESP-r, as shown for two of the clothing items monitored in Figure's 5.38 and 5.39, resulting in poor agreement with the measured data. As already discussed in the review of surface boundary conditions and the drying process in sections 4.1.1 and 4.3.1 of Chapter 4, respectively, a more detailed investigation of the drying process would have required a more accurate knowledge of the clothing material moisture properties and hygrothermal conditions at the air-clothing interface, in order to improve and replicate the different stages and dynamics of the drying process being modelled.

5.10 Chapter summary

This chapter has described the main approaches used in the process of verifying and applying ESP-r's integrated moisture modelling domain. The suitability and accuracy of the moisture transfer analysis was assessed using a range of simplified and whole building simulation exercises and analytical results.

An initial series of test exercises designed specifically for assessing the performance of hygrothermal building modelling and to aid in identifying areas where further modelling development may be required, were undertaken. These were devised as part of an International Energy Agency project (Woloszyn et al, 2008). The complexity of the building environments modelled varied from simple monolithic construction

exposed to isothermal boundary conditions, to multilayered construction modelled under real outdoor climate conditions. Key areas were investigated in Test Case 1 through to Test Case 1B, including material moisture property data to highlight the moisture buffering effect associated with different permeable building materials and finishes; indoor moisture loading and heat gains to represent the variable occupancy patterns and activities; the resulting impact of varying the location and quantity of material in a room; and variable indoor air change rates. It was possible to draw comparison between the predicted outcomes produced by ESP-r and, for some of the cases presented, the results from other heat and moisture transfer models. ESP-r was found to produce good agreement with the analytical data provided in the simplified test cases, both in terms of profile and magnitude, and for cases with and without the inclusion of moisture permeable materials in the building envelope. ESP-r's predictions were compared to results from other simulation tools and reasonable consensus could be seen in the final modelling outcomes between all of the tools. The same outcome could not be reached, between ESP-r's predictions and other tools however, as the modelling complexity of the buildings was increased by the introduction of real outdoor climate conditions, thus resulting in a more dynamic indoor environment. A wide range of results was produced by all of the simulation tools used and the agreement with measured data was reduced significantly. Identifying the sources of error in the models would require further investigation of the individual modelling components, such as the material moisture properties and the resulting performance under more dynamic indoor climate conditions.

This uncertainty was further highlighted in Test Case 2 designed to assess the impact of varying the ventilation rate, position and quantity of a permeable building material. An environmental test chamber was modelled using ESP-r, so that predictions could then be compared to the measured results taken from the laboratory set up. Reasonable agreement could be achieved between measured data and ESP-r predictions for a case where all indoor wall surfaces were clad with a moisture permeable material. However, significant ESP-r's predictions were underestimating absolute humidity significantly when compared to the measured data when only the ceiling or the floor was finished with a moisture permeable material. Although a similar moisture profile produced, the difference in magnitude might suggest that a more detailed representation of the temperature and moisture distributions in the environmental chamber could be incorporated in order to enhance the modelled hygrothermal conditions between the air and each hygroscopic surface in the ESP-r model. In addition, the use of a fixed air change rate to model the air supply and extraction system in the test chamber may not have adequately represented the air flow characteristics at different locations within the test chamber. Further analysis of the impact of surface boundary conditions would also be needed to improve understanding of its influence on moisture transfer between the air

and hygroscopic building materials and whether or not the assumption of well-mixed air conditions is suitable.

Having presented the initial cases used to verify the ESP-r moisture model performance, its application in a recent EPSRC funded project investigating the impact of indoor laundry drying on the indoor environmental conditions was presented. A multiple parameter analysis was run. A building model consisting of a living and nonliving space was created to identify which building parameters, including a variable levels of natural ventilation, different internal wall material finishes, heavy and light moisture loading schemes, building fabric quality and dynamic outdoor climate conditions, had a significant influence on the indoor relative humidity conditions. The study indicated the more pronounced effects of infiltration and moisture loading on indoor humidity conditions, although the moisture buffering capacity of permeable building material was still seen to have a significant role in moderating the peak indoor relative humidity. Confidence in the results produced from the multiple parameter study was questioned however, given the uncertainty arising from the initial verification exercises described above and the moisture model predictions produced under dynamic indoor climate conditions. This was a key aspect of the further development undertaken during this research.

The final two verification cases presented in the chapter, highlighted the potential for improvements to be made during the course of this research with respect to firstly, the modelling of dynamic moisture transfer conditions and the associated hygrothermal response of moisture permeable building material, presented in section 5.8. Using standard available moisture permeability properties for two sample materials, agreement between ESP-r's modelled predictions and the measured data for the resultant surface moisture flux taken from a laboratory experiment was poor. This outcome was repeated when looking at the second area of model development undertaken, which was to look at moisture release sources in the context of laundry drying. A linear rate of surface drying was modelled in ESP-r, as was described in section 5.9, highlighting the current modelling deficiency and need to develop the modelling of this transient, dynamic process.

The modelling presented in the following chapter is the result of the development work that has been carried out to address the three main issues that were presented at the beginning of this chapter. The chosen areas of development were focused on expanding the material moisture properties available to model the hygrothermal response of moisture buffering material in ESP-r, given the unsatisfactory agreement achieved between measured and predicted results produced from modelling of a dynamic moisture loading experimental procedure. This development responds to the points made firstly about the suitability of hygrothermal properties applied in moisture modelling and secondly, ensuring the dynamic nature of material moisture response

characteristics is accounted for. Lastly, advancement of the modelling of the surface evaporation process in ESP-r, with specific focus on the drying process of clothing items, has been carried out. The impact of this indoor moisture production activity was discussed in the multiple parameter study presented in section 5.7. Further empirically based verification of the current surface evaporation model, highlighted the ineffectiveness of the current method to replicate the true nature of this process, including the relationship between the surface boundary conditions and the moisture transfer processes taking place within the drying material. By focusing on this aspect of the drying process in the development of ESP-r's surface evaporation model, it was possible to improve the representation of the drying behaviour of laundry items. Chapter 6 will present the progress made during this research in developing these specific components of integrated moisture modelling in ESP-r described above.

CHAPTER 6

Developments in the modelling of moisture buffering and moisture release in ESP-r

Chapter overview

This chapter presents the work undertaken to develop the integrated moisture model of the simulation tool ESP-r. These changes have been implemented to address the areas identified for modelling advancement, as a result of the empirical verification exercises presented in Chapter 5, which include an improved representation of material moisture properties; and modelling of surface moisture evaporation associated with the process of clothes drying. Subsequently, an analytical study is presented to further highlight the importance of developing the modelling of transient surface boundary conditions within ESP-r.

As a result of the implementation of this development work, improved agreement was observed between measured data and ESP-r predictions for both empirical case studies presented in sections 5.8 and 5.9 of chapter 5. The final analytical study also highlighted the transient nature of the moisture permeability of stagnant air in relation to surface temperature variations and the effect this has on the moisture permeability of the material.

6.0 Introduction

This chapter presents the development work undertaken to advance the integrated moisture modelling facility of ESP-r. This has been in response to the issues highlighted in the series of empirical model verification steps presented in the previous chapter. More specifically, the development work has resulted with the improved modelling of material moisture properties, including the moisture permeability of materials exposed to dynamic moisture loading conditions; and secondly, improved modelling accuracy of the drying behaviour of clothing material, in the context of passive indoor laundry drying.

The hygrothermal modelling outcomes presented in Chapter 5 were based on a set of empirical verification and analytical exercises. The exercises discussed from section 5.1 to 5.6 were taken from a recent International Energy Agency project (Woloszyn and Rode, 2008), which aimed to address the specific topic of whole building heat, air and moisture transfer modelling development. A range of building parameters known to influence the heat and moisture transfer behaviour observed in the indoor environment were specified in the model descriptions provided for these verification cases, including the boundary conditions; rates of air infiltration; and the range of hygroscopic porous materials in the building envelope. The moisture transfer solver built into ESP-r was examined by simulating these exercises. Analytical data was available for an initial case involving the modelling of impermeable internal wall surfaces that resulted in good agreement between ESP-r predictions and the analytical solutions

provided. Moisture transfer properties of the building envelope material are neglected during this calculation, thus directing the focus on the ability to model the step change in indoor relative humidity resulting from a moisture injection period and the rate of infiltration, as part of the air mass balance. A second analytical case incorporating the moisture buffering potential of hygroscopic porous building material was also modelled. The current approach adopted in ESP-r to model the hygrothermal interaction between the indoor air and the building envelope fabric indicated the use of a standard material moisture property to determine the moisture content of the material was not suitable for this particular case.

Inter-model comparison was also made possible for some of the test cases, a process which highlighted the wide range in magnitude and dynamic variability of predictions made by different heat and moisture transfer modelling approaches, including ESP-r's, in section 5.2.4 of Chapter 5. This level of uncertainty in the context of building related heat and mass transfer processes can be attributed to several sources of error, including:

- differences between real climate conditions and those assumed in the simulation;
- differences between the actual effect of occupant behaviour and those assumed by the operator of the building simulation tool;
- differences between the reality of heat and mass transfer processes and their representation in building simulation (Judkoff et al, 1983).

The boundary conditions of the buildings modelled in a section of the verification exercises were specified as isothermal and with fixed relative humidity conditions. The indoor air conditions were also specified with constant temperature conditions; and set step changes for heat gains and moisture production periods were scheduled, thus discounting the potential error arising from the first two points described above in the simple modelling cases. However, as mentioned above, the wide distribution of predictions, produced by all of the simulation tools, presents uncertainty in a number of potential areas, including that of suitable representation of heat and moisture transfer mechanisms, such as the hygrothermal interaction between the indoor air and the building envelope material modelled using material and surface boundary transfer properties.

The building related parameters mentioned above were further assessed as part of a multiple parameter study, conducted during a project investigating the impact of indoor passive drying of laundry on indoor relative humidity conditions. ESP-r was applied to model this process within the context of a whole building simulation. Key factors, including the level of natural ventilation and air tightness of the building

envelope, were identified as the primary factors influencing the moderation of indoor relative humidity, in addition to the moisture buffering capacity provided by the material lining the internal wall surfaces. Confirmation of this inherent ability of hygroscopic materials to moderate indoor peak relative humidity in the indoor building environment has already been described in Chapter 2 and in other studies (Ramos et al 2010). Better understanding of the strongly coupled processes associated with this interaction is required In order to develop the modelling of this hygrothermal performance, within integrated whole building simulation.

The uncertainty arising from the use of standard material properties in building simulation and the complex hygrothermal conditions observed at material surface boundary was assessed using ESP-r's current moisture modelling capabilities. Two empirical verification studies were presented in sections 5.8 and 5.9 of Chapter 5, designed to investigate (i) the use of standard material moisture properties when modelling short term, high moisture production schemes; and (ii) the surface evaporation rate of passive indoor drying of laundry, respectively. The context for the second verification study was provided in section 5.7 of Chapter 5, which describes the influence of this occupant related activity on indoor relative humidity conditions. The specific moisture modelling development work undertaken to address the issues identified in these specific cases is presented in sections 6.2 and 6.3.

6.1 Study of simplified monolithic construction

Modelling of a simplified building construction exposed to isothermal conditions was described as part of an initial study presented in section 5.3 of Chapter 5. The building envelope was composed of aerated concrete and a step change in indoor relative humidity was applied for a period of 8 hours, by injecting 500 g/h of moisture. Analytical solutions were provided for an initial case, which did not take into account the moisture buffering capacity of the building construction material; and for a case where this characteristic of the building construction was included. Predictions from ESP-r's modelling of an impermeable building construction, which excluded a solution for the moisture transfer in the construction material by not specifying relevant moisture capacity or moisture permeability properties, produced acceptable agreement with the analytical solution, as was shown in Figure 5.5 of Chapter 5.

The second study introduced the moisture buffering capacity of the aerated concrete in the analytical solution. The results shown below were produced using ESPr's current method for representing the moisture capacity characteristics of aerated concrete during simulation; and by implementing a linear function for determining the moisture content of the specified material (aerated concrete), as shown in Equation (6.0).

$u = 0.0661\varphi$

Equation (6.0)

where u is the gravimetric moisture content of the material (kg/kg), 0.0661 is an experimentally derived coefficient and φ represents the relative humidity. A corresponding moisture capacity function was also implemented in the ESP-r moisture model.

6.1.1 Results from modelling of monolithic construction

As can be seen in Figure 6.1, the standard Hansen equation used for determining the moisture content in ESP-r resulted in the overestimation of the peak relative humidity during the moisture injection period. The correlation between ESP-r predictions and the analytical solution was improved with the addition of a function representing the sorption characteristics of the aerated concrete as a linear form,

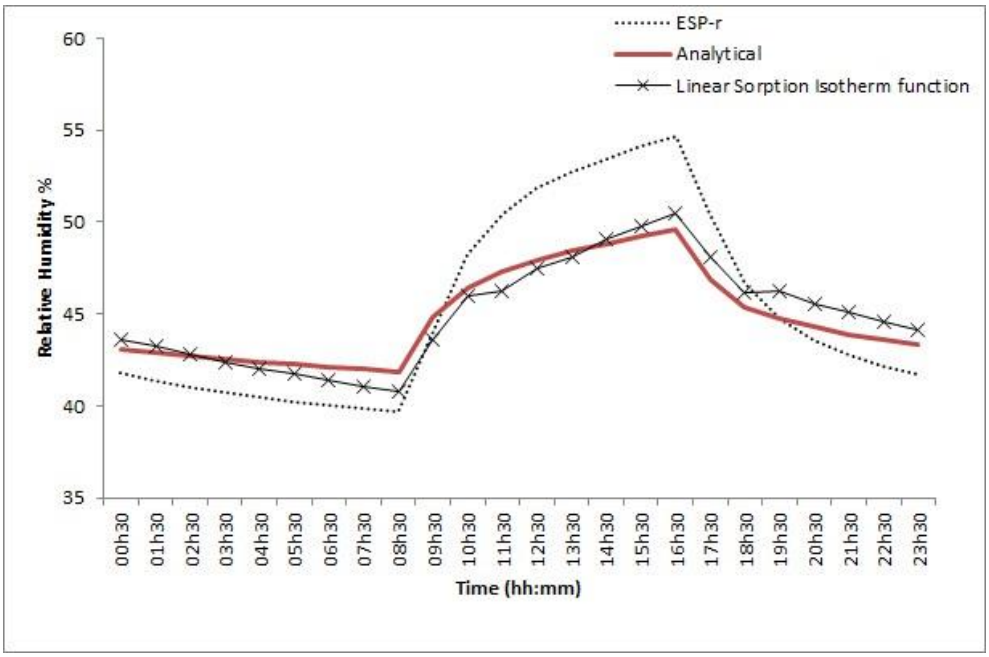

Figure 6.1 Comparison between relative humidity predictions using the standard ESPr moisture absorption isotherm; a new linear function; and an analytical solution.

A sensitivity study of the convective heat transfer coefficient applied to the internal wall surfaces of the building model highlighted the impact of this property on the resulting indoor relative humidity predictions made by ESP-r, which can be seen in the figure below. The linear sorption isotherm function for the aerated concrete was in use during these simulations.

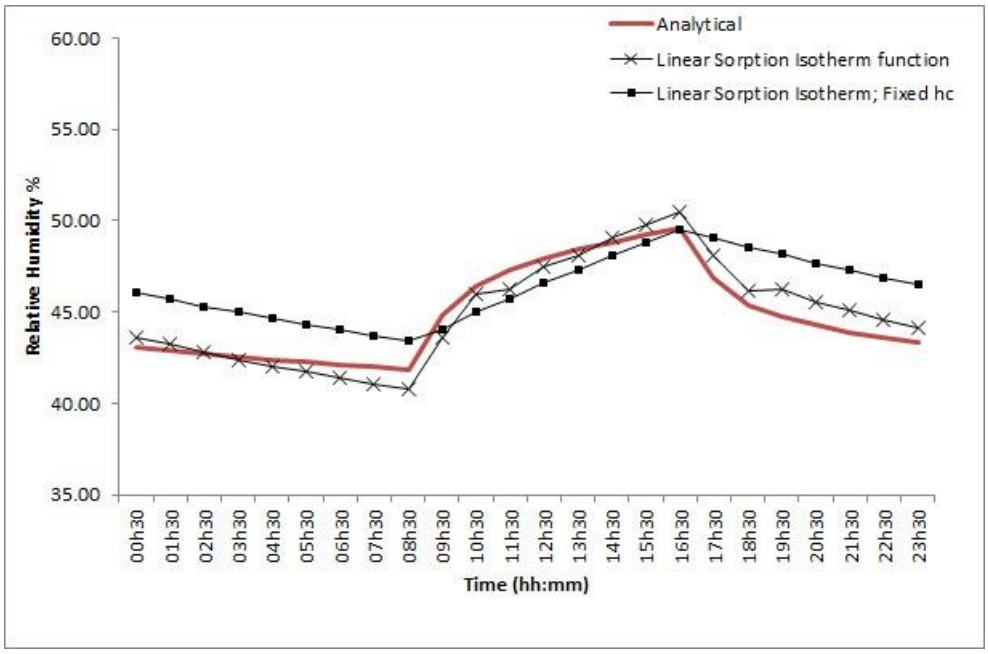

Figure 6.2 Impact of convective heat transfer coefficient on ESP-r relative humidity predictions**.**

Figure 6.2 emphasises the influence of the convective surface heat transfer coefficient on the resulting rate of surface moisture transfer. The use of a fixed convective heat transfer coefficient value (labelled 'Fixed hc' in the graph) produces good agreement between ESP-r's predictions and the analytical values for peak relative humidity during the period of moisture injection however, the indoor relative humidity either side of this period does not decrease in accordance with the profile or magnitude of the analytical result. The release of moisture back into the space from the material during the desorption phase may be overestimated in ESP-r due to the effects of using a single function to represent both sorption phases of the material, thus discounting potential hysteresis effects in the porous medium; and the adoption of a constant value for the convective heat transfer coefficient of the wall, which does not take into account the possible variations in the surface boundary conditions, including buoyancy effects that could be induced by changes in the air temperature at the material surface.

As discussed in section 4.7.1.3 of Chapter 4, calculating the convective surface heat transfer coefficient in ESP-r is based on the buoyancy effects driven by variations in temperature. The indoor relative humidity results produced by ESP-r using this modelling approach are also displayed in Figure 6.2 (time series plot with crosses marking data points). Improved correlation is seen in terms of the dynamic response profile of predicted indoor relative humidity when compared to the analytical solution and in comparison to the other simulation tools used to model this exercise, as shown in Figure 6.3.

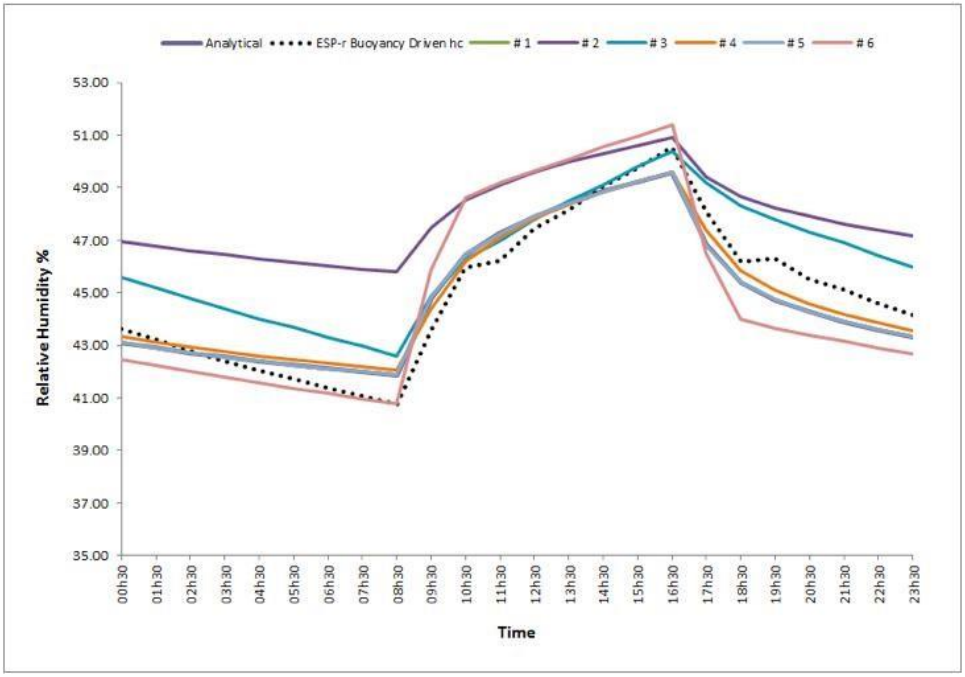

Figure 6.3 Inter-model comparison of indoor relative humidity and comparison to analytical solution

Peak indoor relative humidity during the moisture injection period is slightly over estimated indicating a reduced rate of mass transfer during the period of maximum indoor relative humidity in the model. This difference could be accounted for due to the use of a constant moisture permeability value for the material, neglecting the influence of changes in indoor relative humidity when calculating this property; and as a result of underestimating the surface convective heat transfer coefficient, which would consequently produce a lower value for the convective mass transfer coefficient when using the integrated heat and mass transfer analogy found in ESP-r.

Given the main outcome of this study was to highlight the importance of modelling the dynamic response of hygroscopic building materials, the following section presents the steps taken to develop an improved approach in ESP-r to model moisture transfer behaviour during short duration, intense moisture loading conditions. This study focused on gaining understanding of the current approach used in ESP-r to model the interaction between dynamic moisture loading conditions and hygrothermal building materials. Initial comparison between measured and predicted results indicated a poor level of agreement.

6.2 Study of materials exposed to short duration, high moisture loading

The focus of this investigation was to determine the suitability of standard material moisture properties when used to model the response of hygroscopic building materials exposed to dynamic moisture loading conditions. Comparison between the surface moisture flux data obtained from an experimental procedure (described in

section 5.8) and modelling predictions achieved using ESP-r's existing moisture modelling facility was then made to ascertain the level of agreement achieved. Furthermore, and in light of the uncertainty pertaining to the surface boundary conditions across the samples used in the environmental test chamber, subsequent analyses of the spatial discretisation applied to the modelled material sample; and the impact of the convective surface transfer coefficient on the surface moisture flux were undertaken. These were carried out given the knowledge of the interrelated nature that exists between the moisture transfer process and surface boundary conditions.

6.2.1 Development of material moisture response characteristics

Modelling the moisture response characteristics of the material samples being tested required sorption isotherm and moisture permeability data to be applied in ESPr's moisture modelling methodology. The moisture absorption performance of the materials in question was measured as part of the investigation using the experimental technique described in section 3.3.5. The coefficients of the derived sorption isotherm function were then applied to the ESP-r moisture model. The transfer coefficients however, required to implement the default format of ESP-r's moisture permeability function (described in section 3.3.3 of Chapter 3) were not measured for the specific materials tested at the time of the investigation. In order to overcome this issue, a solution was found by using available data in the model, in the form of the vapour diffusion resistance factor.

As was shown in section 5.8.3, initial attempts at modelling the surface moisture flux resulted in poor agreement between ESP-r's modelling predictions and the measured data. Further investigation focused on the impact of the material moisture transfer properties on the modelling predictions, which involved the introduction of derived moisture permeability functions for the Clayboard and Painted Gypsum Plasterboard into ESP-r's moisture modelling facility. The functions were derived using regression analysis of measured data obtained from two separate research studies and then introduced to ESP-r's integrated moisture model. The first of these studies was by (Goto Y et al, 2012), which looked at the incorporation of the MBV model into a whole building simulation tool to investigate the effect of moisture buffering materials (one of which was Clayboard) on indoor relative humidity and temperature conditions; and the subsequent impact on energy consumption and indoor air quality. The second source of material moisture property data for the Painted Gypsum Plasterboard was obtained from the experimental data provided in the third common exercise of the International Energy Agency (IEA) Annex 41 (Lengsfeld and Holm, 2006). The data included was the standard diffusion thickness, which represents the air layer thickness equivalent to the depth of vapour diffusion. As already described in section 3.3.4 in Chapter 3, this property is preferred due to its suitability for representing thin layers. Figure's 6.4 and 6.5 display

the respective data for each material, with the corresponding functions given underneath.

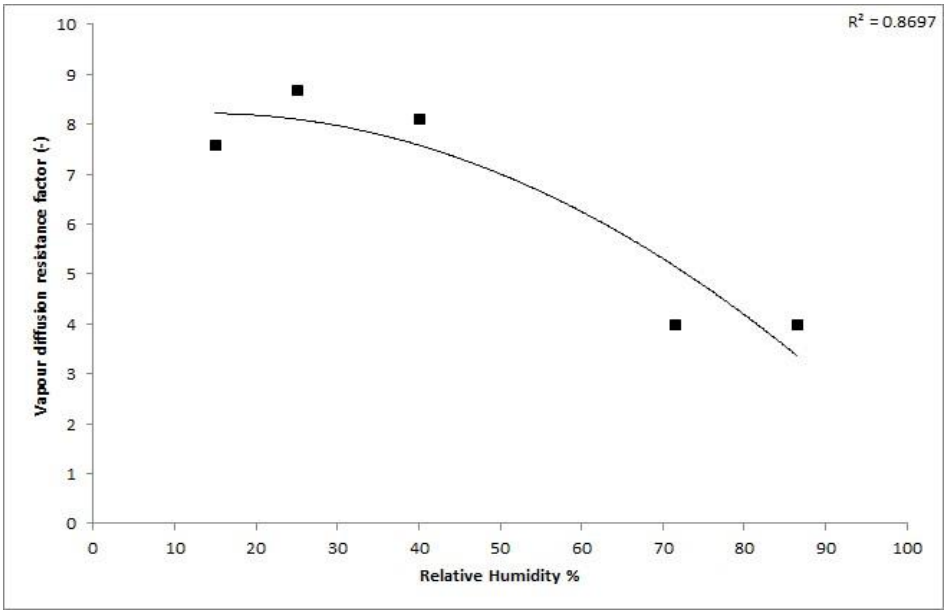

Figure 6.4 Clayboard vapour diffusion resistance factor across relative humidity range.

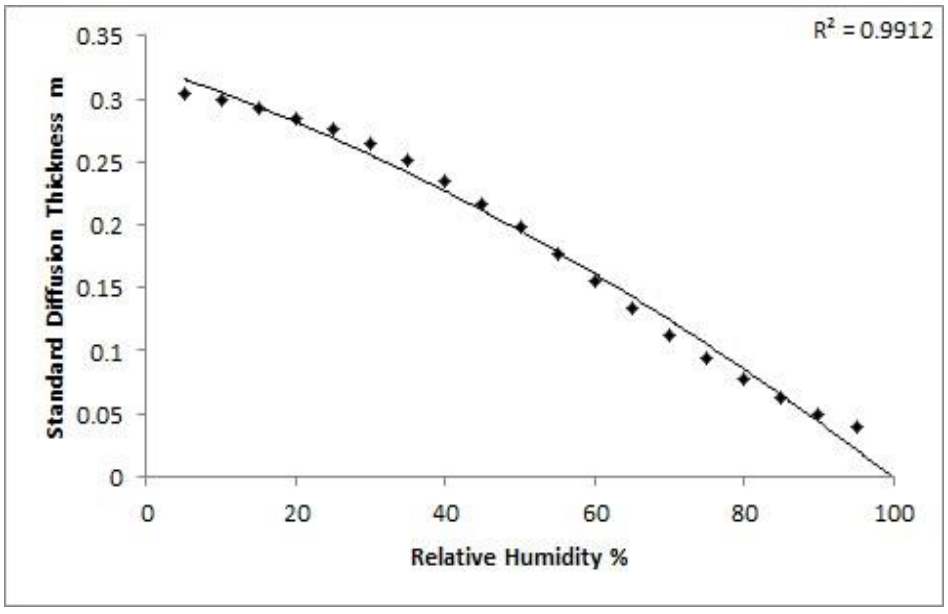

Figure 6.5 Painted Gypsum Plasterboard standard diffusion thickness across relative humidity range.

Based on the curve fitting shown in Figure's 6.4 and 6.5, the following polynomial equations were incorporated into ESP-r's integrated moisture model to represent the moisture permeability □□(kg/m.s.Pa) characteristics of both the Clayboard and Painted Gypsum Plasterboard, respectively:

$$\frac{\delta_a}{\mu = a\varphi^2 + b\varphi + c}$$

Equation (6.1)

$$d = \frac{}{(af^2d + a.bdf + c)}$$

Equation (6.2)

The coefficients a, b and c have been provided in Table 6.0 for the two materials. Equation (6.2) incorporates the inverse of the vapour diffusion resistance factor. This is presented in the equation by dividing the thickness of the sample *d* (m) by the standard diffusion thickness (m) (represented by the polynomial in Equation (6.2)). This development was made to help account for the recognised increase in moisture permeability a porous material undergoes, as a result of elevated material moisture content, and thus promoting the integration of dynamic material property functions in whole building simulation.

	Moisture permeability data transfer coefficients		
	a	**b**	**c**
PGP	-0.13	-0.196	0.326
CB	-9	2.445	8.05

Table 6.0 Permeability transfer coefficients derived from curve fitting for Painted Gypsum Plasterboard (PGP) and Clayboard (CB).

At this point, it is important to recognise the potential influence associated with the method used to model the material samples being tested. Particular focus is on the approach adopted to account for the paint layer applied to the Gypsum Plasterboard, as already in section 5.6.5 of Chapter 5. This issue is now discussed in the following section.

6.2.1.1 Influence of spatial discretisation on moisture response

Without exact knowledge of the thickness of the paint layer applied, it was assumed that it had a negligible effect on the overall thickness of the sample material.

This meant that the thickness of the paint layer was accounted for within that of the plasterboard layer. Having adopted this modelling assumption, certain physical factors such as the potential moisture capacity associated with the paint layer (had it been modelled as an individual layer); the method used to apply the paint (Svennberg K, 2006); and its composition i.e. binder concentration, as presented in section 2.5.2 in Chapter 2, would be neglected. The moisture permeability coefficients (presented in Table 6.0) were therefore used to model the paint and the plasterboard as a single layer. It was assumed that by minimising the number of layers, in this way and hence the number of nodes per layer, would provide a more stable platform for the modelling solution, as was mentioned in section 4.1.3 of Chapter 4. The spatial discretisation process is a balancing act essentially, between the distribution of material layers and their interaction with boundary conditions, which includes those at the surface.

The complex, non-linear nature of moisture transfer at the surface of hygroscopic building materials is known to create difficulty in maintaining a stable modelling solution. Given the emphasis on the modelling of the materials' moisture response in this study, it was acknowledged that the combined effect of the surface boundary conditions and the spatial discretisation scheme applied when modelling surface moisture flux should be investigated. A sensitivity analysis of the spatial discretisation scheme applied to the material being modelled was conducted. The resulting effect on the accuracy of surface moisture transfer modelling predictions was then assessed. The material used in this analysis was a sample of unpainted gypsum plasterboard, chosen due to the lack of adequate material property data available to represent the moisture permeability of a painted material (at the time of conducting the analysis). Measured surface moisture flux data was produced using the same experimental procedure described in section 5.8.1 for this material and used to compare to ESP-r modelling predictions.

The spatial discretisation schemes used in the sensitivity analysis are presented below in Table 6.1. A one-way and equi-distant (both coarse and fine) gridding scheme was tested. The two-way expansion method was not included in the study as there was only one exposed surface in the material sample, with the remaining surfaces sealed using an aluminium foil.

Discretisation scheme	**Number of moisture nodes per layer**	**Number of layers**	**Thickness of layers (m)**
Equi-distant gridding (coarse)	6	5	0.0025
Equi-distant gridding (fine)	6	8	0.0015625

One-way expansion	6	4	0.001, 0.0015, 0.003, 0.0065
One-way expansion	6	5	0.0015, 0.002, 0.0022, 0.0025, 0.0043

Table 6.1 Discretisation schemes used to assess influence on mass transfer rate.

Results from this analysis are presented in Figure 6.6, indicating satisfactory agreement was achieved between the measured and predicted surface moisture flux when applying an equi-distant and fine gridding scheme.

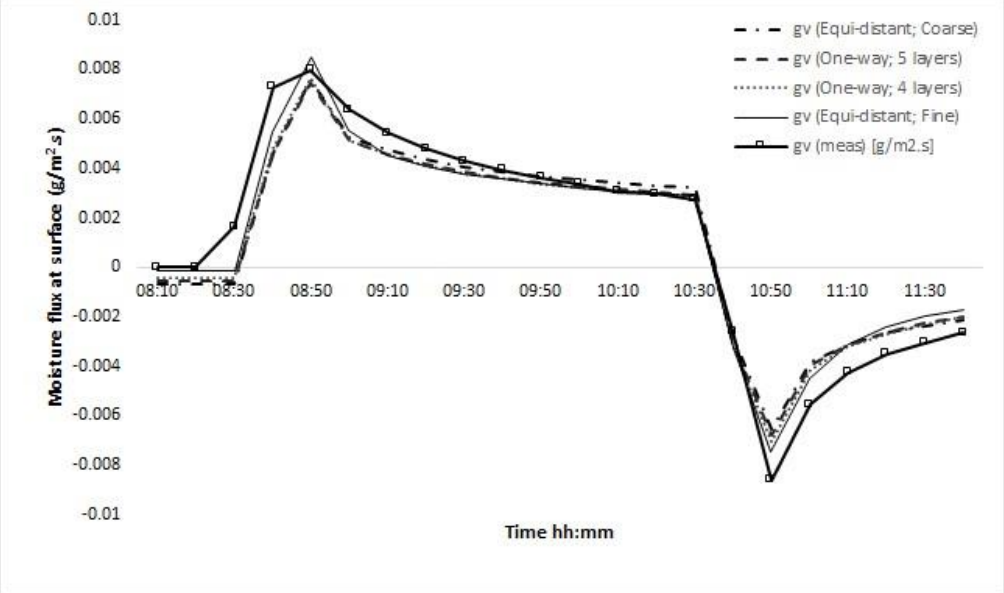

Figure 6.6 Comparison between measured data and ESP-r predictions of surface moisture flux to highlight the impact of different spatial discretisation schemes.

A negligible difference was seen when applying the remaining discretisation schemes and consequently the combined equi-distant, fine gridding approach was taken forward when modelling the moisture response characteristics of the Clayboard and Painted Gypsum Plasterboard samples exposed to short duration, high intensity moisture production regimes.

6.2.2 Outcomes of developed moisture response modelling

Having applied the chosen discretisation scheme to the two materials described in the initial specification of this investigation (Section 5.8.1), a comparison between the experimental data and the surface moisture flux predicted using ESP-r was made. Figures 6.7 and 6.8 present a comparison between the modelling results produced when a constant vapour diffusion resistance factor was used as a means of determining the moisture permeability of the two sample materials, and a relative humidity dependent moisture permeability function. It is shown that improved agreement between the measured data and ESP-r predictions was reached for both of the materials when a

relative humidity dependent function for moisture permeability was used. In both figures, a significant difference in magnitude between the surface moisture flux measured and that predicted remained during the peak moisture loading period i.e. when relative humidity was set at a constant 90%RH. Improved agreement is also observed across the period where a step change in relative humidity occurred. This was most apparent in the case of the Painted Gypsum Plasterboard when relative humidity decreased from 90%RH to 50%RH. However, results in Figure 6.7 show that a delay in the modelled Clayboard response to the changing relative humidity conditions occurred before and after the period of constant relative humidity.

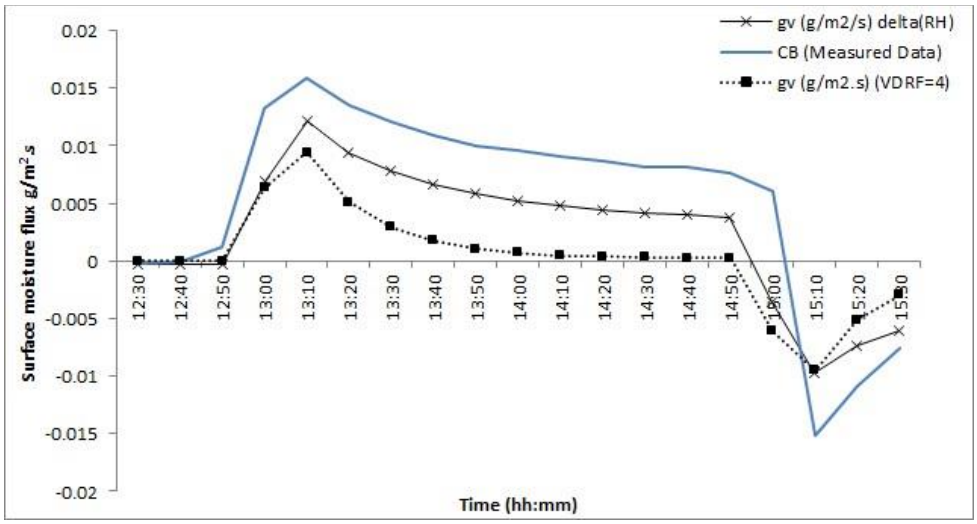

Figure 6.7 Comparison of Clayboard surface moisture flux between measured and predictions for (a) moisture permeability as a function of RH (delta (RH)); and (b) a vapour diffusion resistance factor equal to 4.

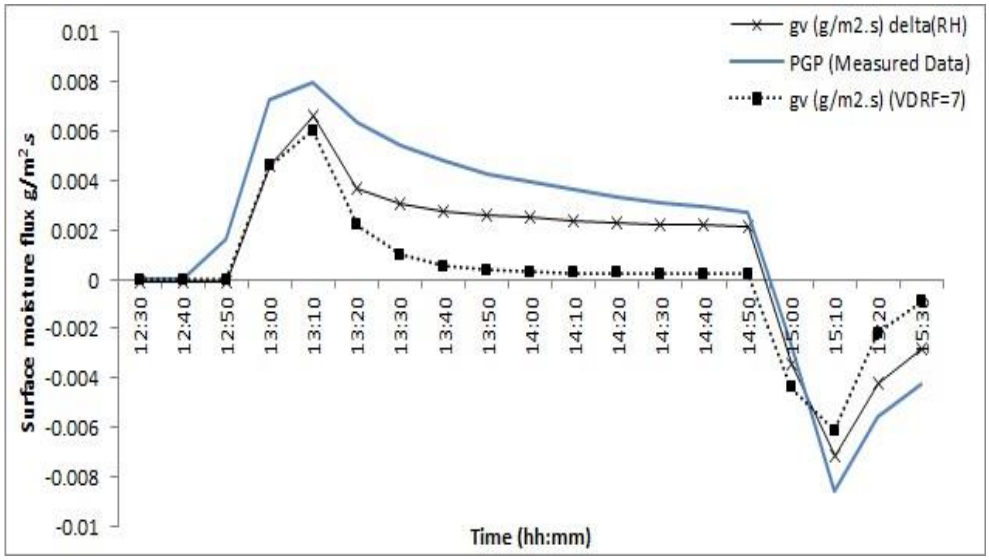

Figure 6.8 Comparison of Painted Gypsum Plasterboard surface moisture flux between measured and predictions for (a) moisture permeability as a function of RH (delta (RH)); (b) a vapour diffusion resistance factor equal to 7.

A summary of the results comparison presented in the two graphs above is provided in the next section.

6.2.3 Discussion

A level of uncertainty surrounding the outcomes of this form of empirical verification exists. Firstly, errors may arise as a consequence of the steps taken during the experimental procedure, pertaining to the operational features of the environmental test chamber. The environmental chamber used in the study was originally designed to determine the moisture permeability of thin material layers e.g. permeable membranes. Determining this material property experimentally requires a high air velocity across the surface of the sample placed in the environmental chamber, so as to reduce the resistance to moisture transfer. An air velocity of 0.5 m/s was applied during this particular procedure, and maintained during the course of the empirical verification study presented here (a value that would generally exceed the air velocity conditions experienced in the indoor environment). Secondly, the sample weighing process is another area where uncertainty could arise between numerical modelling and empirical procedure. This process requires temporary lowering of the material samples to the weighing scale positioned at the base of the chamber, and involves deactivating the environmental air conditioning system. A further hygrothermal response from the material samples could therefore be induced as a result of reactivating the air conditioning unit.

Finally, the potential for inaccuracies to arise, as a result of uncertainty over the suitability of the developed material moisture permeability functions, was also considered. Using material moisture property data that has been determined under a single set of boundary conditions, to an experimental procedure using different boundary conditions, is often questioned (Scheffler G, 2008). This practice is of particular concern when information regarding the measurement process is unavailable. This issue was pertinent to this study, as the data used when modelling the Painted Gypsum Plasterboard was taken from a single source and detail of the boundary conditions was not provided (Lengsfeld and Holm, 2006). The influence of the surface boundary conditions on the modeling predictions formed the focus of an additional analysis presented in the following section. The aim of the analysis was to investigate the influence of the surface convective transfer coefficient on the reliability of the moisture transfer modelling.

6.2.3.1 Analysis of moisture transfer at the interfacial region

The complex hygrothermal interaction occurring at a material surface requires accurate representation of the surface transfer parameters and boundary conditions. One such parameter is the convective heat transfer coefficient, which has already been

highlighted in section 4.3.1 as a key surface parameter influencing the overall moisture transfer rate. Given its intrinsic link to the surface boundary conditions, a study was conducted to determine the potential impact of a range of convective heat transfer coefficients on modelling predictions. The results from this study are presented in the figures below, highlighting the variable effect associated with this surface transfer parameter.

As is shown in Figure's 6.9 and 6.10, an improved resultant surface mass flux predictions is achieved, when varying the convective heat transfer coefficient, in comparison to the impact associated with the newly applied material moisture permeability properties.

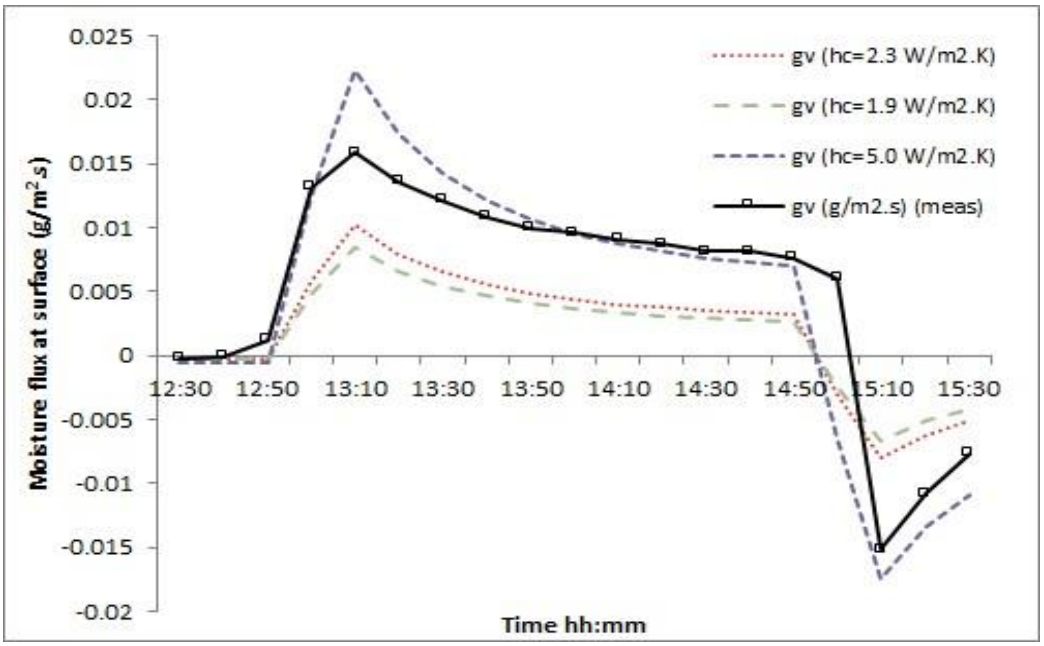

Figure 6.9 Impact of convective heat transfer coefficient on surface moisture flux predictions for Clayboard.

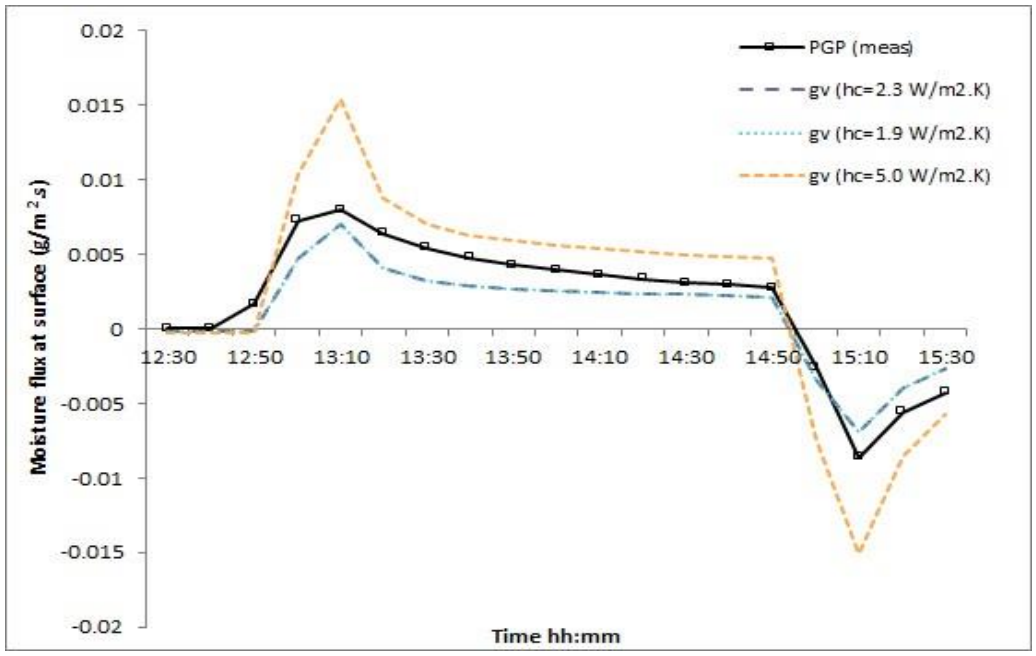

Figure 6.10 Impact of convective heat transfer coefficient on surface moisture flux predictions for Painted Gypsum Plasterboard.

Results from the sensitivity analysis indicate modelling the convective heat transfer coefficient as a variable parameter would produce a more realistic reflection of the actual conditions, in contrast to applying a fixed value. The true value would lie in the range between 1.9 and 5.0 W/m^2.K over the surface mass transfer process. This assumption was made in response to the overestimation of the predicted surface moisture exchange occurring during the initial stage of moisture injection in the test chamber. The level of agreement is seen to improve at the latter stage of the high moisture injection period, when a heat transfer coefficient of 5.0 W/m^2.K is used. Values of 1.9 and 2.3 W/m^2.K were seen to under predict the amount of moisture transfer at the material surface. Given the sensitivity of predictions to the surface convective heat transfer coefficient, a more detailed study of the airflow conditions in the experimental procedure would be required.

Further detailed study of the airflow conditions used in the experimental setup was not undertaken, yet, the critical influence of the convective heat transfer coefficient continued to be investigated in the context of the second area of moisture modelling development presented below. This work developed the existing surface evaporation model found in ESP-r based on the empirical verification procedure described in section 5.9 of Chapter 5. This work also refers to the important point made in the introduction of Chapter 5 about accurately accounting for the relationship between the boundary conditions, in this case at the surface of a material, and the resultant hygrothermal behaviour. Accurate modelling of moisture transfer at the interfacial region now becomes the focus of the following section.

6.3 Development of the surface evaporation model

The second empirical verification study presented in Chapter 5, section 5.9 investigated the correlation between measured data and the simulated outcomes produced by ESP-r for the rate of surface evaporation. A constant air change rate was applied in the model and fixed indoor air temperature and relative humidity boundary conditions were used. The hygrothermal material properties of the drying surface were neglected also. The initial simulation outcomes presented in Chapter 5 indicated a linear rate of evaporation from the drying surface being modelled under these conditions and so further development of the existing surface evaporation model was undertaken.

6.3.1 Adaptation of the surface evaporation model

The model development process involved introducing and comparing variants of the original evaporative rate calculation used in ESP-r, originally presented in Chapter 5. The rate of evaporation from a wetted material surface is not a simple and linear function dependent solely on the vapour pressure and temperature gradients across the surface of the drying material and the surrounding air in contact with this surface. ESP-r's current method for modelling evaporation is analogous to evaporation from a wetted surface, represented as a floating surface within a whole building model. This method however, does not account for the hygrothermal properties of the material drying and therefore liquid and vapour diffusion processes associated with the transport processes taking place in the pore structure of the material during the different drying stages are not represented. The figure below highlights the two stages of drying taking place in porous material and the relevant factors driving the process during each stage.

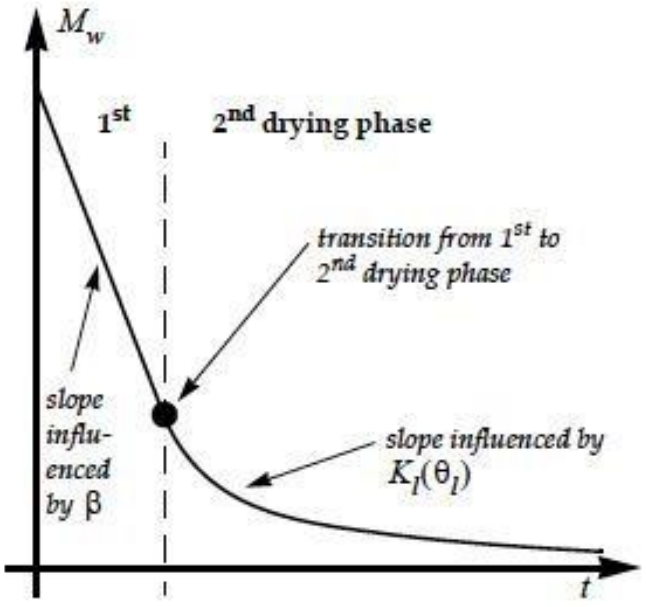

Figure 6.11 First and second stages of the drying process (Scheffler, 2008) (where K_l represents the hydraulic conductivity of the material as a function of the liquid moisture content θ_l)

The model was adapted to reflect the profile associated with the drying of porous media, as shown in the figure above. Components introduced to the surface evaporation model to improve the level of agreement between the measured data and ESP-r predictions, included the addition of an initial mass of moisture reflecting the storage capacity of the material; and an additional variable seen in Equation (6.3) that was termed an 'evaporative history coefficient', e_h for the purpose of this investigation. This initial step improved the correlation between the measured data and predictions as can be seen in Figure 6.12 (displayed in subsection 6.3.2). The variable was calculated by subtracting the ratio between the moisture evaporated and the initial moisture at the material surface from unity (the value of which represented no evaporation having taken place) after each time step. This is shown in the equation below:

$$e_h = 1.0 - \frac{m^e}{m_i}$$

Equation (6.3)

where m_e and m_i are the evaporated mass of moisture from the surface node and the initial mass of moisture (kg) at the material surface node, respectively. Prior to the activation of the evaporation process, e_h will equal one. Finally, four different equations for calculating the surface evaporation rate were added. Equation (6.4) was adapted from the original expression used in ESP-r, Equation (6.5), with the addition of the evaporative history coefficient. (Tang et al, 2004) found the process of drying from a wetted surface to be proportional to the exponent of the difference in the vapour pressure gradient at the interface between fluid and solid. Having reviewed existing expressions used to determine the evaporation rate, their study assumed the function given in Equation (6.6) shown below, which was subsequently added to the surface evaporation model in ESP-r. The convective mass transfer coefficient, calculated using the heat and mass transfer analogy adopted in ESP-r, was also incorporated into this equation, given the limited data on the exact hygrothermal surface boundary conditions. Equation (6.7) applied the same approach to model the evaporation rate as Equation (6.6) with the addition of the evaporative history coefficient. The four equations described above are now presented:

$$ev = e_h \cdot h_c \cdot A_s(\rho_{surf} - \rho_{air})/C_p$$

Equation (6.4)

$$ev = h_c A_s(\theta_{surf} - \theta_{air})/C_p$$

Equation (6.5)

$$ev = h_m A_s(p_{sat,surf} - (\phi\, p_{sat,air}))^{expt}$$

Equation (6.6)

$$ev = e_h h_m A_s(p_{sat,surf} - (\phi\, p_{sat,air}))^{expt}$$

Equation (6.7)

where h_m is the convective mass transfer coefficient (s/m) and is derived in ESP-r using the Lewis relation displayed below that incorporates a heat and mass transfer analogy.

$$h_m = h_c M_{H2o}(0.85)$$
$$\rho C_p R T$$

Equation (6.8)

The value 0.85 represents the Lewis number at standard atmospheric pressure; R is the universal gas constant (J/kmole.K); and M_{H2O} is the molecular mass of vapour (kg/kmole). Initial simulations showed that the predicted results were very sensitive to the value of the exponent used in equations (6.[1]) and (6.7). A sensitivity analysis carried out to assess the level of impact associated with the exponent value, found that a fixed value of 1.18 would be applied to equation (6.6) and 1.2 to equation (6.7).

---

[1] .3.2 Outcomes from developed modelling approach

Figures 6.12 to 6.17 plot the resultant drying rates predicted using the developed modelling approach. The graphs draw comparison between ESP-r's predictions for the drying rates calculated using each of the four variants of the evaporation rate equations and the measured data for the selected clothing items. The level of agreement between the measured data and the predictions though varied depending on the clothing item modelled and for the different stages of the drying process.

The humidity ratio (kg/kg) at the modelled drying surface is calculated based on the surface temperature and the moisture content. The moisture content of the air is calculated as part of the air mass balance for all of the zones in a model at each time step and accounts for the moisture introduced to the indoor air as a result of any evaporative sources being modelled.

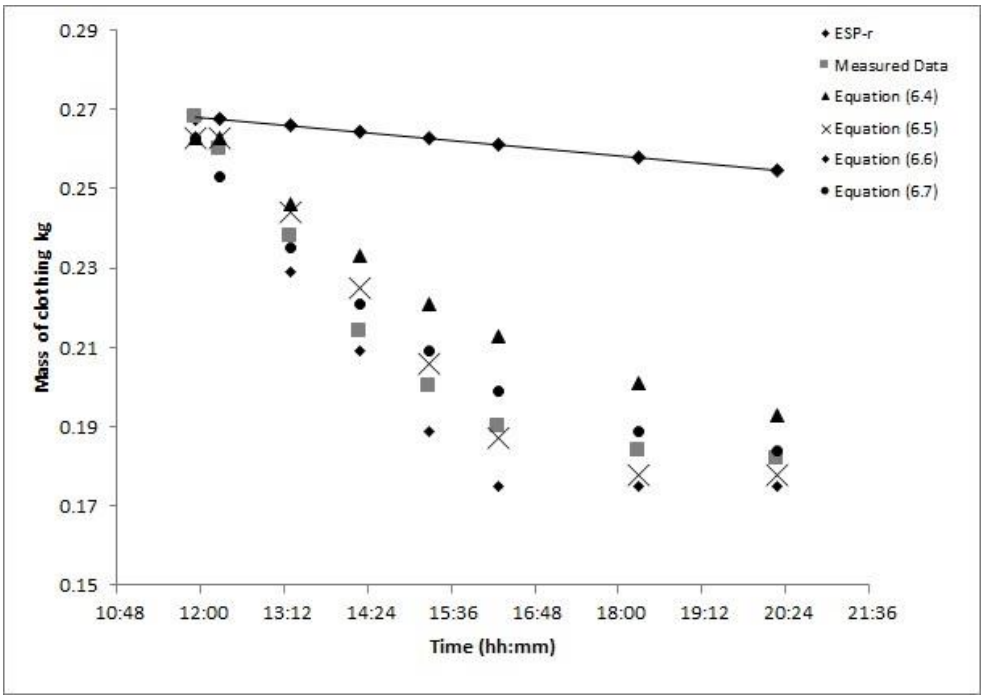

Figure 6.12 Evaporation rates predicted for T-shirt.

The results presented in Figure 6.12 highlight the positive impact achieved through the introduction of the new methodology implemented in ESP-r's surface modelling capabilities. A significant difference between the original results (labelled 'ESP-r') and the measured data is shown, resulting in the characteristic curve of the porous material drying performance also not being achieved. By only accounting for transfer effects at the interfacial region, which in this case refers to the effect of the humidity ratio gradient on the mass transfer rate, the influence of moisture transfer within the material on the drying process is not represented.

The developed modelling approach shows that the drying performance of the porous material is better represented when the combined effect of surface transfer phenomena and moisture transfer within the porous material is considered. The improved agreement between modelled and actual measured data was repeated for a number of clothing items, including a Towel, Facecloth, Jeans, Shirt and Cotton Top, the results from which are presented in the figures below.

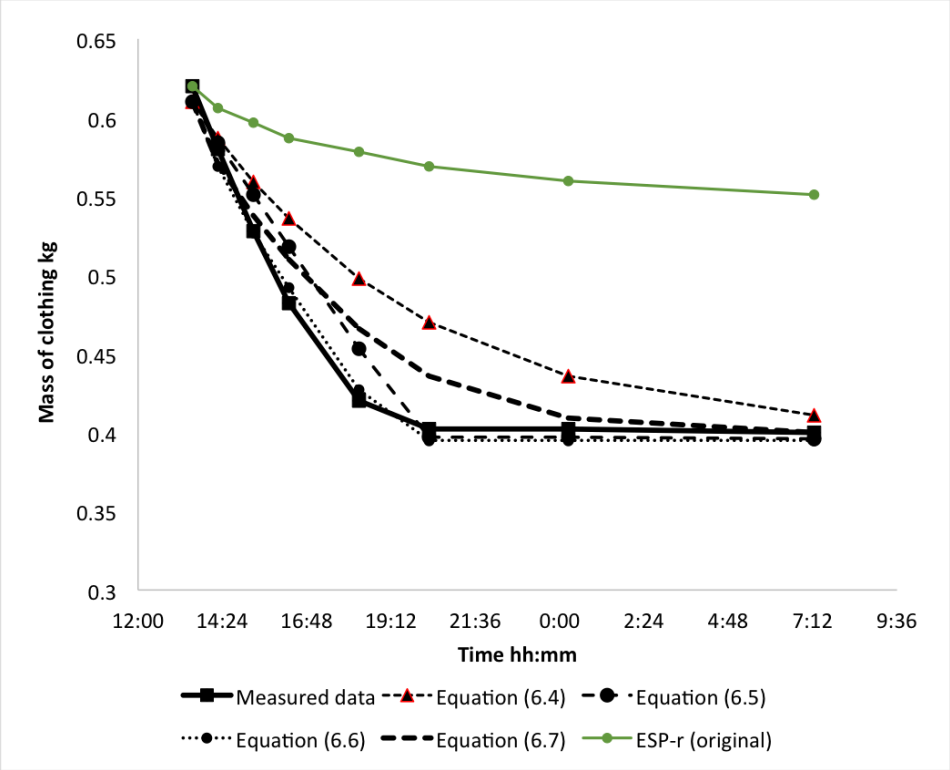

Figure 6.13 Evaporation rates predicted for Towel.

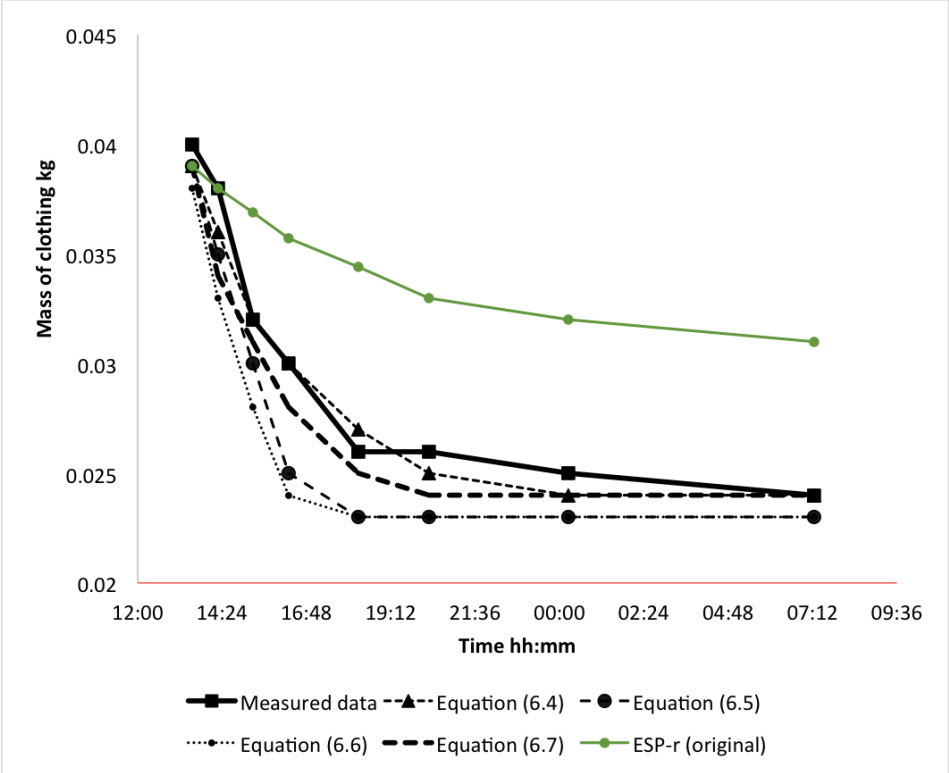

Figure 6.14 Evaporation rates predicted for Facecloth.

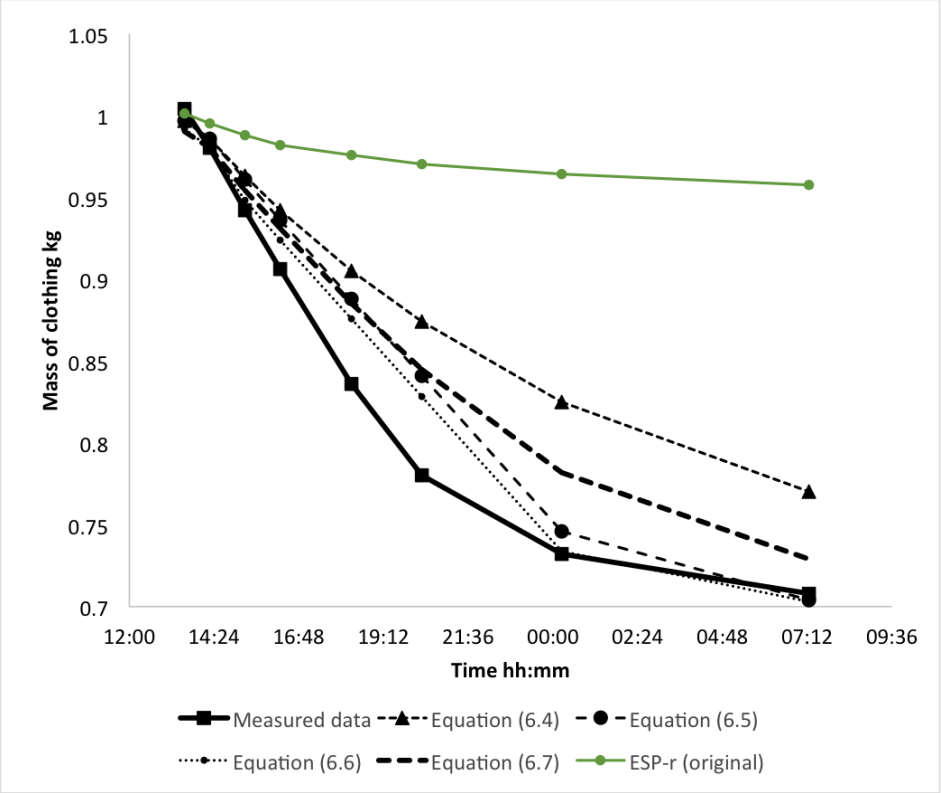

Figure 6.15 Evaporation rates predicted for Jeans.

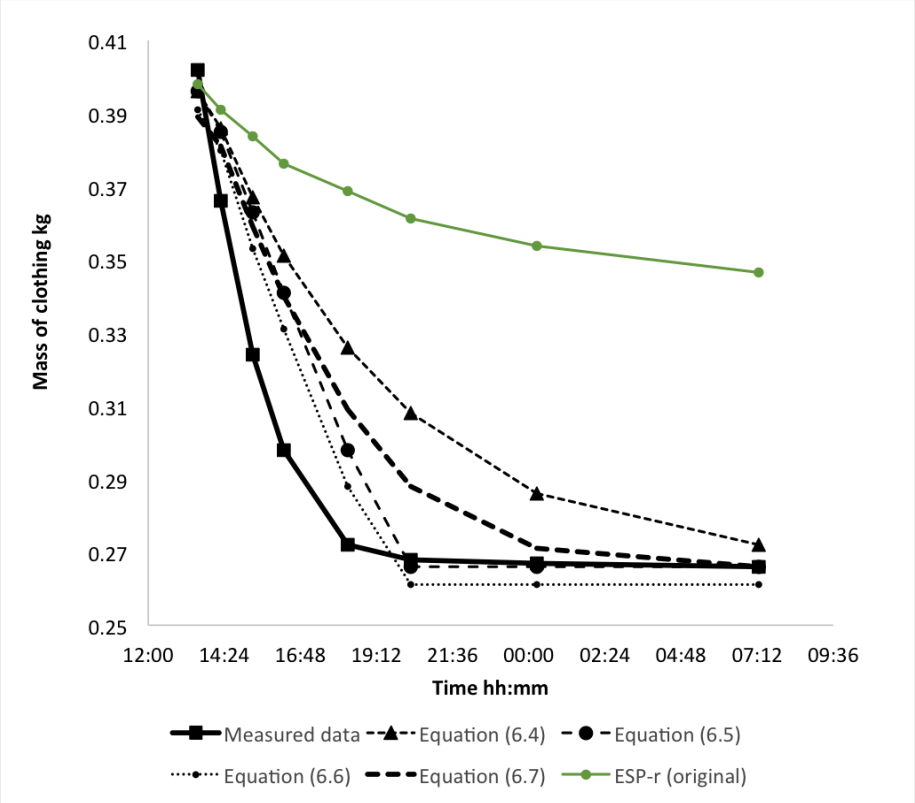

Figure 6.16 Evaporation rates predicted for Shirt.

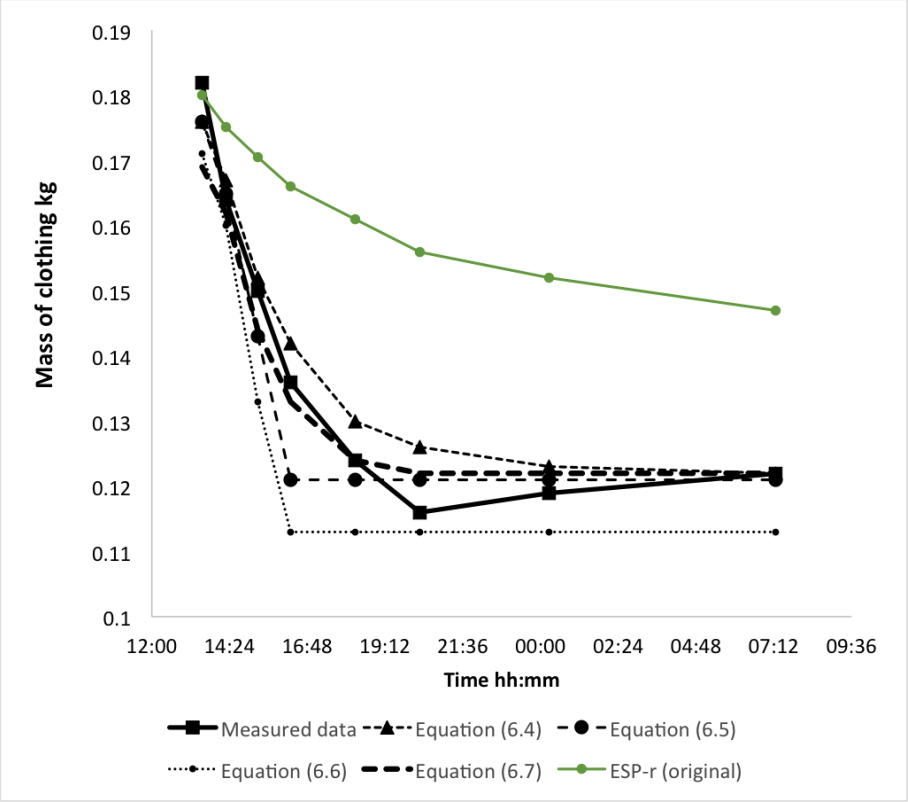

Figure 6.17 Evaporation rates predicted for Cotton top.

The level of agreement achieved in the results presented is discussed in the next section, with reasons given for the improved modelling performance but also the causes of poor agreement.

6.3.3 Discussion

Predictions made using Equation (6.4) improved the correlation with measured data, in terms of the expected profile of the drying process, as is shown in the example drying curve displayed in Figure 6.11. A significant difference arises between all but two of the clothing items modelled when comparing the magnitude of the predictions made using Equation (6.4) and the measured data. This would indicate that despite the numerical adaptation introduced, there are additional parameters not accounted for in this particular modelling approach. Improved agreement between predictions and measured data was seen for the Facecloth and the Cotton top, which were the two smallest items modelled but also, with respect to the material composition, items that would respond primarily to the fluctuations in boundary conditions.

Outcomes from the modelling study using Equation (6.5) did not improve the drying profile correlation between measured data and model predictions for the clothing items tested. In the cases where a shorter time was required to reach a dry weight equilibrium, the predicted rate of drying during the initial stage of the process (as highlighted in Figure 6.11) was linear. However, the transition phase between the first and second stages of drying, where the hygrothermal properties would become the primary factors

dictating the rate of moisture transfer through the pore structure of the material to the surface, was not adequately modelled. This aspect of the modelling process was most apparent when modelling the Jeans, indicating a low liquid conductivity in the fabric and hence the need to model the liquid transfer properties associated with this type of material.

The final two evaporation rate equations produced reasonable agreement between the predicted drying rate and the measured data. Using Equation (6.6) resulted with improved correlation in relation to the drying profile observed in the measured data. The difference in magnitude between the measured and predicted sets of data was smaller when modelling clothing items that required less time to reach a dry equilibrium state in comparison to the items considered with greater moisture storing capacity such as the Jeans and the Towel. Applying Equation (6.7) resulted in improved predictions when modelling the Towel, but in the remainder of the cases an overestimation of the rate of drying, predominantly during the initial drying stage, was seen as a consequence perhaps of the amplification effect associated with using an exponent value greater than 1. Modelling the Jeans again indicated that further knowledge of the hygrothermal properties of the materials being tested would improve the model.

Further consideration of the relationship between the surface temperature conditions of a material and the resulting moisture transfer characteristics is presented in the following section. This analytical study highlights the importance of taking into account the transient nature of the surface temperature conditions in relation to its potential impact on hygrothermal material behaviour. Measured data from the empirical verification study presented in section 6.3 was used to conduct an analysis of the effect of changing temperature conditions on the resulting moisture permeability of a material.

6.4 Considering the transient effects of surface temperature

This study was conducted to highlight the sensitivity of a materials hygrothermal performance to changing surface boundary conditions and hence the associated impact this may have on simulation outcomes. The specific focus of the study was on the relationship between the surface moisture diffusion coefficient property and the moisture permeability of stagnant air.

6.4.1 Methodology for analysing the moisture permeability of stagnant air

The time series air temperature and relative humidity data obtained from the clothes drying experiment discussed in section 5.9 was recorded using a 1-min time step interval. This data was then used to determine the hygrothermal properties required to calculate the moisture diffusion coefficient of air across the entire measurement period, which was approximately 21 hours. The properties calculated included the saturation vapour pressure, which was then used to determine the equivalent vapour pressure values at the recorded temperature. Figure 6.18 displays the resultant vapour pressure profile and the measured temperature profile across the recorded period.

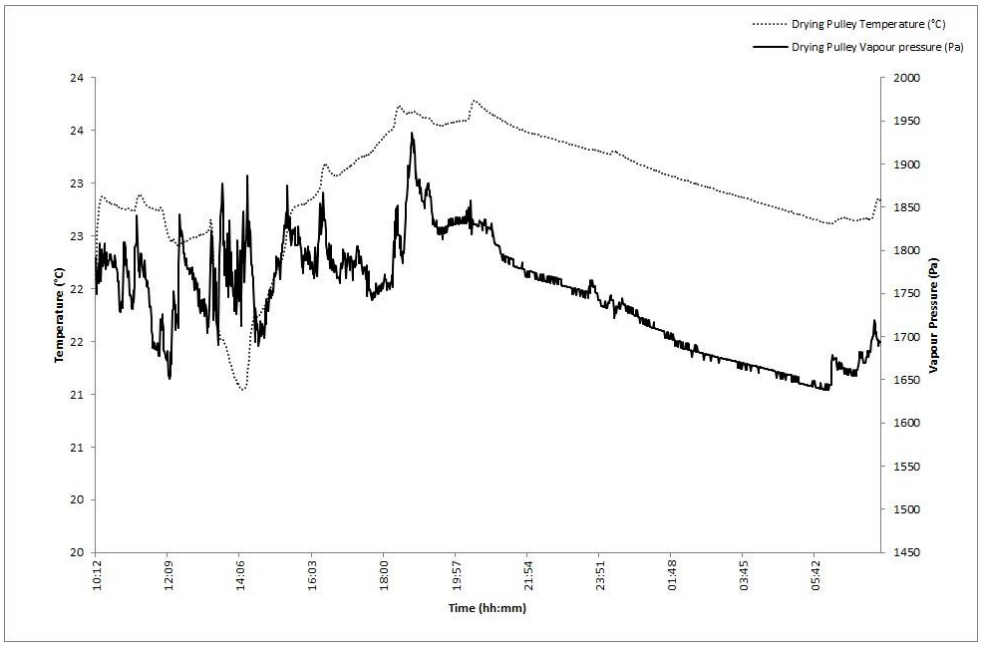

Figure 6.18 Measured temperature and calculated vapour pressure profiles at surface of drying pulley.

Following this, the values were then substituted accordingly into the different empirical correlations derived for the moisture diffusion coefficient of air (already presented in Chapter 3 section 3.3.3), to produce a transient profile of the moisture diffusion coefficient values for air.

Subsequently, a time series profile of the moisture permeability of stagnant air was calculated. The results for this were applied into the standard formula used to determine the material moisture permeability in ESP-r, shown below, to create a moisture permeability profile for an arbitrary Gypsum Plasterboard surface exposed to the measured hygrothermal conditions.

$$\square_a$$

$$\square_p \square$$

$$\delta_a(T) = \frac{D^{aw}(T)}{R_v T}$$

Equation (6.9)

The dependency of both the moisture permeability of stagnant air and the moisture diffusion coefficient of air on the air temperature and additional surface boundary conditions has been identified in empirical studies and is represented by the following expression:

$$\delta_a(T) = \frac{D^{aw}(T)}{R_v T}$$

Equation (6.10)

where δ_a is the moisture permeability of stagnant air (kg/m.s.Pa); D_{aw} is the binary diffusion coefficient for an air and vapour mixture (m^2/s); R_v is the ideal constant for water vapour (J/kg.K); and T is the air temperature (K). The relevance of this property when applied to a practical moisture transfer scenario, such as the passive clothes drying, becomes increasingly important given the different stages of drying taking place, the driving forces associated with each of the related transfer processes, and material characteristics such as the surface pore structure that will determine the length of time the initial rate of drying will take place over (Metzger et al, 2007). This study did not consider the complete set of boundary conditions and material parameters influencing the rate of moisture transfer from a wetted surface, but instead focused on presenting one physical aspect and accounting for its transient behaviour, i.e. its dependency on changes in the material surface temperature. Additional temperature dependent air properties, such as the air density, would also need to be considered as part of this nonlinear, natural convective process, given its use in the heat and mass transfer analogy shown in equation (6.8).

6.4.2 Results from modelling transient air temperature conditions

Empirical studies on the effect of a temperature dependent value for the moisture permeability of stagnant air have shown the value to be in the order of 10^{-10} kg/m.s.Pa (Kumaran, 1998), which was also achieved in the results presented in this study. Figure 6.19 presents a comparison between the four predicted values of the moisture permeability of stagnant air, which account for the temperature dependency of this property; and the fixed value employed in ESP-r. The four predicted values were produced by substituting the value for the diffusion coefficient of a binary air and vapour mixture (values calculated using the empirical relations of Schirmer, Sherwood, De Vries and Krischer, presented in Chapter 3, section 3.3.3) into equation (6.10) above.

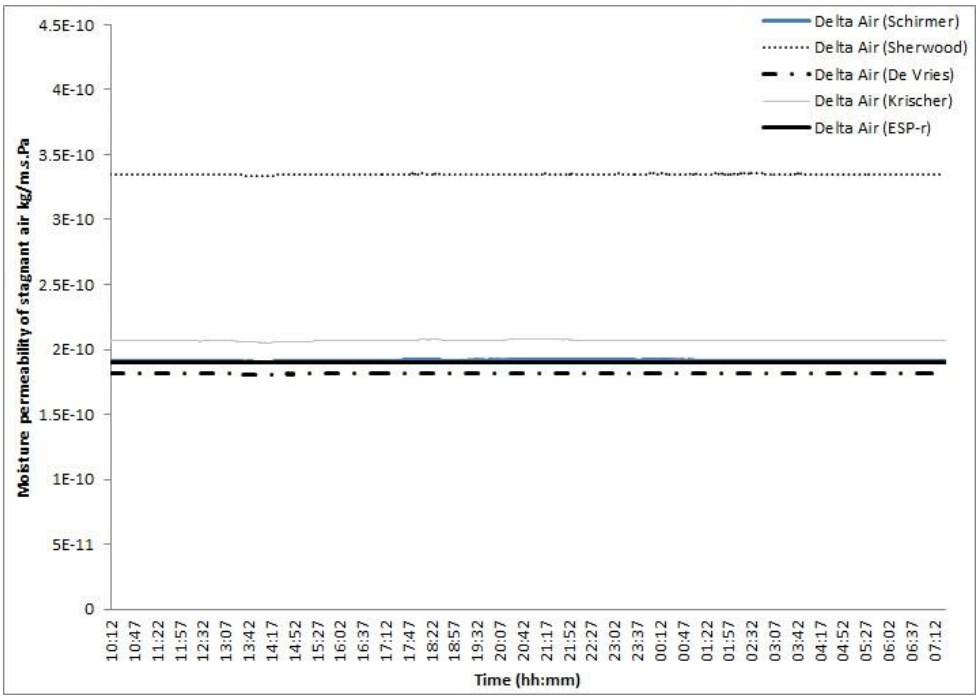

Figure 6.19 Comparison between moisture permeability of stagnant air values calculated using Schirmer, Sherwood, De Vries and Krischer empirical relationships for the diffusion coefficient of stagnant air.

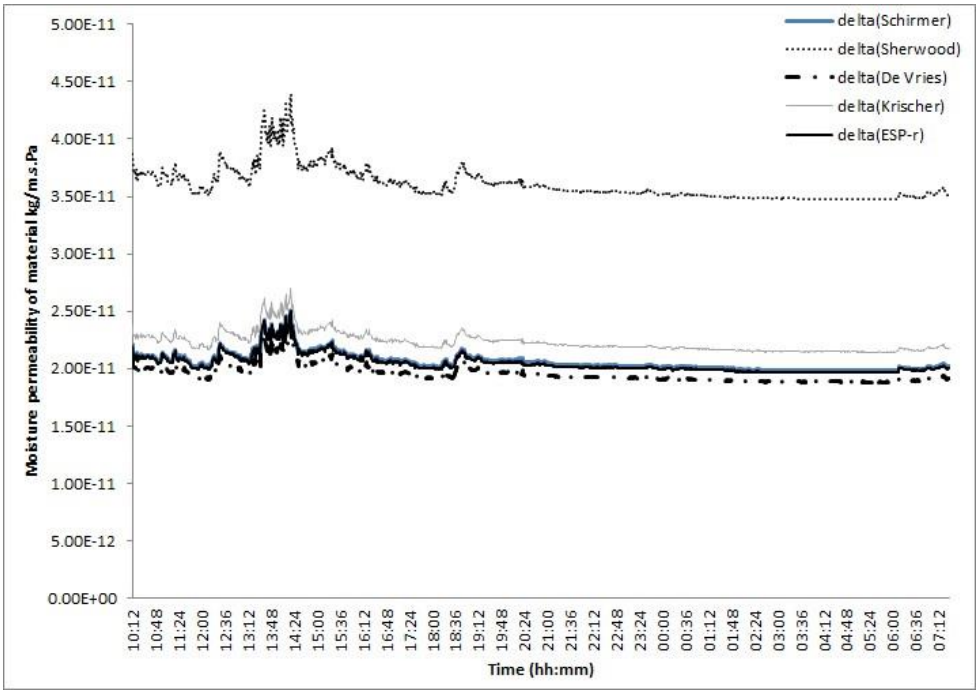

Figure 6.20 Comparison between resultant material moisture permeability values calculated using the temperature dependent moisture permeability of stagnant air

Figure 6.20 presents the resulting effect of accounting for the temperature dependency of the moisture permeability of stagnant air when determining the moisture permeability of a hygroscopic material. The variation of the material moisture permeability over the time period is highlighted during the clothes drying period, emphasising the need for a more detailed and dynamic representation of the surface boundary conditions in simulation.

6.5 Chapter summary

This chapter has presented the results from the development work that has been undertaken as part of the research into advancing the integrated moisture modelling domain found within the ESP-r whole building simulation tool. A key lesson learned was that of the underlying complexity of modelling the interrelated nature of heat, air and moisture transfer processes in the building environment. This high level of complexity became very apparent following an initial set of model verification exercises, carried out to investigate the efficacy of the current moisture model employed in ESP-r. The option for intermodel comparison was made available in these exercises and helped to underline the large number of moisture modelling approaches currently adopted across a wide range of building simulation tools which analyse combined heat, air and moisture transfer processes. This view was founded on observations made of the wide distribution of modelling results produced by these tools, even for simplified, isothermal cases; and the lack of general consensus obtained in the modelling solutions, as to where the source of uncertainty may lie. By introducing added complexity to the specification of a building model, this underlying problem would be exacerbated.

The work undertaken was therefore in response to the weaknesses identified during the moisture modelling verification process. These included the suitability of standard hygrothermal material properties being used to model both isothermal and dynamic hygrothermal conditions in a building. The addition of a new linear function to calculate the moisture buffering performance of simple building construction greatly improved

the level of agreement reached between modelled predictions of the indoor relative humidity conditions and the analytical solution. It was also found that the approach used to model the heat transfer coefficient would significantly impact on both the profile and magnitude of the final solution as well, indicating the potential for further investigation into the sensitivity observed between the model predictions and this surface transfer parameter, despite the use of fixed boundary conditions.

The heightened impact of the surface transfer parameters was also noticed during the first of the two empirical verification studies presented. Improved agreement between the predictive performance of ESP-r and experimental data was achieved when modelling the surface moisture flux of a material with the advancement of the range of moisture permeability functions available in ESP-r to model this material characteristic. The experimental method applied in this study was designed with the aim of replicating dynamic moisture loading conditions observed in the indoor building environment. Without exact knowledge of the airflow regime and surface boundary conditions in the environmental chamber used in the experiment, a fixed convective heat transfer coefficient was adopted in the study. However, further analysis of this surface transfer property indicated a variable coefficient would be more suitable under these hygrothermal conditions.

The second empirical verification case focused on the modelling of surface evaporation. The model developments helped to improve the correlation between the predictions and the measured data taken from a clothes drying monitoring experiment. The differences observed between the predicted and measured drying rate profile may be addressed with the inclusion of hygrothermal material properties for the clothing items modelled, as this particular hygrothermal component of material characterisation is associated with the transition phase between the initial and second stages of drying. At this particular point in the process, a lower moisture content is to be expected in the material and hence the moisture transfer through the material pore structure to its surface is related primarily to the material hygrothermal properties e.g. the hydraulic conductivity.

A final analytical study highlighted the influence of surface boundary conditions on material moisture transfer properties, further emphasising the need for detailed representation of boundary conditions, in particular the surface temperature due to the standard application of the heat and mass transfer analogy in moisture modelling.

Referring to the lesson learned that was mentioned earlier in this section, it is important to address the level of complexity associated with moisture modelling prior to creating a building moisture model. Within an integrated dynamic whole building simulation environment, the level of complexity incorporated into a moisture model will be dictated by the quality of the data available to create it. Uncertainty underlies a number of processes and factors that ultimately influence the application of moisture

modelling within a whole building simulation, including the reliability of experimentally derived material moisture properties; the suitability of governing equations used to represent the heat and mass transfer analogy; and accurate representation of moisture generating activity. The work presented in this thesis has made a contribution to this issue of the difficulty of accurately modelling the complex processes involved in moisture transfer. This has been done by improving the accuracy in the modelling of the moisture buffering phenomenon associated with hygroscopic building material; and through developing the representation of surface evaporation from moisture sources found within the indoor building environment.

CHAPTER 7

Conclusions and Future Work recommendations

Chapter overview

This chapter concludes the work that has been presented in this thesis. An overview of the stated aim and objectives of this research is provided alongside a review of the steps that were taken to realise them. The achievements made during the course of this research are described and it is argued they represent important developmental work in the field of moisture modelling. In light of this work, it is argued that a valuable platform for future development is provided, particularly with regard the experimental and whole building simulation of moisture transfer phenomena, including moisture buffering and the drying process in hygroscopic porous materials, and a series of recommendations for such work is made.

7.0 Conclusions

The aims of this research were to verify and advance the modelling of indoor moisture transfer processes within the context of whole building simulation. The defined objectives of the research were to:

- accurately model the impact of the moisture buffering behaviour associated with hygroscopic porous building materials in the building envelope;
- develop the treatment of surface evaporation from indoor moisture sources.

The moisture modelling domain located within the integrated whole building simulation framework of ESP-r was used in order to meet the stated objectives. This provided a platform from which to model the influence of several building parameters. These included the levels of occupancy and associated production of heat and moisture gains; the indoor air change rate created both naturally and through mechanical schemes; variable outdoor climate conditions; and the interrelated nature of these aspects of building performance as part of a whole building simulation using a defined time step resolution. In doing so, the dynamic whole building integrated approach would help to reflect the dynamic and complex nature of the hygrothermal conditions arising in the indoor building environment. These become critical in accurately modelling the recognised hygrothermal interaction taking place between the indoor air and the hygroscopic porous material found in the building envelope construction, which passively contributes to the moderation of indoor relative humidity conditions. The significance of using simplified surface boundary conditions, and incorporating standard hygrothermal material properties in the modelling methodology to reflect the dynamic and coupled heat and moisture transfer processes occurring at this fluid-solid interface, became apparent in the outcomes produced from the empirical verification studies conducted during the course of this research.

The work presented in this thesis has described the methods used to verify and develop the moisture modelling approaches adopted by ESP-r in response to the issues

highlighted above. Verification of ESP-r's moisture model was based on drawing comparison between measured and analytical data provided in a recent International Energy Agency project and the modelling predictions produced using ESP-r for specific test cases. Additional results produced by other heat and moisture transfer modelling tools were also provided, allowing for inter-model comparison between these tools and ESP-r for the different test cases. Following this initial verification of the existing moisture modelling methodology utilised by ESP-r, the model was applied to investigate the impact of passive indoor drying of laundry on the indoor environment, in particular the relative humidity conditions resulting from this common practice in housing, as part of an EPSRC funded project. The existing modelling platform was used to conduct a multiple parameter study. This included: the impact of variable occupancy profiles; heating and moisture loading schedules, implemented as hourly step changes in sensible and latent heat gains, respectively; different levels of air infiltration and building fabric quality to represent different levels of air tightness and thermal efficiency in the building; and finally a range of internal wall lining materials, so as to evaluate the moisture buffering potential associated with these types of materials.

Further to this study, two additional empirical verification cases were modelled to assess firstly, the suitability of using standard hygrothermal material properties to model the response of hygroscopic porous building materials exposed to short duration, high moisture loading conditions; and secondly, calculation of the evaporation rate from wetted surfaces, in the context of passive indoor laundry drying described in the project above.

The development work presented in this thesis was put forward in response to two primary issues arising from the initial assessment of ESP-r's moisture modelling approach and to those identified during the empirical verification studies. The first includes enhancement of the range of material properties available to model the dynamic response of hygroscopic porous building materials to changes in relative humidity conditions, which also allows for the incorporation of surface coatings to the internal surface of the building envelope construction. The second area of development was in the simulation of the drying process, which incorporated important parameters influencing the duration of the drying period and advanced the modelling of different stages of the surface evaporation process.

The following sections describe the steps taken to implement the developments that have been described above.

7.0.1 Quantification of the moisture buffering effect

Building design has primarily been driven with the aim of improving energy efficiency and thermal performance, taking the forms of increased levels of building air tightness and reduced levels of natural ventilation. The negative effect of these improvements has

been realised in the reduction of indoor air quality. This issue has received less attention in practice due to limited knowledge on effective methods to balance adequate levels of ventilation with efficient use of energy given the context of such diverse and dynamic hygrothermal conditions experienced in the indoor environment. Managing the concentration of indoor air pollutants will therefore also require the appropriate control of indoor relative humidity, which research has shown can induce both discomfort and pose health risks to occupants during extended periods of exposure to indoor relative humidity surpassing 60%RH. Recommended levels of indoor airflow rates are provided in building regulations to address this. However, these are focused on their application being in new housing design thus leading to concern over the existing housing stock already displaying signs of moisture related damage. Exploration of methods for mitigating excessive levels of indoor moisture has also identified the passive moisture buffering effect associated with hygroscopic porous materials found in the building construction and objects commonly found in the domestic housing scene, for example furniture. The positive effect of this material characteristic has been realised in several studies and subsequently its incorporation in whole building hygrothermal modelling has received considerable attention. Developing and optimising the underlying numerical methods used to model this coupled heat, air and moisture transfer behaviour occurring at the surface and through the pore structure, for the range of materials that display this type of moisture buffering effect, becomes critical in assessing its influence on whole building performance assessment.

An outline of numerical methods available to quantify the moisture buffering effect inherent in hygroscopic porous building materials was also given in Chapter 2. The method described included the Effective Moisture Penetration Depth (EMPD) method, the Effective Resistance (ER) and Effective Capacitance (EC) models and a material characterisation method known as the Moisture Buffer Value (MBV). Significant drawbacks associated with these methods were highlighted, emphasising the need for using a dynamic, whole building simulation tool to conduct this research. The boundary conditions applied during the numerical analysis procedures mentioned i.e. the EMPD, ER and EC methods are assumed steady state despite the actual conditions in the indoor building environment being subject to fluctuating occupancy levels and ventilation rates that will impact on both the indoor air temperature and moisture content. The extended time required to compute the material response and determine material moisture properties for each modelled surface is an additional limitation of these approaches. The limiting factors also apply when considering the moisture transfer properties of the materials being assessed. The use of fixed values for these properties and in the case of the Effective Capacitance (EC) model the omission of intrinsic material hygrothermal properties, such as the moisture permeability, is detrimental to the accuracy of the resultant quantification of the moisture performance of the building. This issue was

addressed during the development work presented in Chapter 6, which addressed the interdependency between the moisture permeability of the materials investigated and variations in relative humidity.

7.0.2 Verifying the modelling of hygrothermal material performance

The reduction of indoor air relative humidity achieved as a result of the passive absorption and desorption processes associated with these materials was reviewed, placing emphasis on the accurate representation of this aspect of material performance in the context of building simulation. The techniques available to measure the hygrothermal performance of porous, hygroscopic building materials and the subsequent range of moisture properties derived from this measured data were presented in Chapter 3, which also highlighted the concern raised over the reliability of derived material moisture properties in hygrothermal building simulation as a result of measurement inaccuracies, unrealistic measurement conditions and the heterogeneity inherent in the composition of many porous building materials, invariably leading to the use of simplifying assumptions for material characterisation. An initial example of the effect resulting from the use of different forms of material moisture properties was presented in Chapter 5, for the case of the sorption isotherm function, by drawing comparison between ESP-r predictions for indoor relative humdity and an analytical solution. A simple, monolithic building was modelled with isothermal boundary conditions and a scheduled step change of indoor relative humidity. Applying the existing sorption isotherm function in ESP-r to model the moisture buffering performance of the building envelope resulted in underestimating the rate of absorption during the moisture production period. However, better agreement between ESP-r's predictions and the analytical solution was brought about by implementing a new function to represent this moisture property of the concrete construction.

The significant influence of surface transfer parameters was also identified during a sensitivity study of the effect of the convective heat transfer coefficient in the analytical study described above, comparing ESP-r's standard default method for calculating this property with the application of a fixed heat transfer coefficient.

Additional cases of increased modelling complexity were also presented, providing the opportunity for inter-model comparison of indoor relative humidity predictions, including those of ESP-r. A wide distribution of modelling predictions was seen that emphasised the lack of consensus between the different moisture modelling approaches, and also the potential for uncertainty to arise in the modelling of material moisture properties and the associated surface moisture transfer behaviour.

7.0.3 Modelling surface moisture transfer processes

As described in Chapter 5, ESP-r's integrated moisture modelling domain was used in a recent project to investigate the environmental impact of passive indoor drying

of domestic laundry. This produced evidence indicating that further validation of the existing moisture flow solver was required in the assessment of the hygrothermal performance of moisture buffering building material, and also with respect to the significant influence observed in indoor moisture production. Chapter 6 presented the development work that took place in parallel to further empirical verification studies.

The use of standard material moisture properties to model the response of two material samples exposed to dynamic relative humidity conditions was applied in a laboratory environment. This reflected the short term and high moisture production levels associated with occupant related activities in the indoor environment, such as showering and cooking, and showed that the current use of standardised single values characterising the moisture transfer behaviour of the tested materials was not appropriate when modelling these conditions in ESP-r. Using the surface moisture flux data measured in the experimental procedure, ESP-r predictions underestimated the magnitude of the surface moisture transfer behaviour following the initial step change in relative humidity from 50%RH to 90%RH. This indicated that the influence of material moisture properties was less significant in comparison to the initial vapour pressure gradient produced across the fluid-solid interface. The two materials being tested consisted of a sample of painted gypsum plasterboard and a sample of Clayboard (manufactured as 'Claytec'), a composite comprised of reed, hessian and clay. Additional empirical data was sourced from other experimental investigations involving these materials and existing material property databases in order to derive new moisture permeability functions. This data was represented in the form of the standard vapour diffusion thickness and the vapour diffusion resistance factor across the relative humidity range.

This development produced improved agreement between the measured data and ESP-r predictions in terms of the response profile of each material. However, a difference in magnitude remained. Explaining this difference involved analysis of the influence of the convective heat transfer coefficient, to which the sensitivity of predictions had already been identified during the verification stage of the work presented in this thesis. Without accurate knowledge of the surface airflow conditions or the material surface temperatures inside the environmental chamber used in the experiment, a constant heat transfer coefficient was applied to the model, having calculated a Reynold's number indicating a laminar flow regime. The analytical study showed that a variable heat transfer coefficient would be necessary to further optimise the modelling of this surface moisture transfer process. This result further emphasised the importance of determining appropriate convective heat transfer coefficients when there is modelling uncertainty, which could be achieved through a sensitivity study of the air velocity in the chamber that would help to highlight the potential for moisture transfer at the surface. The simplifying assumption applied in isothermal cases and in

those without detailed knowledge of surface temperature conditions, as was described in Chapter 4, involves the use of a heat and mass transfer analogy. Applying an increased level of detail, with respect to the different fluid flow processes and hygrothermal conditions in the test chamber, would help to address the uncertainty surrounding the modelling of the complex and dynamic interaction taking place at the surface boundary; and also help to identify the factors influencing the different stages of moisture transfer.

7.0.4 Enhancing the surface evaporation model

Developments of the surface evaporation model existing in ESP-r included the addition of an initial material moisture content and advanced representation of the different stages of the drying process, in the context of passive indoor laundry drying. This helped to advance the correlation between measured data and initial ESP-r predictions presented in Chapter 5. An overview of the convective drying process was provided in Chapter 4, describing the general use of heat and mass transfer coefficients to relate heat and moisture fluxes with changes in temperature and vapour pressure conditions. This is a simplified approach adopted to avoid explicit modelling of the complex and variable surface boundary conditions observed at the fluid-solid interface. Research has helped to characterise the different stages of the drying process and define the material properties and environmental parameters, the latter referring to the surface airflow characteristics, temperature and vapour pressure gradients, influencing this process.

The existing surface evaporation model in ESP-r calculated the moisture loss rate from a wetted surface as the product of the vapour pressure gradient (widely used as the primary driving force behind this process) across the interfacial region between the wetted surface and the air and the convective mass transfer coefficient calculated using a Lewis relation. Using experimentally obtained data for the moisture loss rate of a selection of clothes dried passively inside a real house setting described in Chapter 5, the model predictions portrayed a linear rate of evaporation, which did not reflect the true characteristic drying curve presented later in Chapter 6. The introduction of an initial moisture content for the clothing enabled the time step calculation method used in ESPr to account for the remaining moisture in the drying surface, and thus account for the moisture storage capacity of the clothing material modelled. However, the material moisture properties or material composition recognised to influence the moisture diffusion rate from the inside of the material to the surface was not incorporated. It became apparent from modelling clothing items that required a longer period of time to reach an equilibrium dry mass weight that the inclusion of their relevant material moisture properties should be investigated to determine the rate of moisture flow to the material surface, i.e. low hydraulic conductivity of the fabric.

The work described in this thesis has presented the contributions made in expanding the range of material moisture properties that can be applied in future

building moisture modelling applications and improving the representation of the drying process, in the context of passive laundry drying. Additionally, an empirical verification procedure has been devised and outlined in this thesis, which could be further developed with the aim of improving the transition between experimentally derived material moisture properties into the whole building simulation environment.

7.1 Recommendations for Future Work

The outcomes of this research point to several key areas suitable for further study and development in the field of material moisture modelling. These include future development of the empirical verification procedure conducted during the dynamic moisture loading experiment used to evaluate standard hygrothermal material properties; the incorporation of ESP-r's CFD modelled boundary conditions to enhance the detail of this feature entered into the moisture modelling solution; the further expansion of material moisture properties used in the existing moisture model; and finally the continued adaptation of the surface evaporative model to include material moisture property properties and implementation of the pore structure characteristics found in clothing materials. Each of these are now considered in turn and recommendation are made as follows.

7.1.1 Further development of the empirical verification procedure

The experimental procedure used as part of the empirical verification study of the surface moisture flux modelling capabilities of ESP-r was described in Chapter 5. The testing facility was originally designed to measure the moisture permeability of thin layer materials e.g. permeable membranes. A high air velocity is applied to reduce the resistance to moisture transfer at the surface boundary layer above the sample material tested and this consequently creates an unrealistic representation of the indoor air characteristics observed in the building environment. A more detailed investigation of a range of airflow velocities and monitoring of surface temperatures at of the material samples would enhance understanding of the effect these variables have on the convective heat transfer coefficient.

An additional aspect of the experimental facility that may be improved upon is in relation to the weighing procedure. The current mechanism involves lowering of the test samples to the weighing scale and at the same time turning off the air conditioning unit, a process which may interfere with the accurate measurement of the sample weight. This process was not modelled in ESP-r during the empirical verification study. Improving the modelling may therefore require increasing the time step resolution of the experimental procedure, currently set to a minimum of 10 minutes.

7.1.2 Combining CFD with the simulation of surface transfer processes

The importance of increased spatial and temporal resolution of the hygrothermal variability associated with the highly coupled heat and moisture transfer processes

occurring at the surface of porous building materials was discussed in chapter 4. This was highlighted due to the influence of fluctuating boundary conditions observed in the indoor environment, which are intrinsically linked to accurate modelling of the hygrothermal response of porous and hygroscopic materials. Despite surface thermal buoyancy effects and subsequent variations in air density, simplifying assumptions are applied to model the conditions at the surface boundary layer in the form of constant surface moisture transfer coefficients; and through the application of the heat and mass transfer analogy, the use of which still raises concern over its suitability in such highly coupled hygrothermal processes.

To further develop the modelling side of the first empirical verification case presented in Chapter 5, a detailed representation of the fluid flow fields observed within the environmental test chamber could be achieved using the partitioned CFD solver integrated into ESP-r. Detailed boundary conditions for the interior of the environmental test chamber would provide a better estimation of the convective heat transfer coefficients at the surface of the materials being assessed.

7.1.3 Hygrothermal material properties

It is important that the dynamic nature of moisture transfer, both at the surface boundary layer and within the porous structure of hygroscopic building materials as was described in Chapter 4, is required to develop accurate simulation of hygrothermal processes in the indoor building environment. This accuracy is highly dependent on the hygrothermal properties of the materials found both in the building envelope and additional objects present in the building interior, which should be calculated in response to fluctuations of indoor boundary conditions. Despite reasonable agreement achieved in some of the test cases modelled during the initial verification study presented in Chapter 5, the incorporation of the desorption isotherm in the ESP-r moisture modelling domain is recommended to allow for the investigation of hysteresis effects.

An additional study of the moisture permeability of stagnant air further highlighted the influence of dynamic surface boundary conditions, in particular the surface temperature, in Chapter 6. ESP-r currently adopts a constant value for this property. Development of the experimental technique available to measure this particular hygrothermal property is necessary to overcome the current limitations associated with differentiating between the coupled heat and moisture transfer processes. This dynamic aspect should also apply to additional thermophysical properties influenced by moisture conditions in building materials, such as the thermal conductivity.

Further work is required to obtain hygrothermal properties for the clothing materials tested during the verification and development of the surface evaporation model in ESP-r. Differences emerged between the predicted rates of drying and the

measured data, which could be examined further by incorporating the hygrothermal material properties dictating the rate of moisture transfer from the inside of the drying material to its surface.

7.1.4 Incorporating the pore structure in the surface evaporation model Further to the point made above with respect to modelling clothing material as another moisture permeable surface in the ESP-r moisture flow solver, an inter-model comparison could be conducted to assess the same drying process using a pore network model solution. This would involve modelling the homogeneous pore structure of clothing fabric using a series of interconnected sorption sites, which would also provide the potential to introduce liquid transfer modelling and associated properties e.g. the liquid conductivity and porosity, in ESP-r's moisture modelling domain for a specific application.

7.2 Outlook for future building design

With the expansion of the range of material moisture properties available and the enhanced representation of the drying process associated with passive indoor drying in ESP-r's integrated modelling framework, it is possible to further evaluate the hygrothermal performance of the indoor building environment with respect to moisture buffering and indoor moisture release.

Moisture in the indoor environment has become increasingly important as research highlights its potentially negative effects on both indoor air quality and occupant health. The emphasis on indoor air quality has also identified the delicate relationship that exists between this issue and the steps being taken to optimise the building ventilation strategy and energy efficiency. Given the dynamic nature of the hygrothermal conditions that have been described in this thesis, it is hoped this research raises the prospects of further developing the accuracy in modelling these processes within whole building simulation.

References

Abadie M O, Mendonca K C, 2009 'Moisture performance of building materials: From material characterisation to building simulation using the Moisture Buffer Value concept', *Building and Environment,* v44: 388-401

Adan O, Brocken H, 2003, *Determination of liquid water transfer properties of porous building material and development of numerical assessment methods*, Final Technical Report of the HAMSTAD project, http://www.bouw.tno.nl/eng/pdf/Hamstad_finalreport_1.PDF

Al-Homoud MS, 2005, Performance characteristics and practical application of common building thermal insulation materials, *Building and Environment*, 40: 353-366

Allergy UK, *Indoor Allergy Week 2011 'The Rise of 'Home Fever'*, November 2011 *www.allergyuk.org/downloads/resources/reports/IAW_Report_2011.pdf*

Al-Raoush RI, Willson CS, 2005, 'A pore-scale investigation of a multiphase porous media system', *J of Contaminant Hydrology*, 77: 67-89

http://archbps1.campus.tue.nl/bpswiki/index.php/Hamlab

Baker P H, Galbraith G H, Mclean R C, 2009 'Temperature effects on moisture transport in porous building materials', *Building Services Engineering Research and Technology*, v30.

Baker P H, 2014, Personal communication

Beausoleil-Morrison I, 2000, *The Adaptive Coupling of Heat and Air Flow Modelling within Dynamic Whole-Building Simulation*, PhD diss., University of Strathclyde

Belarbi R, Qin M, Ait-Mokhtar A, Nilsson LO, 2008, 'Experimental and theoretical investigation of non-isothermal transfer in hygroscopic building materials', *Building and Environment*, 43: 2154-2162

Blocken B, Carmeliet J, 2004, 'A review of wind-driven rain research in building science', *Journal of Wind Engineering and Industrial Aerodynamics, 92: 1079-1130*

Blunt MJ, 2001, 'Flow in porous media – pore-network models and multiphase flow', *Current Opinion in Colloid & Interface Science*, 6: 197-207

Blunt MJ, Bijeljic B, Dong H, Gharbi O, Iglauer S, Mostaghimi P, Paluzny A, Pentland C, 2013, 'Pore-scale imaging and modelling', *Advances in Water Resources*, 51: 197216

Bluyssen PM, 2009, 'Towards an integrative approach of improving indoor air quality', *Building and Environment*, 44: 1980-1989

Burch DM, 1997, *Manual of MOIST – A PC program for predicting heat and moisture transfer in building envelopes (Release 3.0*), Building and Fire Research Laboratory, National Research of Standards and Technology, Gaithersburg, MD, USA

Carmeliet J, 1992, 'Some critical remarks on the numerical modelling of the coupled heat and vapour transfer by the control volume method', *International Energy Agency Annex* 24, Vol. 5, Task 1

Carmeliet J, de Wit M H D, Janssen H, 2005 'Hysteresis and moisture buffering of wood', *7th Nordic Building Physics Symposium*, Reykjavik

Carmeliet J, Descamps F, Houvenaghel G, 1999, 'A multiscale network model for simulating moisture transfer properties of porous media', *Transport in Porous Media,* 35: 67-88

Cerolini S, D'Orazio M, Di Perna C, Stazi A, 2009, Moisture buffering capacity of highly absorbing materials, *Energy and Buildings*, 41: 164-168

Chen ZQ, Shi MH, 2005, 'Study of heat and moisture migration properties in porous building materials', *Applied Thermal Engineering*, 25: 61-71

Clapp RB, Hornberger GM, 1978, 'Empirical equations for some soil hydraulic properties', *Water Reservoir Resource*, 14(3): 601-604

Clarke JA, 2001, *Energy Simulation in Building Design,* 2nd ed., Oxford & Woburn MA: Butterworth-Heinneman

Clarke JA, 2013, 'Moisture flow modelling within the ESP-r integrated building performance simulation system', *Journal of Building Performance Simulation*, 6: 385-399

Cockroft JP, 1979, *Heat Transfer and Air Flow in Buildings,* PhD thesis, University of Glasgow

Colburn AP, 1933, 'A method of correlating forced convection heat transfer data and a comparison with fluid friction', *Transactions of the American Institute of Chemical Engineers*, 29: 174-210

Comings EW and Sherwood TK, 1934, 'The Drying of Solids. VII Moisture Movement by Capillarity in Drying Granular Materials,' *Industrial and Engineering Chemistry 26* (10): 1096–1098

Coutelieris FA, Delgado JMPQ, 2012, Chap. In: *Transport Processes in Porous Media, Advanced Structured Materials*, Volume 20, ISBN 978-3-642-27910-2

Cunningham M J, 1988 'The Moisture Performance of Framed Structures – A Mathematical Model', *Building and Environment,* 23: 123-135

Cunningham MJ, 1992, 'Effective Penetration Depth and Effective Resistance in Moisture Transfer', *Building and Environment*, 27 (3): 379-386

Cunningham M J, 1992 'Effective Penetration Depth and Effective Resistance in Moisture Transfer', *Building and Environment,* 27: 379-386

Curtis R, 2007 *DAMP – Causes and Solutions, INFORM Information for Historic Building Owners*, Historic Scotland, Technical Conservation, Research and Education Group

Daisey JM, Angell WJ, Apte MG, 2003, 'Indoor air quality, ventilation and health symptoms in schools: an analysis of existing information', *Indoor Air*, 13: 53-64

d'Ambrosio AFR, Dell'Isola M, Ficco G, Tassini F, 2012, 'Experimental analysis of air tightness in Mediterranean buildings using the fan pressurization method', *Building and Environment*, 53: 16-25

Defraeye T, Blocken B, Derome D, Nicolai B, Carmeliet J, 2012, 'Convective heat and mass transfer modelling at air-porous material interfaces: Overview of existing methods and relevance', *Chemical Engineering Science*, 74: 49-58

De Freitas VP, Abrantes V, Crausse P, 1996* 'Moisture migration in building walls – Analysis of the interface phenomena', *Building and Environment,* v31, 99-108

Delgado JMPQ, Ramos NMM, De Freitas VP, 2006, 'Can moisture buffer performance be estimated from sorption kinetics?',*J of Building Physics*, 29: 281-299

Delgado JMPQ, Barreira E, Ramos NMM, de Freitas VP, 2013*, Hygrothermal Numerical Simulation Tools Applied to Building Physics*, ISBN 978-3-642-35002-3

Derluyn H, Derome D, Carmeliet J, Stora E, Barbarulo R, 2012, 'Hysteretic moisture behaviour of concrete: Modelling and analysis', *Cement and Concrete Research*, 42: 1379-1388

Descamps F, 1996, *Continuum and discrete modelling of isothermal water and air flow in porous media*, PhD thesis, KUL, Belgium

De Vries D A, 'The theory of heat and moisture transfer in porous media revisited'*, Int J of Heat and Mass Transfer*, v30, 1987, pp1343-1350

Dill M J, 2000 'A review of testing for moisture in building elements', *Construction Industry Research and Information Association,* CIRIA Publication C538, CIRIA, ISBN 0 86017 538 3

Dimitroulopoulou C, 2012, 'Ventilation in European dwellings: A review', *Building and Environment*, 47: 109-125

Eitelberger J, Hofstetter K, 2011 'Prediction of transport properties of wood below the fiber saturation point – A multiscale homogenization approach and its diffusion coefficient', *Composites Science and Technology,* 71: 145-151

El Diasty R, Fazio P, Budaiwi I, 1993, 'The dynamic modelling of air humidity behaviour in a multi-zone space', *Building and Environment*, 28: 33-51

Emmerich SJ, Persily AK, Nabinger SJ, 2002, *Modeling Moisture in Residential Buildings with a Multizone IAQ Program,* Proc.: Indoor Air, 9th Int. Conf. on Indoor Air Quality, Monterrey, California, USA

Fatt I, 1956, 'The network model of porous media I, Capillary pressure characteristics', *Trans AIME*, 207: 144-159

Ficker T, 2003, 'Non-isothermal steady-state diffusion within Glaser's condensation model', *Int J of Heat and Mass Transfer*, 46: 5175-5182

Galbraith GH, 1992, *Heat and Mass Transfer Within Porous Building Materials*. PhD diss., University of Strathclyde

Galbraith G H, Mclean R C, Kelly D, 1997 'Moisture permeability measurements under varying barometric pressure', *Building Research and Information,* 25: 348-353

Galbraith G H, McLean R C, Guo J, 1998 'Moisture permeability data: Mathematical presentation', *Building Services Engineering Research and Technology,* 19: 31-36

Galbraith GH, Li J, McLean RC, Baker PH, 2001, 'The influence of Space Discretisation on the accuracy of numerical simulation of heat and moisture transport in porous building material', *Building Physics*, 25: 143-160

Gayo E, De Frutos J, Palomo A, Massas S, 1996, 'A Mathematical Model Simulating the Evaporation Processes in Building Materials: Experimental Checking through Infrared Thermography', *Building and Environment*, 31: 469-475

Ge H, Yang X, Fazio P, Rao J, 2014, 'Influence of moisture load profiles on moisture buffering potential and moisture residuals of three groups of hygroscopic materials', *Building and Environment*, 81: 162-171

Goto Y, Wakili K G, Frank T, Stahl T, Ostermeyer Y, Ando N, Wallbaum H, 2012, 'Heat and moisture balance simulation of a building with vapor-open envelope system in subtropical regions', *Building Simulation*, 5: 301-314

Hagentoft CE, 2001, *Introduction to Building Physics*. Lund: Studentlitteratur. ISBN 9144-01896-7

Hameury S, 2005 'Moisture buffering capacity of heavy timber structures directly exposed to an indoor climate: a numerical study', *Building and Environment,* 40: 1400-1412

Hall C, Hoff WD, Nixon MR, 1986, 'Water movement in Porous Building Materials-VI. Evaporation and Drying in Brick and Block Materials', *Building and Environment,* 19: 13-20

Hansen K K, 1986, *Sorption Isotherms: A Catalogue*, Technical Report 162/86, Building Materials Laboratory, Technical University of Denmark

Harmathy TZ, 1969, 'Simultaneous moisture and heat transfer in porous systems with particular reference to drying', *I & EC Fundamentals*, 8(1): 92-103

Haverinen U, Husman T, Pekkanen J, Vahteristo M, Moschandreas D, Nevalainen A, 2011,

Characteristics of Moisture Damage in Houses and Their Association with Self-Reported Symptoms of the Occupants, *Indoor Built Environment*, 10: 83-94

Hens H S L C, 2007, *Building Physics – Heat, Air and Moisture, Fundamentals and Engineering Methods with Examples and Exercises*, ISBN 978-3-433-01841-5

Hersoug LG, 2005, 'Viruses as the causative agent related to "dampness" and the missing link between allergen exposure and onset of allergenic disease', *Indoor Air*, 15: 363:366

IEA 1991. *Condensation and Energy: Catalogue of Material Properties*. Annex XIV Report, International Energy Agency

IEA Annex 23 Final Report, 1996, Multizone Air Flow Modelling, Evaluation of COMIS

IEA Annex 24 Final Report, 1996. See: Kumaran K, 1996.

IEA Annex 41, 2008, *Whole Building Heat, Air and Moisture Response*, (www.ecbcs.org/annexes/annex41.htm).

Incroprera FP, Dewitt DP, 2002, *Fundamentals of Heat and Mass Transfer*, 5th Ed., John Wiley & Sons, ISBN 0-471-38650-2

James C, Simonson CJ, Taludkar P, Roels S, 2010, 'Numerical and experimental data set for benchmarking hygroscopic buffering models', *Int J of Heat and Mass Transfer,* 53: 3638-3654

Janssen H, Blocken B, Carmeliet J, 2007 'Conservative modelling of the moisture and heat transfer in building components under atmospheric excitation', *Int J of Heat and Mass Transfer*, 50: 1128-1140

Janssen H, Roels S, 2008 'The dependable characterisation of the moisture buffer potential of interior claddings', *Proceedings of the 'Nordic Symposium on Building Physics 2008'*

Janssen H, Roels S, 2009 'Qualitative assessment of interior moisture buffering by enclosures', *Energy and Buildings,* v41: 382-394

Janssen H, 2011 'Thermal diffusion of water vapour in porous materials: Fact or fiction?', *Int J of Heat and Mass Transfer*, v54, 2011 / 54: 1548-1562

Johannesson B, Janz M, 2009 'A two-phase moisture transport model accounting for sorption hysteresis in layered porous building constructions', *Building and Environment,* 44: 1285-1294

Jokisalu J, Kurnitski J, Korpi M, Kalamees T, Vinha J, 2009, 'Building leakage, infiltration, and energy performance analyses for Finnish detached houses', *Building and Environment*, 44: 377-387

Jones AP, 1999, 'Indoor air quality and health', *Atmospheric Environment*, 33: 4535-4564

Judkoff R, Wortman D, O'Doherty B, Burch J, 1983, 'A methodology for validating building energy analysis simulations', SERI/TR-254-1508, Solar Energy Research Institute, Golden, CO.

Judkoff R. and Neymark J. (1995), *International Energy Agency Building Energy Simulation Test (BESTEST) and Diagnostic Method*, IEA Energy Conservation in Buildings and Community Systems Programme Annex 21 Subtask C and IEA Solar Heating and Cooling Programme Task 12 Subtask B

Karagiozis A, 2001, 'Advanced Numerical Models for Hygrothermal Research', Ch. in; Trechsel HR (ed), *Moisture Analysis and Condensation control in building envelopes,* West Conshohocken, PA, ASTM, MNL40

Keresteciogl u A, Gu L, 1990, Theoretical and computational investigation of simultaneous heat and moisture transfer in buildings: "Evaporation and condensation" theory, 96(1): 455-464

Krus M, 1996, *Moisture Transport and Storage Coefficients of Porous Mineral Building Materials, Theoretical Principles and New Test Methods,* 1995 (English version published in 1996), Report based on PhD Thesis

Kumaran M K, 1998, 'An alternative procedure for the analysis of data from the cup method measurements for determination of water vapour transmission properties', *J of Testing and Evaluation*, 26: 575-581

Kumaran MK, 2004, IEA-Annex 24: *Heat, air and moisture transfer in insulated envelope parts. Final report*. In: Task 3: material properties, vol. 3. Belgium: Acco Leuven

Kumaran M K, 2006 *A Thermal and moisture property database for common building and insulation materials*, National Research Council Canada, NRCC-45692

Kumaran K, International Energy Agency, IEA Annex 24, 1996, Final Report, Task 3: Material Properties

Kumaran K, Sanders CH, 2007 IEA Annex 41 Moisture Engineering Subtask 3, *Boundary Conditions and Whole Building HAM Analysis, Final Report*, Draft 28th August

Kunzel H M, 1995, *Simultaneous Heat and Moisture Transport in Building Components; One and two-dimensional calculation using simple parameters*, ISBN 3-8167-41037

Kunzel H M, Zirkelbach D, Sedlbauer K, 2003, *Predicting Indoor Temperature and Humidity Conditions including Hygrothermal Interactions with the Building Envelope*, Proc. 1st International Conf. on Sustainable Energy and Green Architecture, Bangkok

Kunzel H M, Holm A, Zirkelbach D, Karagiozis A N, 2005, 'Simulation of indoor temperature and humidity conditions including hygrothermal interactions with the building envelope', *Solar Energy,* 78: 554-561

Kwiatkowski J, Woloszyn M, Roux J-J, 2009 'Modelling of hysteresis influence on mass transfer in building materials', *Building and Environment*, 44: 633-642

Laverge J, Van Den Bossche N, Heijmans N, Janssens A, 2011, Energy saving potential and repercussions on indoor air quality of demand controlled residential ventilation strategies, *Building and Environment*, 46: 1497:1503

Laurindo JB, Prat M, 1996, 'Numerical and experimental network study of evaporation in capillary porous media. Phase distributions', *Chem Eng Science*, 51: 5171-5185

Lengsfeld K, Holm A, 2006, Annex 41 – Subtask 1, Common Exercise 3 additional information for Step 4 (Whole building heat and moisture analysis), *'Two real exposure rooms at FhG'*

International Energy Agency (IEA) Annex 41. See: Lengsfeld and Holm, 2006.

Lengsfeld K, 2008, IEA Annex 41 – Subtask 1, Modelling Principles and Common Exercises, Common Exercise 3, *Test building with two parallel rooms.* Lengsfeld K, 2008

Li Q, Rao J, Fazio P, 2009 'Development of HAM tool for building envelope analysis', *Building and Environment*, 44: 1065-1073

Li Y, Fazio P, Rao J, 2012 'An investigation of moisture buffering performance of wood panelling at room level and its buffering effect on a test room', *Building and Environment,* 47: 205-216

Li Y, Fazio P, Rao J, 2012, 'Numerical investigation of the influence of room factors on HAM transport in a full-scale experimental room', *Building and Environment*, 50: 114-124

Lstiburek J, 2001, Moisture, Building Enclosures and Mold, *HPAC Engineering*

Lu X, 2003, 'Estimation of indoor moisture generation rate from measurement in buildings', *Building and Environment,* 38: 665-675

Ludwig N, Redaelli V, Rosina E, Augeli F, 2004, 'Moisture detection in wood and plaster by IR thermography', *Infrared Physics and Technology,* v46: 161-166

Maneval J, Whitaker S, 1988, 'Effects of saturation heterogeneities on the interfacial mass transfer relation', *Proc. of the 6th International Drying Symposium*, Versailles, 499506

Masmoudi W, Prat M, 1991, 'Heat and mass transfer between a porous medium and a parallel external flow. Application to drying of capillary porous materials', *Int. J. Heat Mass Transfer*, 34: 1975-1989

Massey B, 2006, *Mechanics of Fluids* (8th ed), ISBN 0-415-36206-7

Meadow JF, Altrichter AE, Kembel SW, Kline J, Mhuireach G, Moriyama M, Northcutt D, O'Connor TK, Womack AM, Brown GZ, Green JL, Bohannan BJM, 2014, Indoor airborne bacterial communities are influenced by ventilation, occupancy, and outdoor air source, *Indoor Air*, 24: 41-48

Mendes N, Winkelmann FC, Lamberts R, Philippi PC, 2003, 'Moisture effects on conduction loads', *Energy Buildings,* 35: 631-644

Mendes N, Philippi P C, 2005 'A method for predicting heat and moisture transfer through multilayered walls based in temperature and moisture content gradients',

Int J of Heat and Mass Transfer, 48: 37-51

Menon RA, Porteous CDA, 2012, *Design Guide: Healthy Low Energy Home Laundering*, MEARU, The Glasgow School of Art. 5.3

Metzger T, Irawan A, Tsotsas E, 2007, 'Influence of Pore Structure on Drying Kinetics: A Pore Network Study', *American Institute of Chemical Engineers*, Fluid Dynamic and Transport Phenomena, 53: 3029-3041

Miller J D, 1992, 'Fungi as contaminants in indoor air, *Atmospheric Environment*', 26a: 2163-2172

Miller CT, Christakos G, Imhoff PT, McBride JF, Pedit JA, Trangestein JA, 1998, 'Multiphase flow and transport modelling heterogeneous porous media: challenges and approaches', *Advances in Water Resources*, 21: 77-120

Molenda CHA, Crausse P, Lemarchand D, 1992, 'The influence of capillary hysteresis effects on the humidity and heat coupled transfer in a non-saturated porous medium', *Int J of Heat and Mass Transfer*, 35: 1385-1396

Mortensen LH, Rode C, Peuhkuri R, 2005, *Effect of airflow velocity on moisture exchange at surfaces*, Trondheim, Oct 26-28

Nakhi AE, 1995, *Adaptive Construction Modelling within Whole Building Dynamic Simulation*, PhD Thesis, University of Strathclyde

Nasrallah SB and Pere B, 1988, 'Detailed study of a model of heat and mass transfer during convective drying of porous media', *Int J of Heat and Mass Transfer,* 31/5: 957-967

Neale A, Derome D, Blocken B, Carmeliet J, 2007, Determination of surface convective heat transfer coeffcients by CFD', *11th Canadian Conference on Building Science and Technology, Banff, Alberta*

Nikitsin VI, Backiel-Brzozowska B, 'Determination of capillary tortuosity coefficient in calculations of moisture transfer in building materials', 2013*, Int J of Heat and Mass Trans*, 56: 30-34

Nordisk Innovations Center 2005, *Moisture Buffering of Building Materials, Report*, BYGDTU, ISBN 87 7877 195 1

Osanyintola O F, Taludkar P, Simonson J, 2006, 'Effect of initial conditions, boundary conditions and thickness on the moisture buffering capacity of spruce plywood', *Energy and Buildings*, 38: 1283-1292

Osanyintola O F, Simonson C J, 2006, 'Moisture buffering capacity of hygroscopic building materials: Experimental facilities and energy impact', *Energy and Buildings*, 38:1270-1282

Padfield T, 1998 *The role of absorbent building materials in moderating changes of relative humidity*, Doctoral Thesis, Department of Structural Engineering and Materials, Technical University of Denmark

Pandey RN, Srivastava SK, Mikhailov MD, 1999, 'Solutions of Luikov equations of heat and mass transfer in capillary porous bodies through matrix calculus: a new approach', *Int J of Heat and Mass Trans,* 42: 2649-2660

Parliamentary office of Science and Technology (POST), 2010, 'UK Indoor Air Quality', POSTNOTE, Number 366, 2010, www.parliament.uk/documents/post/postpn366_indoor_air_quality.pdf

Pedersen CR, 1990, *Combined heat and moisture transfer in building constructions*, Dissertation, Technical University of Denmark

Pedersen C R, 1992, 'Prediction of Moisture Transfer in Building Constructions', *Building and Environment*, 27: 387-397

Peeters L, Beausoleil-Morrison I, Novoselac A, 2011, 'Internal convective heat transfer modelling: Critical review and discussion of experimentally derived correlations', *Energy and Buildings*, 43: 2227-2239

Peuhkuri R, Rode C, Hansen K K, 2008, 'Non-isothermal moisture transport through insulating materials', *Building and Environment*, 43: 811-822

Philipson M C, Baker P H, Davies M, Ye Z, McNaughtan, Galbraith G H, McLean R C, 2007, 'Moisture measurement in building materials: an overview of current methods and new approaches', *Building Services Engineering Research and Technology,* 28: 303316

Plathner P, Littler J, Cripps A., 1998, *Modelling water vapour conditions in dwellings*. Third International Symposium on Humidity and Moisture, National Physical Laboratory, London, vol. 2, pp. 64–72

Plathner P, Woloszyn M, 2002, 'Interzonal air and moisture transport in a test house: experiment and modelling', *Building and Environment*, 37: 189-199

Platts-Mills TAE, De Weck AL, 1989, 'Dust mite allergens and asthma – a worldwide problem', *Journal of Allergy & Clinical Immunology*, 83: 416-427

Porteous CA, Sharpe TR, Menon RA, Shearer D, Musa H, Baker PH, Sanders CH, Strachan PA, Kelly NJ, Markopoulos A, 2012, 'Energy and environmental appraisal of domestic laundering appliances', *Building Research and Information*, 40: 679-699

Prachayawarakorn S, Prakotmak P, Soponronnarit S, 2008, 'Effects of pore size distribution and pore-architecture assembly on drying characteristics of pore networks', *Int J of Heat and Mass Trans*, 51: 344-352

Prat M, 2002, 'Recent advances in pore-scale models for drying of porous media', *Chem Eng Journa*l, 86:153-164

Prat M, 2007, 'On the influence of pore shape, contact angle and film flows on drying of capillary porous media', *Int J of Heat and Mass Transfer*, 50: 1455-1468

Qin M, Belarbi R, Ait-Mokhtar A, Nilsson L O, 2008 'Non-isothermal moisture transport in hygroscopic building materials: modelling for the determination of moisture transport coefficients', *Transport Porous Med*., 72: 255-271

Qin M, Belarbi R, Ait-Mokhtar A, Olof-Nilsson L, 2009, 'Coupled heat and moisture transfer in multi-layer building materials', *Construction and Building Materials*, 23: 967-975

Raimondo M, Dondi M, Mazzanti F, Stefanizzi P, Bondi P, 2007, Equilibrium moisture content of clay bricks: The influence of the porous structure, *Building and Environment*, *v42, Issue 2, 926-932.*

Ramos N M M, de Freitas V P, 2012, 'The Evaluation of Hygroscopic Inertia and its Importance to the Hygrothermal Performance of Buildings', in JMPQ Delgado (ed.), *Heat and Mass Transfer in Porous Media,* v13, Springer, Berlin, 978-3-642-21966-5

Ramos N M M, Delgado J M P Q, de Freitas V P, 2010, 'Influence of finishing coatings on hygroscopic moisture buffering in building elements', *Construction and Building Materials,* 24: 2590-2597

Riffat S B, 1989 'Interzone air movement and effect on condensation in houses', *Applied Energy,* 32: 49-69

Robert-Hughes R, (ed.) Fox W, Scott-Marshall A, 2011, *The Case for Space: the size of England's new homes*, RIBA

Rode C, Holm A, Padfield T, 2004, 'A review of humidity buffering in the interior spaces', *J of Thermal Envelope and Building Science*, 27: 221-226

Rode C, Peuhkuri R, Hansen KK, Time B, Svennberg K, Arfvidsson J, Ojanen T, 2005, NordTest project on moisture buffer value of materials, AIVC Conference 'Energy performance regulation', Brussels, September 21-23

Rode C, Peuhkuri R, Time B, Svennberg K, Ojanen T, 2007, 'Moisture Buffer Value of Building Materials', *Journal of ASTM International,* Volume 4, No.5

Roels S, Carmeliet J, Hens H, Adan O, Brocken H, Cerny R, Pavlik Z, Ellis A T, Hall C, Kumaran K, Pel L, Plagge R, 2004, A comparison of Different Techniques to Quantify Moisture Content Profiles in Porous Building Materials, *J of Thermal Envelope and Building Science*, 27: 261-276

Roels S, Janssen H, 2006, A comparison of the NordTest and Japanese test methods for the moisture buffering performance of building material, *Journal of Building Physics*, 30: 137-161

Roels S, Taludkar P, James C, Simonson C J, 2010, 'Reliability of material data measurements for hygroscopic buffering', *Int J of Heat Mass Transfer,* 53: 53555363

Rouchier S, Janssen H, Rode C, Woloszyn M, Foray G, Roux J J, 2012, 'Characterization of fracture patterns and hygric properties for moisture flow modelling in cracked concrete', *Construction and Building Materials*, 34: 54-62

Sanders C, 1988, 'Condensation effects on structure durability'. *Building Services: CIBSE Journal*

Scheffler GA, 2008, *Validation of hygrothermal material modelling under consideration of the hysteresis of moisture storage*, PhD Thesis, University of Technology, Dresden

Schirmer R, 1938, Die Diffusionzahl von Wasserdampf-Luftgemischen und die Verdampfungsgeschwindigkeit, VDI Beiheft Verfahrenstechnik, 6, 170

Scottish Housing Conditions Survey, 2012, www.scotland.gov.uk/Resource/0043/00439879.pdf

Sherman M H, Walker I S, Meeting residential ventilation standards through dynamic control of ventilation systems, *Energy and Buildings,* Volume 43, 2011

Simonson CJ, Salonvaara M, Ojanen T, 2002, 'The effect of structures on indoor humidity – possibility to improve comfort and perceived air quality', *Indoor Air*, 12: 243-251

Singh J, 2001, 'Review: Occupational Exposure to Moulds in Buildings', *Indoor and Built Environment*, 10: 172-178

Stafford J V, 1988, 'Remote, non-contact and in-situ measurement of soil moisture content: a review', *Journal of Agricultural Engineering Research*, 41: 151-172

Steeman HJ, Janssens A, Carmeliet J, De Paepe M, 2009, 'Modelling indoor air and hygrothermal wall interaction in building simulation: Comparison between CFD and a well-mixed zonal model', *Building and Environment*, 44: 572-583

Steeman HJ, Janssens A, De Paepe M, 2009, 'On the applicability of the heat and mass transfer analogy in indoor air flows', *Int J of Heat and Mass Transfer*, 52: 1431-1442

Steeman HJ, T'Joen C, Van Belleghem M, Janssens A, De Paepe M, 2009, 'Evaluation of the different definitions of the convective mass transfer coefficient for water evaporation into air', *Int J of Heat and Mass Transfer*, 52: 3757-3766

Steskens P, Rode C, Janssen H, 2008, 'Influences of the indoor environment on Heat, Air and Moisture conditions in the building component: Boundary conditions modeling', *11DBMC Int. Conf. on Durability of Building Materials and Components,* ISTANBUL, May 11th-14th

Svennberg K, 2006 *Moisture Buffering in the Indoor Environment*, Doctoral Thesis, Building Physics LTH, Lund University

Swirska-Perkowska J, 2011, 'Estimation of moisture superficial diffusivity in porous materials,' *Int J of Heat and Mass Trans*, 54: 692-697

Tang R, Etzion Y, 2004, 'Comparative studies on the water evaporation from a wetted surface and that from a free water surface', *Building and* Environment, 39: 77-86

Tariku F, Kumaran K, Fazio P, 2010, 'Integrated analysis of whole building heat, air and moisture transfer', *Int J of Heat and Mass Transfer*, 53: 3111-3120

Tenwolde A, Pilon CL, 2007, The effect of indoor humidity on Water Vapor release in homes, *Thermal Performanceof the Exterior of Whole Buildings X*, Atlanta, USA

Threlkeld JL, 1998, *Thermal Environment Engineering*, 3rd ed., pp. 191-193, Prentice-Hall, Englewood Cliffs, NJ

Tinga W R, Voss W A G, Blossey D F, 1973 'Generalised Approach to Multi Phase Dielectric Mixture Theory', *J of Applied Physics*, 44: 3897-3902

Topcuoglu O, Altinkaya S A, Balkose D , 2006 'Characterization of waterborne acrylic based paint films and measurement of their water vapor permeabilities', *Progress in Organic Coatings,* 56: 269-278

Trechsel H R, 2001 ed. *Moisture Analysis and Condensation Control in Building Envelopes*, ASTM manual series, Philadelphia, ISBN 0-8031-2089-3

Trechsel HR, Vigener NW, 2009, Investigating Moisture Damage caused by Building Envelope Problems, *American Society for Testing Materials*, MNL18-2ND

Van Belleghem M, Steeman HJ, Steeman M, Janssens A, De Paepe M, 2010, 'Sensitivity analysis of CFD coupled non-isothermal heat and moisture modelling', *Building and Environment*, 45: 2485-2496

Van Belleghem M, Steeman M, Willockx A, Janssens A, de Paepe M, 2011, 'Benchmark experiments for moisture transfer modelling in air and porous materials', *Building and Environment*, 46: 884-898.

Vereecken E, Roels S, Janssen H, 2009, 'In situ determination of the moisture buffering potential of room enclosures', Conf. Proc., 11th International IBPSA Conference, Glasgow, Scotland July 27-30

Waters E H, 1965 'Measurement of moisture in concrete and masonry with special reference to neutron scattering techniques', *Nuclear Structural Engineering*, 2: 494-500

Webb RL, 1990, 'Standard Nomenclature for Mass Transfer Processes', *Int Comm. Heat Mass Transfer,* 17: 529-535

Welty J, Wicks C, Wilson R, Rorrer G, 2001 *Fundamentals of Momentum, Heat and Mass Transfer*, 4th ed., John Wiley & Sons, New York

Whitaker S, 1977, 'Simultaneous heat, mass and momentum transfer – a theory of drying', *Advances in Heat Transfer*, 13: 119-203

Wolkoff P, Kjaergaard SK, 2007, 'The dichotomy of relative humidity on indoor air quality', *Environment International*, 33: 850-857

Woloszyn M, Rode C, 2008, IEA Annex 41, Subtask 1: *Modelling Principles and Common Exercises*.

Woloszyn M, Kalamees T, Abadie MO, Steeman M, Kalagasidis AS, 2009, 'The effect of combining a relative humidity sensitive ventilation system with the moisture buffering capacity of materials on indoor climate and energy efficiency of buildings', *Building and Environment*, 44: 515-524

Worch A, 2004, 'The behaviour of vapour transfer on building material surfaces: The vapour transfer resistance', *J of Thermal Envelope and Building Science*, 28[2], pp. 187-200

Wormald R, Britch A L, 1969, 'Methods of measuring moisture content applicable to building materials', *Building Science,* v3: 135-145

www.claytec.de *www.gintronic-instruments.com*

www.womersleys.co.uk/acatalog/Building_Products_2_6.html *www.wufi.de*

Wyrwal J, Marynowicz A, 2002, 'Vapour condensation and moisture accumulation in porous building wall', *Building and Environment*, 37: 313-318

Yang X, Fazio P, Ge H, Rao J, 2012, 'Evaluation of the moisture buffering capacity of interior surface materials and furniture in a full-scale experimental investigation', *Building and Environment,* 47: 188-196

Yoshino H, Mitamura T, K Hasegawa, 2009, 'Moisture buffering and effect of ventilation rate and volume rate of hygrothermal materials in a single room under steady state exterior conditions', *Building and Environment,* 44: 1418-1425

Yoshino H, Mitamura T, Hasegawa K, 2008, IEA Annex 41 – Subtask 1, Modelling Principles and Common Exercises, Common Exercise 2, *Small chamber test (THU test room) in the climate chamber*

Zhang H, Yoshino H, Hasegawa K, 2012, 'Assessing the moisture buffering performance of hygroscopic material by using experimental method', *Building and Environment*, 48: 27-34